nature genetics

Article

https://doi.org/10.1038/s41588-022-01213-w

Multi-ancestry genome-wide association analyses identify novel genetic mechanisms in rheumatoid arthritis

In the format provided by the authors and unedited

Supplementary Note

Comparison between the fixed-effect and random-effect meta-analysis

To compare the outputs of the fixed-effect meta-analysis with those of the random-effect meta-analysis, we applied MR-MEGA to the same sets of cohorts and conducted a multi-ancestry meta-analysis. Although MR-MEGA detected associations similar to our results, the associations were systematically weaker than the fixed-effect meta-analysis we employed in our multi-ancestry GWAS. This study identified 122 significant autosomal loci using fixed-effect meta-analysis. Among the 122 lead variants in this study, 117 showed weaker signals in MR-MEGA results (one-sided sign test *P* value = 4.1×10^{-29}; **Supplementary Figure 1**). On the flip side, MR-MEGA identified 83 significant autosomal loci. Even among the 83 lead variants of the MR-MEGA, 69 showed weaker signals in MR-MEGA results (one-sided sign test *P* value = 3.4×10^{-10}). MR-MEGA demonstrates the highest power in the situation where allelic effect heterogeneity between cohorts is correlated with ancestry[1], suggesting that the RA risk loci identified so far confers relatively homogeneous risk across ancestries.

Identification of associated loci

We detected 108 genome-wide significant loci ($P < 5 \times 10^{-8}$) in this multi-ancestry study: 106 autosomal loci and two loci on the X chromosome (**Supplementary Tables 4** and **5**). We observed almost identical effect sizes between this multi-ancestry GWAS and the previously reported 100 RA risk alleles[2] (Pearson's $r = 0.98$ and $P = 2.8 \times 10^{-82}$; **Supplementary Figure 2**; **Supplementary Table 3**). EUR-GWAS identified three additional autosomal loci which were not significant in multi-ancestry GWAS (**Supplementary Table 4**). GWAS of seropositive RA additionally detected 13 autosomal loci (**Supplementary Table 4**). In total, we detected significant signals at 122 autosomal loci outside of the MHC locus and two loci on the X chromosome (**Supplementary Table 4** and **5**). Among these 124, 34 autosomal loci were novel (**Table 1**). Notably, 25 novel loci had not been implicated in any other autoimmune diseases (**Supplementary Table 4; Methods**). We provided Manhattan and QQ plots in **Supplementary Figure 3**.

We note that among these 124 loci, 16 were not associated at genome-wide significance level in the multi-ancestry GWAS (**Supplementary Table 4**). These loci may represent ancestry-specific or seropositive RA-specific loci but may also represent statistical fluctuation. For completeness, we included all these loci in our downstream analyses.

Power gain of multi-ancestry GWAS

To evaluate the source of the power gain in the multi-ancestry GWAS other than the sample size, we conducted a down-sampling test where the multi-ancestry GWAS has almost identical sample size as EUR-GWAS (the down-sampled multi-ancestry GWAS: 22,253 cases and 73,080 controls; and the EUR-GWAS: 22,350 cases and 74,823 controls). Compared with the EUR-GWAS, the down-sampled multi-ancestry GWAS detected more loci (**Supplementary Figure 4; Supplementary Note**), which is probably attributed to the allele frequency diversity in our multi-ancestry cohorts.

Genetic risk differences between seropositive and seronegative RA

The presence or absence of autoantibodies (rheumatoid factor and anti-citrullinated peptide antibodies) defines two major subgroups of RA: seropositive and seronegative RA[3]. We tested the differences in genetic signals between them at the 122 significant autosomal loci. Although their effect sizes were significantly correlated in general (Pearson's $r = 0.76$; $P = 3.2 \times 10^{-23}$), the effect sizes of seronegative RA were generally smaller than seropositive RA (one-sided sign test P value = 8.3×10^{-17}; **Extended Data Figure 2**). The smaller effect sizes at the detected loci might reflect greater polygenicity and clinical heterogeneity of seronegative RA. The effect size gap was prominent for some genes; we found significant heterogeneity in effect size estimates at the nine loci: *CCR6, CTLA4, NFKBIE-TMEM151B, PADI4, PTPN22, RAD51B, SMIM20-RBPJ, TNFRSF14-AS1*, and *UBASH3A* ($P_{het} < 0.05/122$; **Extended Data Figure 2**), which might suggest etiological differences between seropositive and seronegative RA. For example, *CCR6* has critical roles in B cell antibody production[4,5]. Together, these findings suggested generally shared genetic risks between seropositive and seronegative RA outside of the MHC locus, although substantial differences exist around biologically relevant genes.

Our study had insufficient power to detect significant signals for seronegative RA outside of the MHC region due to a limited sample size (4,515 cases of seronegative RA). Although we observed shared genetic risks between them (**Extended Data Figure 2**), this analysis was restricted to the loci detected in all RA or seropositive RA. To unveil the specific etiology of seronegative RA further, we need cohorts that are larger and have better representation of seronegative RA.

Comparison of fine-mapping resolution among different GWAS settings

To discuss the benefit of multi-ancestry study design in fine-mapping, we utilized three different GWAS settings; multi-ancestry (meta-analysis using all of five ancestries), EUR-, and EAS-GWAS. The 95% credible sets were smaller in the multi-ancestry GWAS than the EUR- and EAS-GWAS (one-sided paired Wilcoxon text $P = 1.1 \times 10^{-9}$ and 2.6×10^{-18}, respectively; **Supplementary Figure 4a**). Similarly, posterior inclusion probability (*PIP*) was higher in the multi-ancestry GWAS than the EUR- and EAS-GWAS (one-sided paired Wilcoxon text $P = 3.1 \times 10^{-11}$ and 6.1×10^{-15}, respectively: **Supplementary Figure 4b**).

To confirm the reason why multi-ancestry study design provided finer resolution results, we conducted a down-sampling experiment. We excluded 10 cohorts from EUR-GWAS and meta-analyzed them with similar-sized 10 cohorts from EAS, AFR, SAS, and ARB (down-sampled multi-ancestry GWAS; 22,253 cases and 73,080 controls in total); down-sampled multi-ancestry GWAS has almost identical sample size as in full sized EUR-GWAS (22,350 cases and 74,823). Even in this setting, the 95% credible sets were still smaller in the multi-ancestry setting (**Supplementary Figure 4c**). Similarly, *PIP* was still higher in the multi-ancestry setting (one-sided paired Wilcoxon text $P = 3.6 \times 10^{-5}$; **Supplementary Figure 4d**). We also confirmed that the down-sampled multi-ancestry GWAS detected more loci compared with the EUR-GWAS (**Supplementary Figure 4e).** These results suggested that the improved fine-mapping resolution in the multi-ancestry GWAS was not only due to the increase in sample size but also due to diversified LD structures and allele frequency spectrum.

Sample sizes required to detect ancestry-specific signals

In this study, we detected ancestry-specific signals only for EAS and EUR. Although ancestry-specific signals are relatively few, they include predominantly large effect size variants, many of which are missense, and hence they are valuable resources to understand the etiology of RA. Therefore, we sought to assess the sample size required to detect ancestry-specific signals. Since the true effect size and MAF of the causal variants are unknown, we assumed the lead variants of EUR-GWAS are the proxy of the causal variants. We selected 57 autosomal variants that passed genome-wide significance in EUR-GWAS, including three EUR-specific signals: rs2476601, rs34536443, and rs9826420 (see the definition in the main text). Using these variants, we conducted the power analysis and estimated the odds ratio corresponding to the sample size and MAF with the following conditions: power = 0.5, α = 5 x 10^{-8}, and the case-control ratio = 0.23 (the actual ratio in EUR-GWAS) (**Supplementary Figure 5**). This analysis suggested that this study was underpowered to detect specific signals in non-EUR and non-EAS ancestries. For example, we need around 5,000 and 10,000 samples to detect equivalents of the *PTPN22* missense variant (rs2476601) and the *TYK2* missense variant (rs34536443) in non-EUR, respectively (**Supplementary Figure 5**).

Effect size similarities between ancestries

We examined the extent to which genetic effects are shared across ancestries. We focused on the 30 fine-mapped variants (*PIP* > 0.5; **Methods**). The **Supplementary Figure 6** showed the correlation of the effect sizes for the fine-mapped variants between ancestries, which ranged from 0.56 to 0.91. To quantify the influence of the sample size differences or the effect size standard errors on the correlation estimates, we conducted extensive simulation tests. We assumed the true effect size is the same across ancestries (i.e., the true correlation = 1) and randomly sampled effect sizes 1,000 times using the observed standard errors in each ancestry. We then evaluated the distribution of the correlation estimates (**Supplementary Figure 7**). The simulated correlation estimates were dependent on the size of standard errors in each ancestry: we observed the lowest simulated correlation in the Arab ancestry with the largest effect-size standard errors (due to the smallest sample size). The **Supplementary Figure 7** showed the observed correlation with the red vertical line, and we confirmed that the observed

correlation was within the expected range (rank-based *P* value > 0.354). These results are consistent with the identical effect sizes across ancestries at the fine mapped loci.

We compared effect sizes in EUR-GWAS with those in non-EUR-GWASs. We only found two variants with significant heterogeneities (**Supplementary Figure 6, 8,** and **9**); rs3093017 located at the *CCR6* locus (OR = 0.89 (0.87-0.92) in EUR-GWAS; OR = 0.82 (0.80-0.85) in EAS-GWAS; P_{het} = 1.4 x 10^{-4} < 0.05 / (30 x 5)) and esv3585367 located at the *PADI4* locus (OR = 0.92 (0.90-0.95) in EUR-GWAS; OR = 0.83 (0.80-0.86) in EAS-GWAS; P_{het} = 1.0 x 10^{-6} < 0.05 / (30 x 5)). Although rs3093017's effects were uniform within each ancestry, esv3585367 had a significant effect size heterogeneity within EAS cohorts (P_{het} = 2.5 x 10^{-4}); this remained significant even after restricting this analysis to seropositive RA (P_{het} = 5.8 x 10^{-4}) (**Supplementary Figure 8 and 9**; **Supplementary Table 4**). Therefore, these heterogeneous signals might suggest genetic differences among cohorts, rather than differences between EUR and EAS, which probably highlighting clinical heterogeneity in our GWAS. These results suggested that we need more efforts to collect clinically uniform samples to infer differences in genetic risk across ancestries.

Partitioning heritability

In the analysis of S-LDSC using IMPACT annotations, we detected significant enrichments in 114 annotations in either of EUR and EAS (P < 0.05/707 = 7.1 x 10^{-5}; **Figure 5a** and **Supplementary Table 11**). Although four out of 114 significant annotations were derived from non-immune cells, controlling the effect of $CD4^+$ T cell T-bet annotation canceled out all four enrichments. Among annotations with significant enrichments, the one which explained the largest fraction of EUR heritability was $CD4^+$ T cell T-bet annotation (90%; S.E. = 11%). This annotation explained 94% (S.E. = 12%) of EAS heritability consistent with analyses on previous GWAS results[6]. However, it is important to note that $CD4^+$ T cells do not explain all heritability. Moreover, the contribution of $CD4^+$ T cells to RA heritability might be overestimated when other causal cell types share similar regulatory regions with $CD4^+$ T cells. Therefore, this finding does not exclude the possible contribution of other cell types and tissues.

In addition to IMPACT annotations, we analyzed 396 histone mark annotations and found significant enrichment in 55 annotations in either of EUR or EAS ($P < 0.05/396 = 1.3 \times 10^{-4}$; **Supplementary Table 12**); among them, the annotation of H3K4me1 in PMA-I stimulated primary $CD4^+$ T cells explained the largest fraction of heritability of EUR (52%; SE = 5.7%). However, controlling the effect of $CD4^+$ T cell T-bet IMPACT annotation cancelled out all significant enrichments of histone mark annotations (**Extended Data Figure 7**). Moreover, controlling the effect of H3K4me1 in PMA-I stimulated primary $CD4^+$ T cells was unable to cancel out significant enrichments of $CD4^+$ T cell T-bet annotation (**Extended Data Figure 7**). Therefore, we confirmed that $CD4^+$ T cell T-bet annotation can explain a large fraction of RA heritability and it outperforms histone mark annotations.

PRS performance comparison with the previous GWAS

To understand the impact of increased sample size in this GWAS, we compared the PRS performance of our multi-ancestry GWAS with that of the previous multi-ancestry GWAS[2]. This GWAS has 1.9 times more cases than the previous GWAS; the number increases to 2.8 when we restrict cases to non-EUR samples. We restricted the PRS validation cohorts to 15 cohorts that were not included in the previous GWAS to avoid over-fitting. This analysis confirmed that our PRS model outperformed that of the previous GWAS (**Extended Data Figure 8**).

PRS performance in UK Biobank samples

Although our strategy has no over-fitting problem using the LOCO approach, we also applied our PRS model to external samples and evaluated its performances. We used the UK Biobank samples (UKBB; 4,617 cases and 316,265 controls of White British ancestry), which was not included in the original analysis. The inclusion criteria of our initial analysis required RA patients to be diagnosed by trained rheumatologists, whereas the case/control information in UKBB was retrieved from the clinical information (ICD-10) in UKBB via phecode and PHESANT software[7]. The liability scale R^2 was 0.086 for UKBB, which was around the same level as in other EUR cohorts (**Supplementary Figure 10**). For EUR cohorts in our study, we used the multi-ancestry PRS with the LOCO approach as in other analyses. On

the other hand, we used the multi-ancestry PRS *without* the LOCO approach for UKBB analysis since UKBB was not included in our GWAS. These results supported that our original PRS evaluation did not have an upward bias due to the over-fitting problem.

Limitations of eQTL analysis

Although we employed a careful approach evaluating GWAS and eQTL signal colocalization by using the intersection of the coloc and SMR results (**Supplementary Tables 9** and **10**), some loci showed extensive pleiotropy; for example, a novel GWAS association around rs55762233 is colocalized with eQTL signals of six genes, among which we prioritized *CILP2* as the candidate causal gene considering its role in the articular cartilage extracellular matrix. To confirm the causal gene at the pleiotropic loci, we require functional experiments, which should be one of the future research directions.

BioBank Japan Project Consortium

Koichi Matsuda. Laboratory of Genome Technology, Human Genome Center, Institute of Medical Science, The University of Tokyo, Tokyo, Japan. Laboratory of Clinical Genome Sequencing, Graduate School of Frontier Sciences, The University of Tokyo, Tokyo, Japan. kmatsuda@edu.k.u-tokyo.ac.jp; Yuji Yamanashi. Division of Genetics, The Institute of Medical Science, The University of Tokyo, Tokyo, Japan. yyamanas@ims.u-tokyo.ac.jp; Yoichi Furukawa. Division of Clinical Genome Research, Institute of Medical Science, The University of Tokyo, Tokyo, Japan. furukawa@ims.u-tokyo.ac.jp; Takayuki Morisaki. Division of Molecular Pathology IMSUT Hospital, Department of Internal Medicine. Project Division of Genomic Medicine and Disease Prevention, The Institute of Medical Science, The University of Tokyo, Tokyo, Japan. morisaki@ims.u-tokyo.ac.jp; Yoshinori Murakami. Department of Cancer Biology, Institute of Medical Science, The University of Tokyo, Tokyo, Japan. ymurakam@ims.u-tokyo.ac.jp; Yoichiro Kamatani. Laboratory of Complex Trait Genomics, Graduate School of Frontier Sciences, The University of Tokyo, Tokyo, Japan. Laboratory of Clinical Genome Sequencing, Graduate School of Frontier Sciences, The University of Tokyo, Tokyo, Japan. kamatani.yoichiro@edu.k.u-tokyo.ac.jp; Kaori Muto. Department of Public Policy, Institute of Medical Science, The University of Tokyo, Tokyo, Japan. krmt@ims.u-tokyo.ac.jp; Akiko Nagai. Department of Public Policy, Institute of Medical Science, The University of Tokyo, Tokyo, Japan. akikongi@ims.u-tokyo.ac.jp; Wataru Obara. Department of Urology, Iwate Medical University, Iwate, Japan. watao@iwate-med.ac.jp; Ken Yamaji. Department of Internal Medicine and Rheumatology, Juntendo University Graduate School of Medicine, Tokyo, Japan. k.yamaji@juntendo.ac.jp; Kazuhisa Takahashi. Department of Respiratory Medicine, Juntendo University Graduate School of Medicine, Tokyo, Japan. kztakaha@juntendo.ac.jp; Satoshi Asai. Division of Pharmacology, Department of Biomedical Science, Nihon University School of Medicine, Tokyo, Japan. Division of Genomic Epidemiology and Clinical Trials, Clinical Trials Research Center, Nihon University. School of Medicine, Tokyo, Japan. asai.satoshi@nihon-u.ac.jp; Yasuo Takahashi. Division of Genomic Epidemiology and Clinical Trials, Clinical Trials Research Center, Nihon

University School of Medicine, Tokyo, Japan. takahashi.yasuo@nihon-u.ac.jp; Takao Suzuki. Tokushukai Group, Tokyo, Japan. takao.suzuki@tokushukai.jp; Nobuaki Sinozaki. Tokushukai Group, Tokyo, Japan. nobuaki.shinozaki@tokushukai.jp; Hiroki Yamaguchi. Departmentof Hematology, Nippon Medical School, Tokyo, Japan. y-hiroki@fd6.so-net.ne.jp; Shiro Minami. Department of Bioregulation, Nippon Medical School, Kawasaki, Japan. shirom@nms.ac.jp; Shigeo Murayama. Tokyo Metropolitan Geriatric Hospital and Institute of Gerontology, Tokyo, Japan. smurayam@bbarjp.net; Kozo Yoshimori. Fukujuji Hospital, Japan Anti-Tuberculosis Association, Tokyo, Japan. yoshimorik@fukujuji.org; Satoshi Nagayama. The Cancer Institute Hospital of the Japanese Foundation for Cancer Research, Tokyo, Japan. snagayama2009@hotmail.co.jp; Daisuke Obata. Center for Clinical Research and Advanced Medicine, Shiga University of Medical Science, Shiga, Japan. dobata@belle.shiga-med.ac.jp; Masahiko Higashiyama. Department of General Thoracic Surgery, Osaka International Cancer Institute, Osaka, Japan. higashiyama-m@higashiosaka-hosp.jp; Akihide Masumoto. IIZUKA HOSPITAL, Fukuoka,Japan. amasumotoh1@aih-net.com; Yukihiro Koretsune. National Hospital Organization Osaka National Hospital, Osaka, Japan. koretune318@hotmail.co.jp; Yukihide Momozawa. Laboratory for Genotyping Development, RIKEN. Center for Integrative Medical Sciences, Yokohama, Japan. momozawa@riken.jp; Nao Otomo. Laboratory for Statistical and Translational Genetics, RIKEN Center for Integrative Medical Sciences, Yokohama, Japan. naoootomo@yahoo.co.jp; Hiroyuki Suetsugu. Laboratory for Statistical and Translational Genetics, RIKEN Center for Integrative Medical Sciences, Yokohama, Japan. hiroyuki-suetsugu@hotmail.co.jp

Ethics Statements

The Consortium for the Longitudinal Evaluation of African Americans with Rheumatoid Arthritis (CLEAR) Registry and Repository. The study was approved by the Institutional Review Boards of the participating institutions: the University of Alabama at Birmingham (Birmingham, Alabama), Emory University (Atlanta, Georgia), The Medical University of South Carolina (Charleston, South Carolina), The University of North Carolina at Chapel Hill (Chapel Hill, North Carolina), and Washington University (St. Louis, Missouri). These studies were conducted in accordance with the Declaration of Helsinki for the protection of human subjects in research. All study participants gave written informed consent.

GENRA. The GENetics of RA in individuals of African ancestry (GENRA) study (which recruited patients with RA) was approved by the National Research Ethics Service Committee London—Dulwich (reference: 11/LO/1244). Controls for the GENRA study were from the South London Ethnicity and Stroke Study (SLESS); this was approved by the Wandsworth Local Research Ethics Committee (reference: 05/Q0803/324). All participants provided consent.

The Epidemiological Investigation of Rheumatoid arthritis, Qatar. The study was approved by the Institutional Review Boards (IRB) of Weill Cornell Medicine-Qatar, Hamad Medical Corporation (Qatar), American University of Beirut (Lebanon), King Faisal Specialist Hospital and Research Center (Kingdom of Saudi Arabia), Jordan Hospital IRB (Amman, Jordan) and the Dubai Scientific Research Ethics Committee, Dubai Health Authority (United Arab Emirates). All included individuals gave their informed consent to participate.

Biobank Japan (BBJ). All participants provided written informed consent as approved by the ethical committees of the RIKEN Yokohama Institute.

Institute of Rheumatology, Rheumatoid Arthritis (IORRA). The study was approved by Tokyo Women's Medical University Ethics Committee (#217I). All participants provided written informed consent as approved by the committee.

Hanyang University. All participants provided written informed consent for the study and the Institutional Review Board of Hanyang University approved this study.

Kyoto University Arthritis Cohort. We obtained approval from the Ethics Committee of Kyoto University Graduate School and the Faculty of Medicine for the study (No. G1006). Written informed consent was obtained from all patients.

Osaka University. The study was approved by the ethical committee of Osaka University (#734). All participants provided written informed consent.

The University of Occupational and Environmental Health. The study was approved by the ethical committee of Osaka University and The University of Occupational and Environmental Health. All participants provided written informed consent.

The Identification of Genes and Proteins Responsible for Rheumatoid Arthritis in Canada. This study was approved by the Mount Sinai Hospital Research Ethics Board. All participants gave their written informed consent for the study. The following individuals are covered by this study: Kathy Siminovitch, Ed Keystone, Chris Amos, Gang Xie and Jinyi Zhang.

The Epidemiological Investigation of Rheumatoid Arthritis, Netherlands. The study was approved by the Ethical Committee of Leiden University Medical Center, Leiden, The Netherlands. All participants gave their written informed consent for the study.

The Epidemiological Investigation of Rheumatoid arthritis (EIRA) in Sweden. The study was approved by the Stockholm Ethical Committee. All participants gave their informed consent prior to their inclusion in the study.

CARDERA. The CARDERA Genetics Cohort combines data from patients recruited to two trials of Combination Anti-Rheumatic Drugs in Early RA (CARDERA-1 and CARDERA-2). CARDERA-1 (Research Ethics Committee reference: MREC (1) 99/04) and CARDERA-2 (Research Ethics Committee reference: MREC 02/1/089) were ethically approved. Approval was obtained to genotype archived DNA from the National Research Ethics Service Committee East of England—Essex (reference: 11/EE/0544). All participants provided consent.

Rheumatoid Arthritis Medication Study (RAMS). RAMS ethical approval was obtained from the National Research Ethics Service Central Manchester Research Ethics Committee and all participants gave their written informed consent.

Biologics in Rheumatoid Arthritis Genetics and Genomics Study Syndicate (BRAGGSS). The North West Ethics committee approved the study and all patients were recruited after giving informed consent.

The UK Manchester cohort of patients with rheumatoid arthritis (RA) - RA arm of the National Repository study (BIRA). All participants were recruited after providing informed consent and the study was approved by the North West Research Ethics Committee.

The Norfolk Arthritis Register (NOAR). All patients were recruited following informed consent with ethical approval obtained from the East of England Cambridgeshire and Hertfordshire Research Ethics Committee (reference 15/EE/0076 IRAS ID 166048).

The Epidemiological Investigation of Rheumatoid arthritis, Umeå, Sweden. The study was approved by the Regional Ethics Committee and all included individuals gave their written informed consent to participate.

Amsterdam UMC, Amsterdam, the Netherlands. The study protocol was approved by the Medical Ethics Committee of the Amsterdam UMC (AMC & Vumc). All study participants gave written informed consent and the study was performed according to the Helsinki Declaration.

Spanish cohort. The study was approved by the Ethic Committe of CSIC. All participants gave written consent, and the study was performed according to the Helsinki Declaration.

The Vanderbilt BioVU cohort study. The study was designated as non-human subjects research by the Vanderbilt University IRB.

Nurses Health Study. The study was approved by the Mass General Brigham Human Subjects Committee. All participants gave their written informed consent to participate.

The i2b2 Rheumatoid Arthritis Study and the Mass General Brigham Biobank. Ethical approval for both studies were obtained from the Institutional Review Board of Mass General Brigham (MGB). Individuals from the MGB Biobank provide written informed consent for genomic studies.

PHARE (France). The study was approved by the Ethic committee of Paris Pitié-Salpétrière, France on 21 January 2003 (CCPPRB/146-13).

CAPEA study (German). The study was approved the CHARITÉ ethics Committee (EA1/091/09) for the clinical investigation and by ethics Committee of the Duesseldorf Medical Faculty (3368) for the biosamples. All participants gave their written informed consent to participate.

Malaysian Epidemiological Investigation of Rheumatoid Arthritis (MyEIRA). The MyEIRA study was approved by the Medical Research and Ethics Committee of the Ministry of Health in Malaysia (KKM/JEPP/02 Jld.1 (86); (14) dlm.KKM/NIHSEC/08/0804/ MRG-2005-12). All participants were given their written informed consent for the study.

References

1. Mägi, R. *et al.* Trans-ethnic meta-regression of genome-wide association studies accounting for ancestry increases power for discovery and improves fine-mapping resolution. *Hum. Mol. Genet.* **26**, 3639–3650 (2017).
2. Okada, Y. *et al.* Genetics of rheumatoid arthritis contributes to biology and drug discovery. *Nature* **506**, 376–381 (2014).
3. Ajeganova, S. & Huizinga, T. W. J. Seronegative and seropositive RA: Alike but different? *Nature Reviews Rheumatology* **11**, 8–9 (2015).
4. Wiede, F. *et al.* CCR6 is transiently upregulated on B cells after activation and modulates the germinal center reaction in the mouse. *Immunol. Cell Biol.* **91**, 335–339 (2013).
5. Lee, B. O. *et al.* CD40, but Not CD154, Expression on B Cells Is Necessary for Optimal Primary B Cell Responses. *J. Immunol.* **171**, 5707–5717 (2003).
6. Amariuta, T. *et al.* IMPACT: Genomic Annotation of Cell-State-Specific Regulatory Elements Inferred from the Epigenome of Bound Transcription Factors. *Am. J. Hum. Genet.* **104**, 879–895 (2019).
7. Millard, L. A. C., Davies, N. M., Gaunt, T. R., Smith, G. D. & Tilling, K. Software Application Profile: PHESANT: a tool for performing automated phenome scans in UK Biobank. *Int. J. Epidemiol.* **47**, 29–35 (2018).

Supplementary Figures

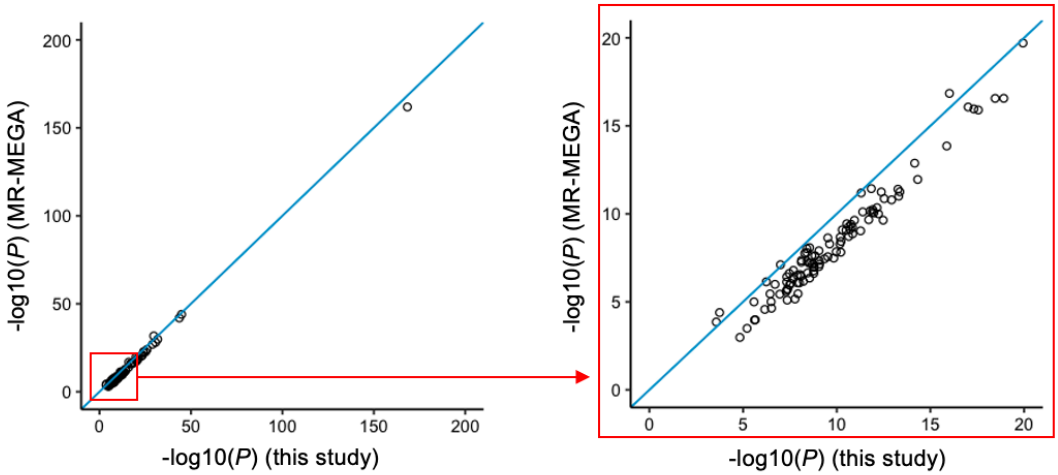

Supplementary Figure 1. *P* value comparison between the fixed-effect and random-effect meta-analysis.
We used the lead variants at the 122 significant autosomal associations. Statistics in each cohort was estimated by a logistic regression test. To calculate *P* values, these statistics were further analyzed by a fixed-effect meta-analysis (our multi-ancestry GWAS; X-axis) and a random-effect meta-analysis (MR-MEGA; Y-axis). The blue line indicates the identity line. On the left, we plotted all 122 variant results. On the right, we provided a zoom-in plot.

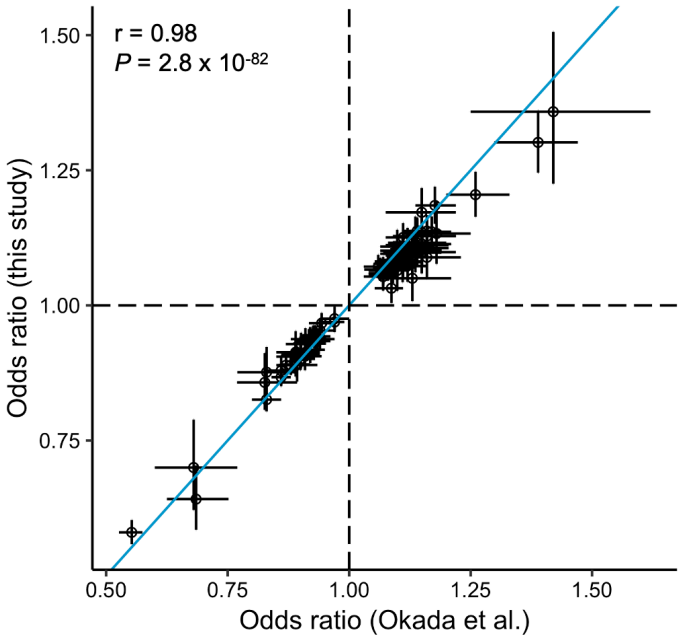

Supplementary Figure 2. Comparison of effect sizes between this and previous GWAS.
We compared effect size estimates between our study (multi-ancestry GWAS) and a previous RA GWAS study at the 100 reported variants[2]. 6:149834574:T:C was excluded due to low imputation quality in our study. Odds ratios and their 95% confidence intervals are provided. *P* values in the multi-ancestry GWAS were calculated by a fixed effect meta-analysis of statistics from logistic regression tests in each cohort.

Multi-ancestry GWAS

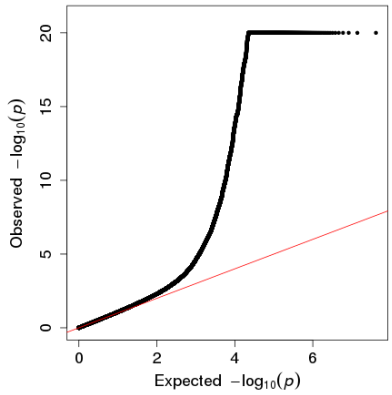

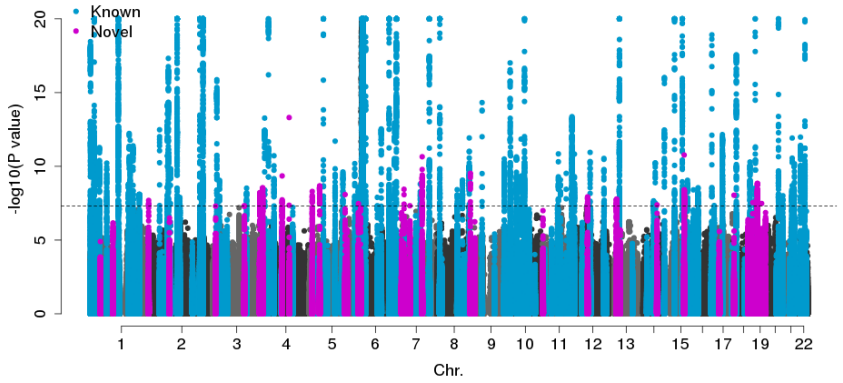

EUR-GWAS

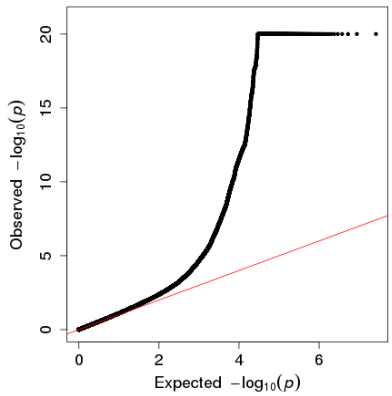

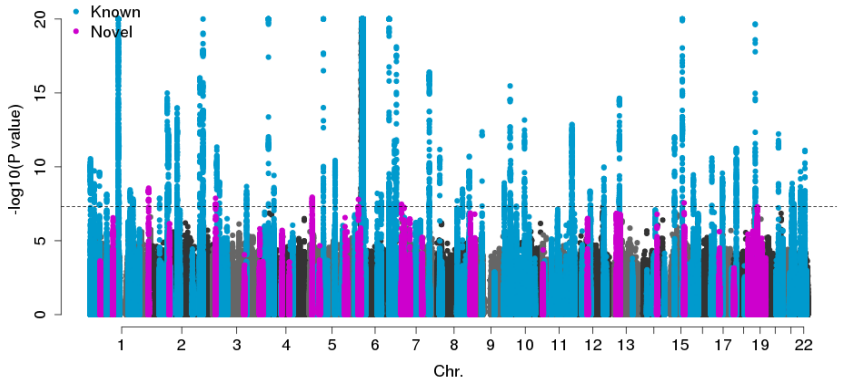

EAS-GWAS

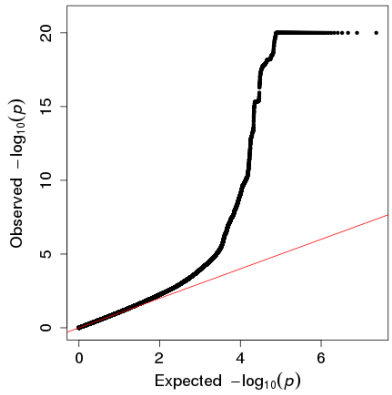

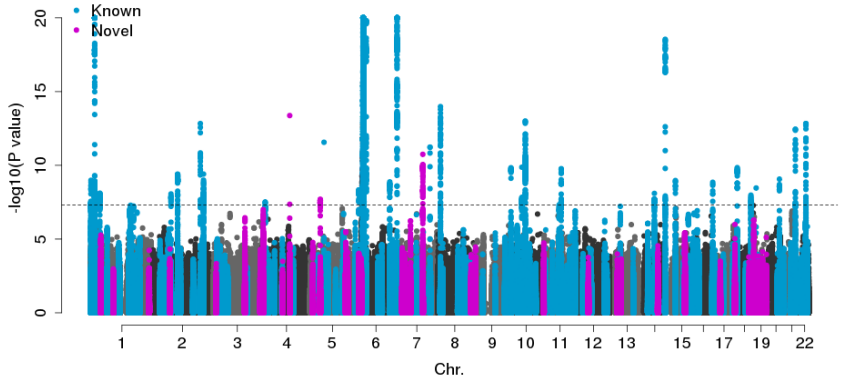

AFR-GWAS

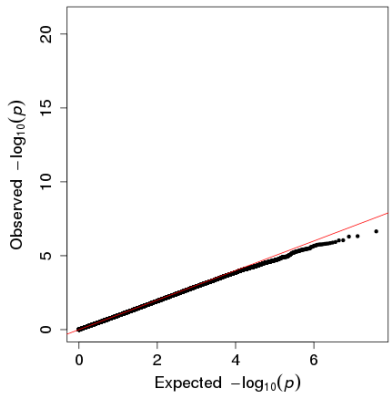

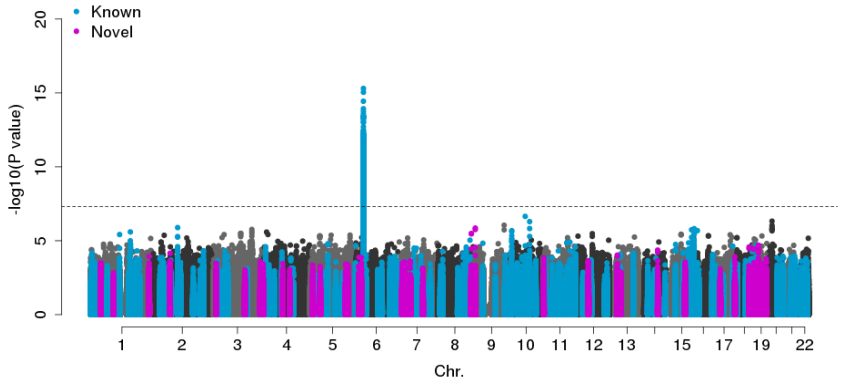

SAS-GWAS

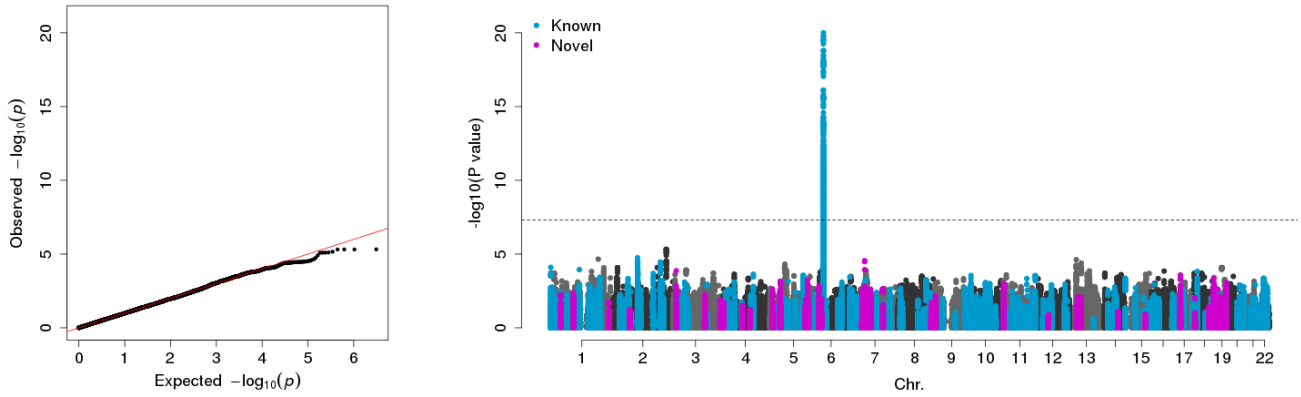

ARB-GWAS

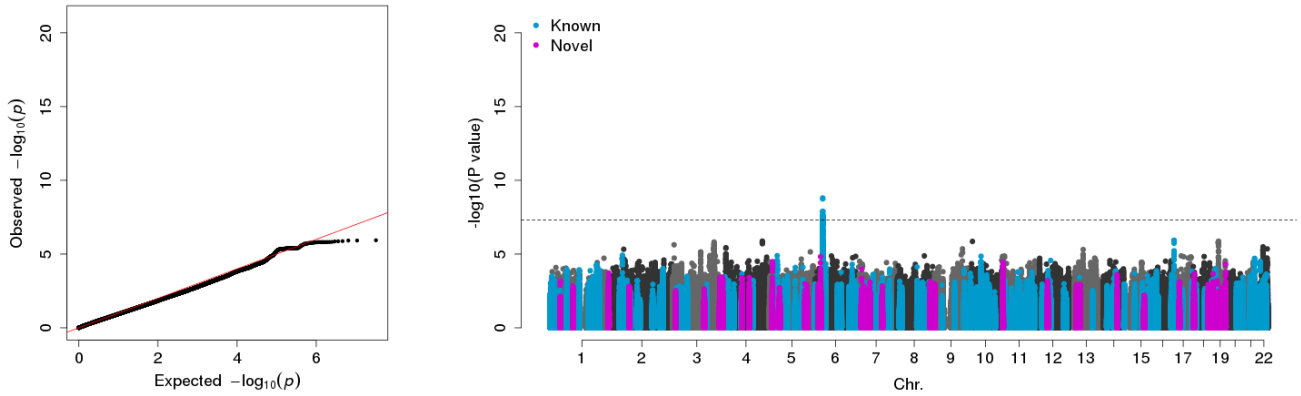

Supplementary Figure 3. QQ plots and Manhattan plots for multi- and single-ancestry GWAS. *P* values were calculated by a fixed effect meta-analysis of statistics from logistic regression tests in each cohort.

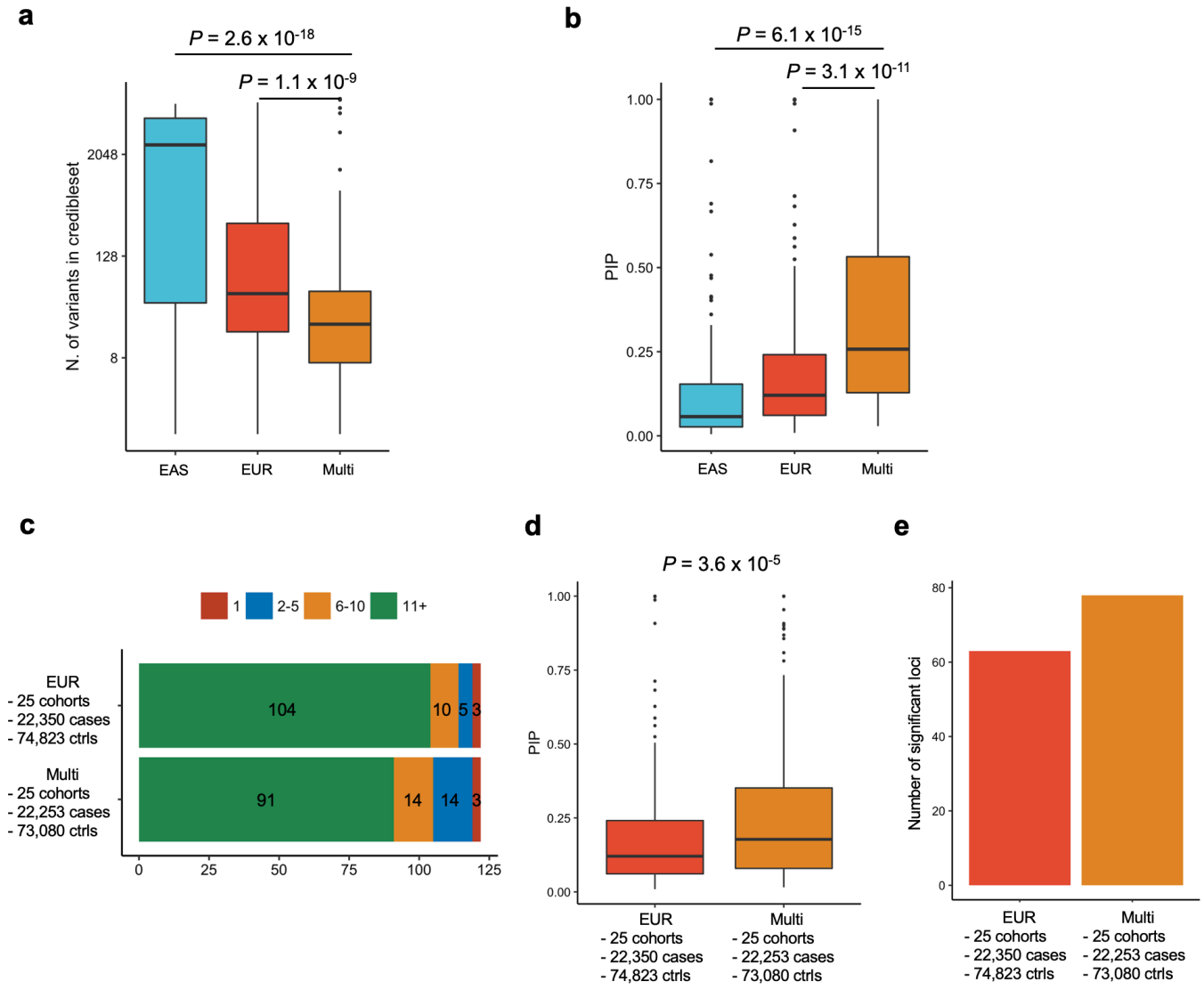

Supplementary Figure 4. GWAS setting influences on fine-mapping resolution.
(a) Number of variants in 95% credible set in three different GWAS settings at the 122 loci analyzed. The differences were assessed by one-sided paired Wilcoxon text (n=122).
(b) The *PIP* of the lead variant in three different GWAS settings at the 122 loci analyzed. The differences were assessed by one-sided paired Wilcoxon text (n=122).
(c) Among 122 loci analyzed, we counted the number of loci whose 95% credible set size was in a specified range. The results from full-sized EUR- and down-sampled multi-ancestry GWAS are provided.
(d) The *PIP* of the lead variant in two different GWAS settings at the 122 loci analyzed. The results from full-sized EUR- and down-sampled multi-ancestry GWAS are provided. The differences were assessed by one-sided paired Wilcoxon text (n=25).
(e) The number of significant loci in full-sized EUR- and down-sampled multi-ancestry GWAS ($P < 5 \times 10^{-8}$). We used the same down-sampled datasets used in **c** and **d**.
Within each boxplot, the horizontal lines reflect the median, the top and bottom of each box reflect the interquartile range (IQR), and the whiskers reflect the maximum and minimum values within each grouping no further than 1.5 x IQR from the hinge.

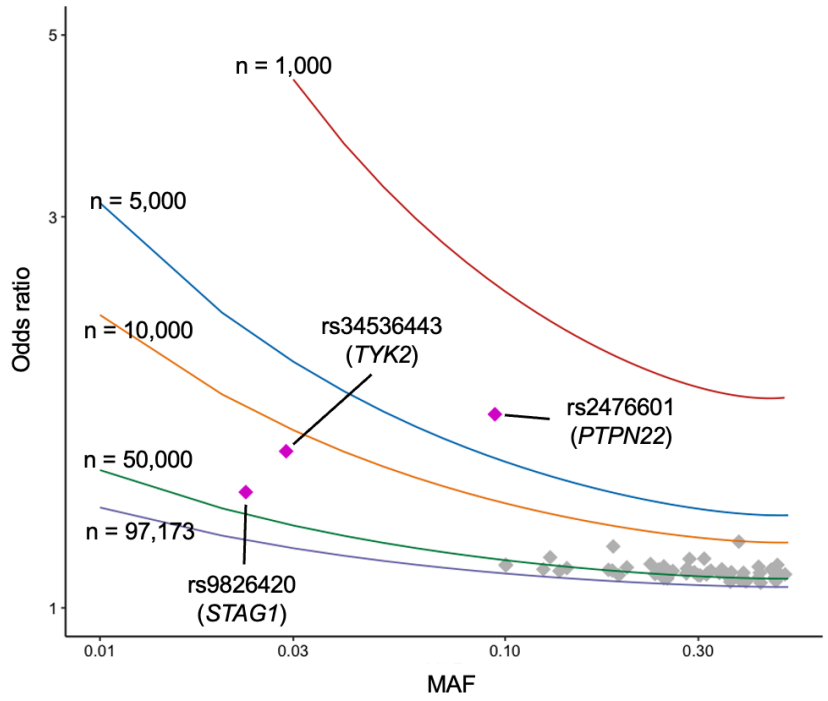

Supplementary Figure 5. Sample sizes and the power of variant discovery.
We selected 57 autosomal variants which passed genome-wide significance in EUR-GWAS, which include three EUR-specific signals: rs2476601, rs34536443, and rs9826420 (see the definition in the main text). Their odds ratios in EUR-GWAS and MAF in EUR are provided. The lines are the results of the power analysis that indicate the odds ratio corresponding to the sample size and MAF with the following conditions: power = 0.5, α = 5 x 10^{-8}, and the case-control ratio = 0.23 (the actual ratio in EUR-GWAS). The sample size of 97,173 is the actual size of this EUR-GWAS.

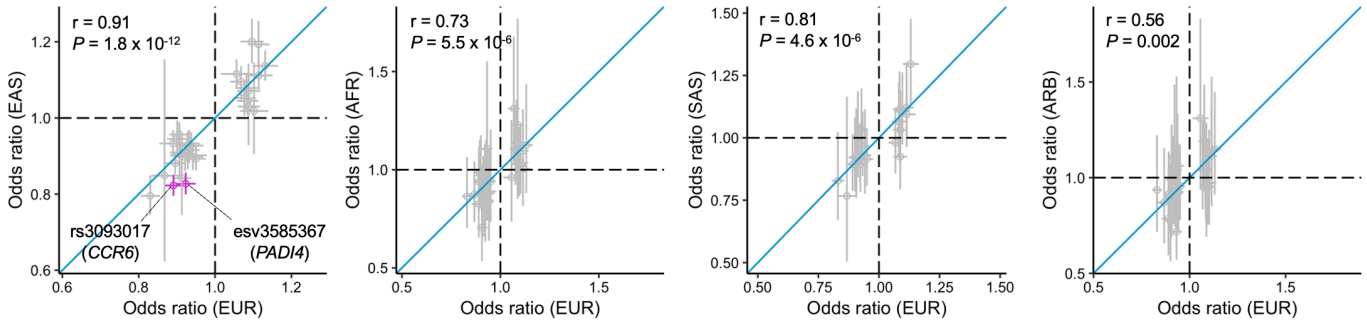

Supplementary Figure 6. Shared GWAS signals across five ancestries.
Odds ratio and its 95% confidence interval of EUR-, EAS-, AFR-, SAS-, and ARB-GWAS at 30 fine mapped variants (*PIP* > 0.5 and MAF greater than 1% in all of EUR, EAS, AFR, and SAS (1KG Phase 3)). rs3093017 and esv3585367 which had a significant heterogeneity in effect size estimate are highlighted by red (Cochran's Q test *P* value < 0.05 / (30 x 5)).

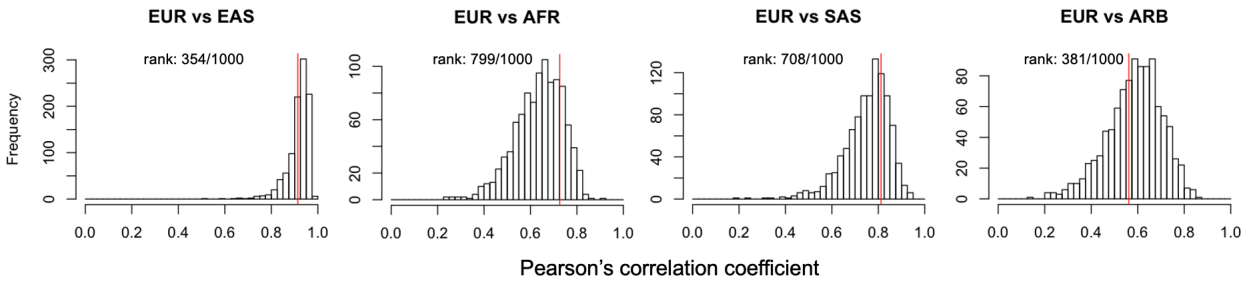

Supplementary Figure 7. The distribution of simulated inter-ancestral effect size correlation at the fine mapped loci.

In this simulation test, we assumed the effect sizes are identical between ancestries (i.e., the true correlation = 1), and evaluated the distribution of inter-ancestral effect size correlation at the 30 fine mapped loci (we used the same variants as in **Supplementary Figure 6**). We utilized observed effect sizes in EUR-GWAS as the true effect size. For each variant in each ancestry, we randomly sampled effect sizes 1,000 times from a normal distribution where the mean is the observed effect size in EUR-GWAS and the S.D. is the observed S.E in the respective ancestry-specific GWAS. The histogram indicates the distribution of the 1,000 simulated effect size correlation and the vertical red line indicates the observed correlation. We used Pearson's correlation. We also provided the rank of the observed correlation from the bottom.

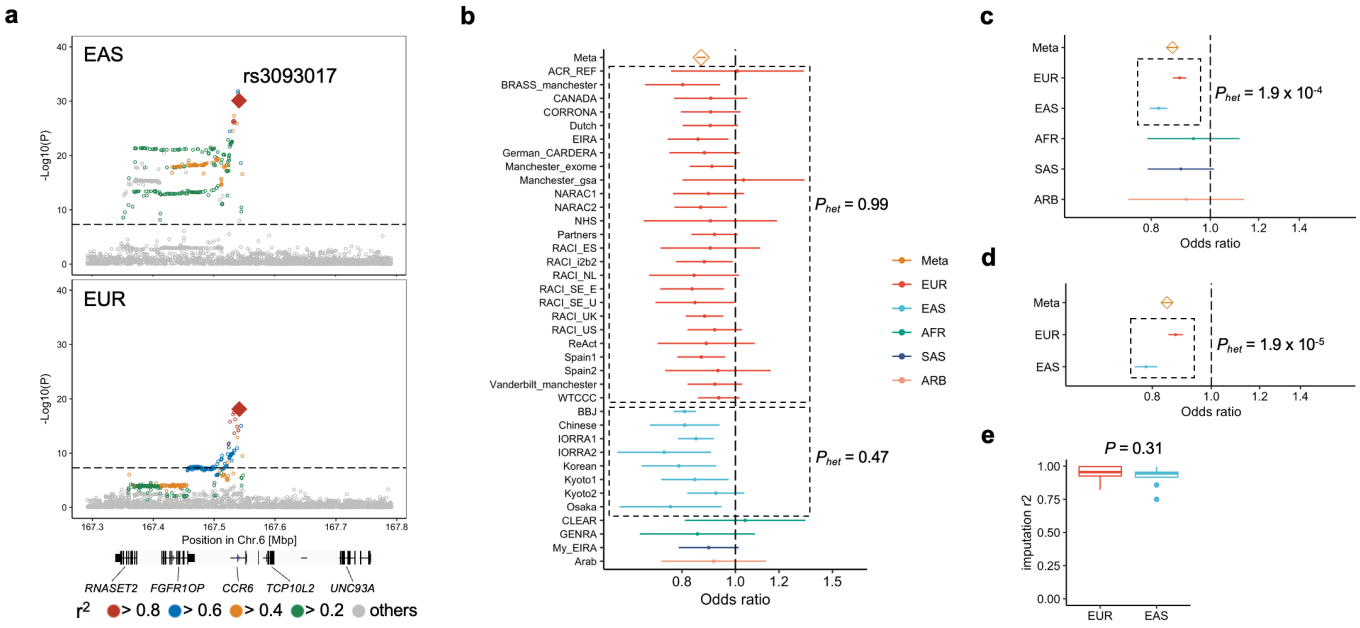

Supplementary Figure 8. Heterogeneous GWAS signals at the *CCR6* locus.
(a) GWAS *P* value plots at the *CCR6* locus. We used EAS- and EUR-GWAS results.
(b) Odds ratio and its 95% confidence interval of each cohort at the fine-mapped variant of the *CCR6* locus (rs3093017; *PIP* = 0.52). Effect size heterogeneity was analyzed by Cochran's Q test (P_{het}).
(c) Odds ratio and its 95% confidence interval of each ancestry at the fine-mapped variant of the *CCR6* locus (rs3093017; *PIP* = 0.52).
(d) same as (c) but cases were restricted to seropositive patients.
(e) Imputation quality (r^2) in EUR and EAS cohorts. The differences were assessed by two-sided Wilcoxon test (n=25 in EUR and 8 in EAS). Within each boxplot, the horizontal lines reflect the median, the top and bottom of each box reflect the interquartile range (IQR), and the whiskers reflect the maximum and minimum values within each grouping no further than 1.5 x IQR from the hinge.

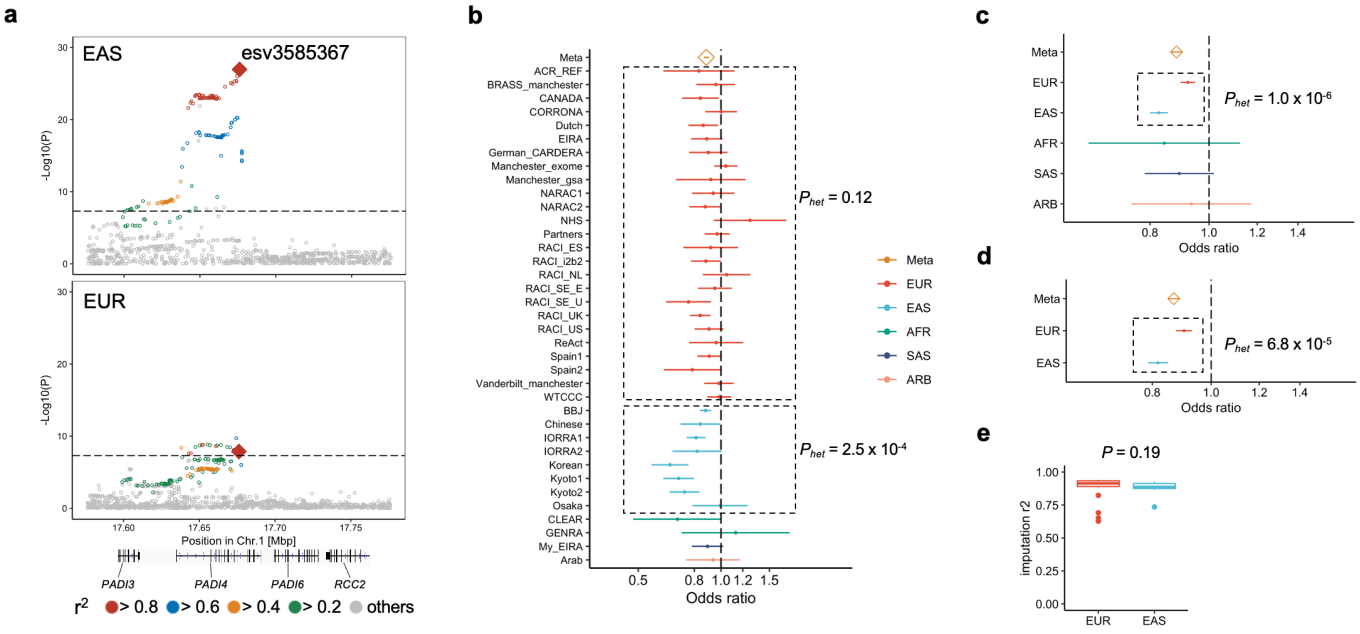

Supplementary Figure 9. Heterogeneous GWAS signals at the *PADI4* locus.
(a) GWAS *P* value plots at the *PADI4* locus. We used EAS- and EUR-GWAS results.
(b) Odds ratio and its 95% confidence interval of each cohort at the fine-mapped variant of the *PADI4* locus (esv3585367; *PIP* = 0.62). Effect size heterogeneity was analyzed by Cochran's Q test (P_{het}).
(c) Odds ratio and its 95% confidence interval of each ancestry at the fine-mapped variant of the *PADI4* locus (esv3585367; *PIP* = 0.62).
(d) same as **(c)** but cases were restricted to seropositive patients.
(e) Imputation quality (r^2) in EUR and EAS cohorts. The differences were assessed by two-sided Wilcoxon test (n=25 in EUR and 8 in EAS). Within each boxplot, the horizontal lines reflect the median, the top and bottom of each box reflect the interquartile range (IQR), and the whiskers reflect the maximum and minimum values within each grouping no further than 1.5 x IQR from the hinge.

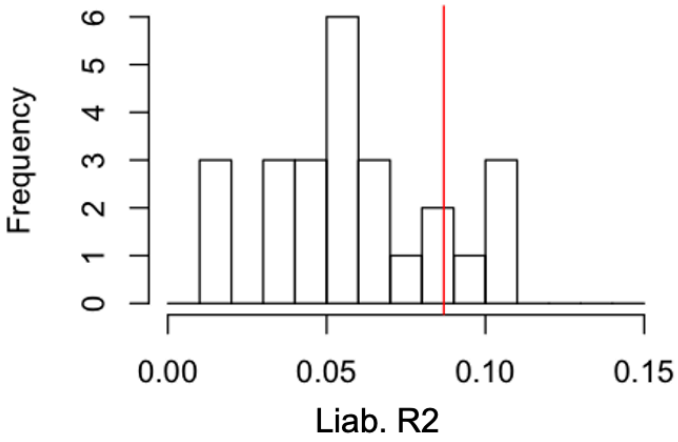

Supplementary Figure 10. The performance of our PRS model in UKBB.
The liability scale R^2 in all EUR cohorts (the histogram) and that in UKBB samples (the red vertical line). For EUR cohorts in our study, we used the multi-ancestry PRS with the LOCO approach. For UKBB analysis, we used the multi-ancestry PRS model without the LOCO approach since UKBB was not included in our GWAS.

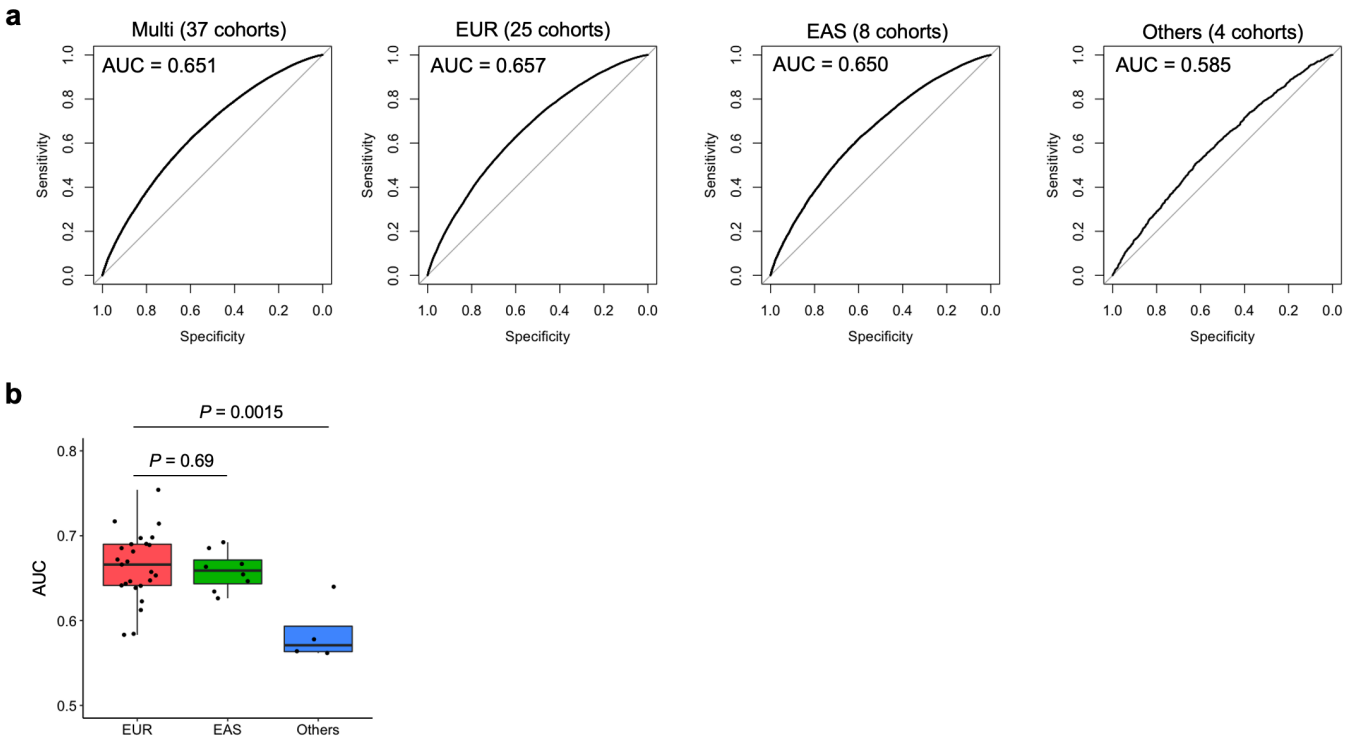

Supplementary Figure 11. AUC and ROC in the PRS analysis.
(a) We calculated AUC using all samples from all ancestries ("Multi") and all samples in each ancestry. We used multi-ancestry PRS with the LOCO approach. Due to small sample sizes in the non-EUR/EAS cohorts, we grouped them into one category ("Others" in panel a and b).
(b) We calculated AUC in each cohort. The differences between ancestries (n=25, 8, and 4, respectively from the left) were evaluated by two-sided Wilcoxon test. We used multi-ancestry PRS with the LOCO approach. Within each boxplot, the horizontal lines reflect the median, the top and bottom of each box reflect the interquartile range (IQR), and the whiskers reflect the maximum and minimum values within each grouping no further than 1.5 x IQR from the hinge.

Supplementary Data

Regional association plots of the associated loci

We provided the LocusZoom plots for all associated loci in this study (124 loci in total). We used *P* values in the GWAS setting with the lowest *P* values (see **Supplementary Table 4** for details). LD information was calculated using combined samples of EAS and EUR in 1KG Phase 3 to reflect haplotypes in both ancestries.
⌖ indicates non-synonymous exonic variants.

<Locus 1>
1:2483961:G:A (rs2258734)
Multi-GWAS (combined)
Known locus

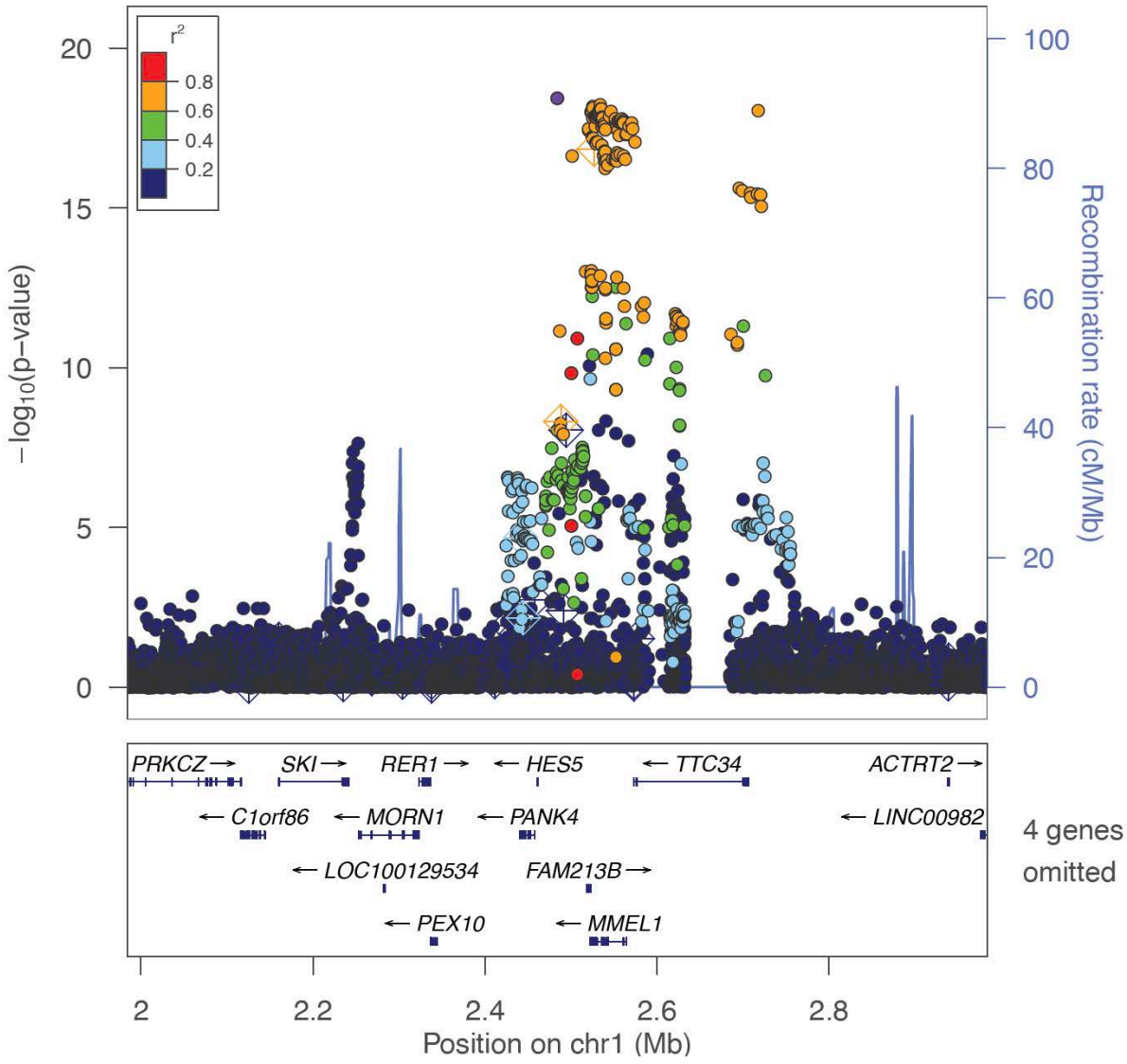

<Locus 2>
1:17676165:A:<CN0> (esv3585367)
Multi-GWAS (combined)
Known locus

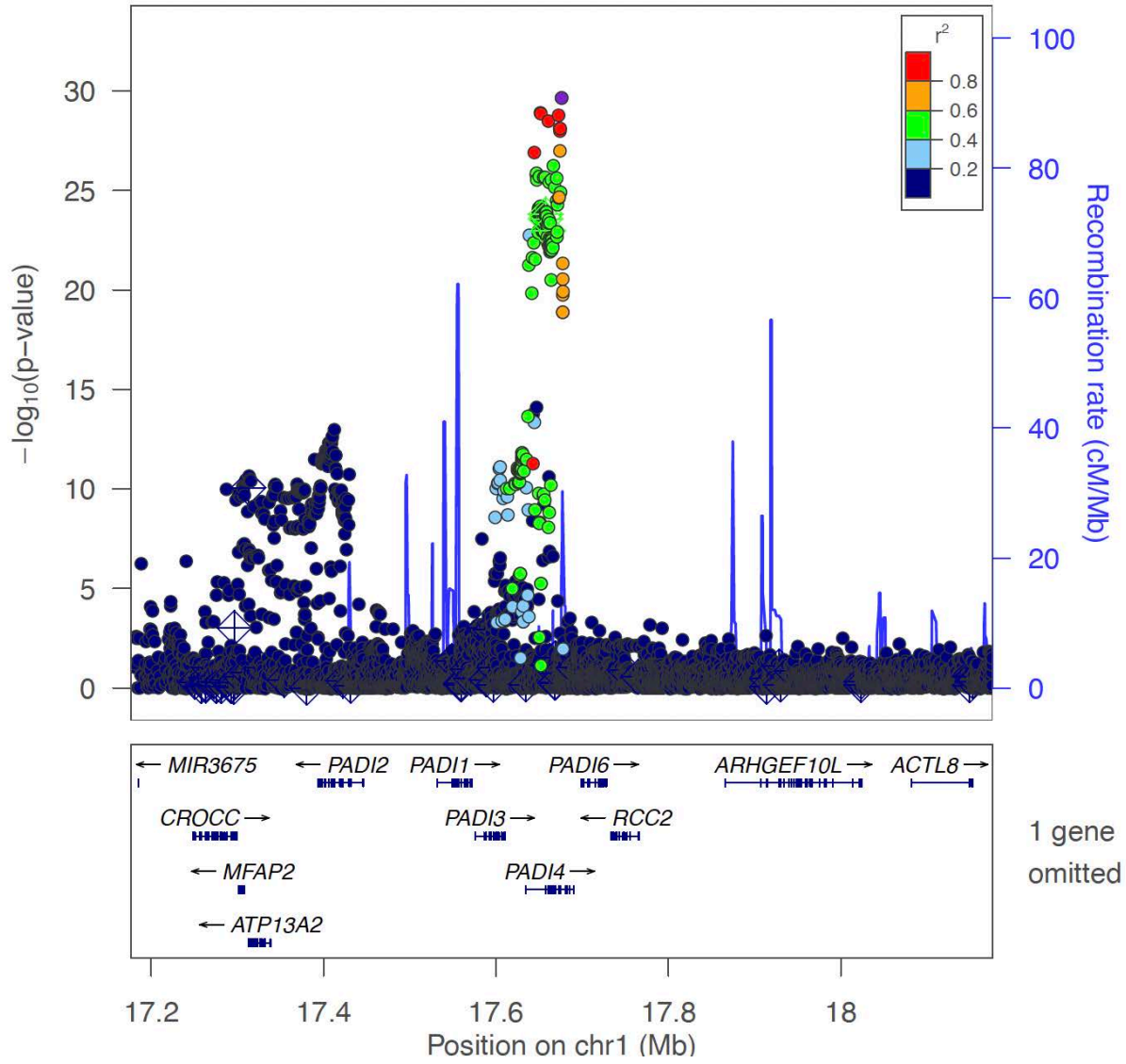

<Locus 3>
1:38622268:T:C (rs7540342)
Multi-GWAS (combined)
Known locus

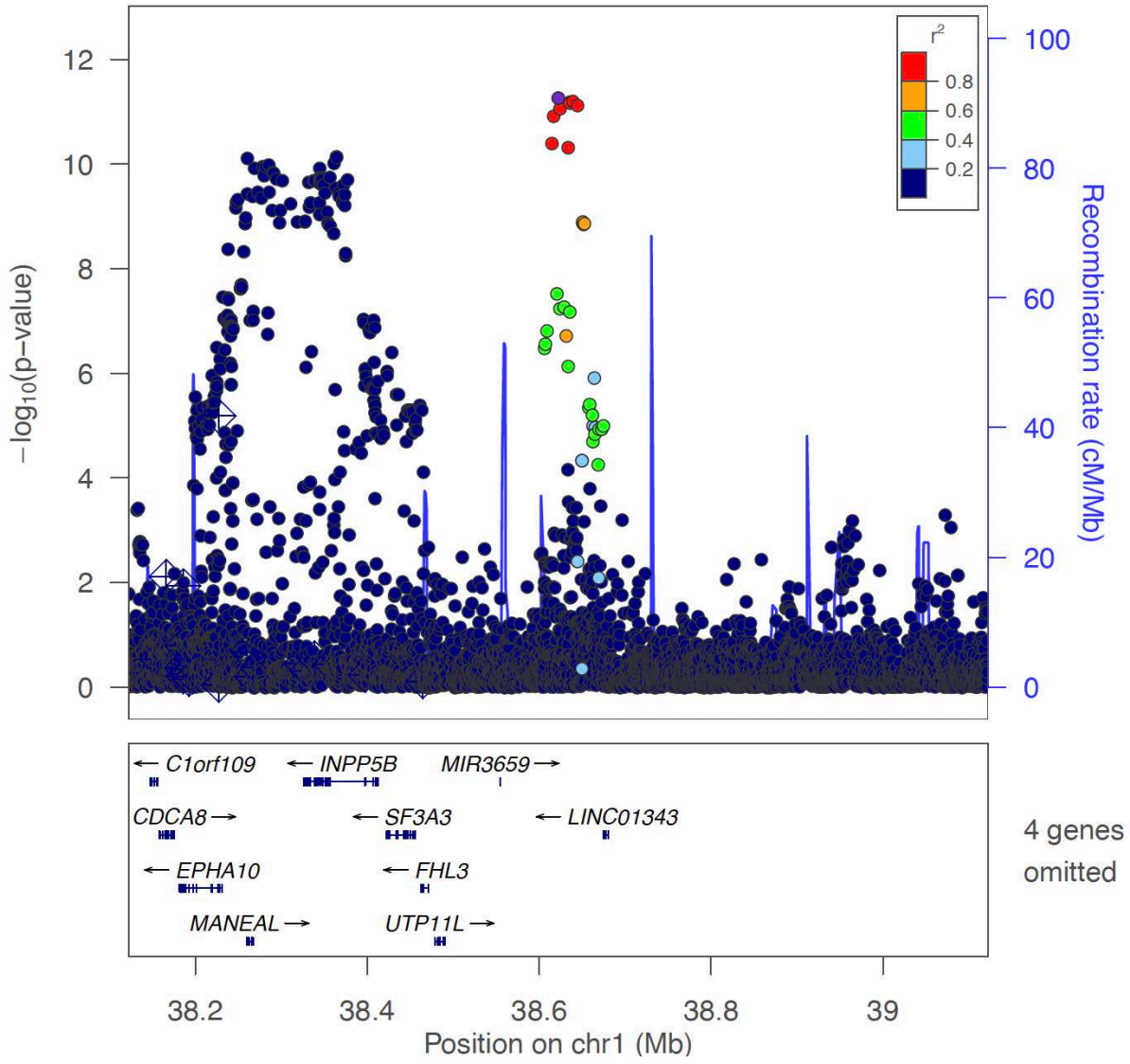

<Locus 4>
1:42166782:G:A (rs41269479)
EAS-GWAS (seroposi)
Novel locus

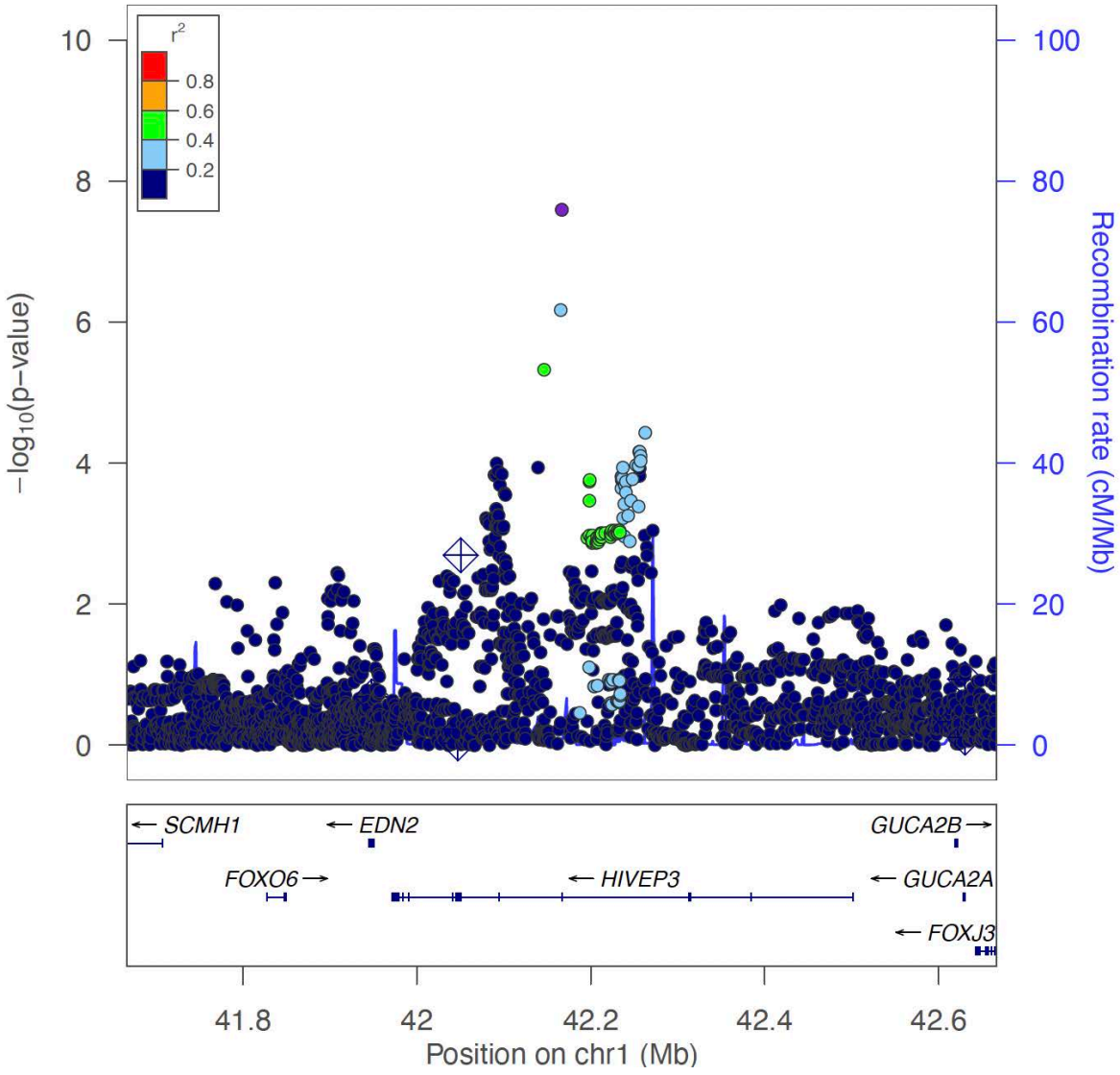

<Locus 5>
1:67798327:T:G (rs4655698)
Multi-GWAS (combined)
Known locus

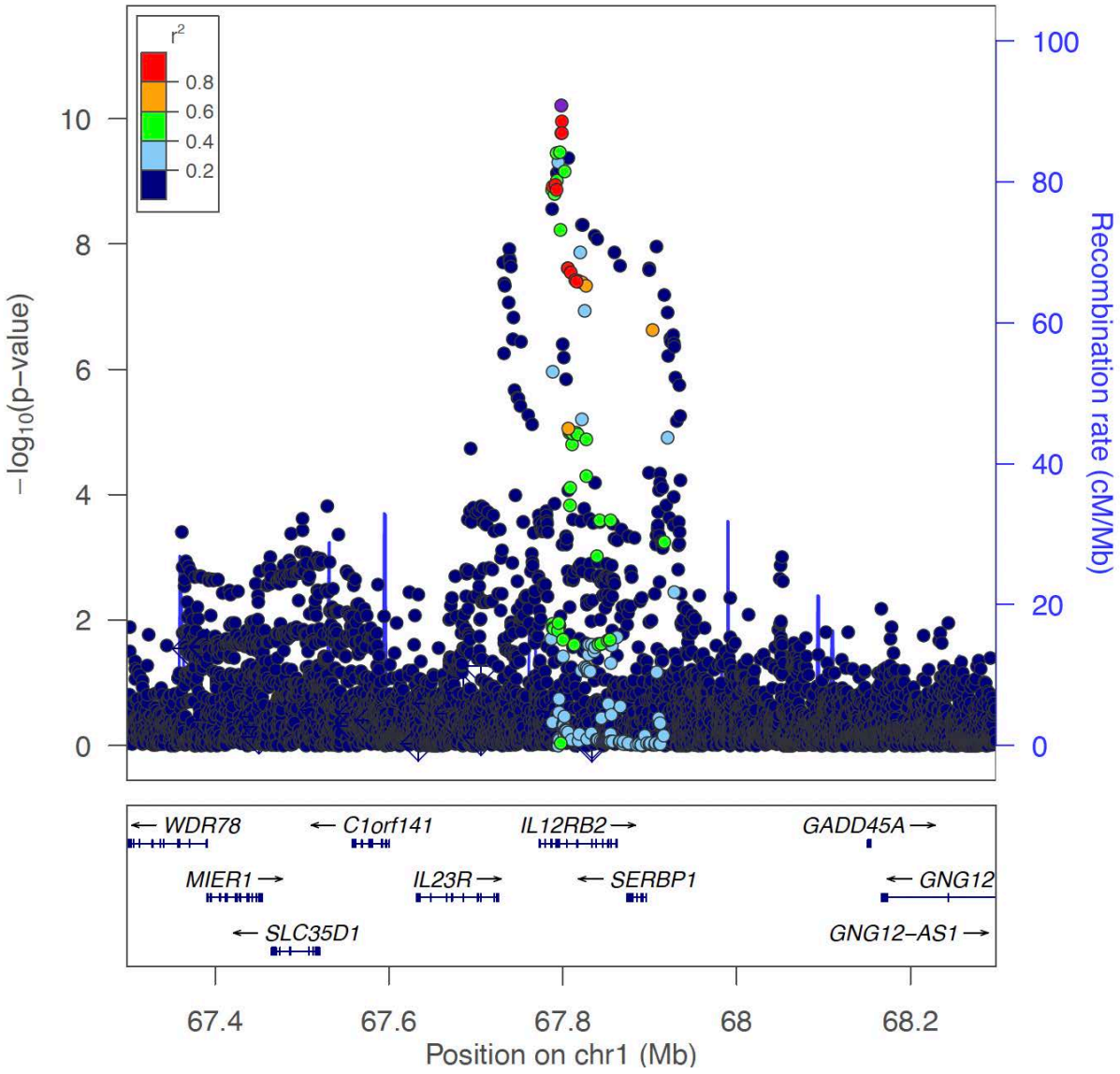

<Locus 6>
1:92940411:C:T (rs41313373)
Multi-GWAS (seroposi)
Novel locus

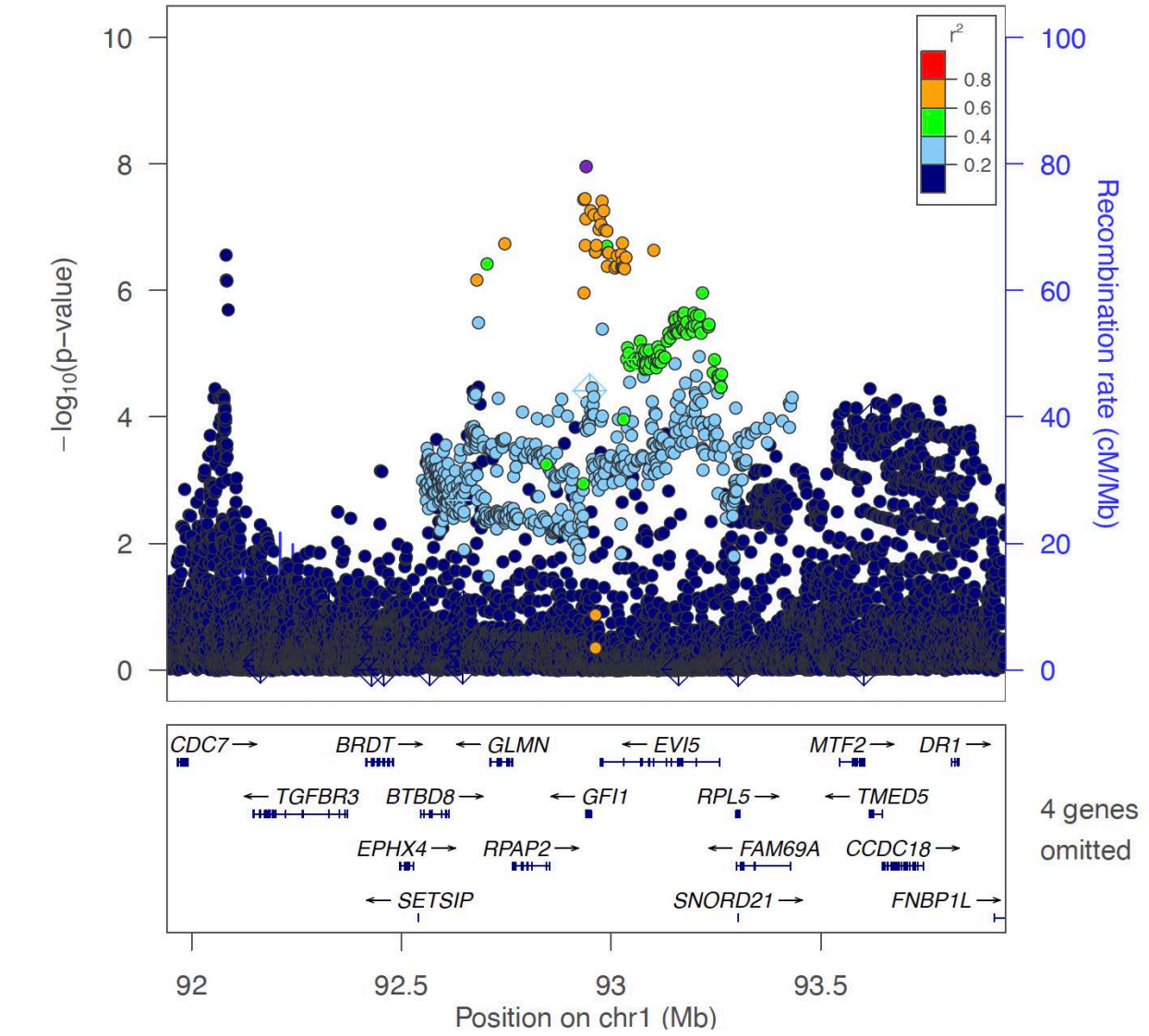

<Locus 7>
1:114377568:A:G (rs2476601)
Multi-GWAS (combined)
Known locus

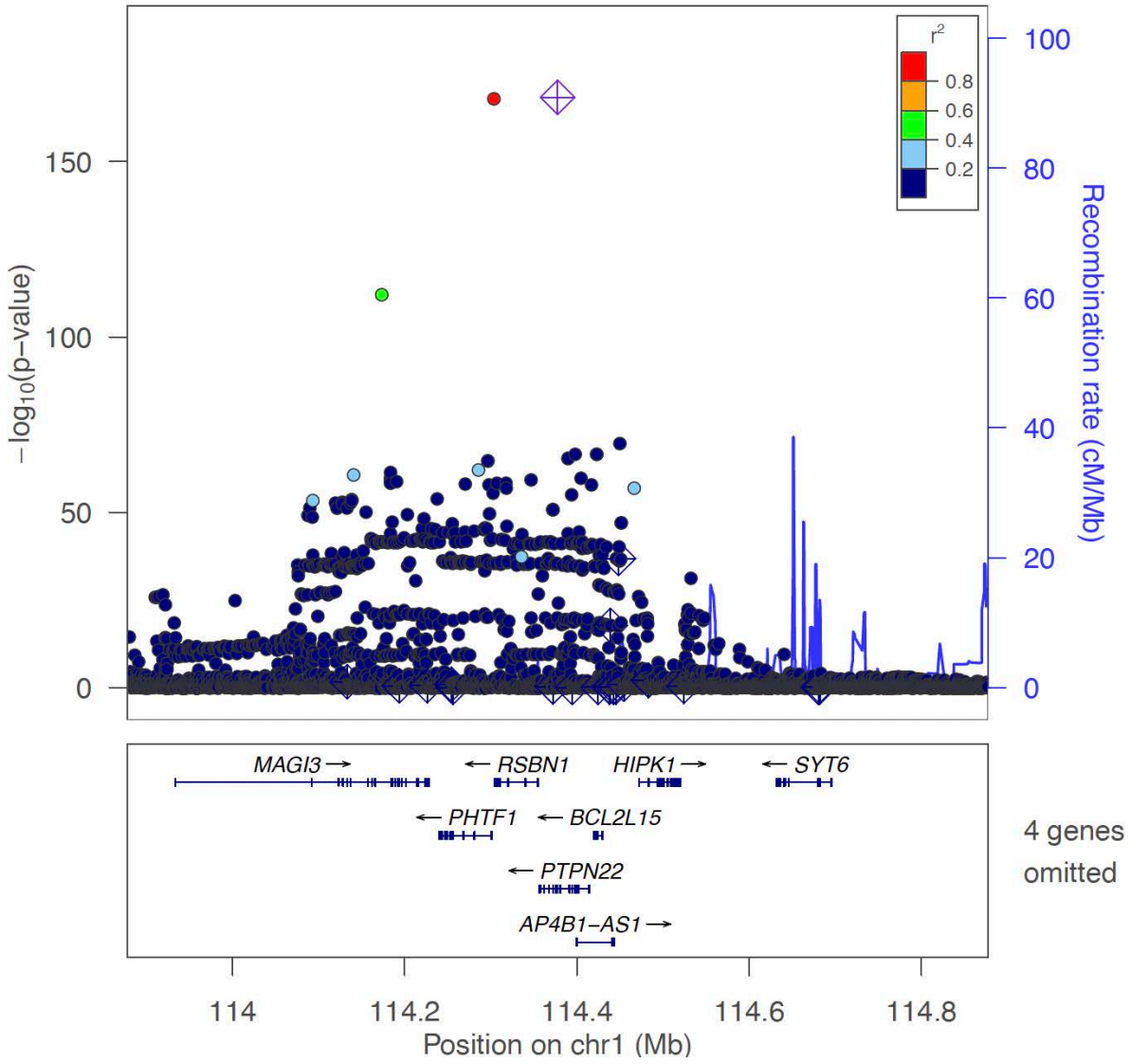

<Locus 8>
1:117280696:C:T (rs798000)
Multi-GWAS (combined)
Known locus

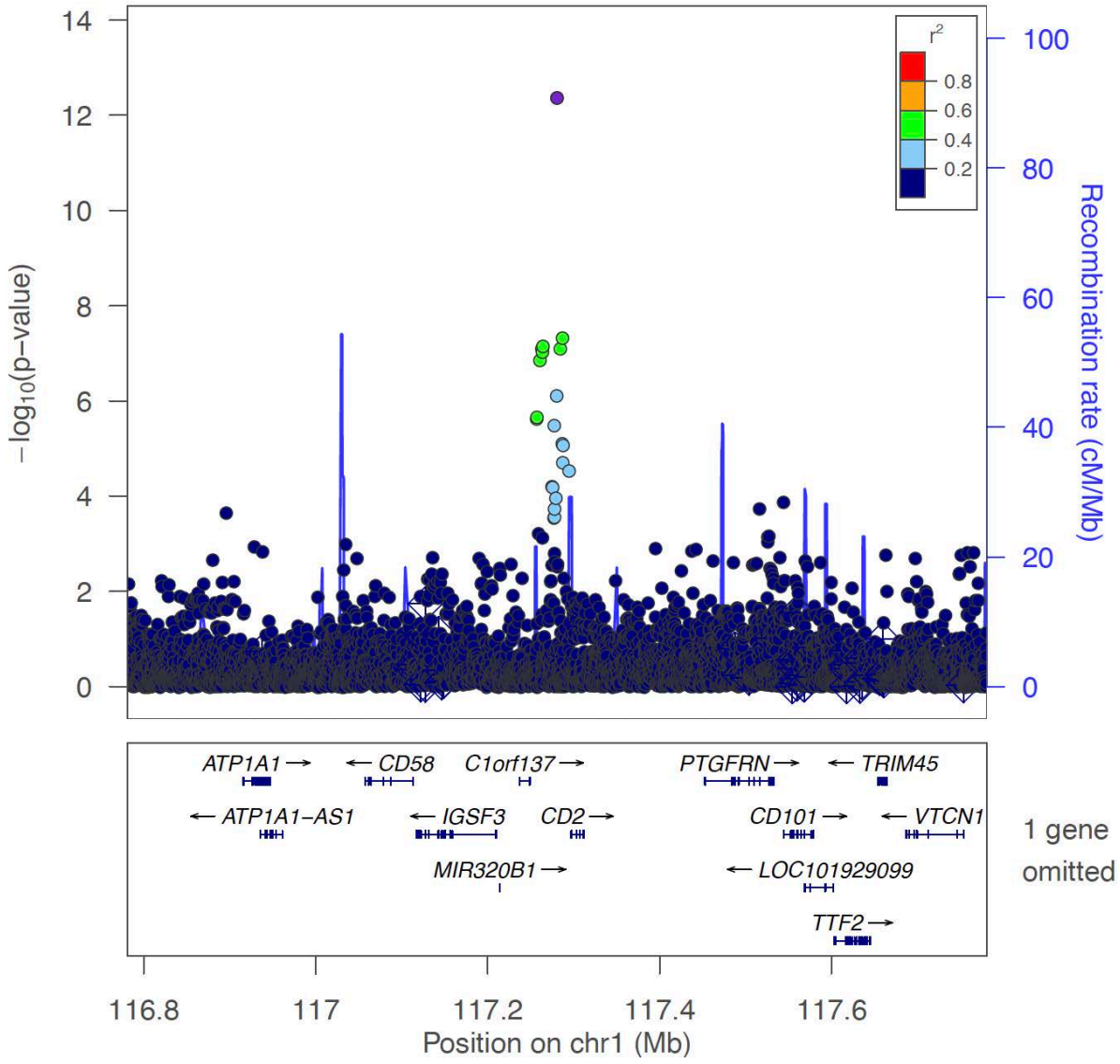

<Locus 9>
1:154425456:G:A (rs12126142)
Multi-GWAS (combined)
Known locus

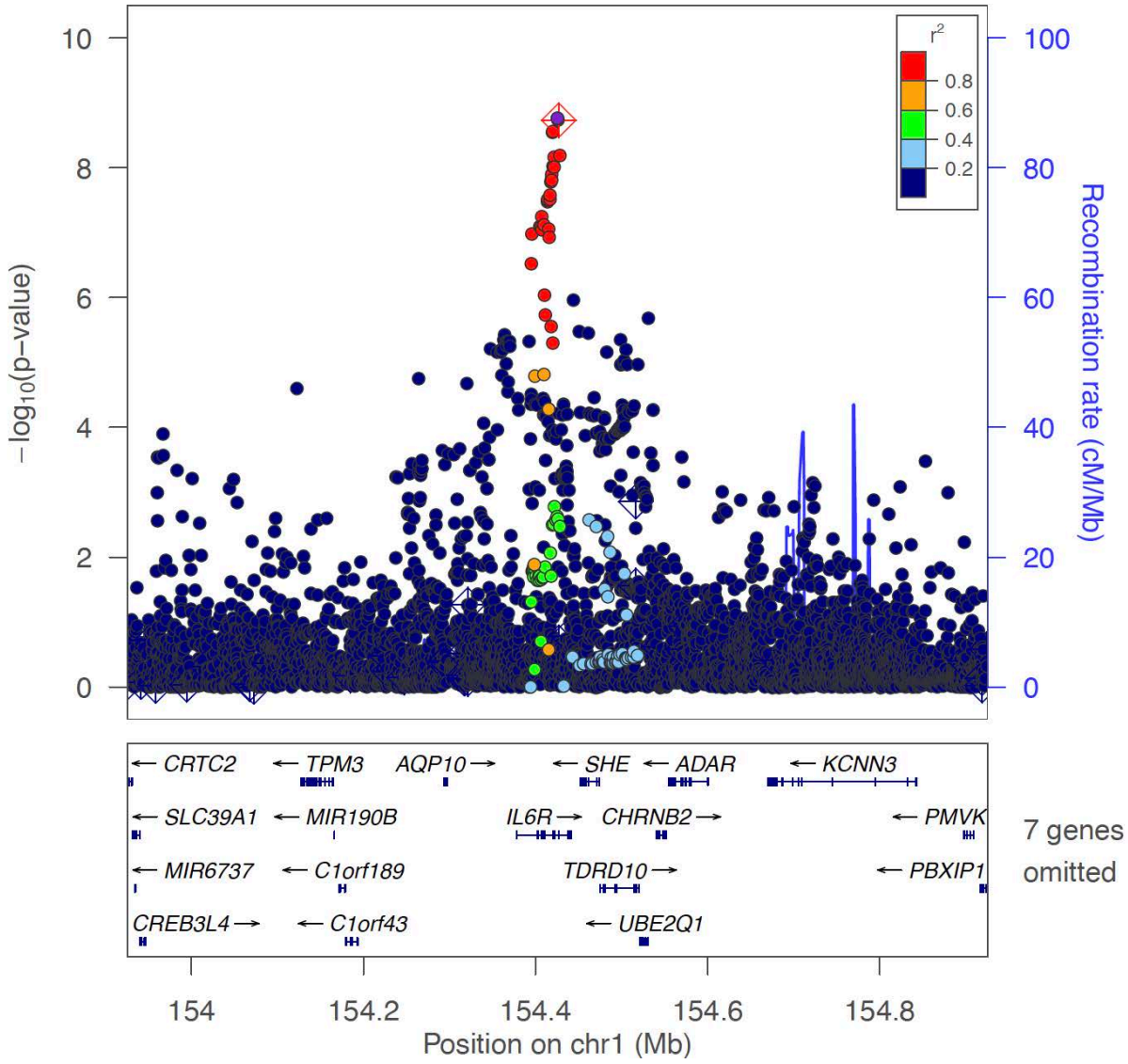

<Locus 10>
1:157686337:G:T (rs2317231)
Multi-GWAS (combined)
Known locus

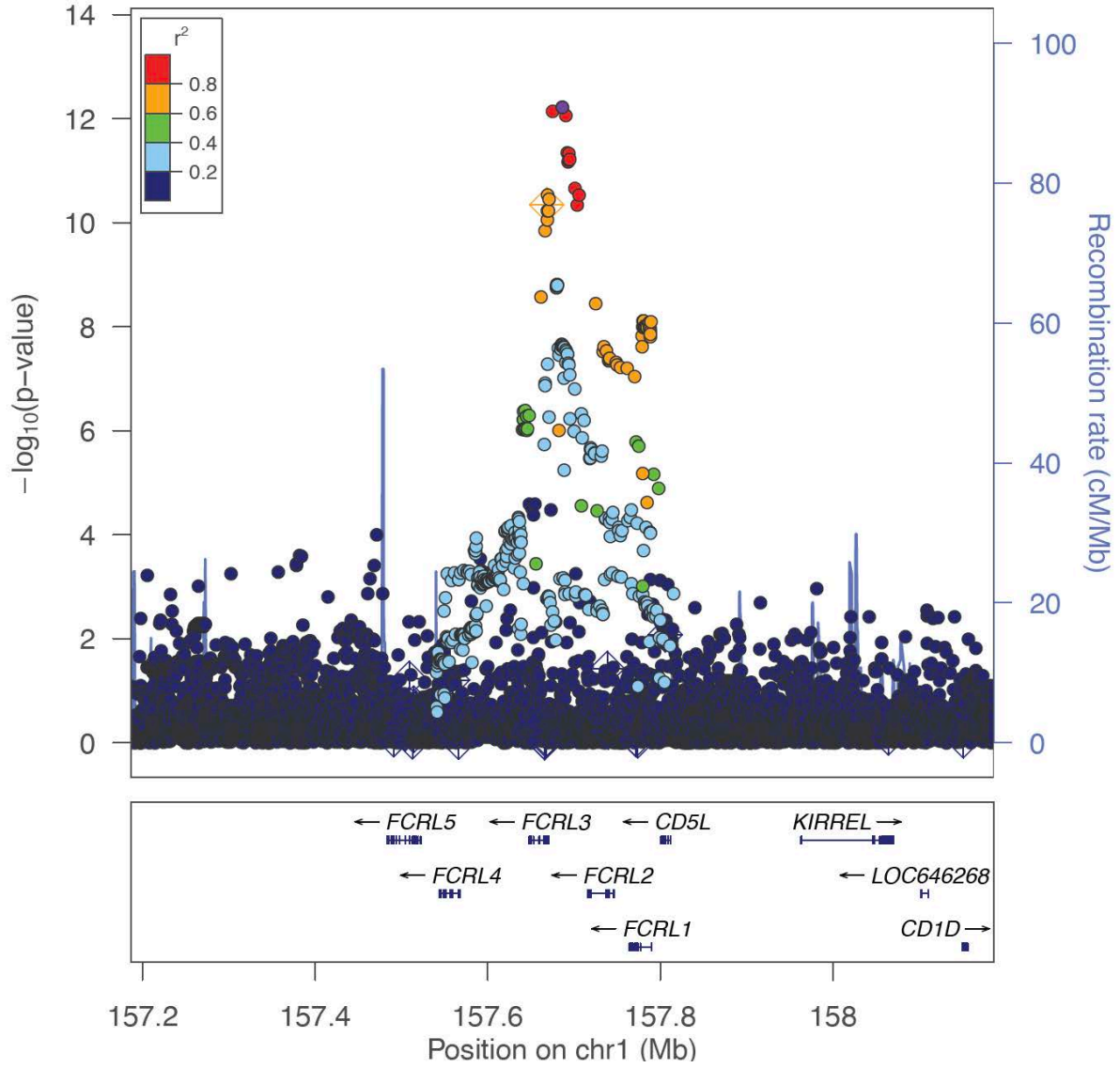

<Locus 11>
1:161519411:C:A (rs10917571)
Multi-GWAS (combined)
Known locus

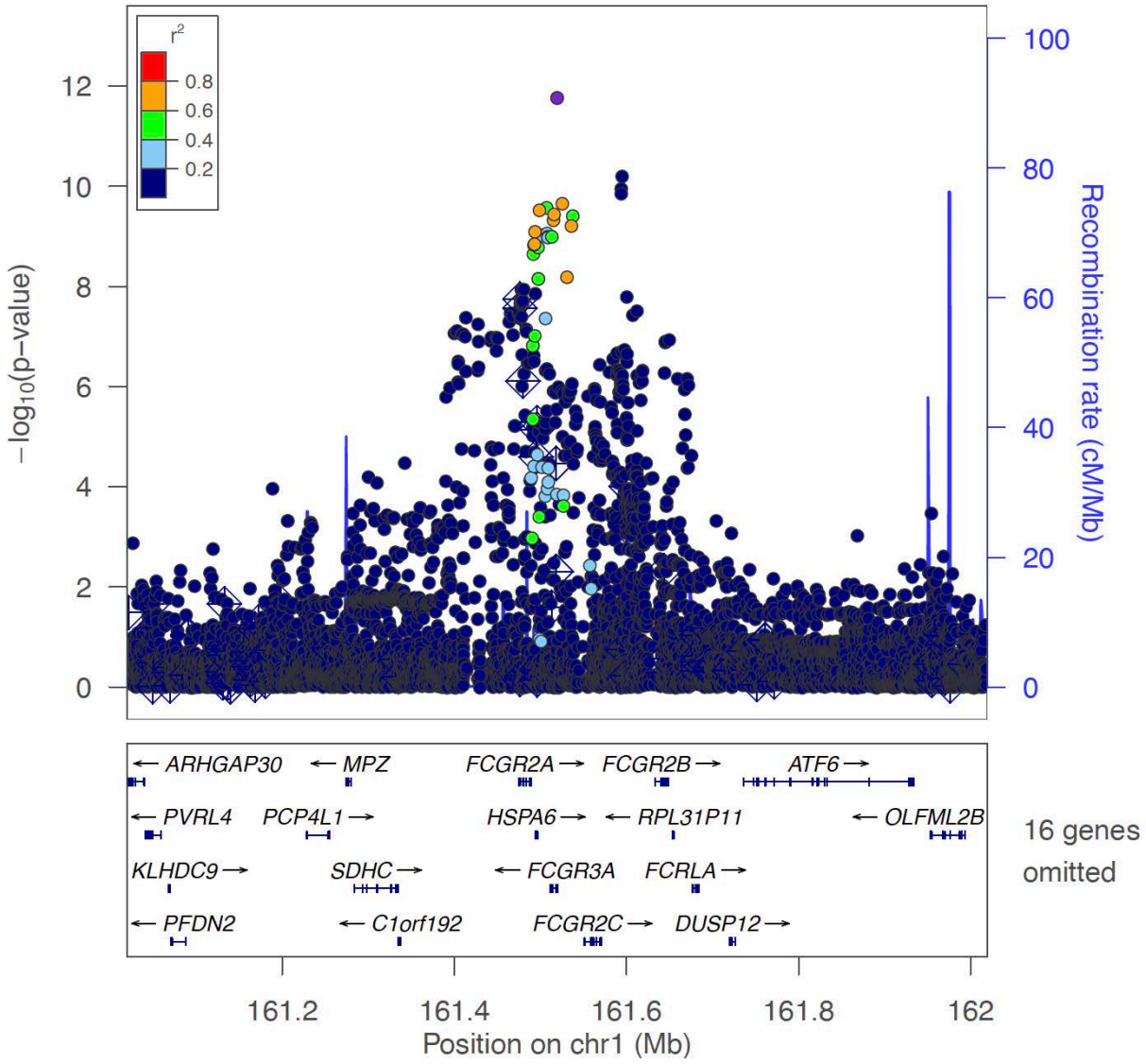

<Locus 12>
1:173306646:G:A (rs6681482)
Multi-GWAS (combined)
Known locus

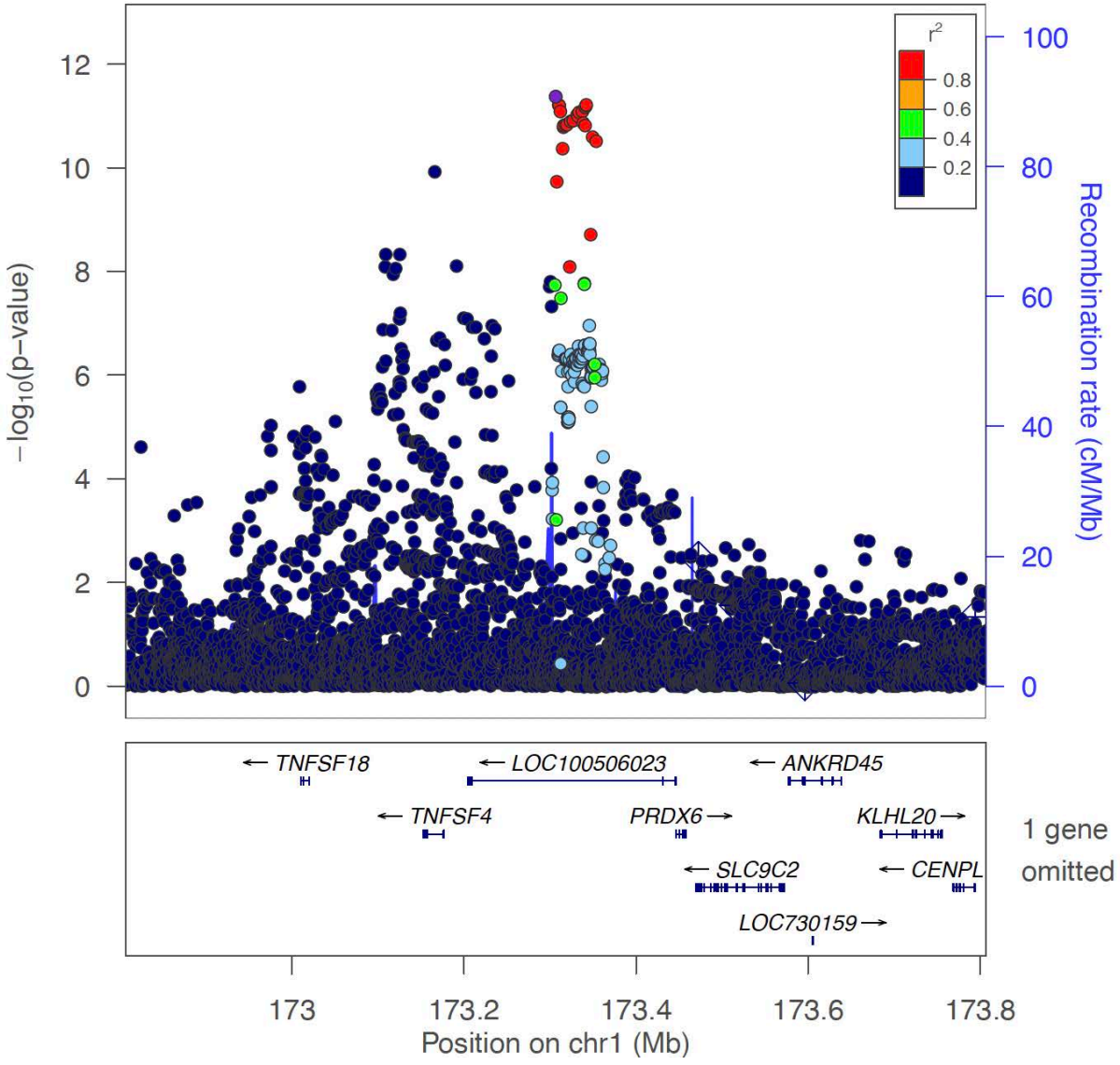

<Locus 13>
1:186604505:T:C (rs12145329)
Multi-GWAS (seroposi)
Known locus

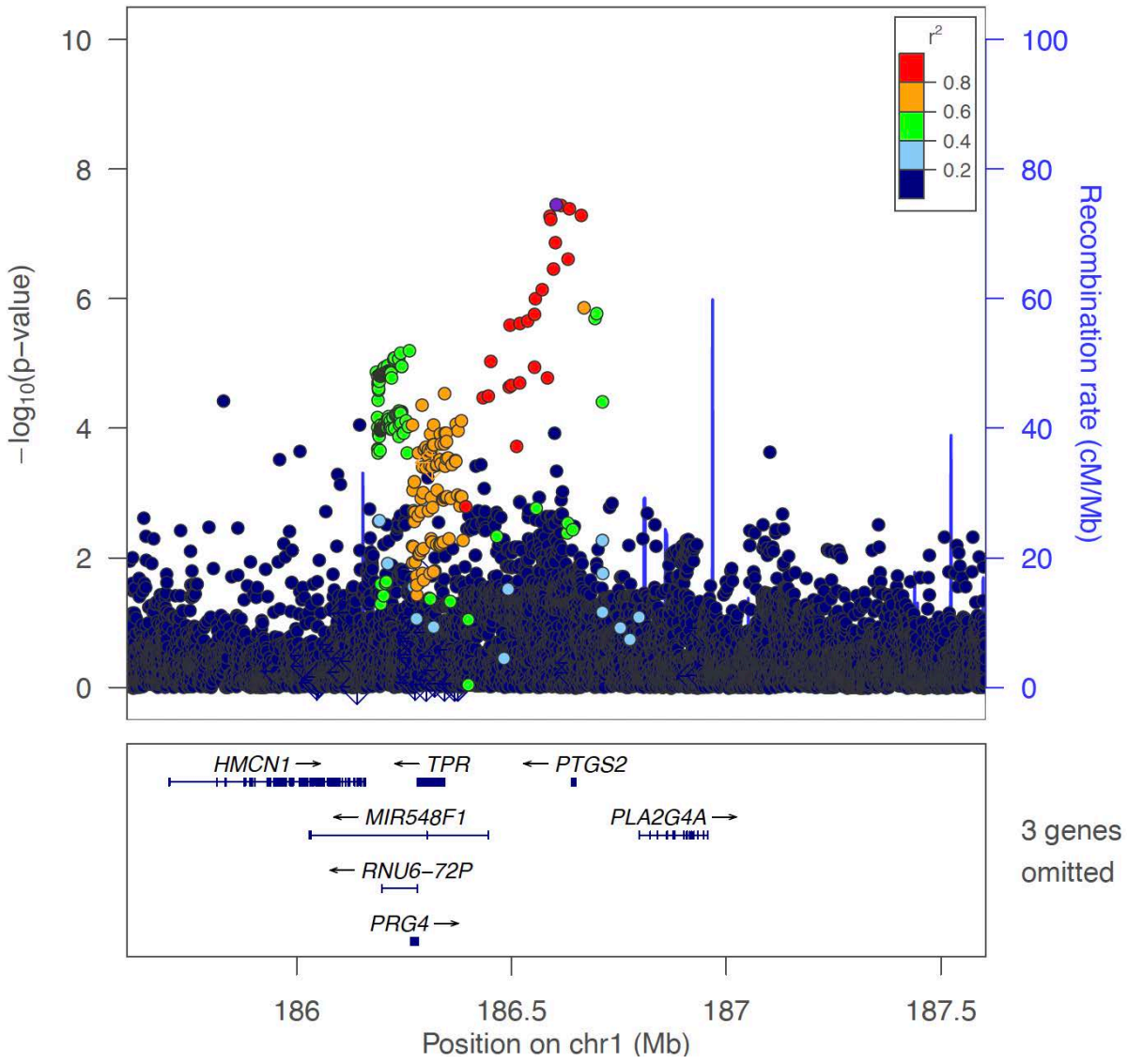

<Locus 14>
1:198584022:A:G (rs28398409)
Multi-GWAS (combined)
Known locus

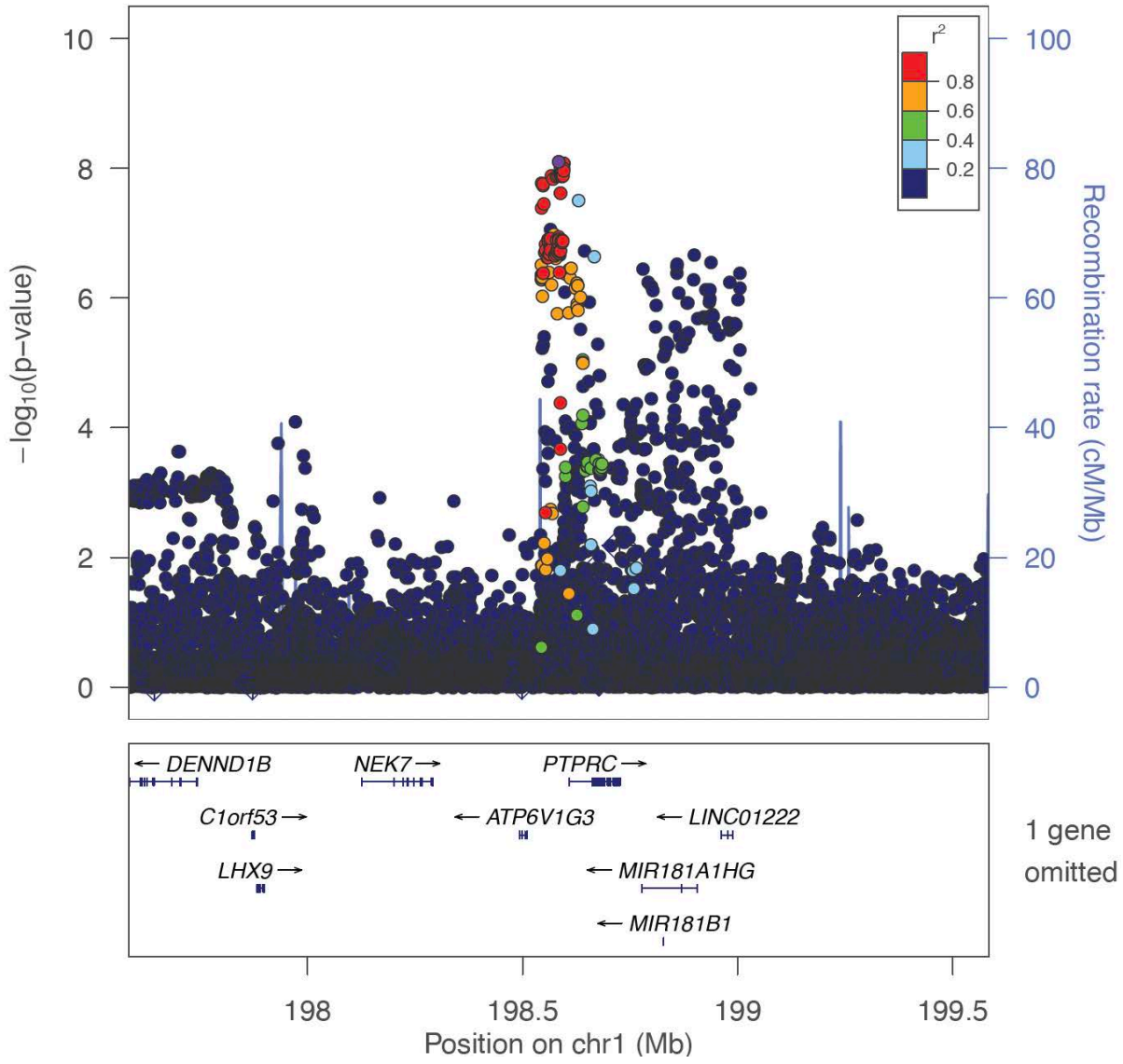

<Locus 15>
1:235800357:CAA:C (rs1188620266)
Multi-GWAS (combined)
Novel locus

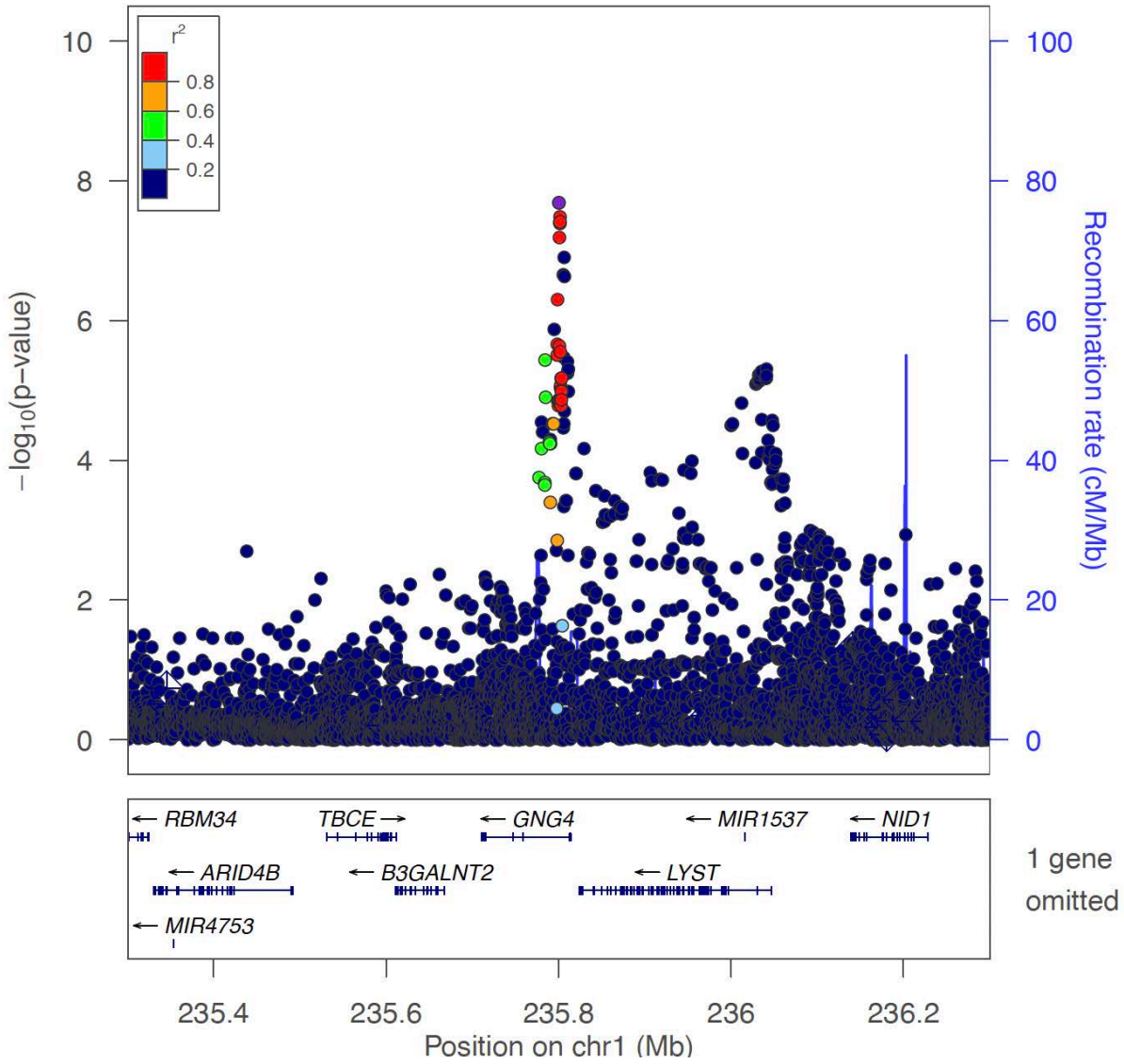

<Locus 16>
2:30449594:G:A (rs10175798)
Multi-GWAS (combined)
Known locus

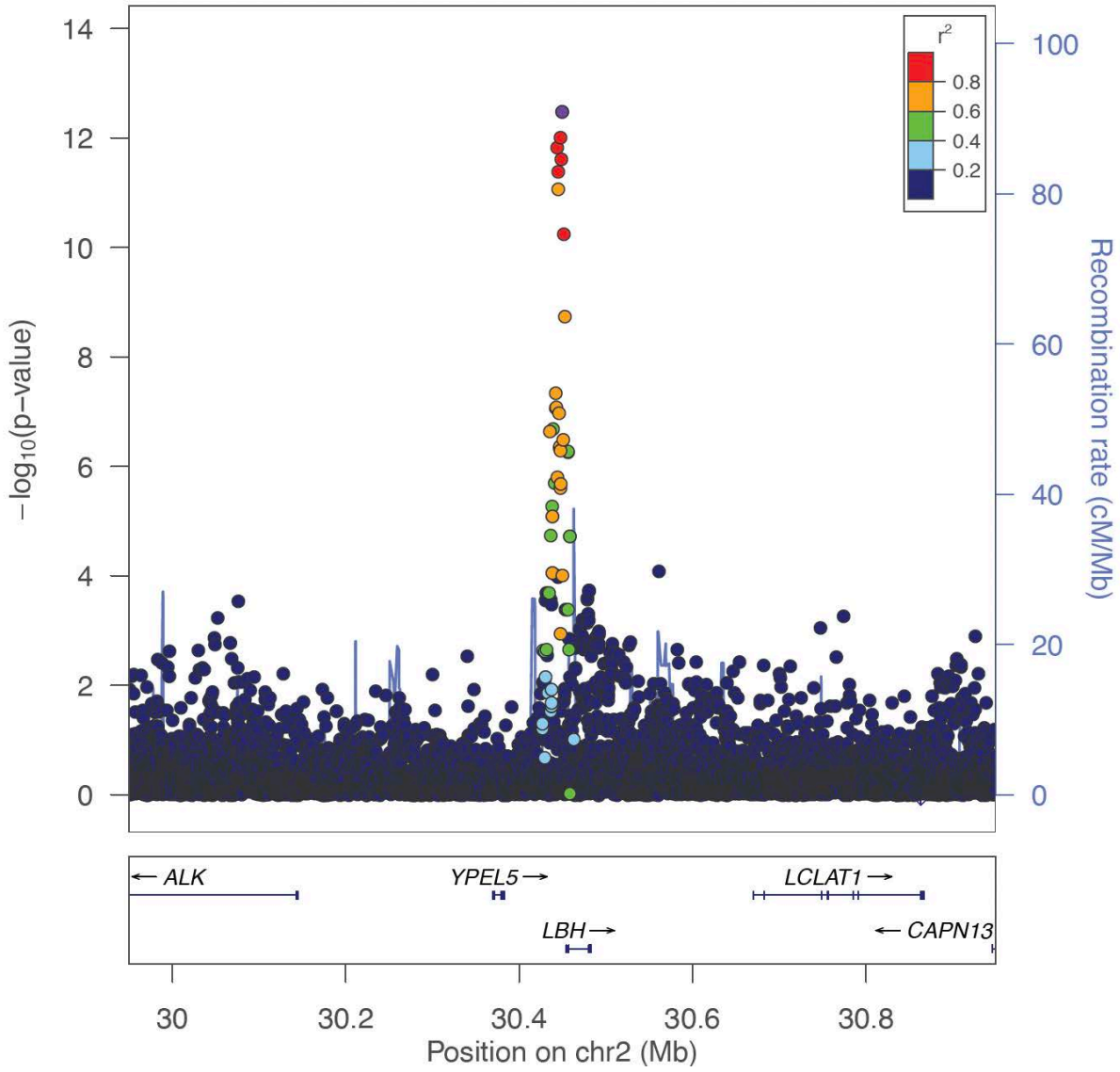

<Locus 17>
2:61097583:A:G (rs55963299)
Multi-GWAS (combined)
Known locus

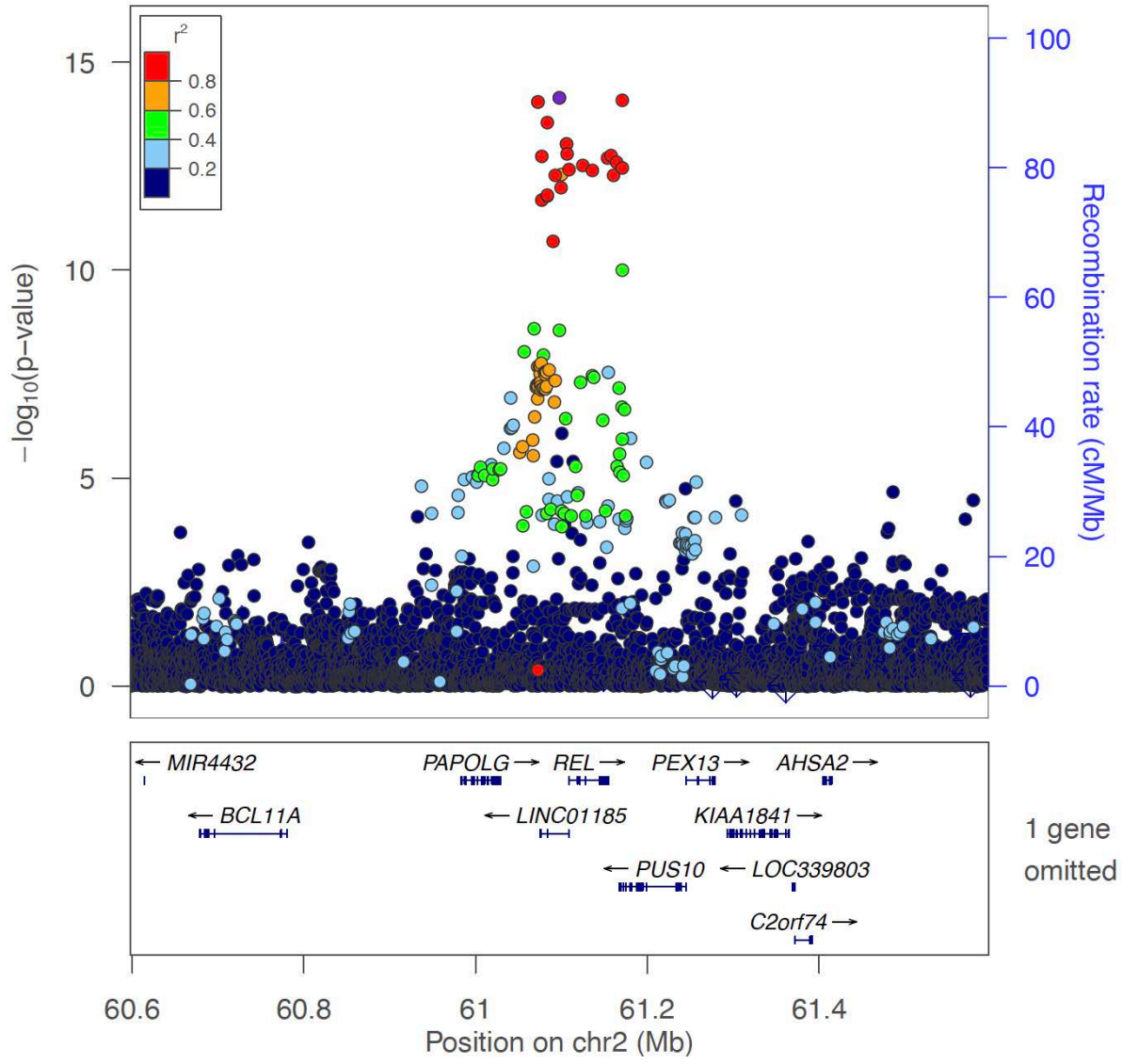

<Locus 18>
2:65598906:G:GA (rs74313386)
Multi-GWAS (combined)
Known locus

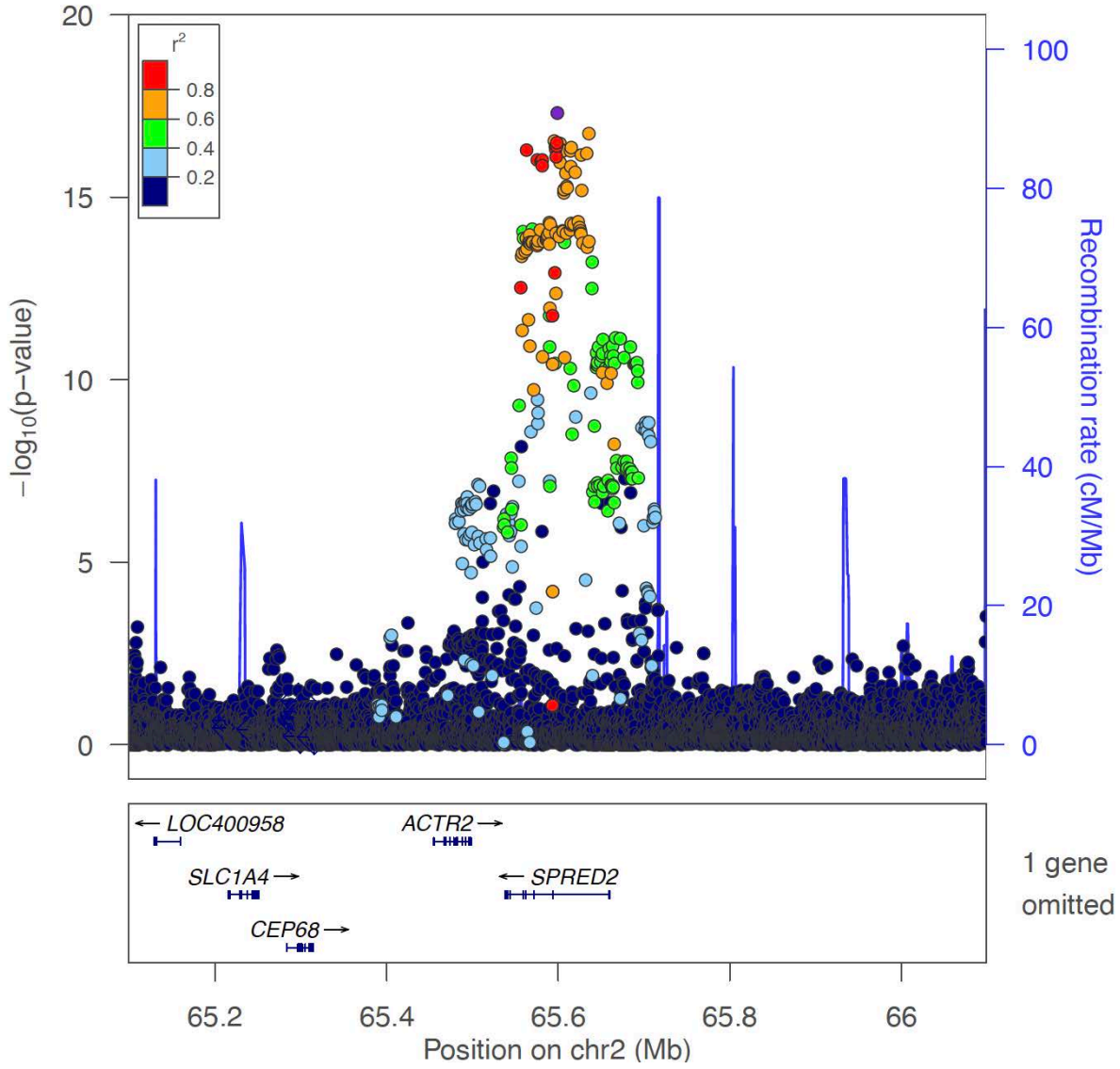

<Locus 19>
2:70209168:TATCCATCC:T (rs143259280)
Multi-GWAS (seroposi)
Novel locus

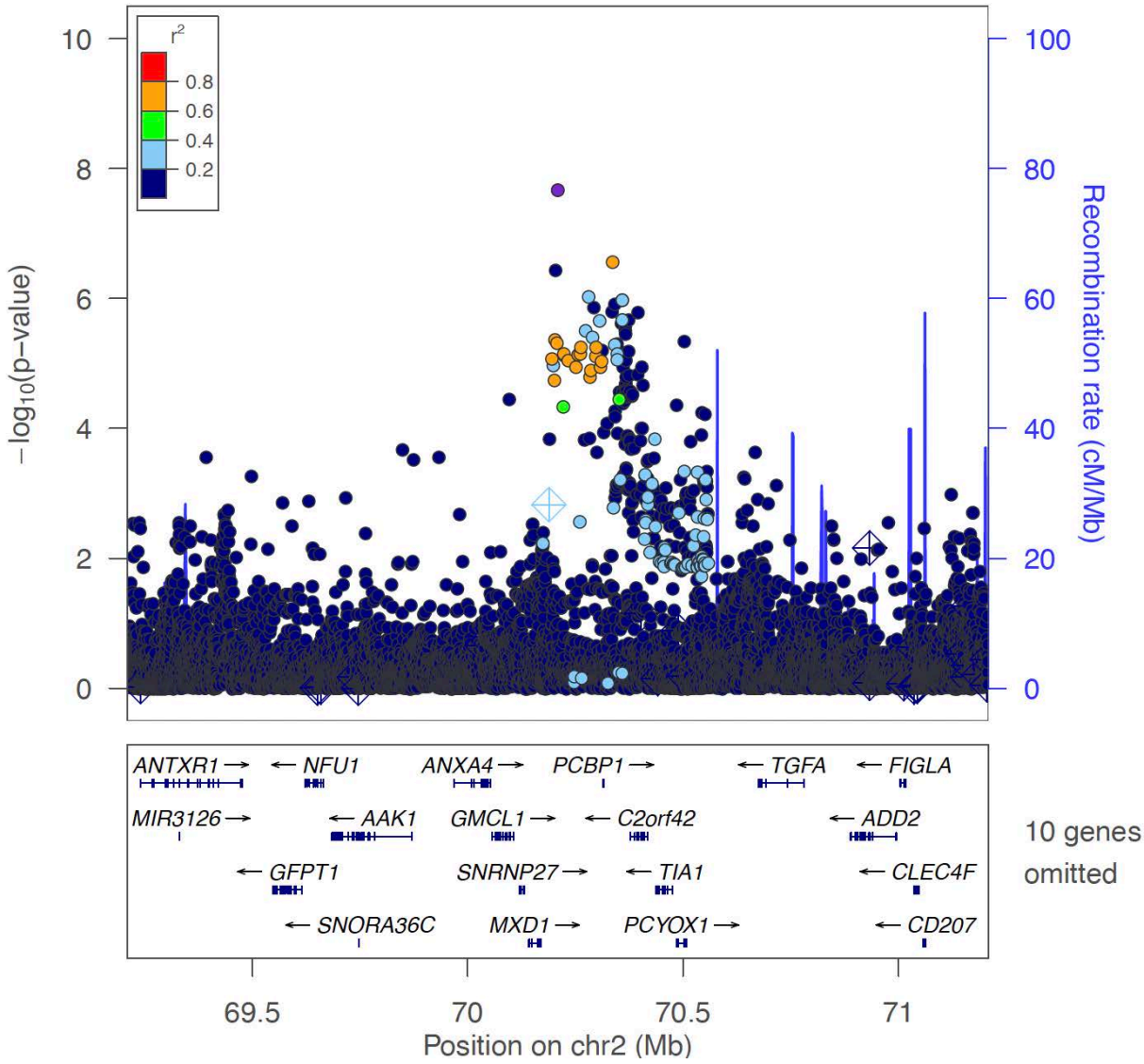

<Locus 20>
2:74219615:T:A (rs28421442)
Multi-GWAS (combined)
Known locus

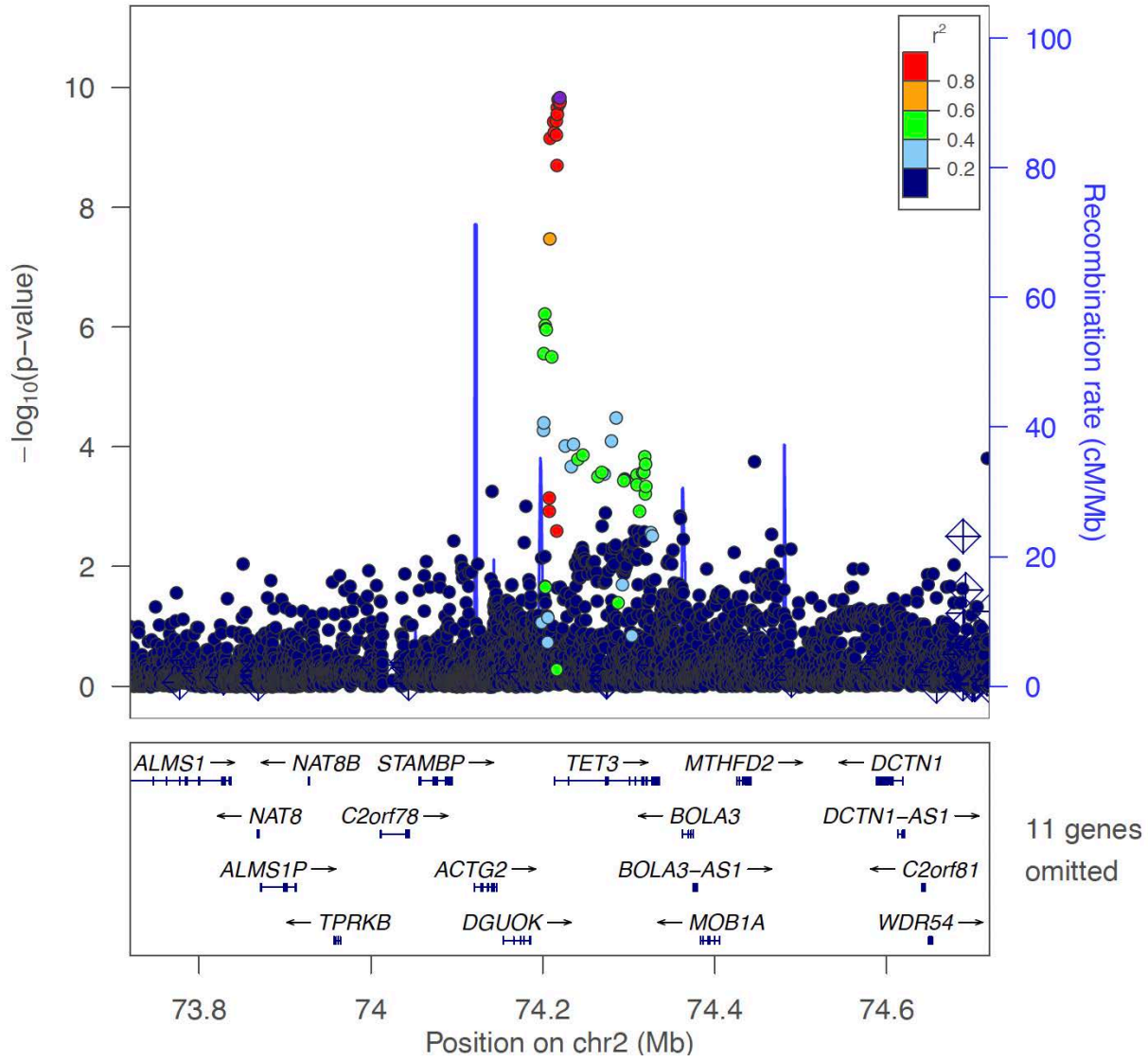

<Locus 21>
2:100761105:C:G (rs12712065)
Multi-GWAS (combined)
Known locus

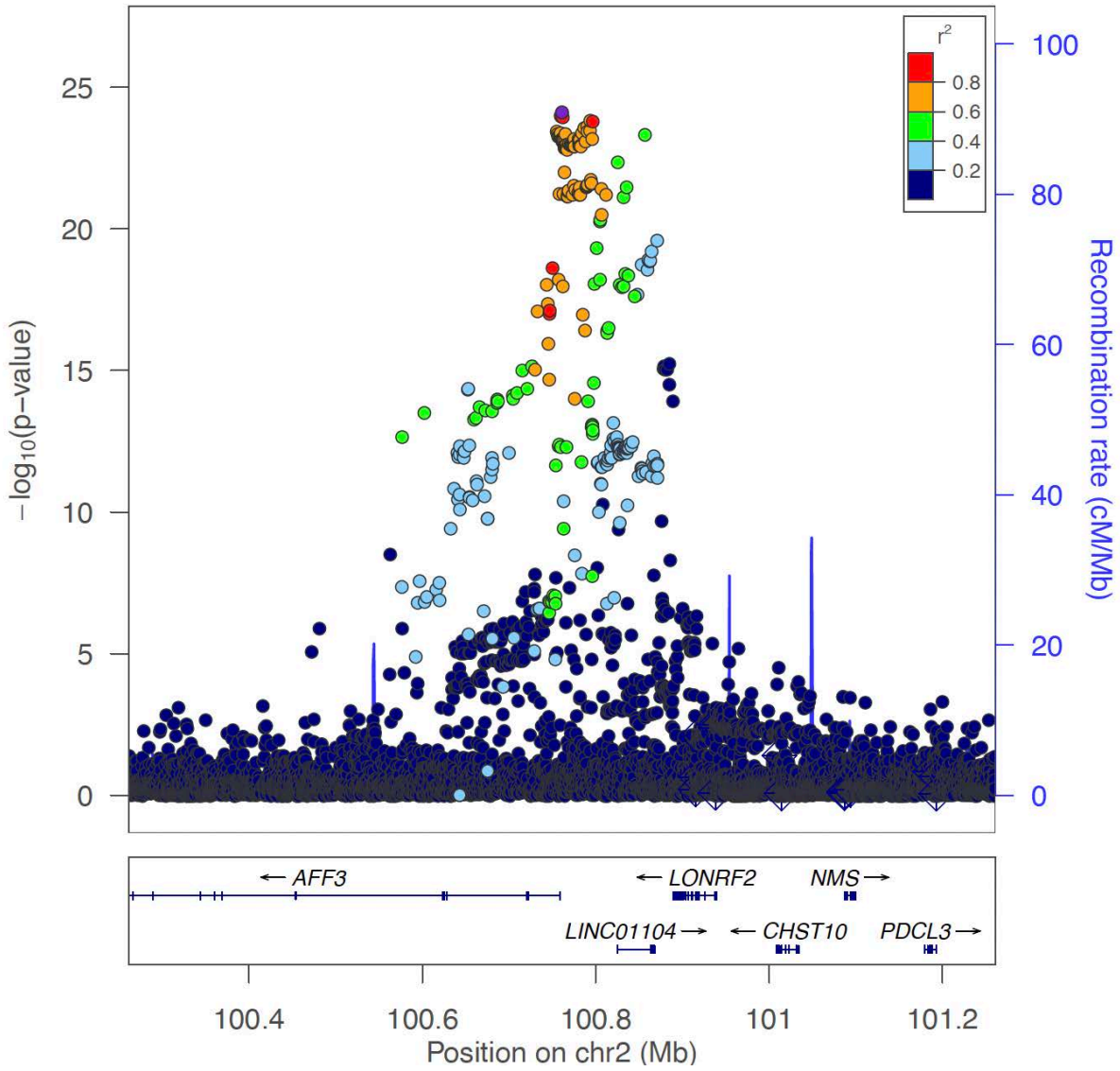

<Locus 22>
2:111605238:A:C (rs13396472)
Multi-GWAS (combined)
Known locus

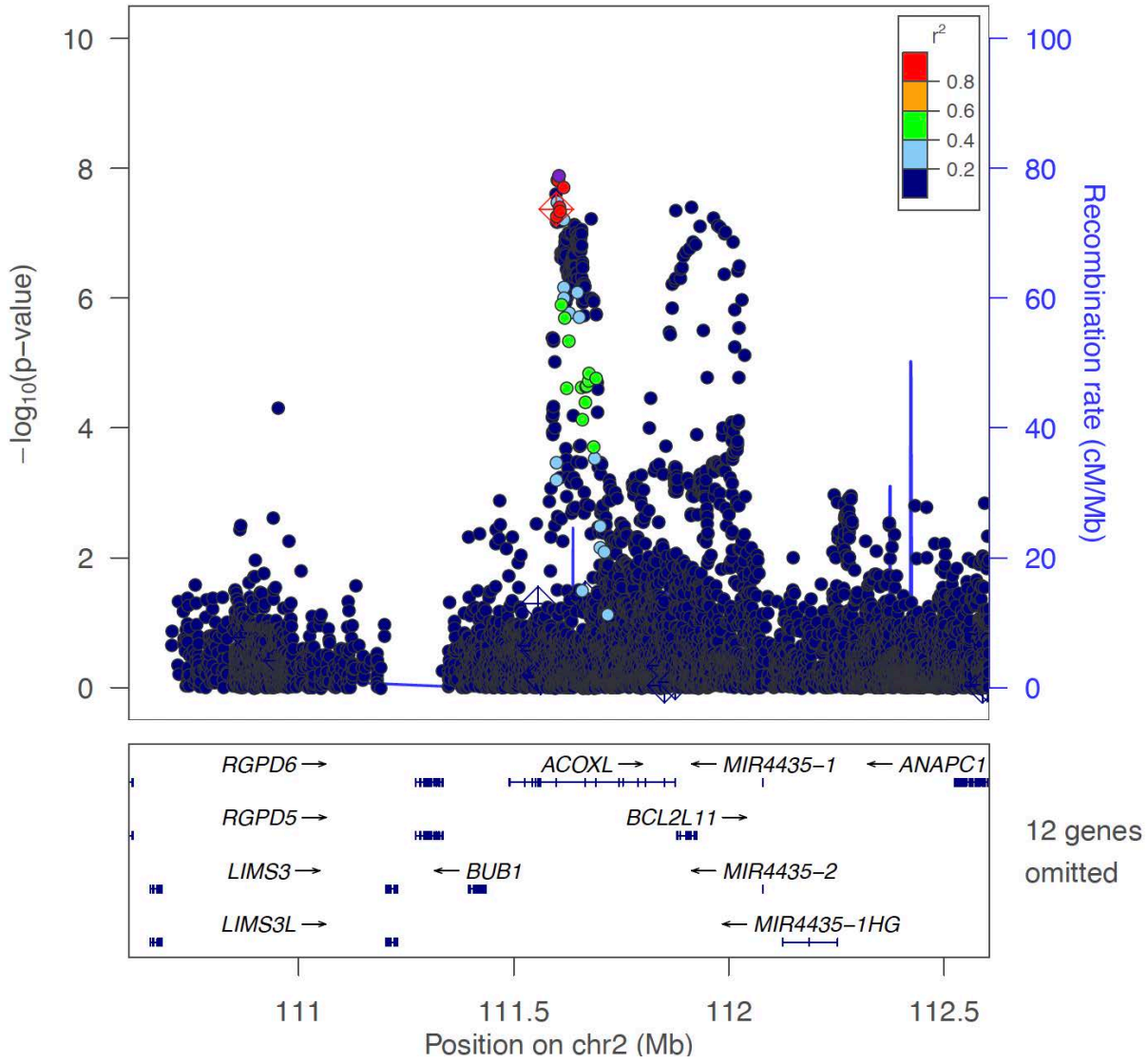

<Locus 23>
2:191943742:C:T (rs11889341)
Multi-GWAS (combined)
Known locus

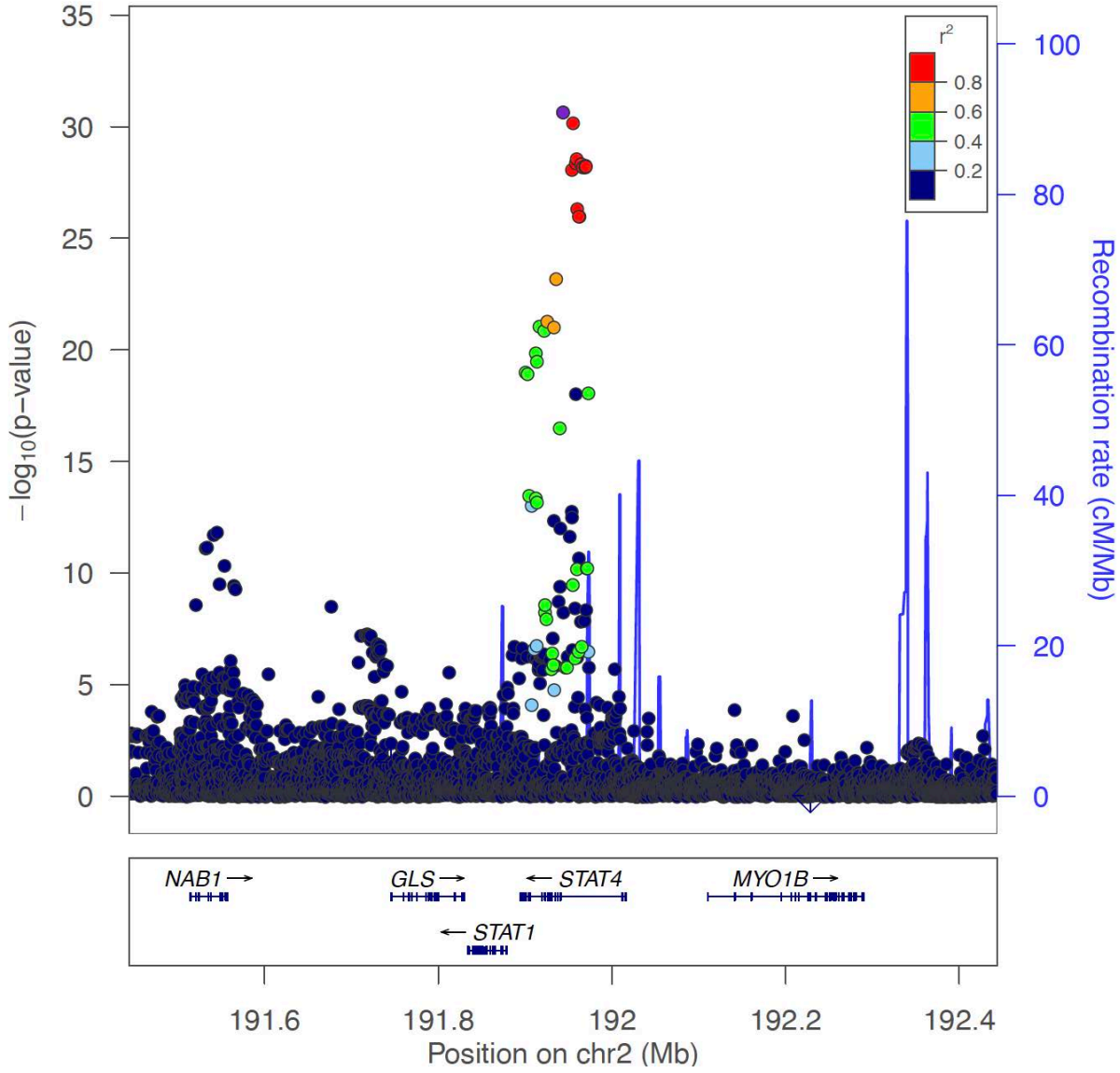

<Locus 24>
2:198914072:G:T (rs10497813)
Multi-GWAS (combined)
Known locus

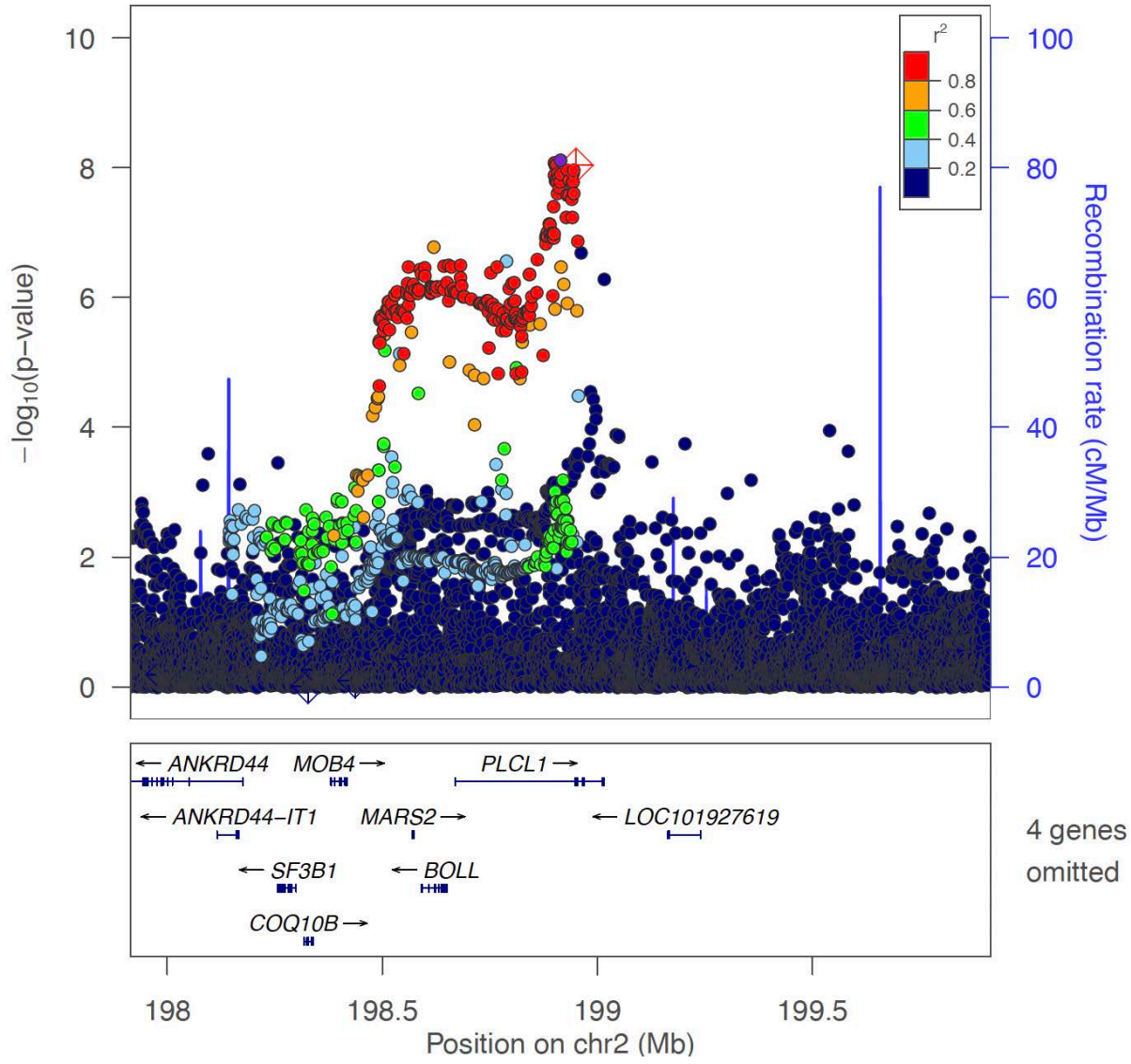

<Locus 25>
2:202151492:C:T (rs2141331)
Multi-GWAS (combined)
Known locus

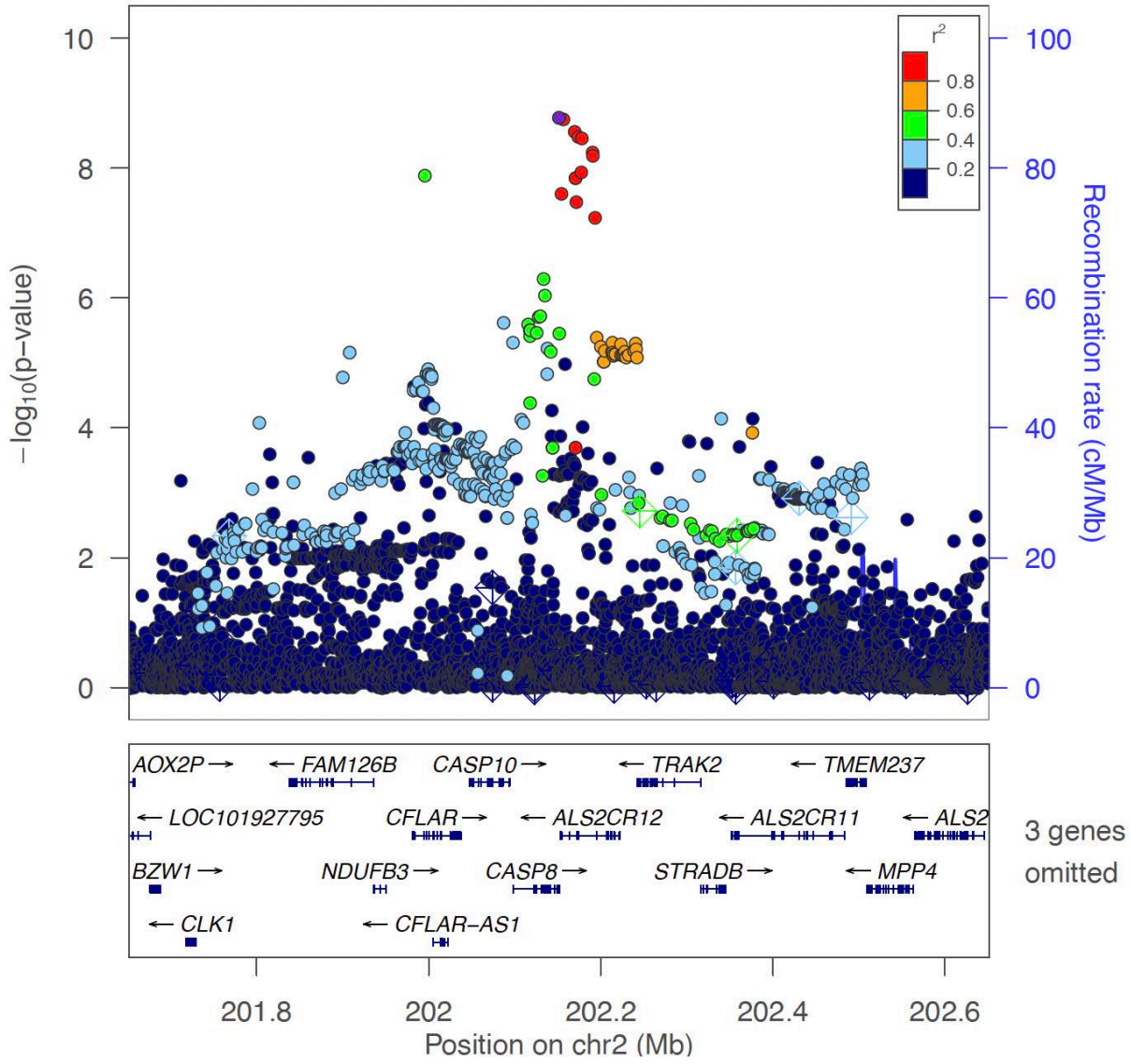

<Locus 26>
2:204738919:G:A (rs3087243)
Multi-GWAS (combined)
Known locus

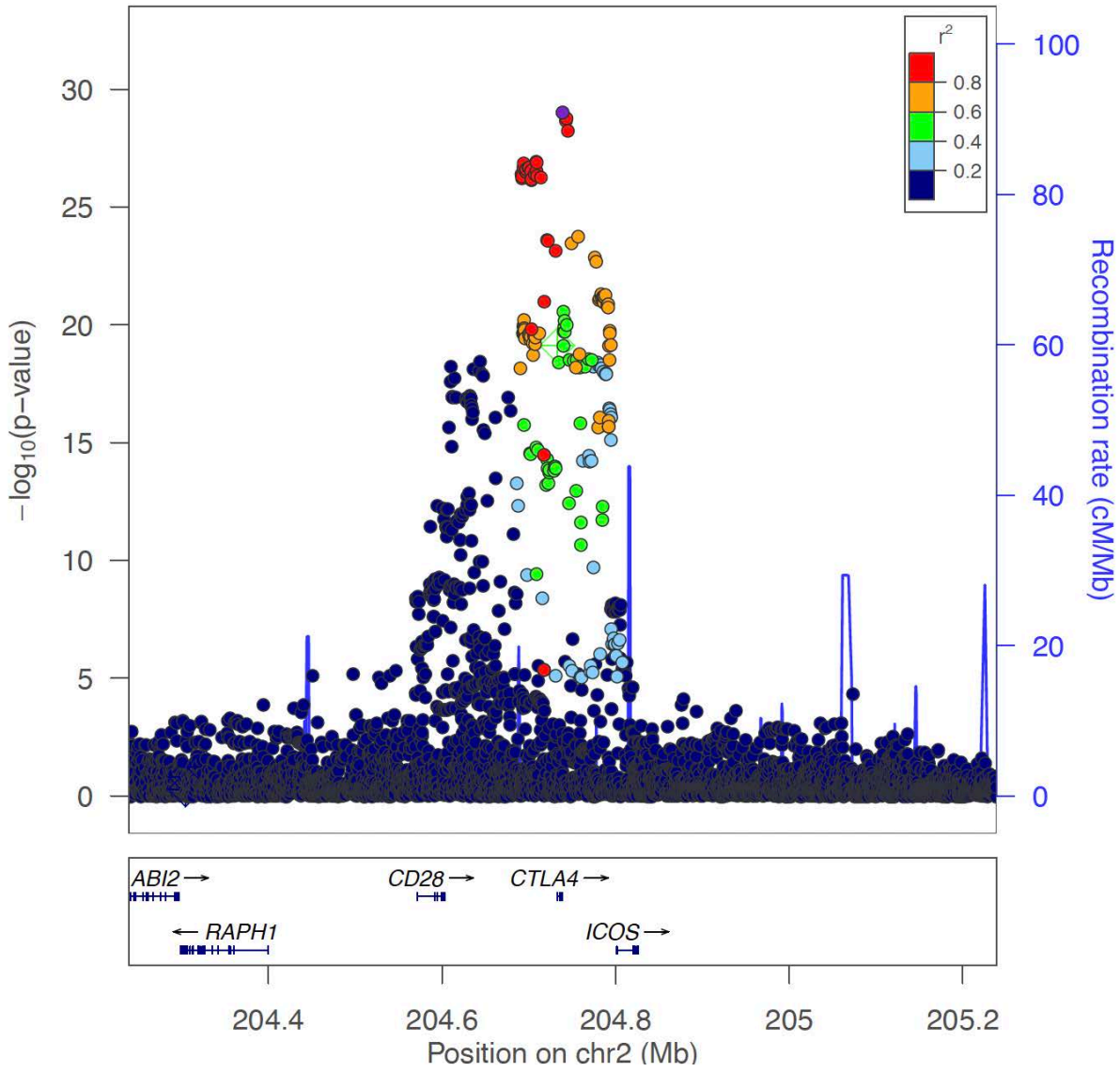

<Locus 27>
3:11984744:G:A (rs77574423)
EUR-GWAS (combined)
Novel locus

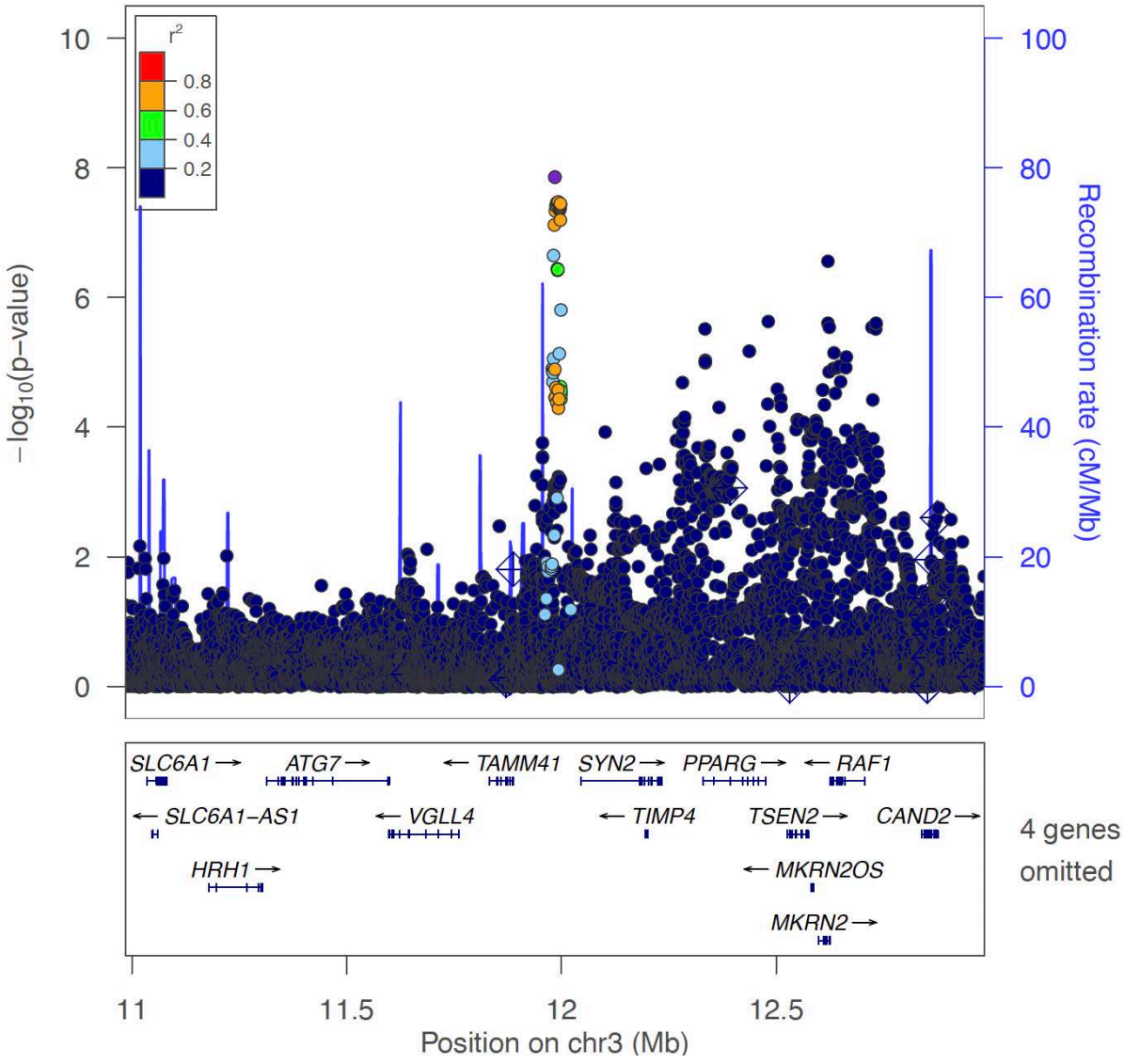

<Locus 28>
3:17046866:G:A (rs5019428)
Multi-GWAS (combined)
Known locus

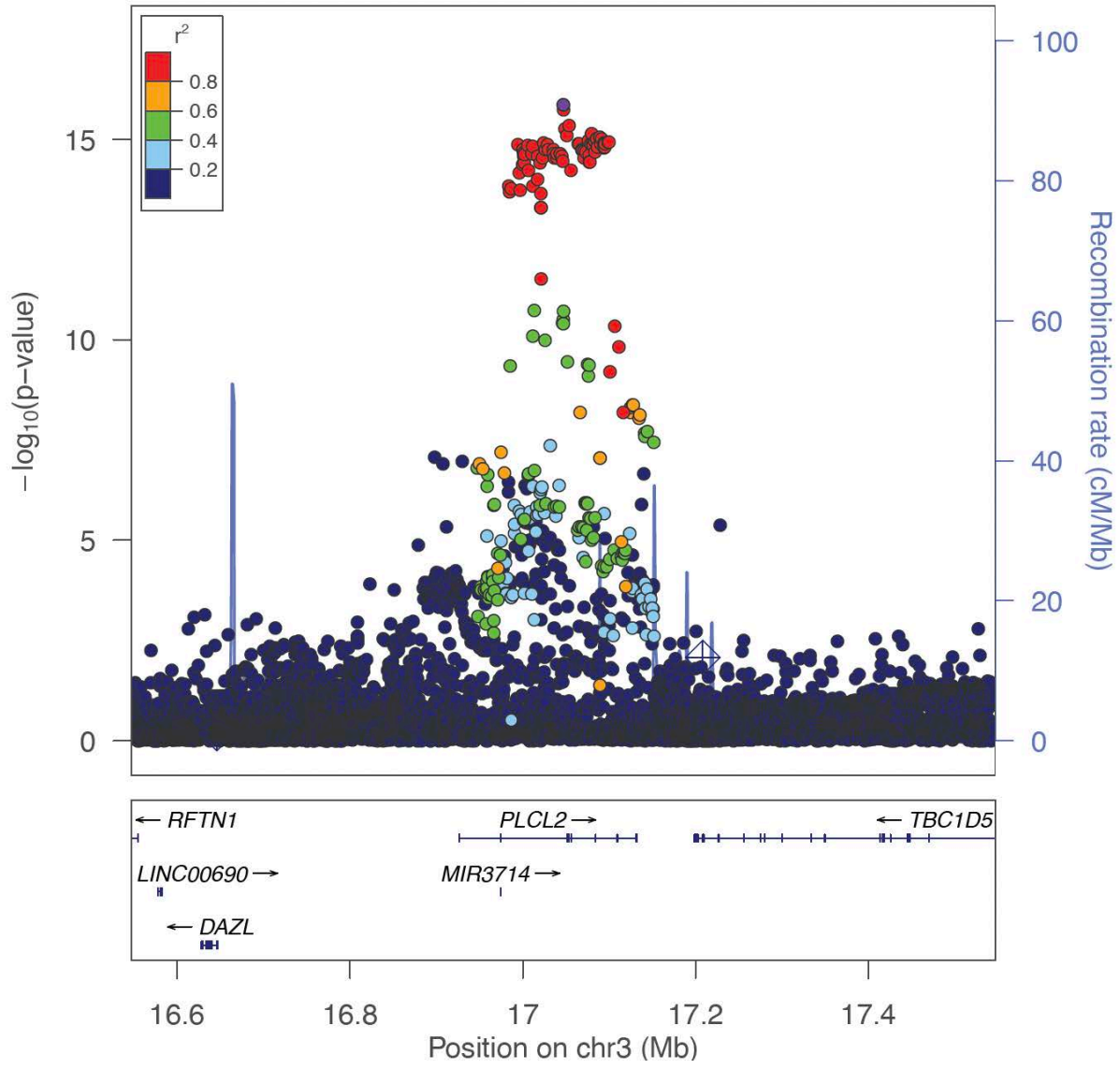

<Locus 29>
3:27777779:G:A (rs9880772)
Multi-GWAS (combined)
Known locus

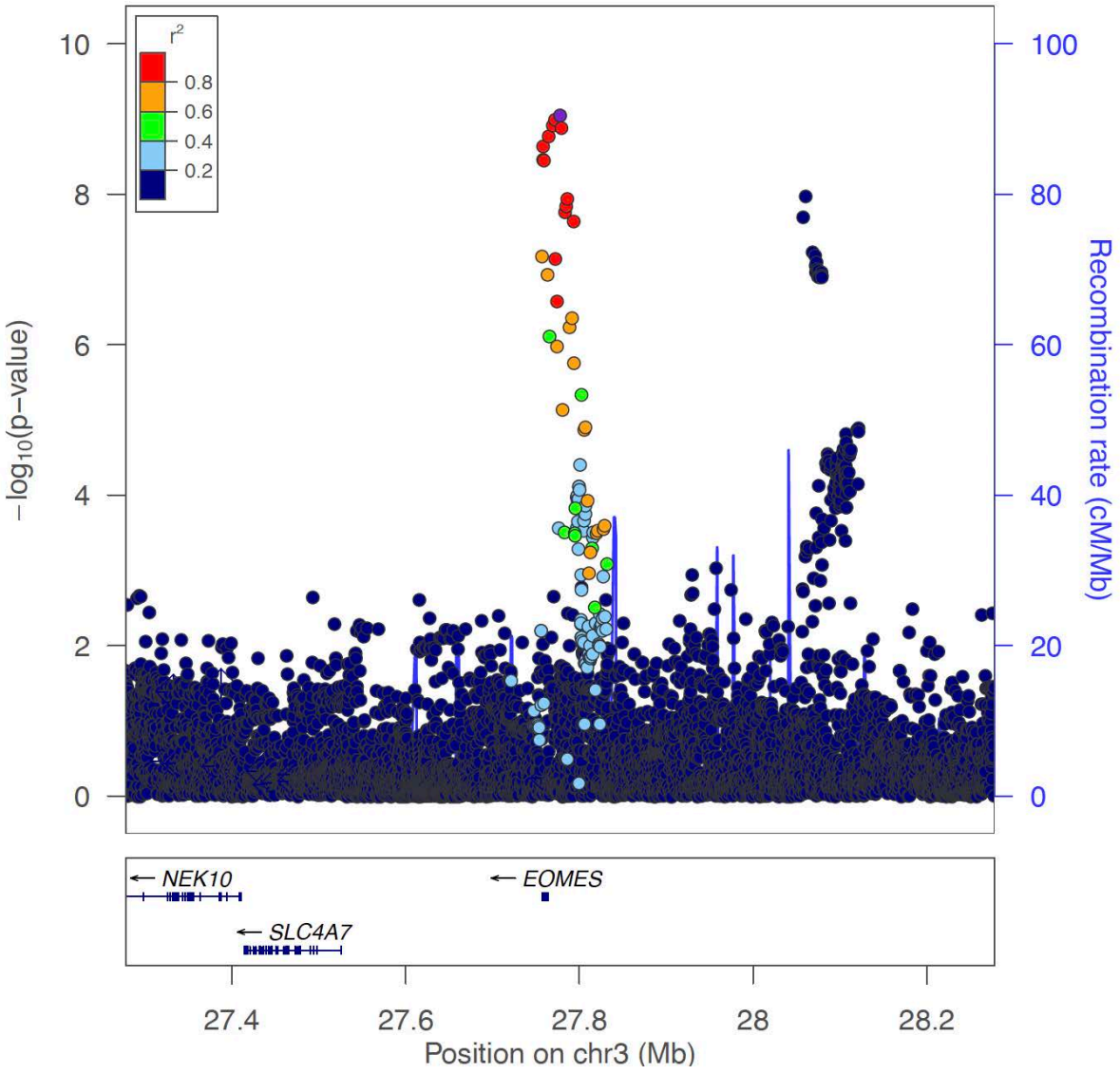

<Locus 30>
3:127292333:G:A (rs62264113)
Multi-GWAS (combined)
Novel locus

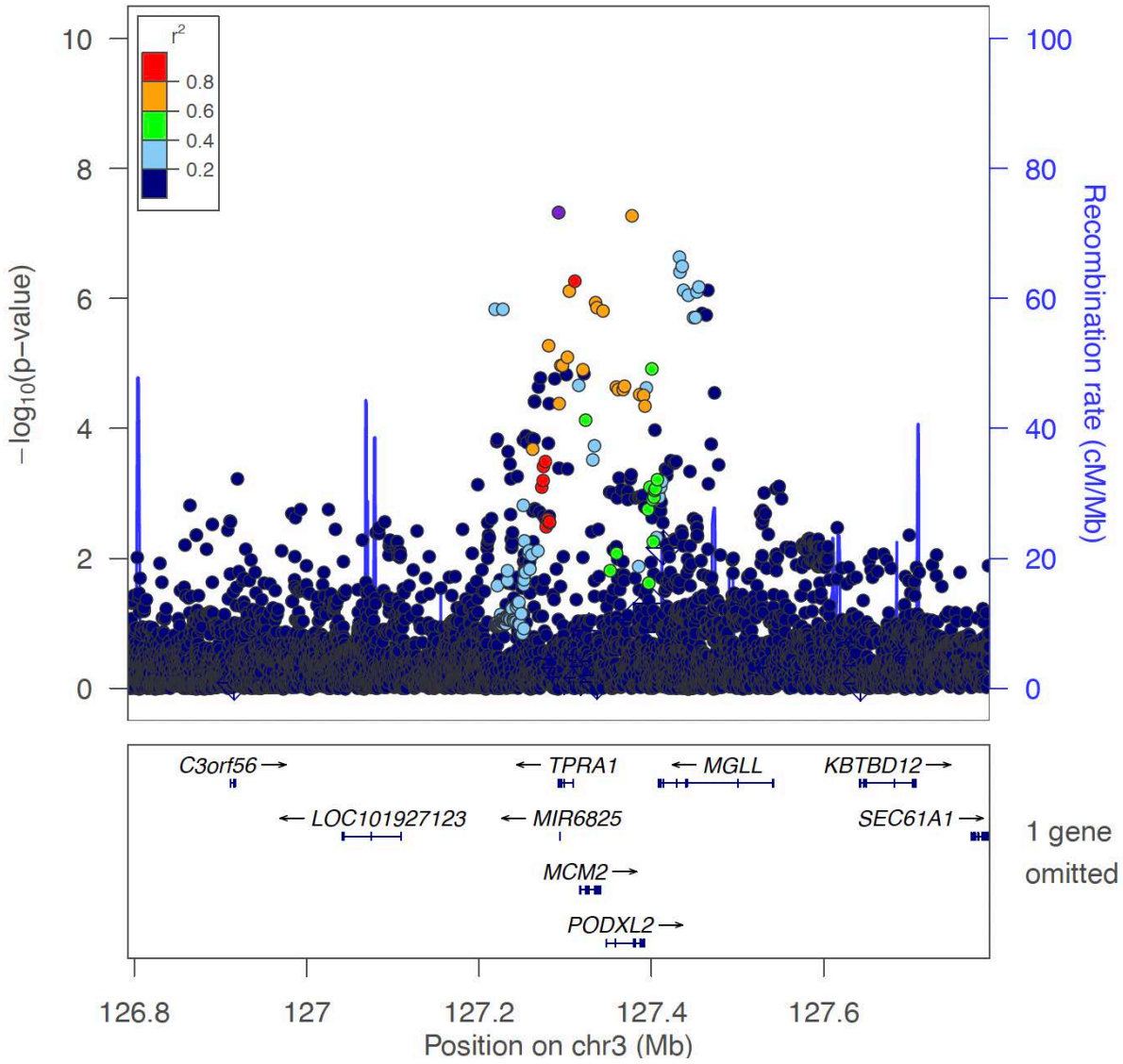

<Locus 31>
3:136317506:G:C (rs9826420)
Multi-GWAS (combined)
Known locus

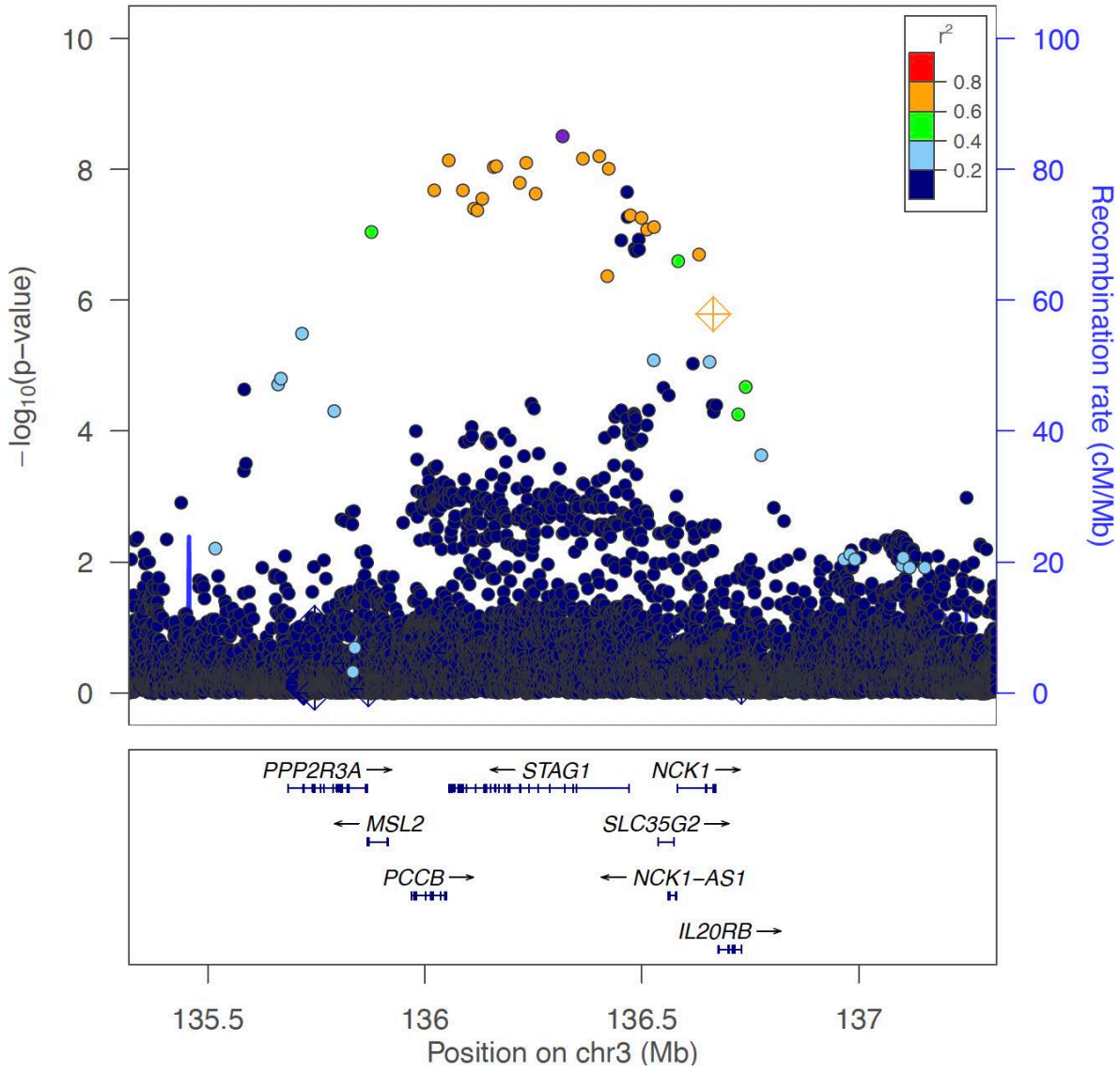

<Locus 32>
3:189306650:A:T (rs4687070)
Multi-GWAS (combined)
Novel locus

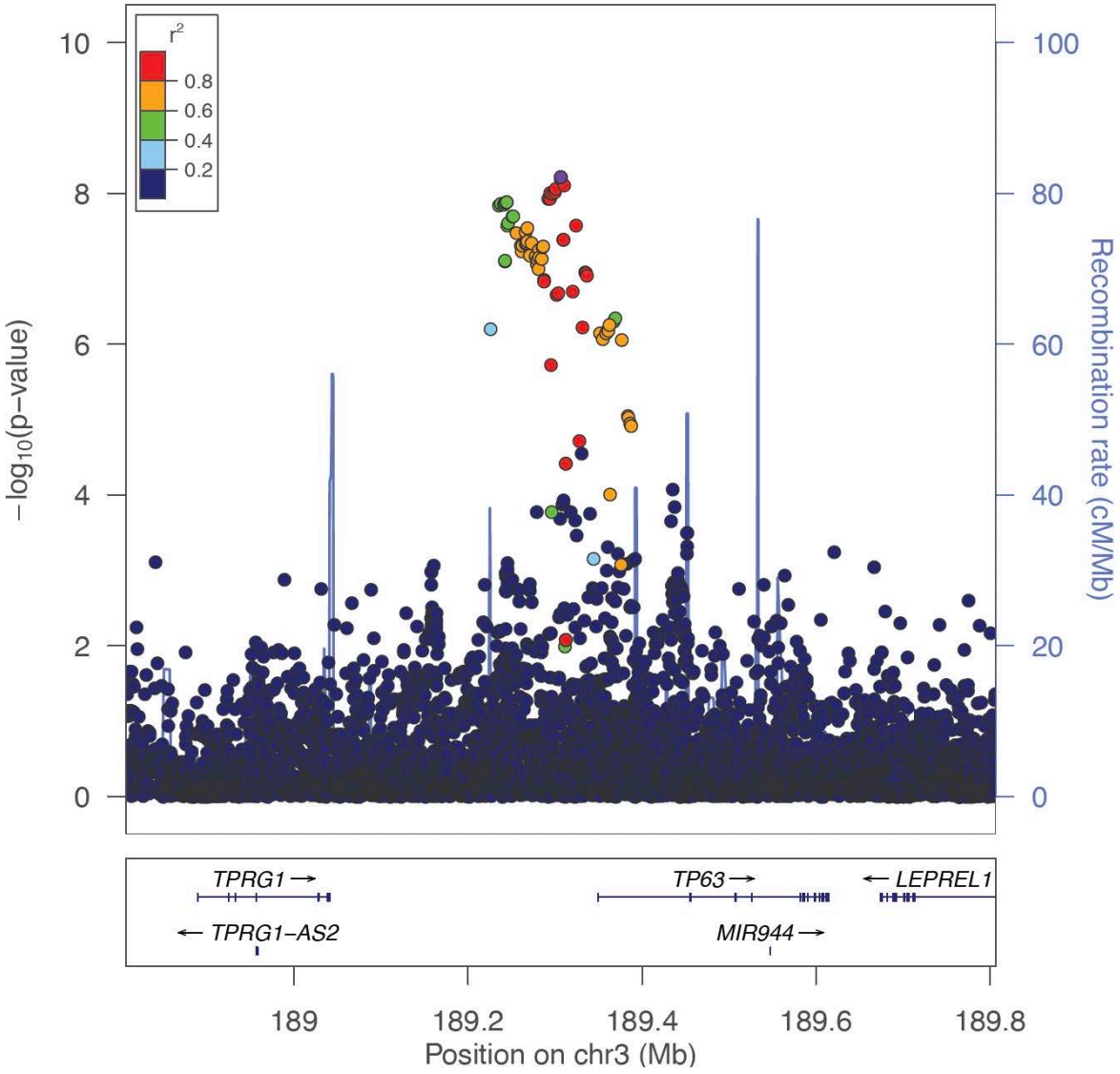

<Locus 33>
4:2722815:T:C (rs4690029)
Multi-GWAS (combined)
Novel locus

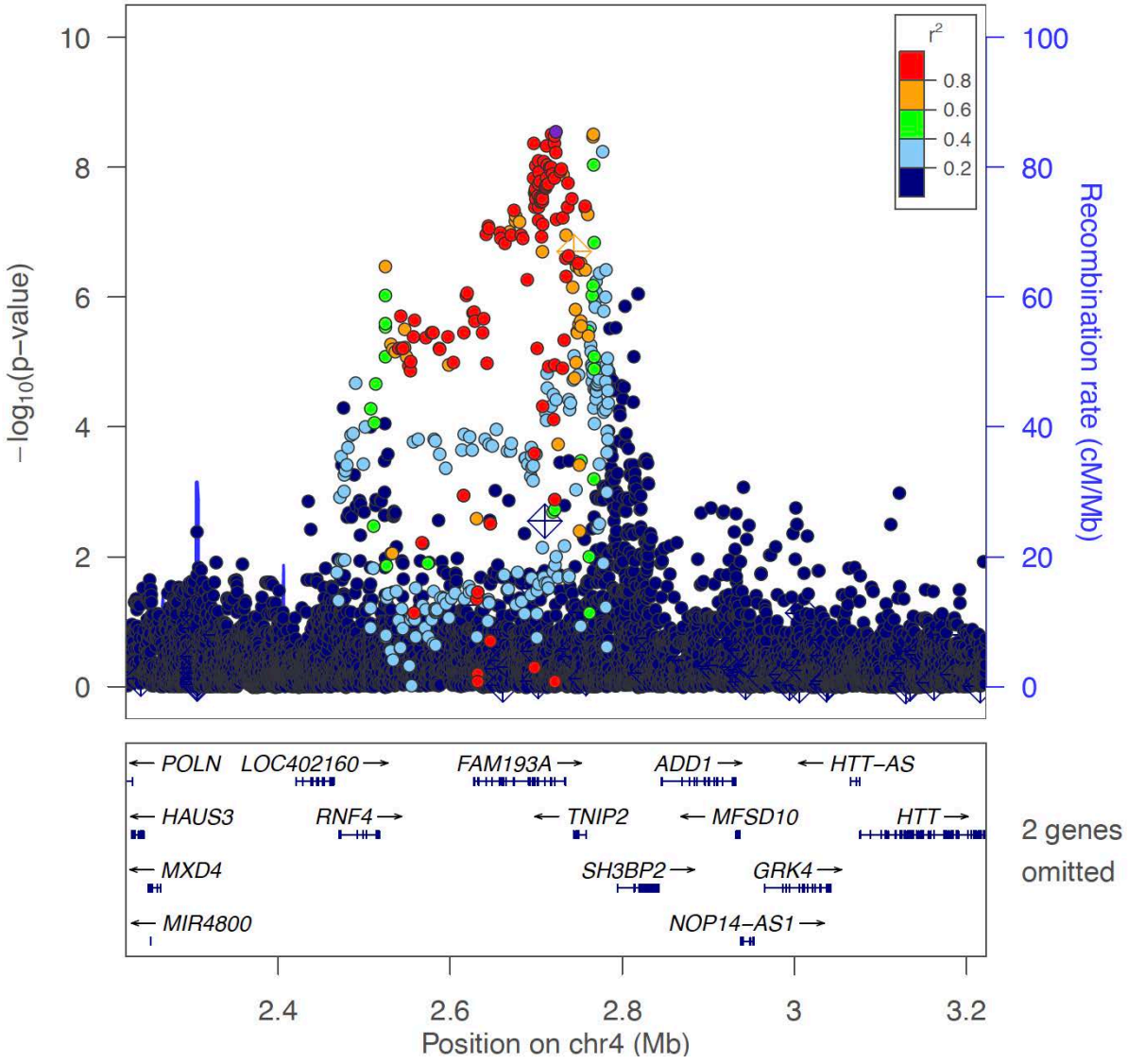

<Locus 34>
4:10709366:T:C (rs6831973)
Multi-GWAS (combined)
Known locus

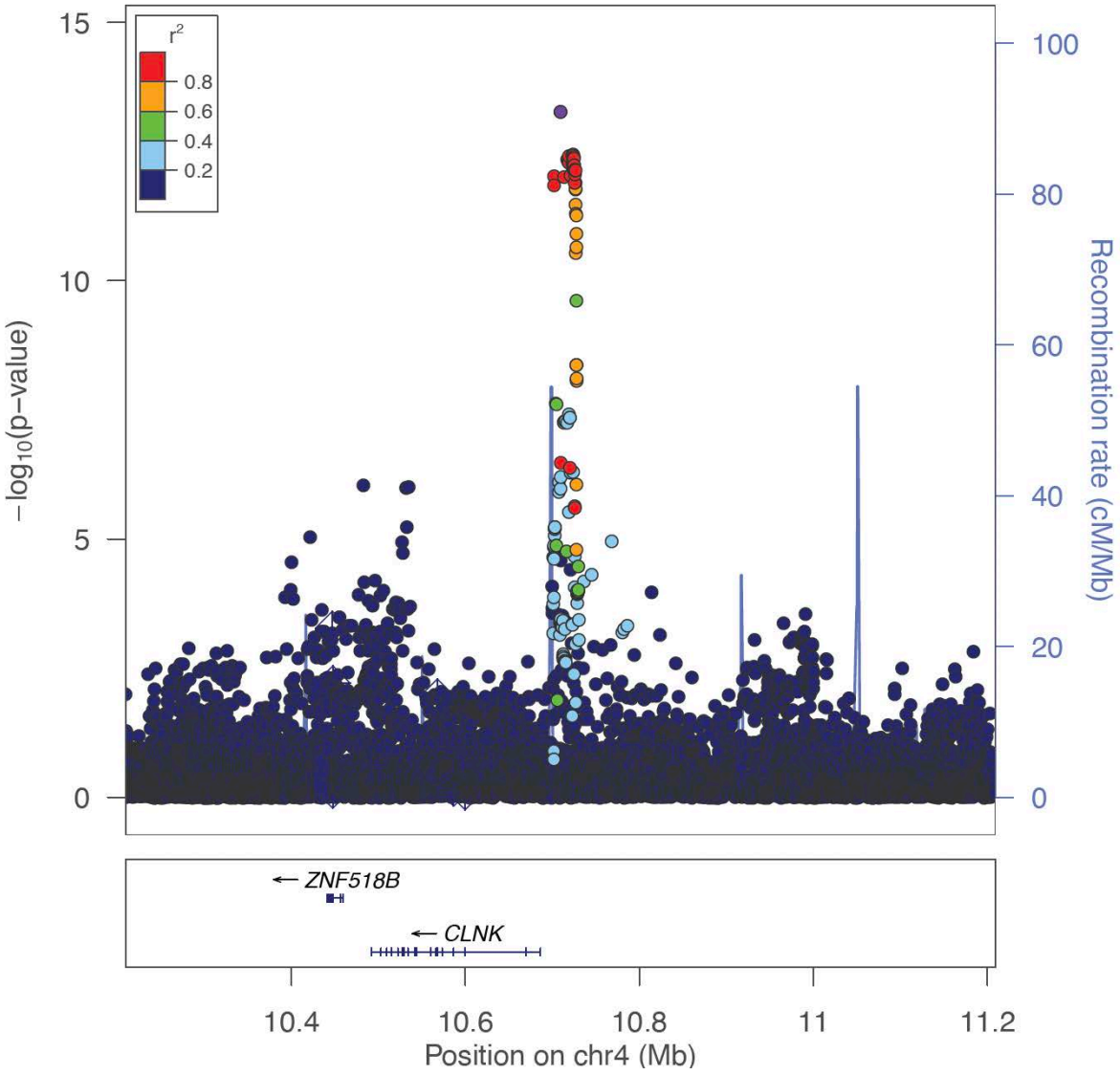

<Locus 35>
4:26117568:T:TA (rs575378713)
Multi-GWAS (combined)
Known locus

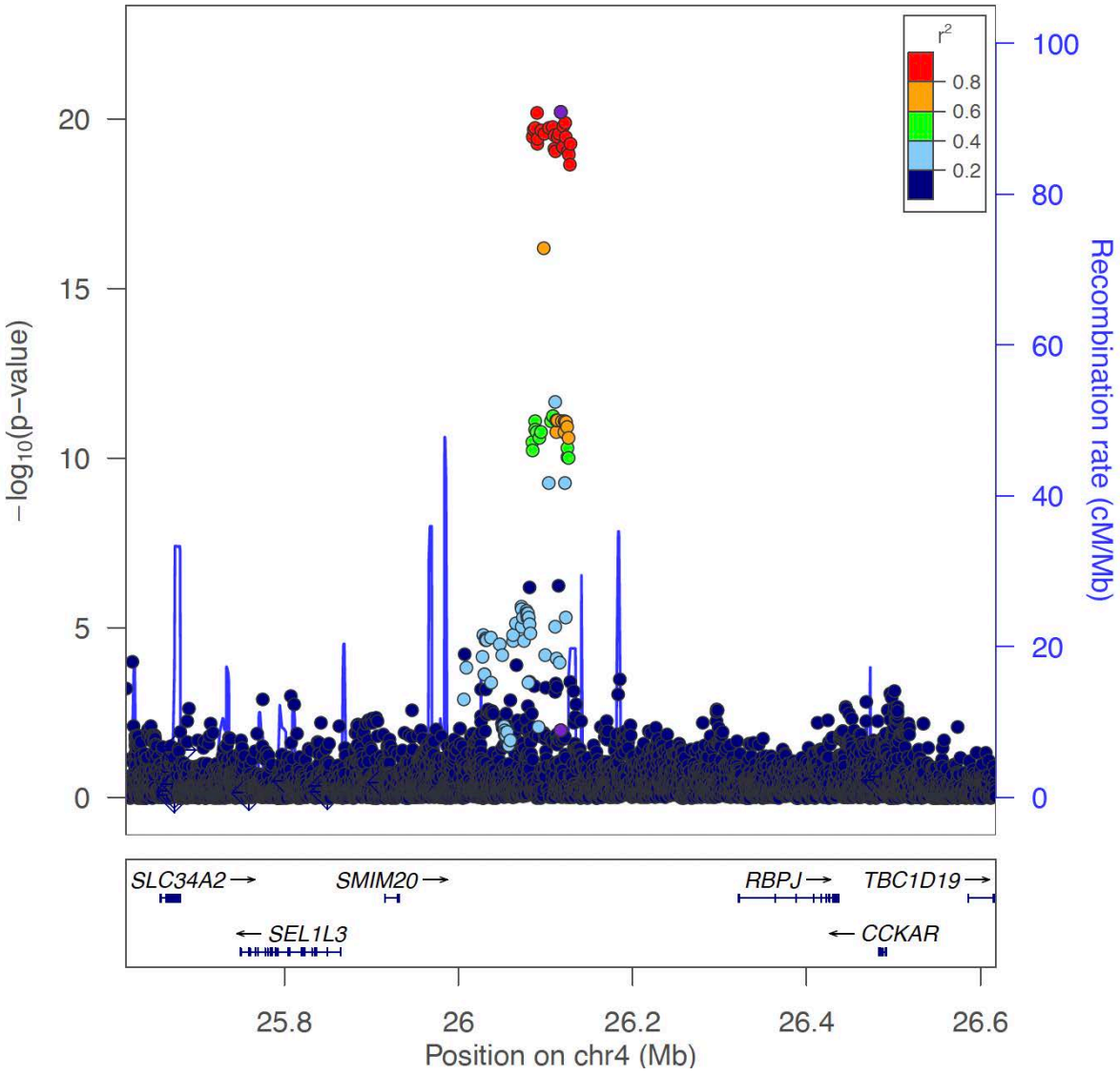

<Locus 36>
4:48220839:G:A (rs2664035)
Multi-GWAS (combined)
Known locus

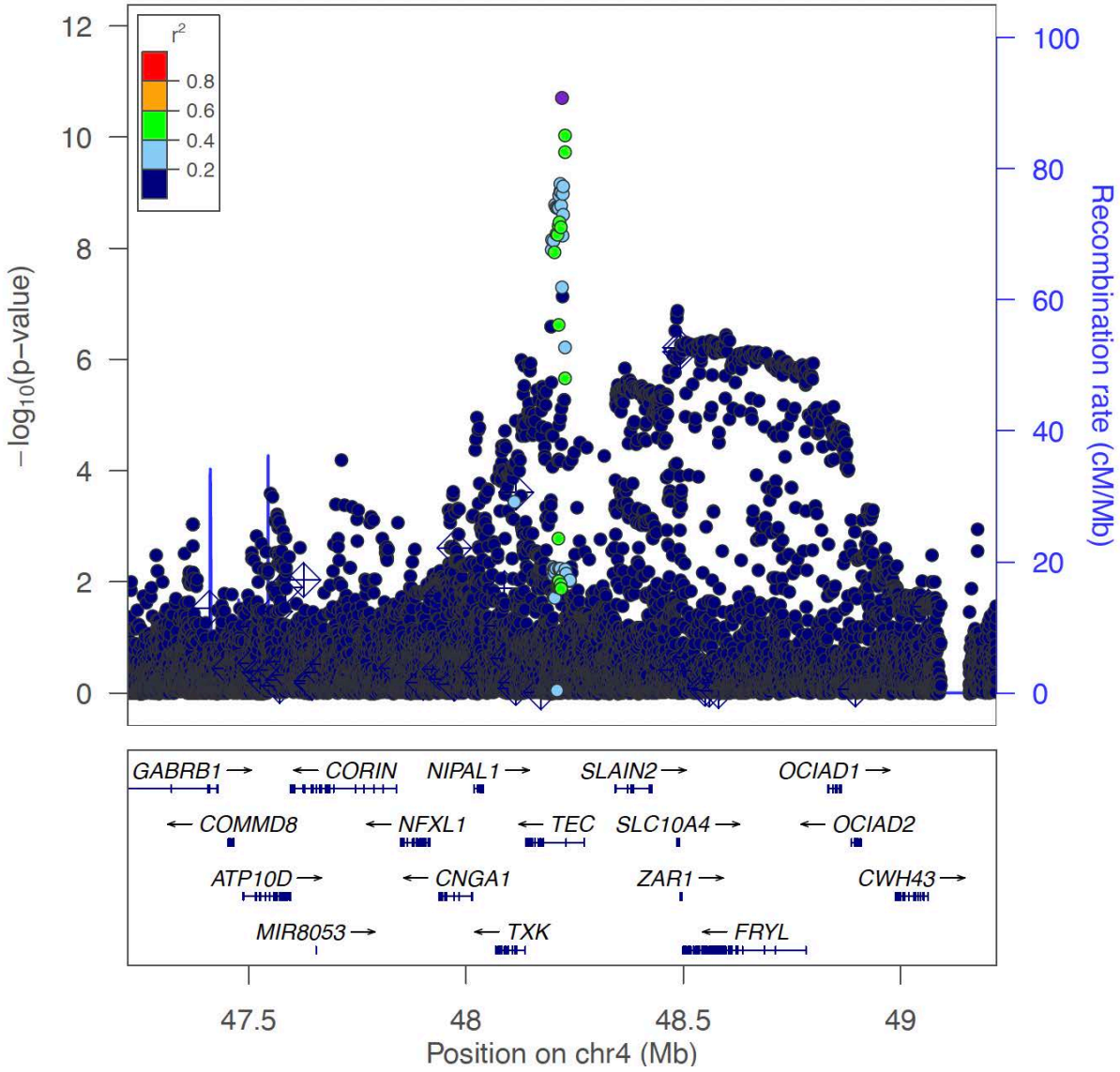

<Locus 37>
4:80952409:GGTGTGTGCATGCACACACAT:G (rs138066321)
Multi-GWAS (combined)
Novel locus

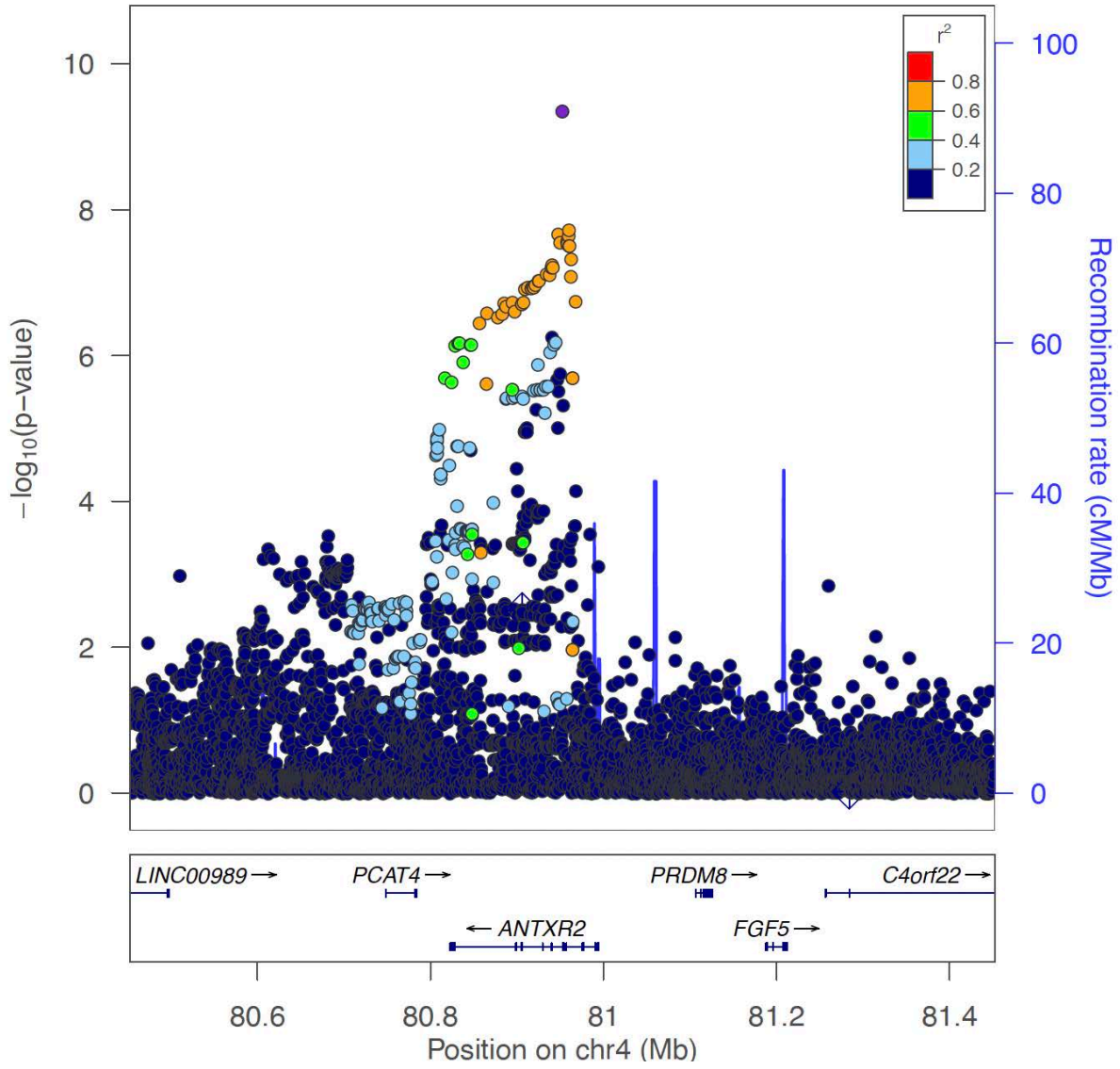

<Locus 38>
4:109061618:G:C (rs58107865)
Multi-GWAS (combined)
Novel locus

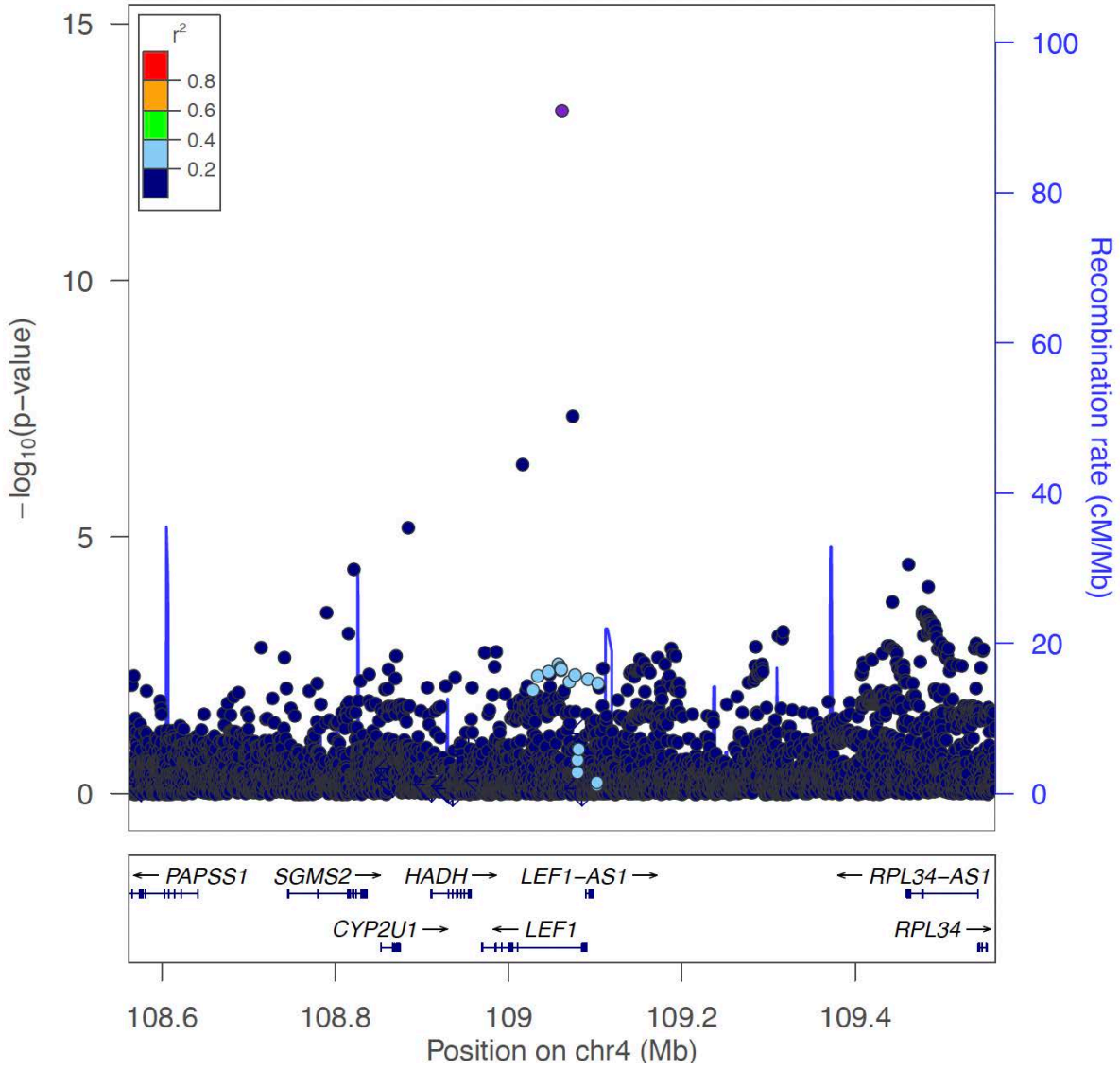

<Locus 39>
4:123043662:A:G (rs6814280)
Multi-GWAS (seroposi)
Known locus

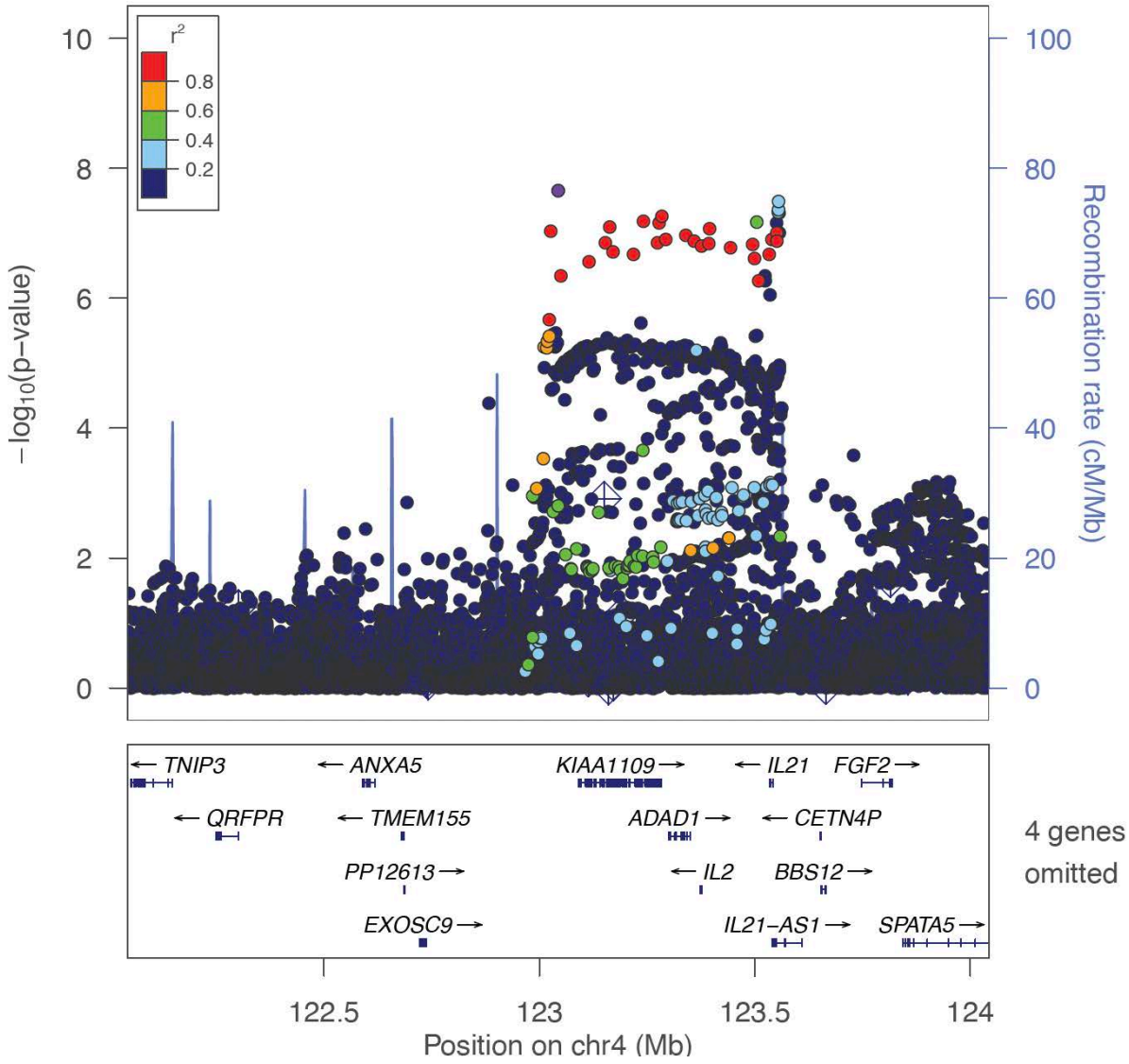

<Locus 40>
5:10704797:T:C (rs2918392)
Multi-GWAS (combined)
Known locus

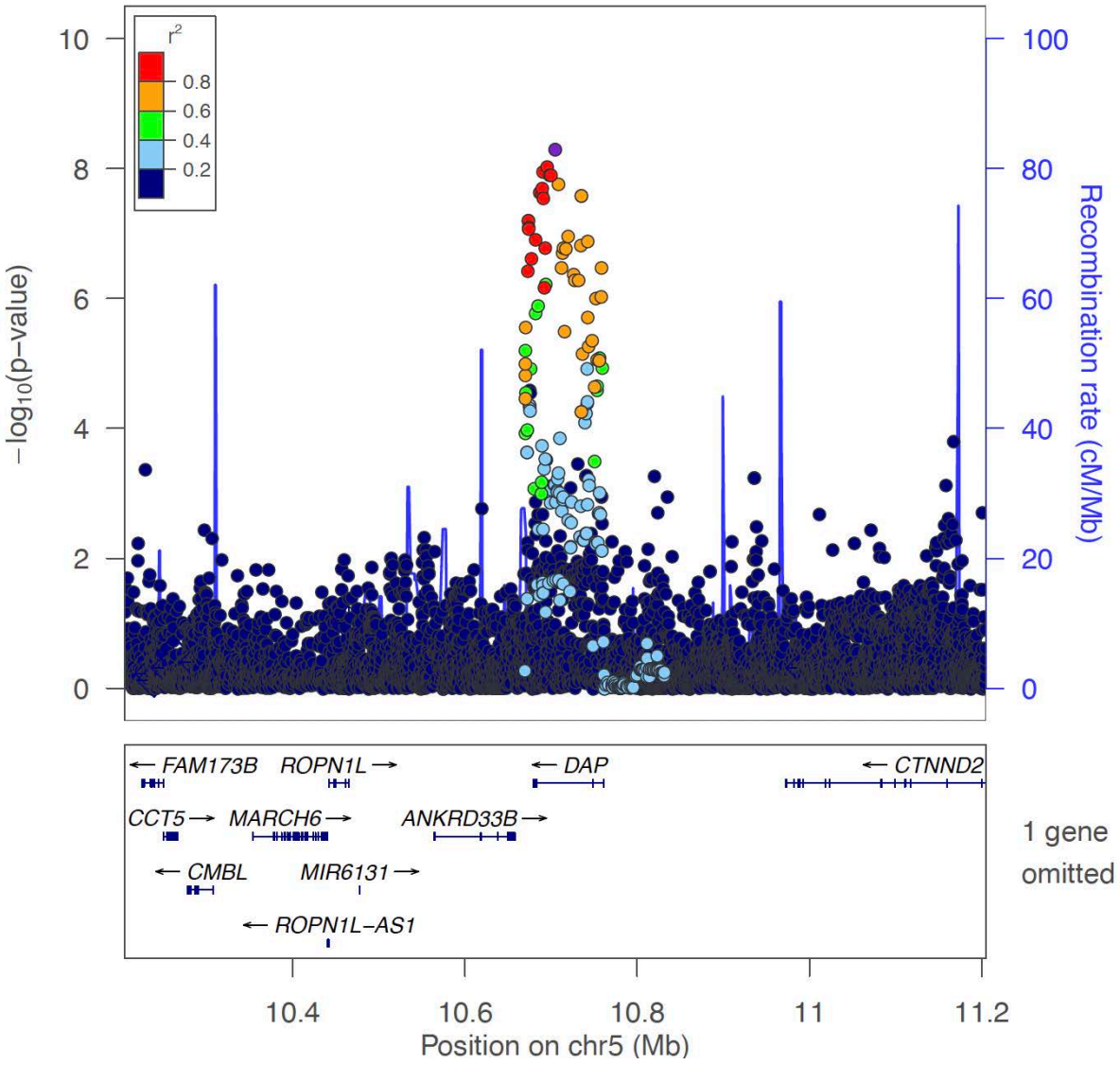

<Locus 41>
5:40499290:G:A (rs56787183)
Multi-GWAS (combined)
Novel locus

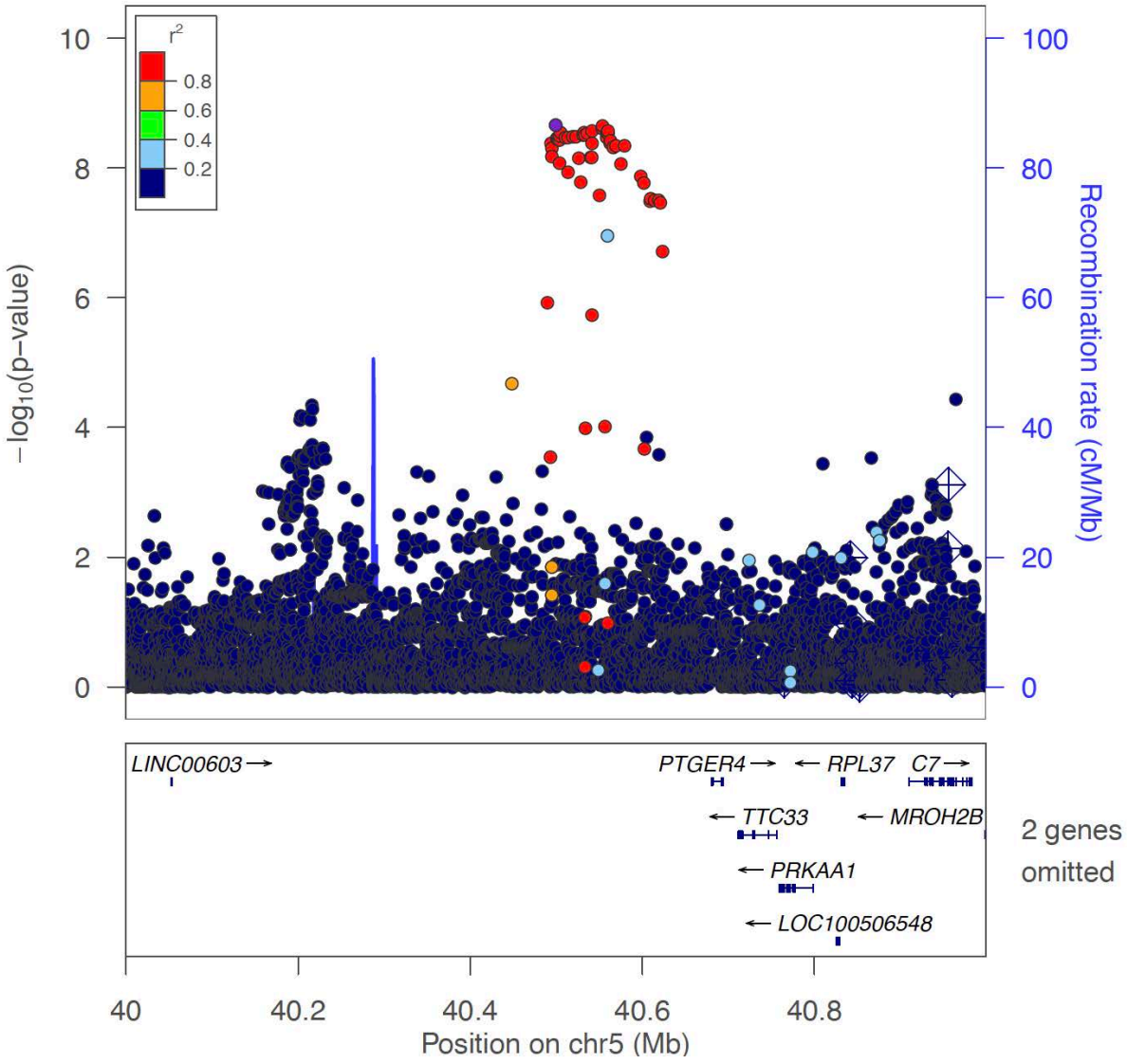

<Locus 42>
5:55444683:G:A (rs7731626)
Multi-GWAS (combined)
Known locus

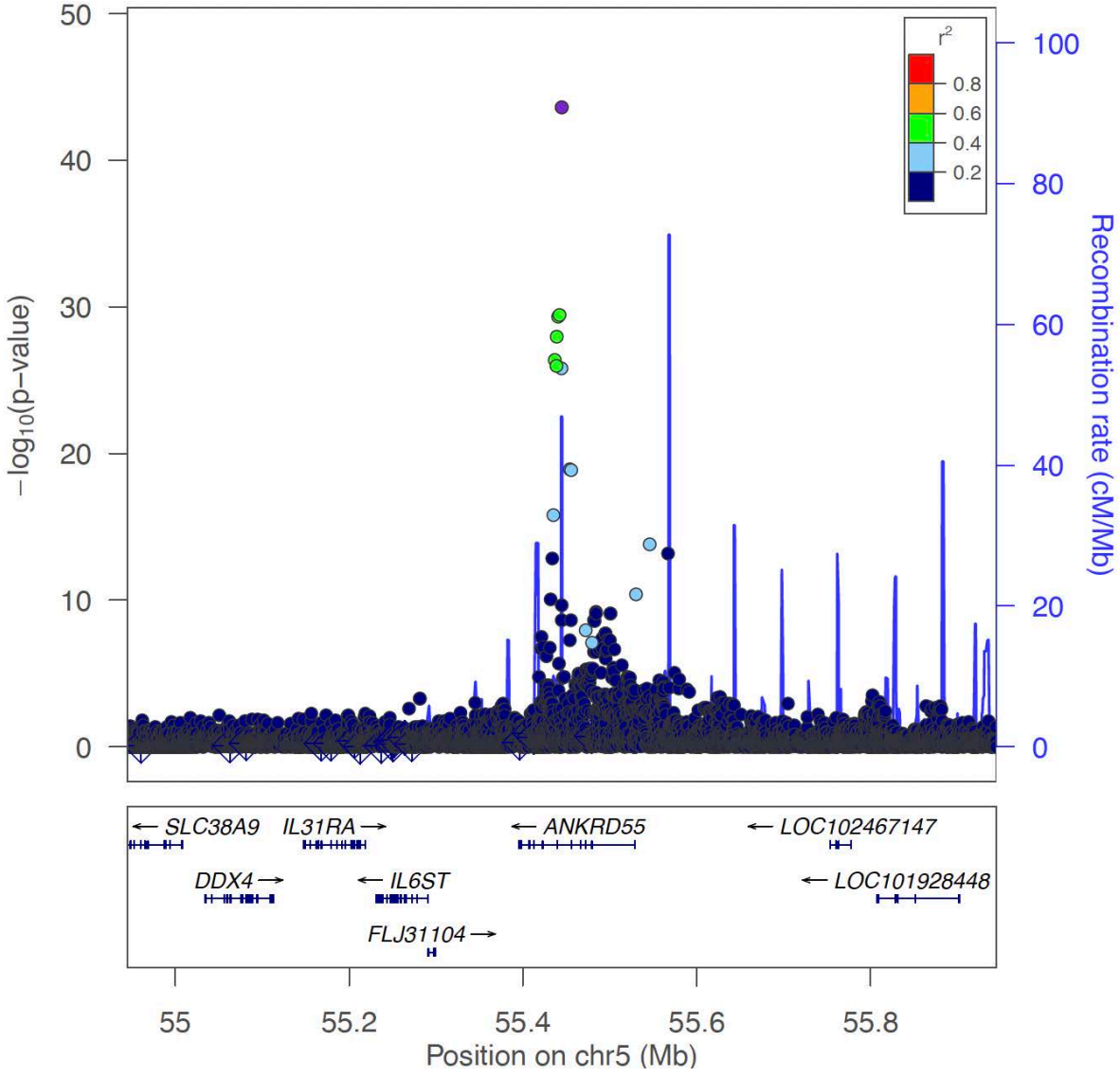

<Locus 43>
5:102604933:A:C (rs187579)
Multi-GWAS (combined)
Known locus

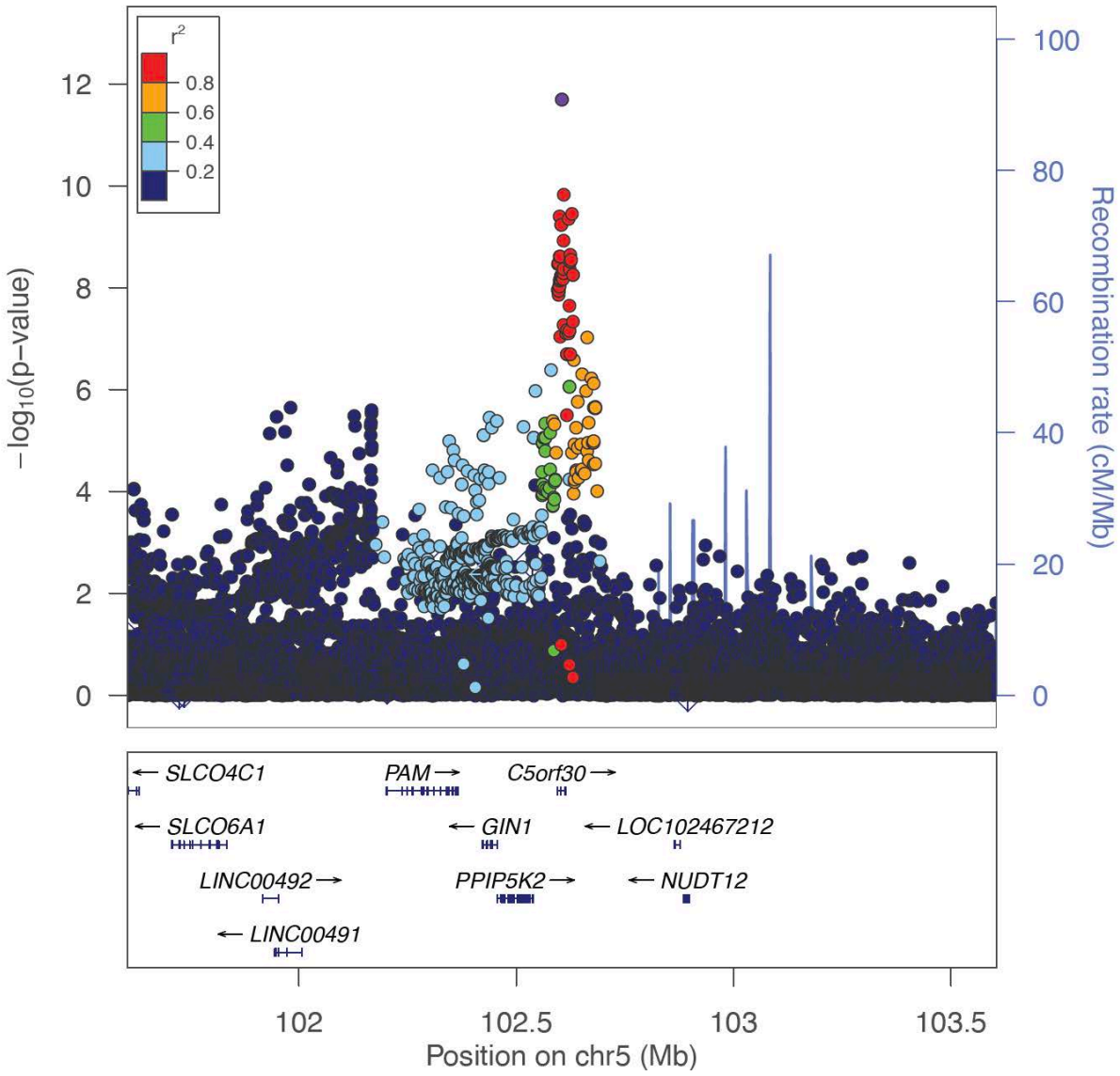

<Locus 44>
5:133839534:C:T (rs12519914)
Multi-GWAS (combined)
Known locus

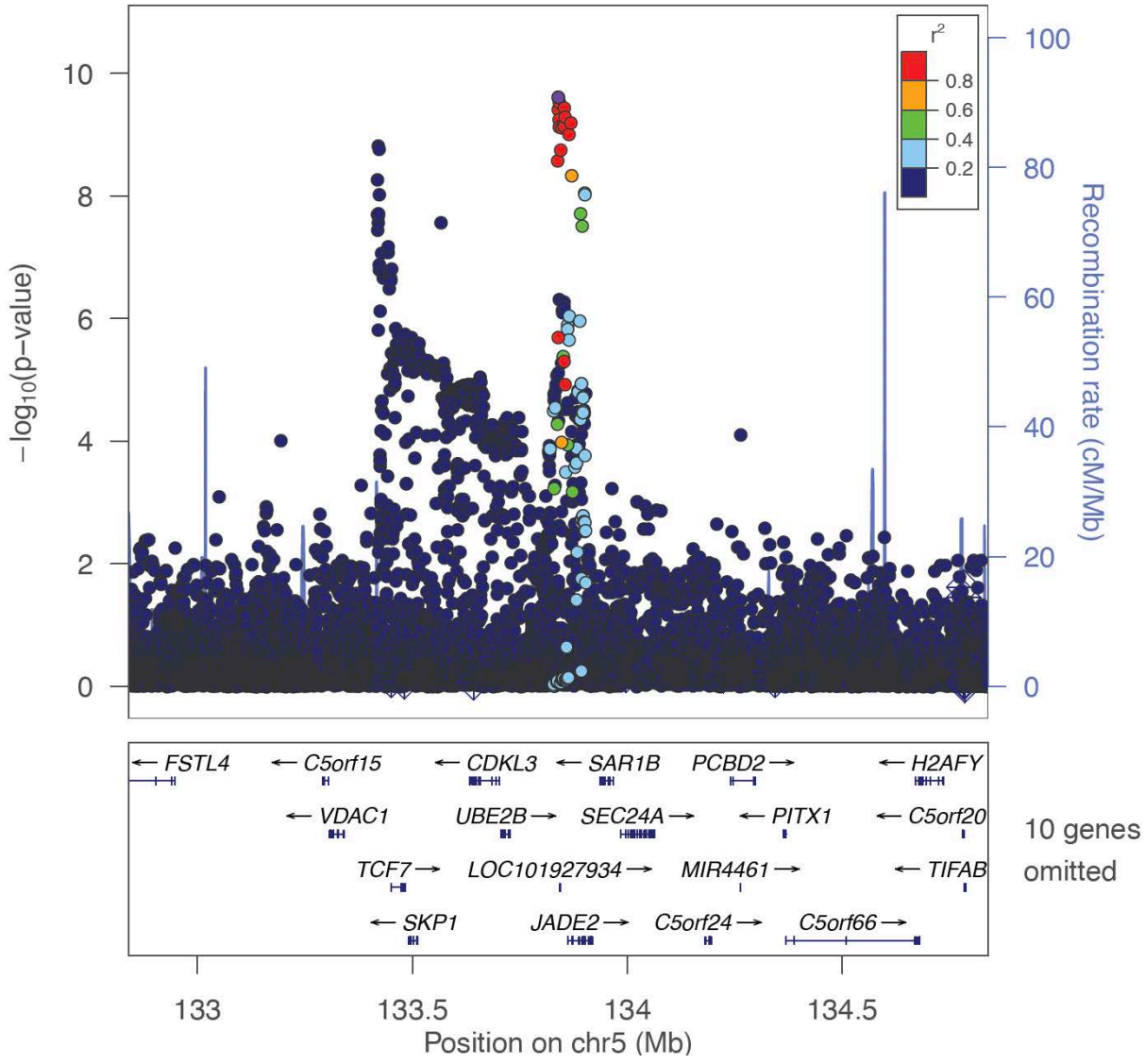

<Locus 45>
5:142604421:A:G (rs244468)
Multi-GWAS (combined)
Novel locus

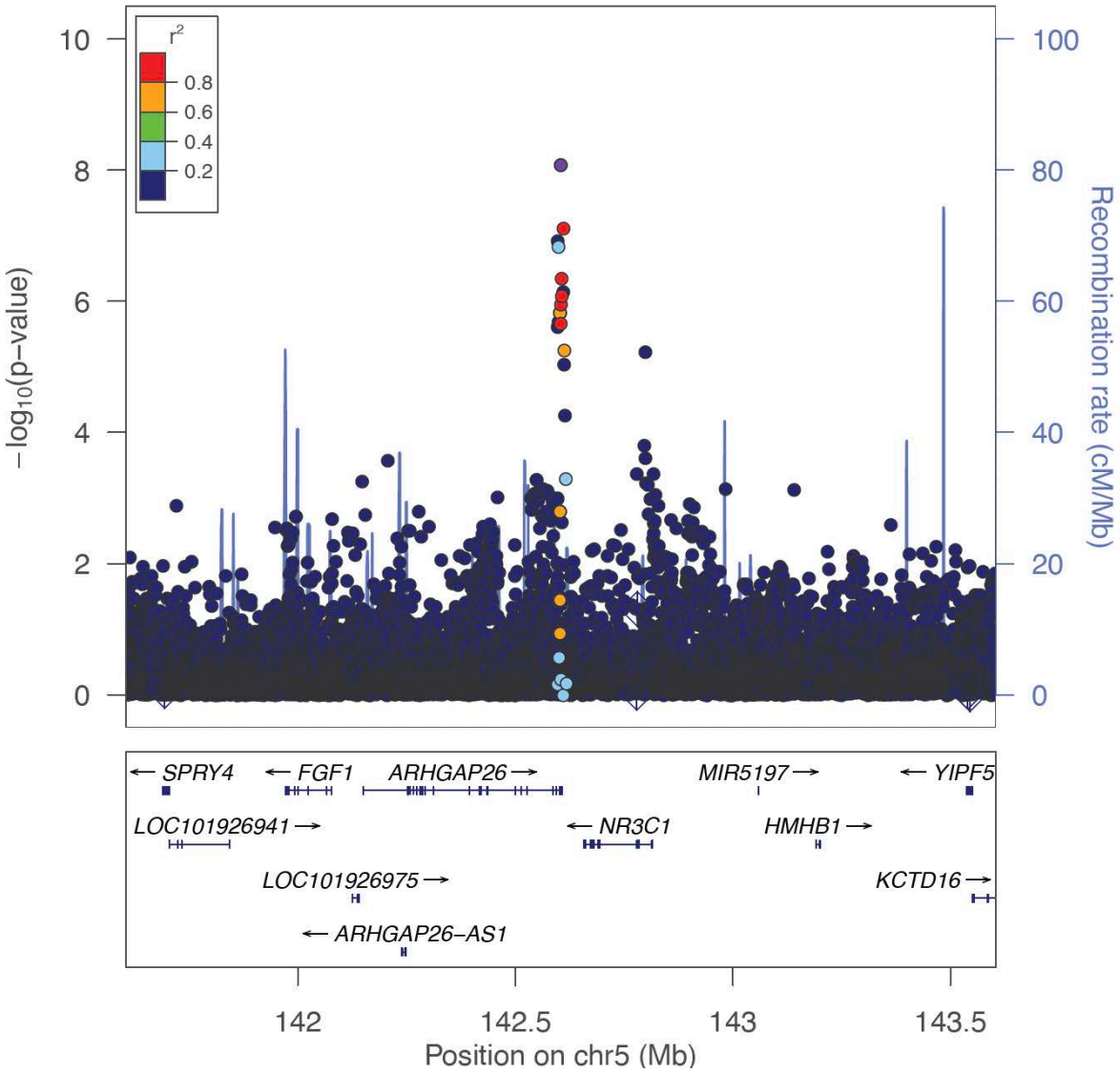

<Locus 46>
5:150438988:C:T (rs1422673)
EUR-GWAS (seroposi)
Novel locus

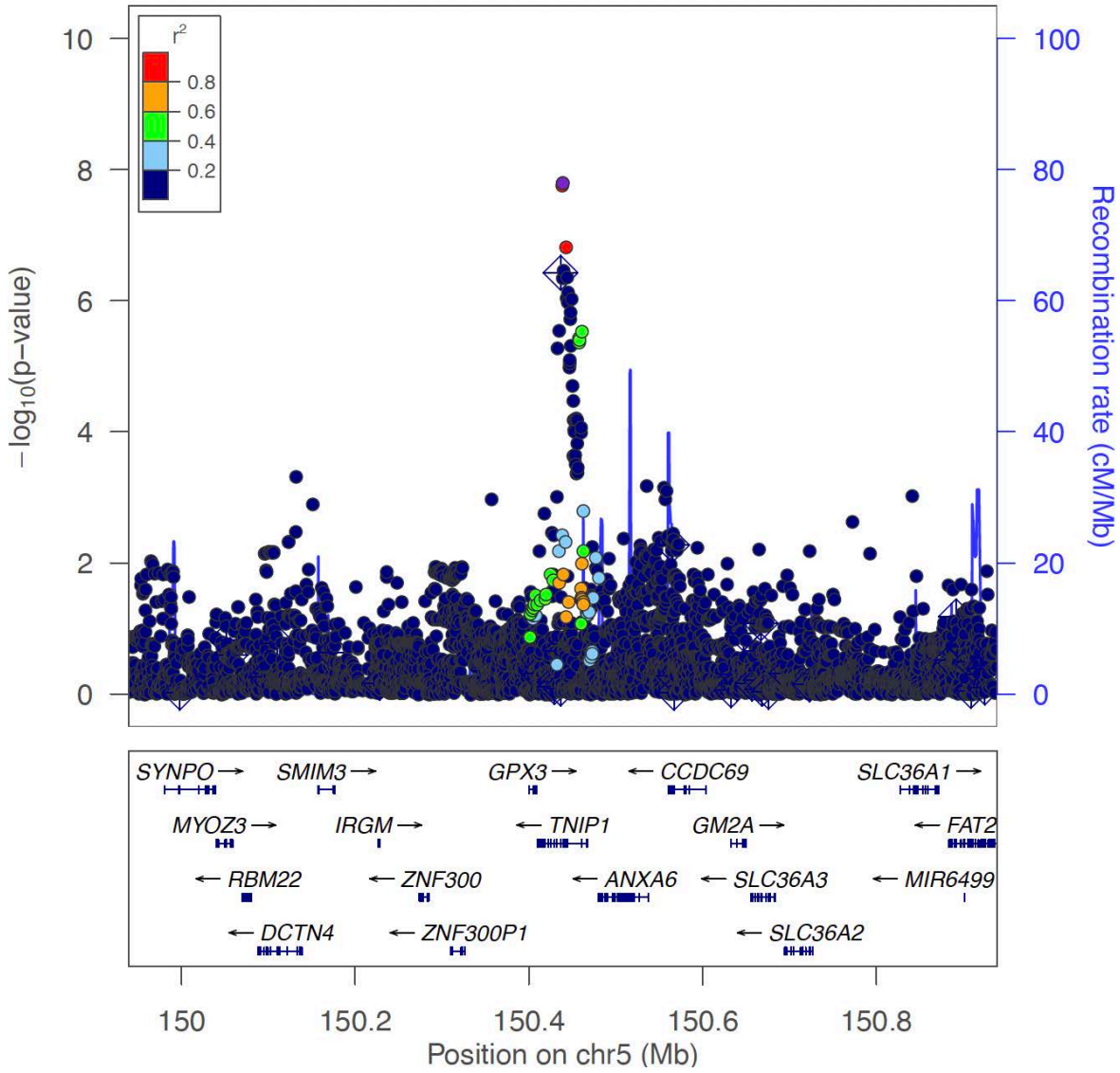

<Locus 47>
6:426268:A:G (rs6930468)
Multi-GWAS (combined)
Known locus

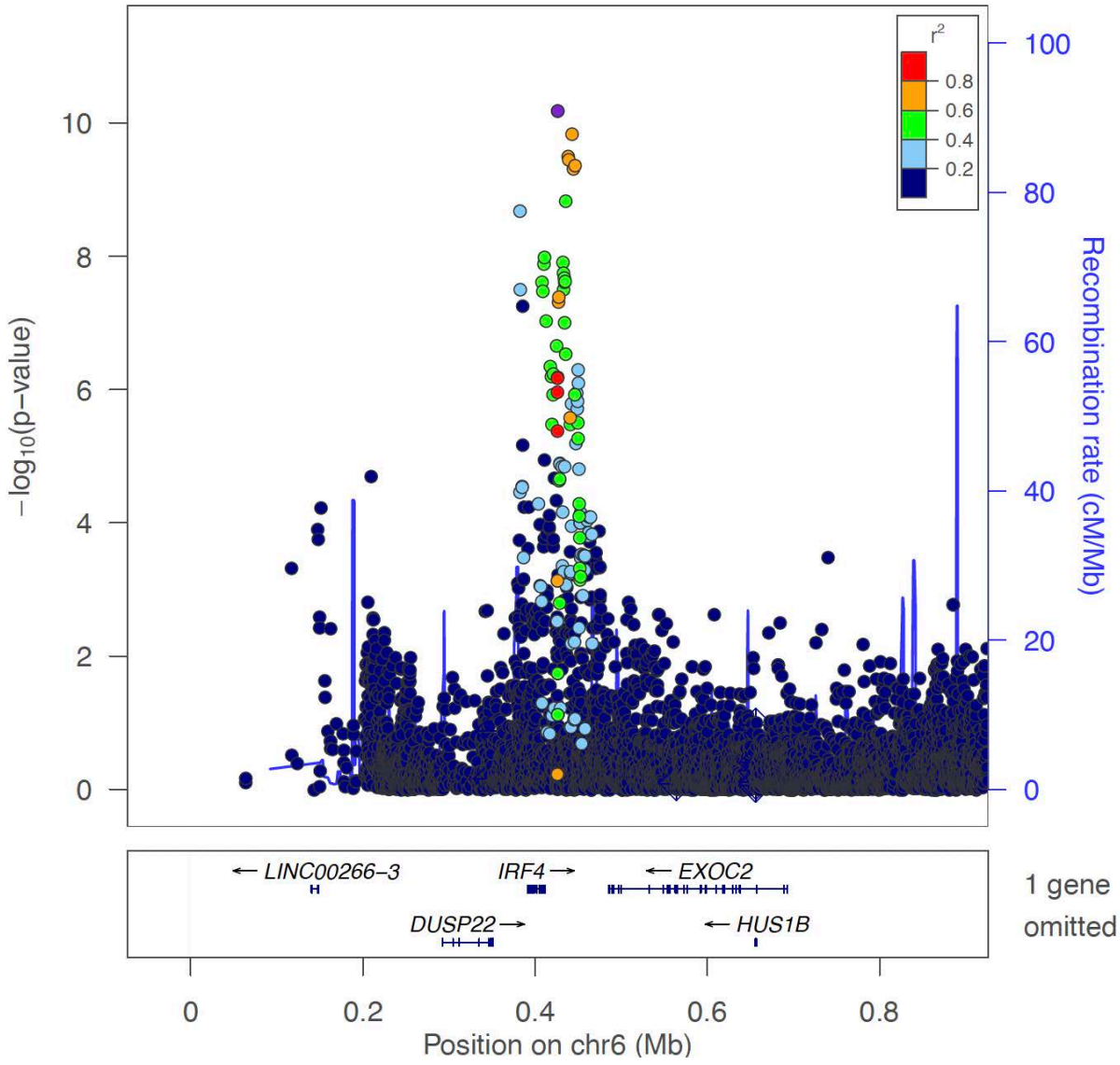

<Locus 48>
6:14107197:C:T (rs12530098)
Multi-GWAS (combined)
Known locus

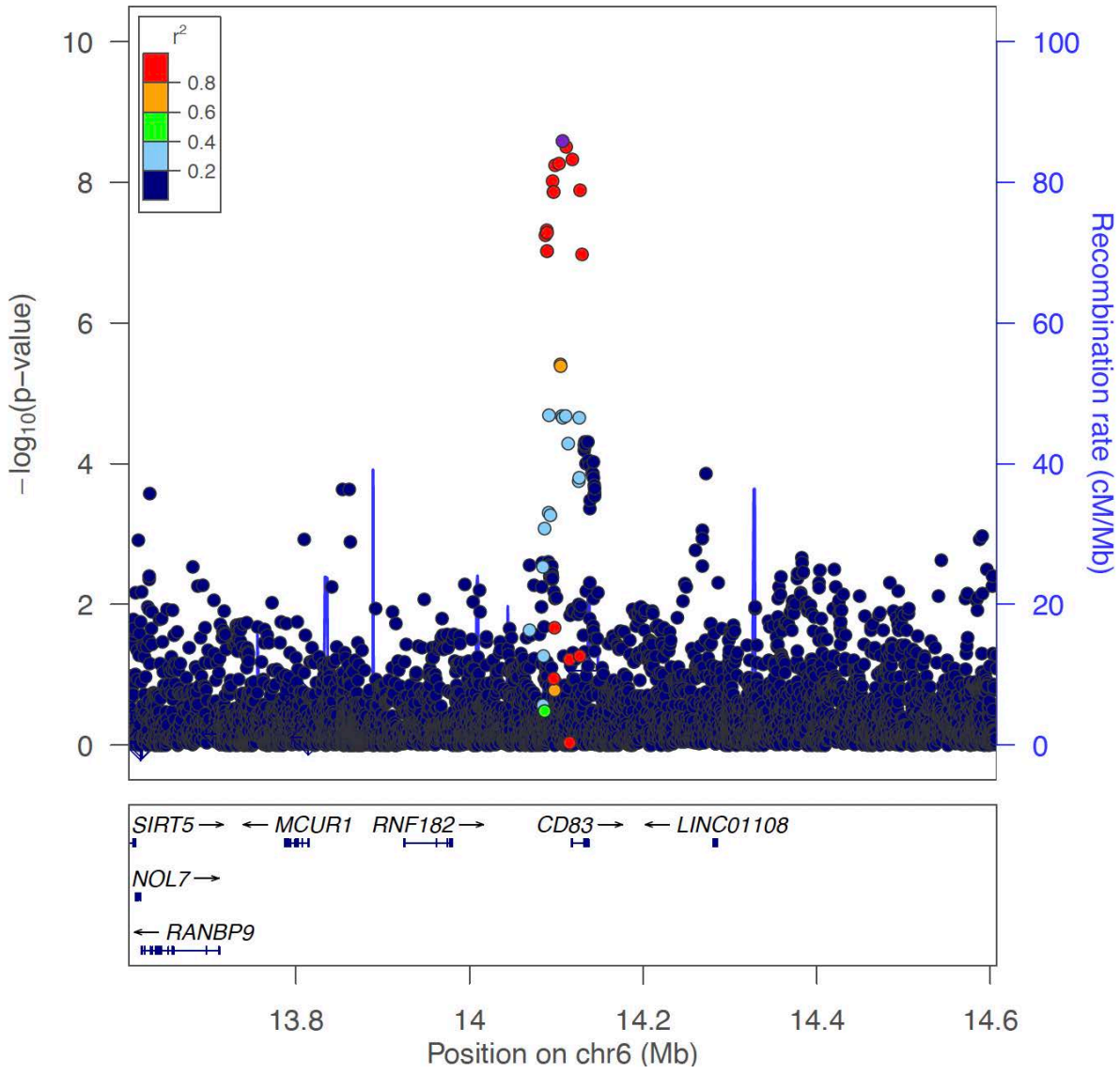

<Locus 49>
6:15195682:C:T (rs113532504)
Multi-GWAS (combined)
Novel locus

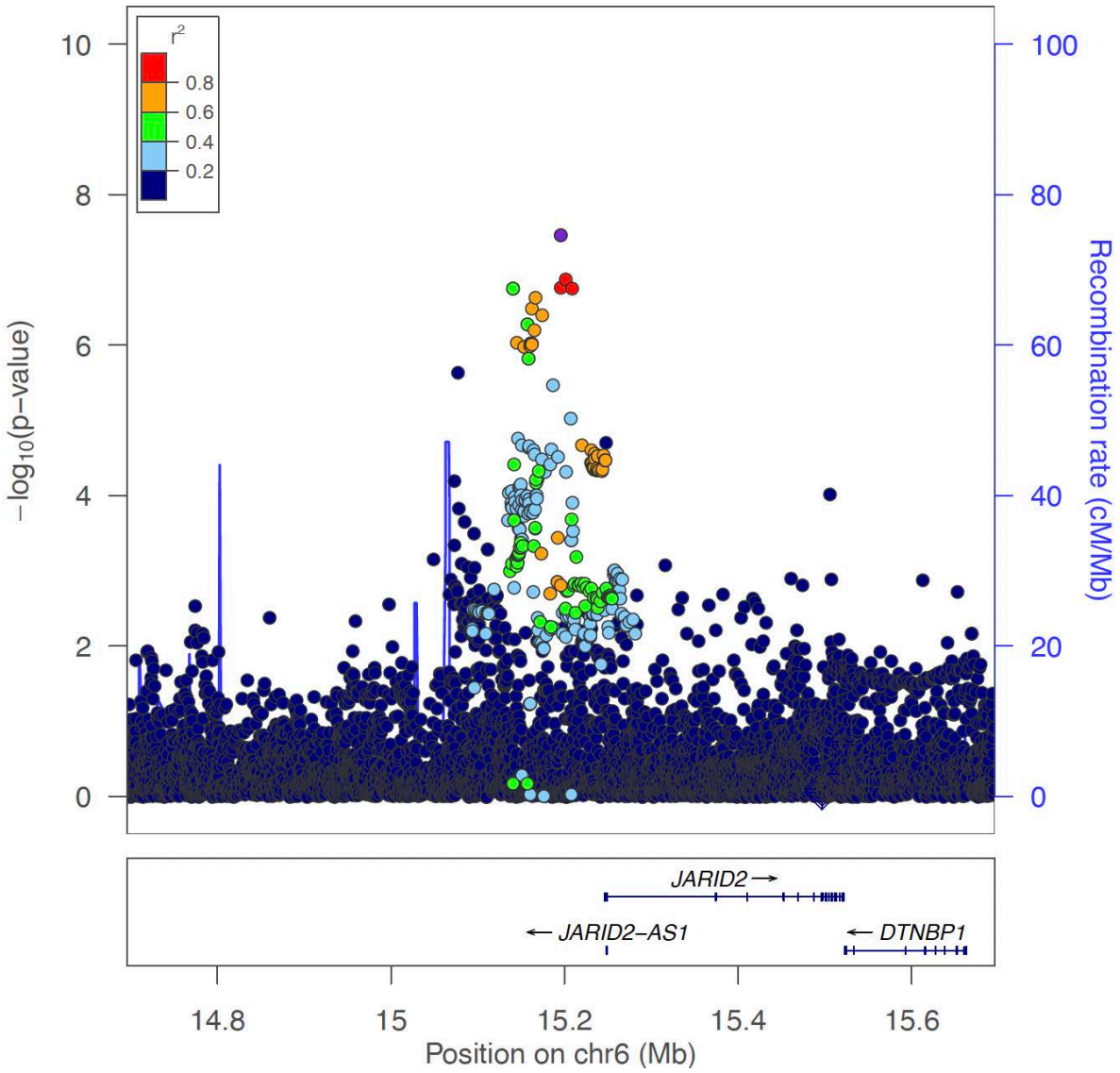

<Locus 50>
6:23925021:A:C (rs67318457)
Multi-GWAS (seroposi)
Novel locus

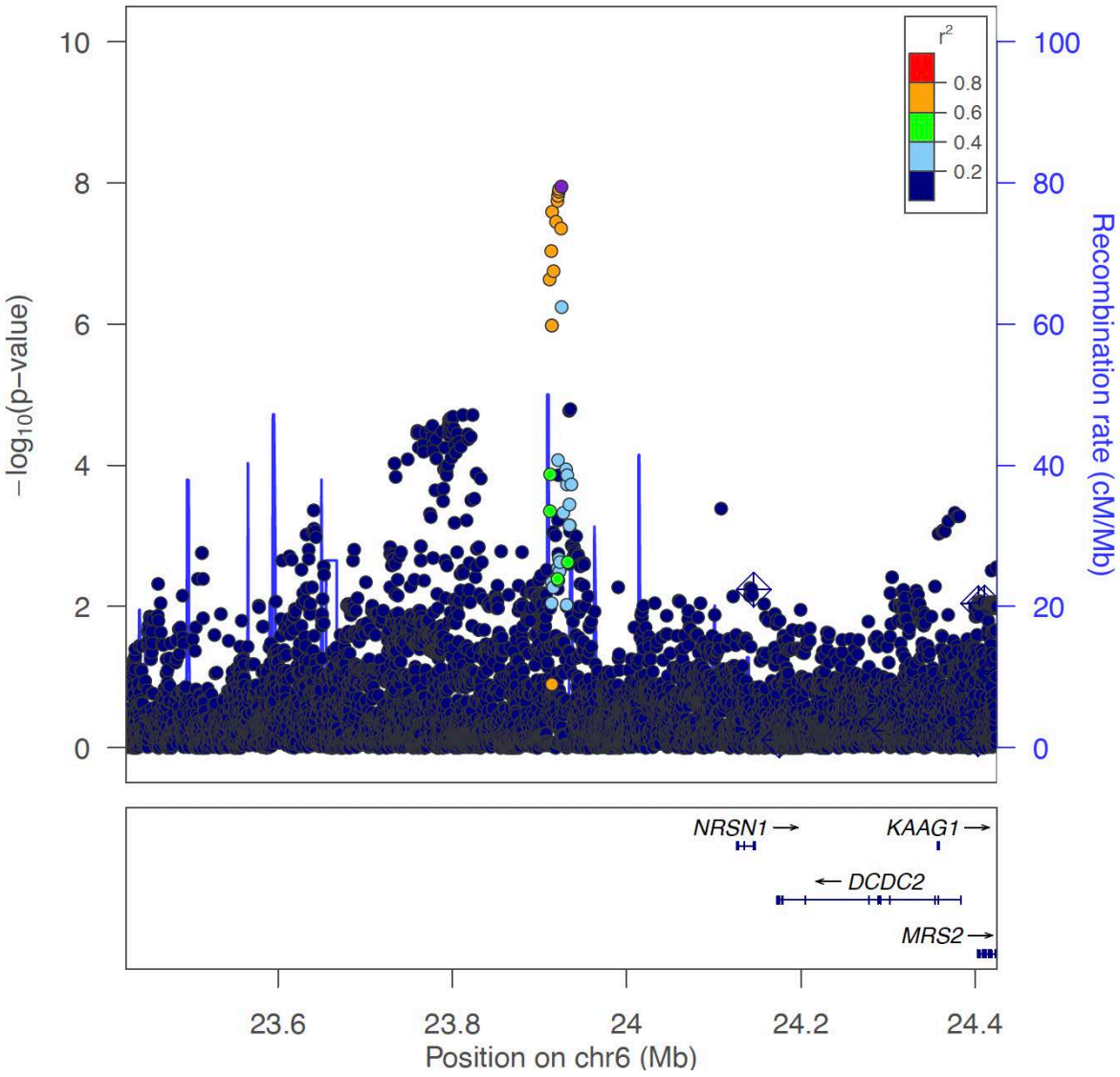

<Locus 51>
6:36381936:G:GA (rs11420145)
Multi-GWAS (combined)
Known locus

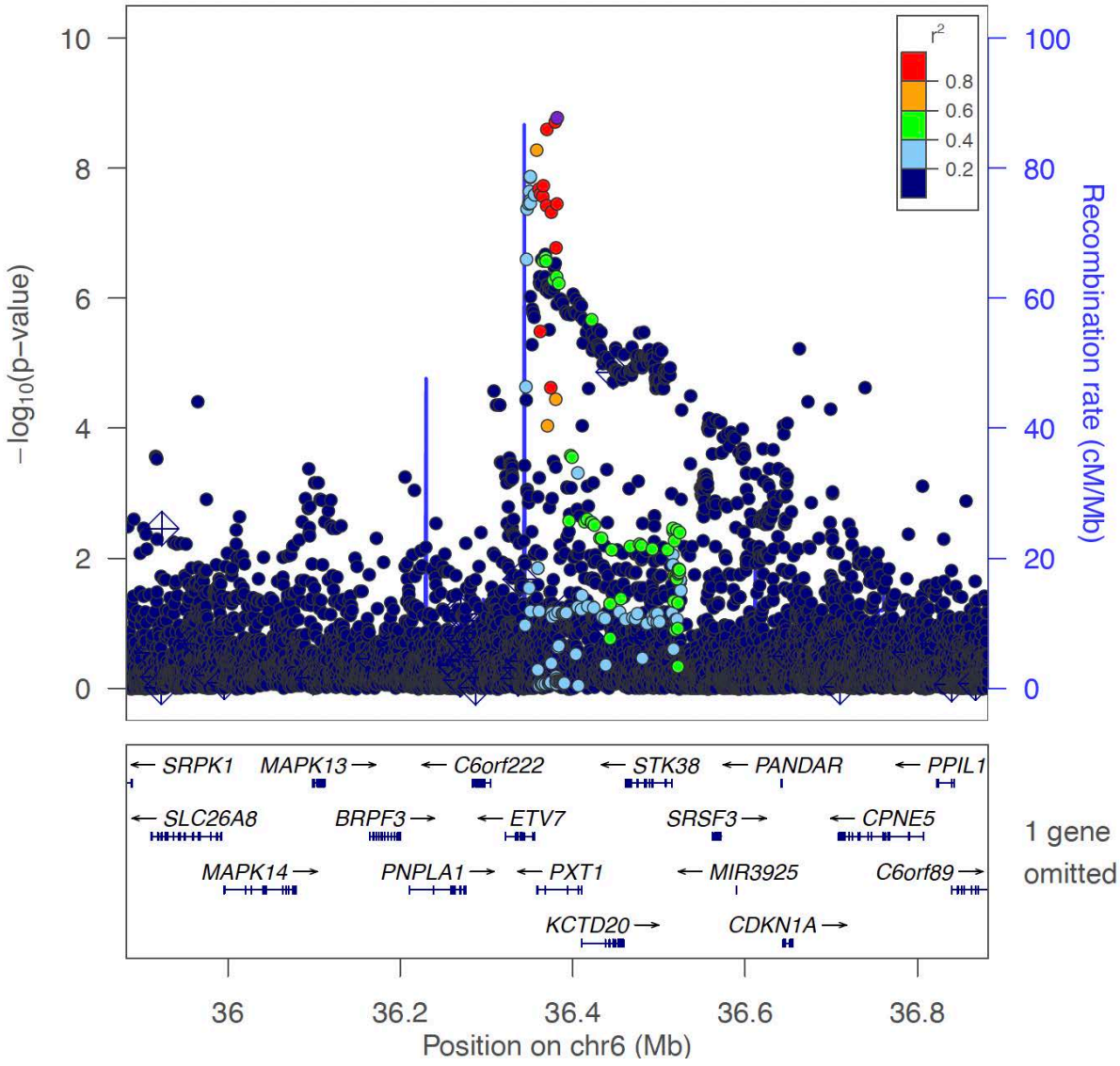

<Locus 52>
6:44234621:G:T (rs28362855)
Multi-GWAS (combined)
Known locus

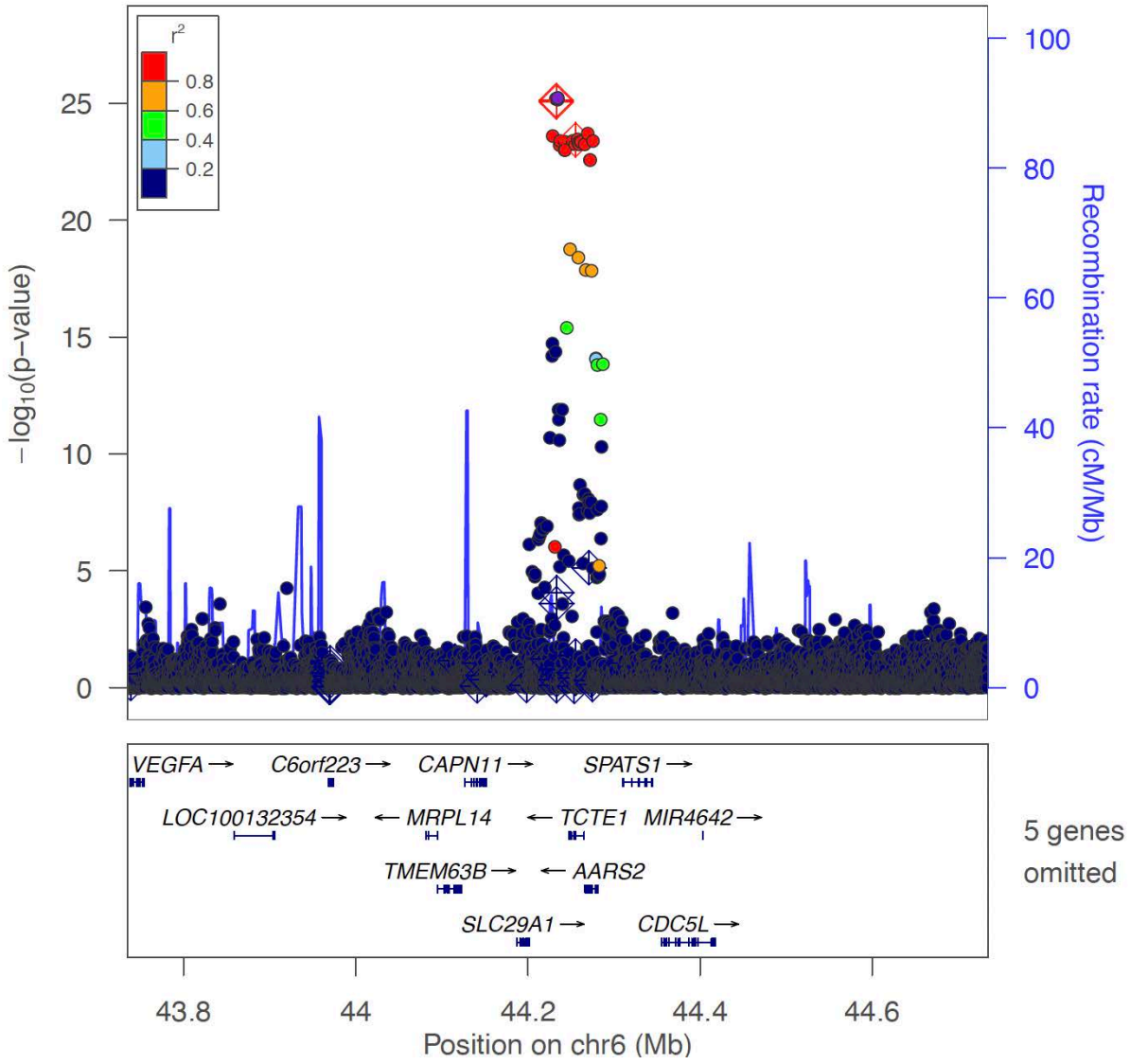

<Locus 53>
6:90976768:G:A (rs72928038)
Multi-GWAS (combined)
Known locus

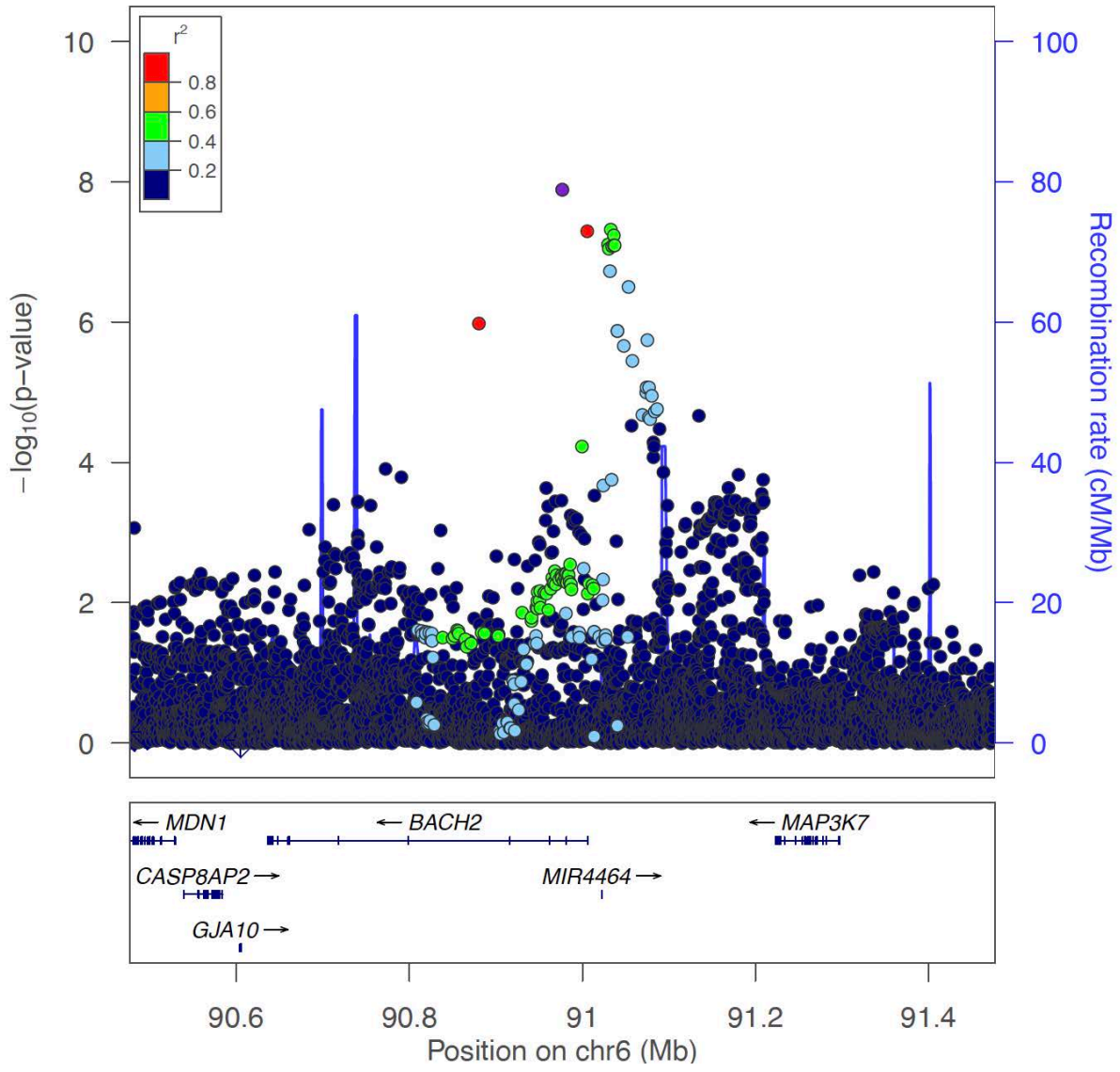

<Locus 54>
6:106727215:C:T (rs3804333)
Multi-GWAS (combined)
Known locus

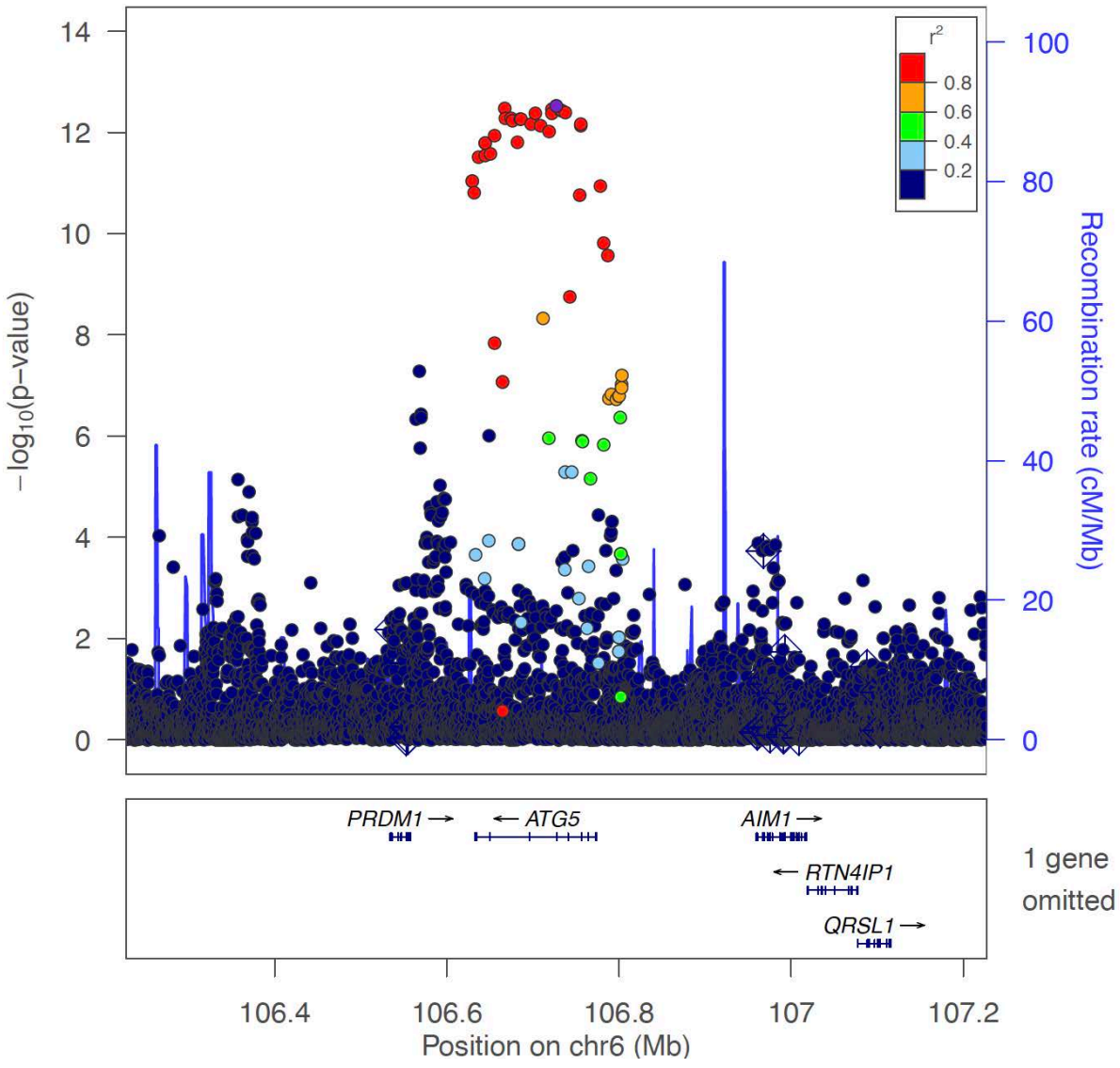

<Locus 55>
6:137999562:GA:G (rs35926684)
Multi-GWAS (combined)
Known locus

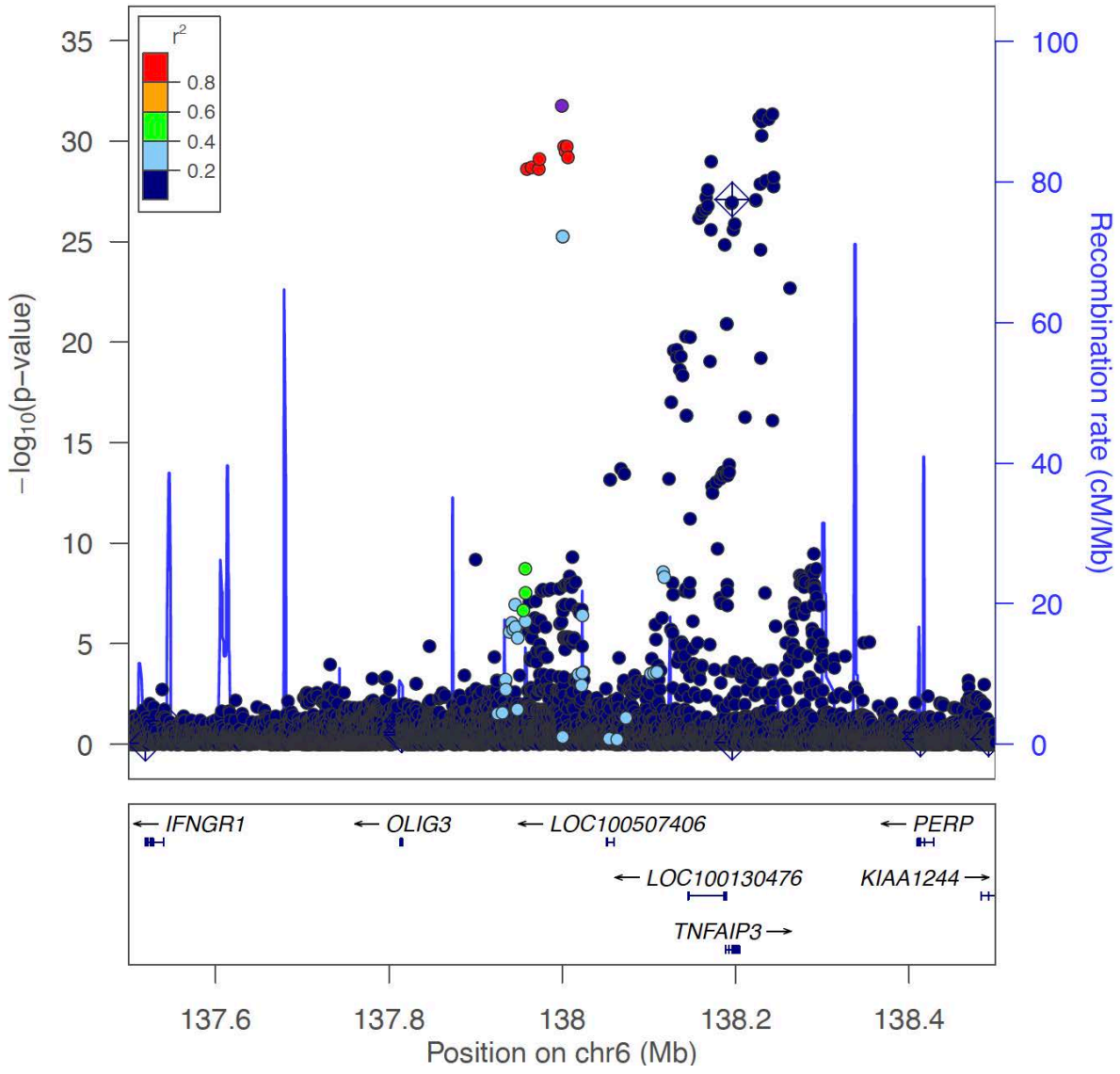

<Locus 56>
6:159503086:A:G (rs2485362)
Multi-GWAS (combined)
Known locus

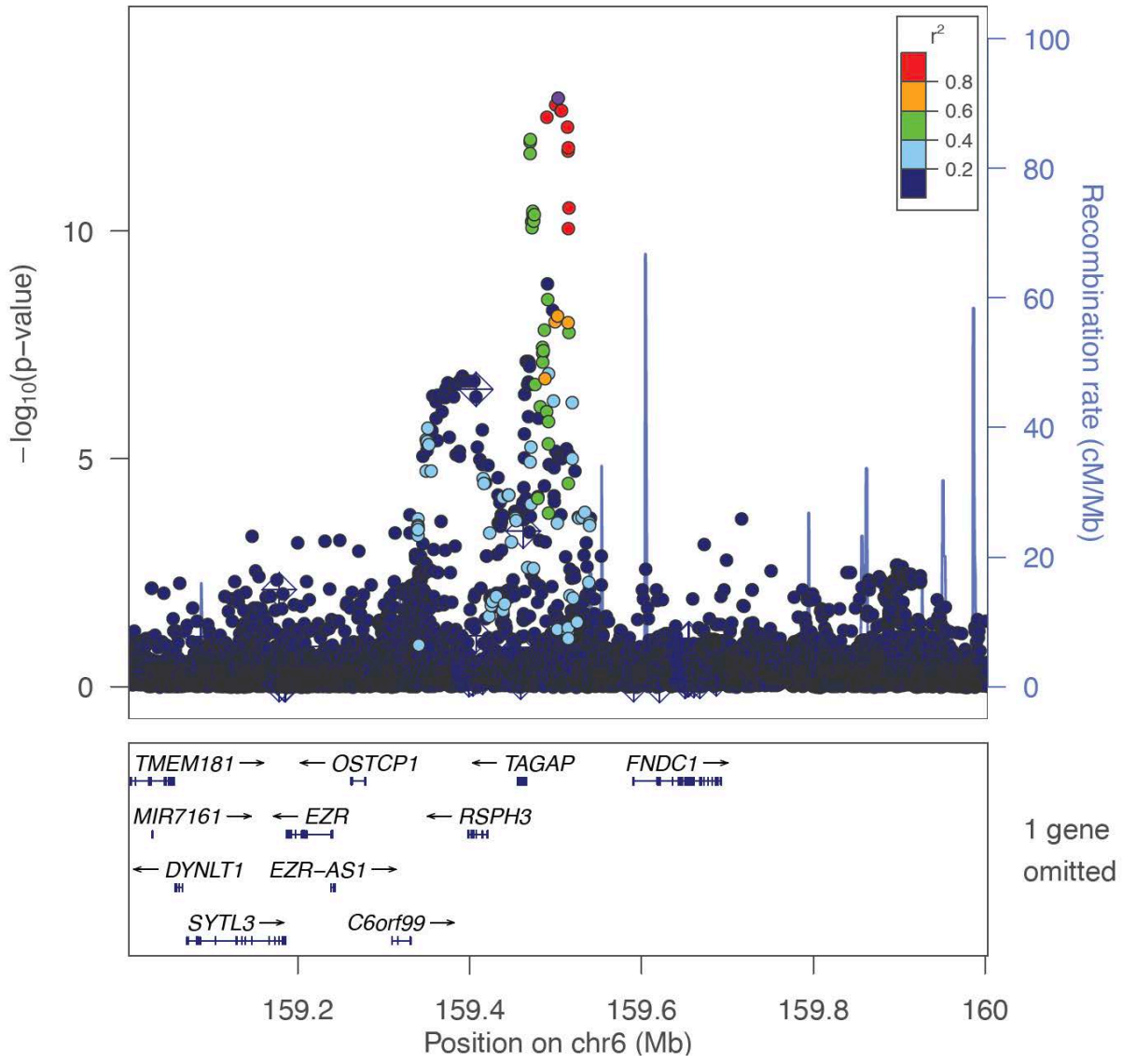

<Locus 57>
6:167541258:C:G (rs3093017)
Multi-GWAS (combined)
Known locus

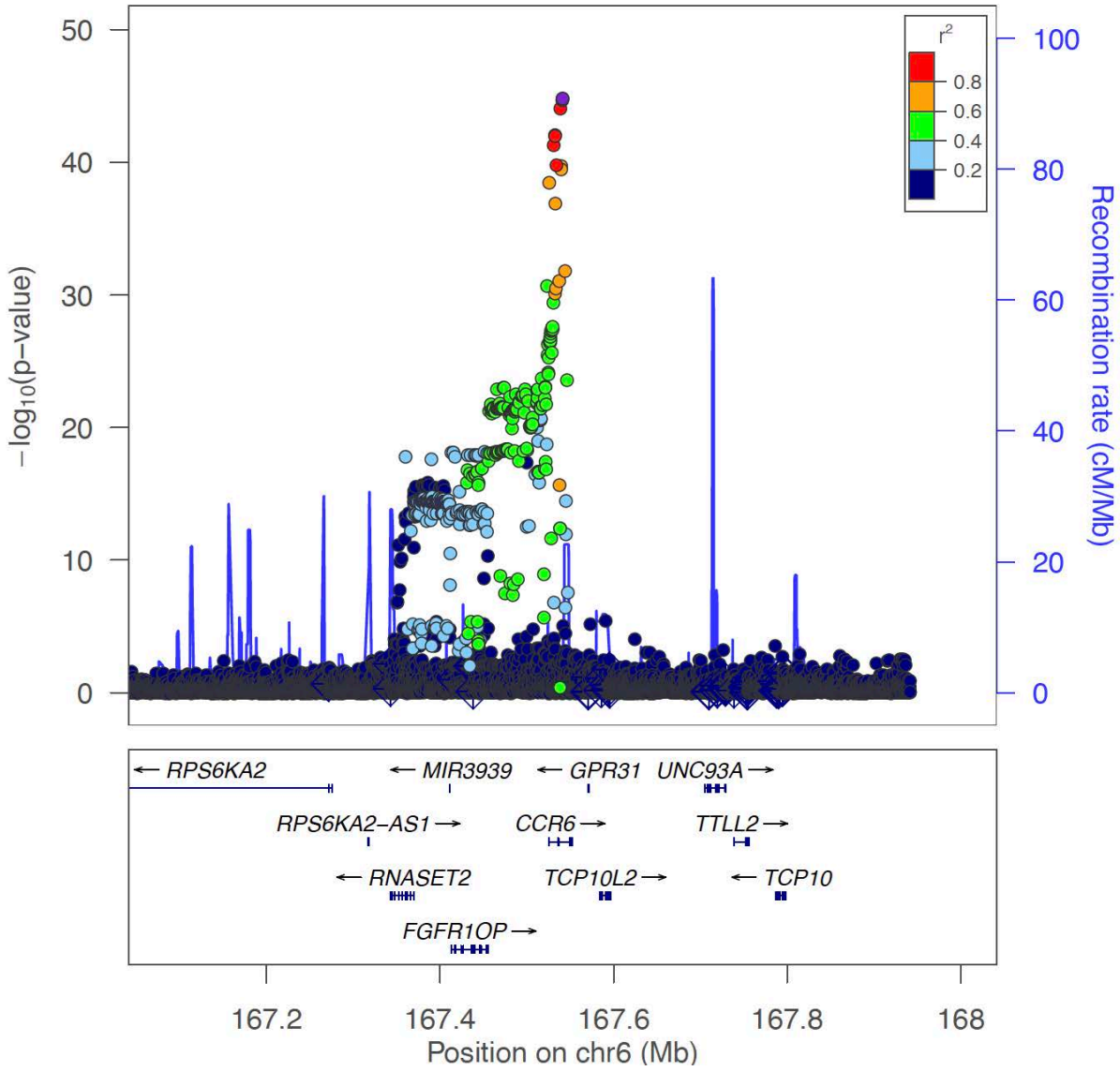

<Locus 58>
7:17207164:T:G (rs940825)
EUR-GWAS (combined)
Novel locus

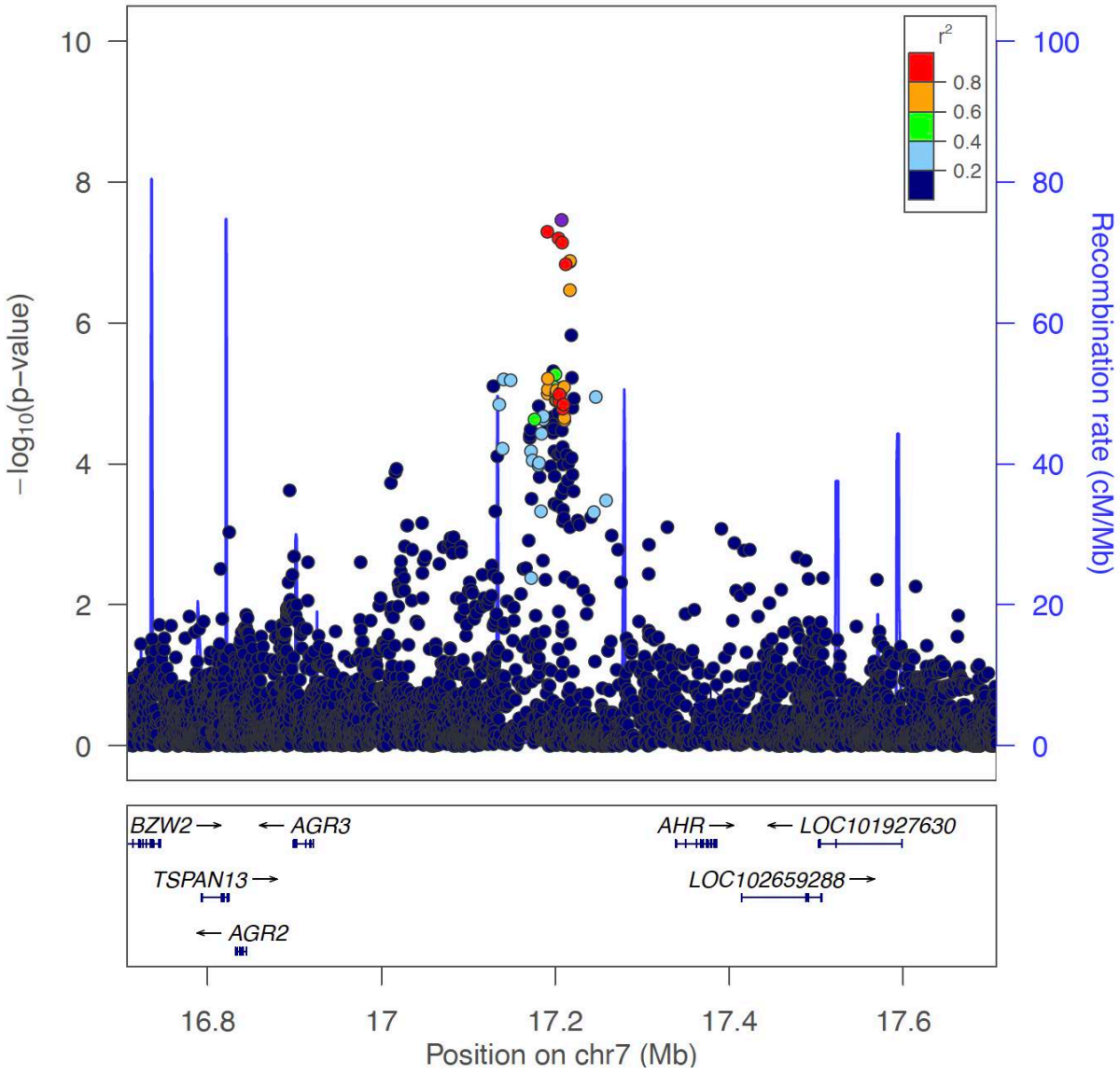

<Locus 59>
7:27084581:C:T (rs182199544)
Multi-GWAS (combined)
Novel locus

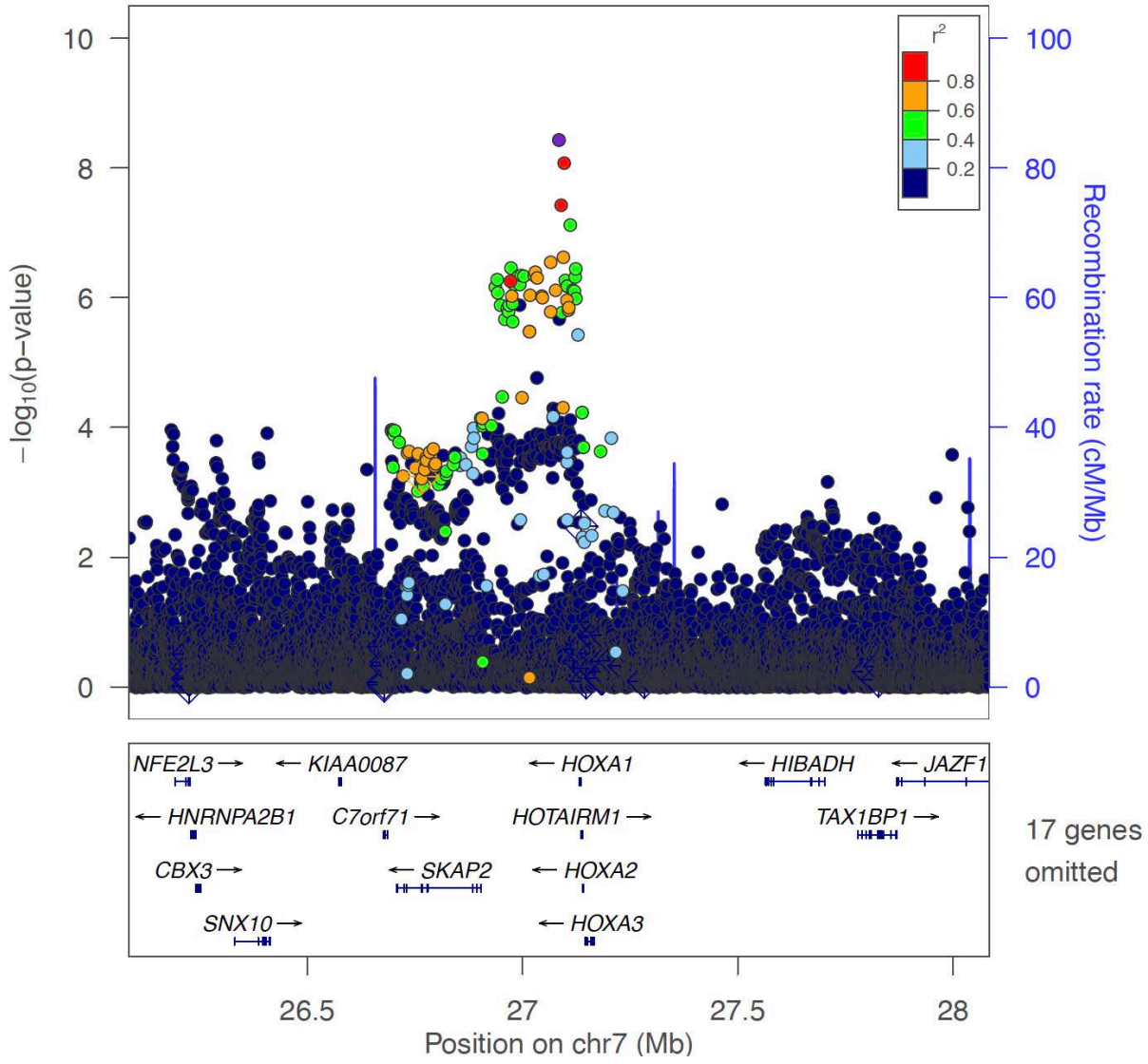

<Locus 60>
7:50361874:A:T (rs6583441)
Multi-GWAS (combined)
Novel locus

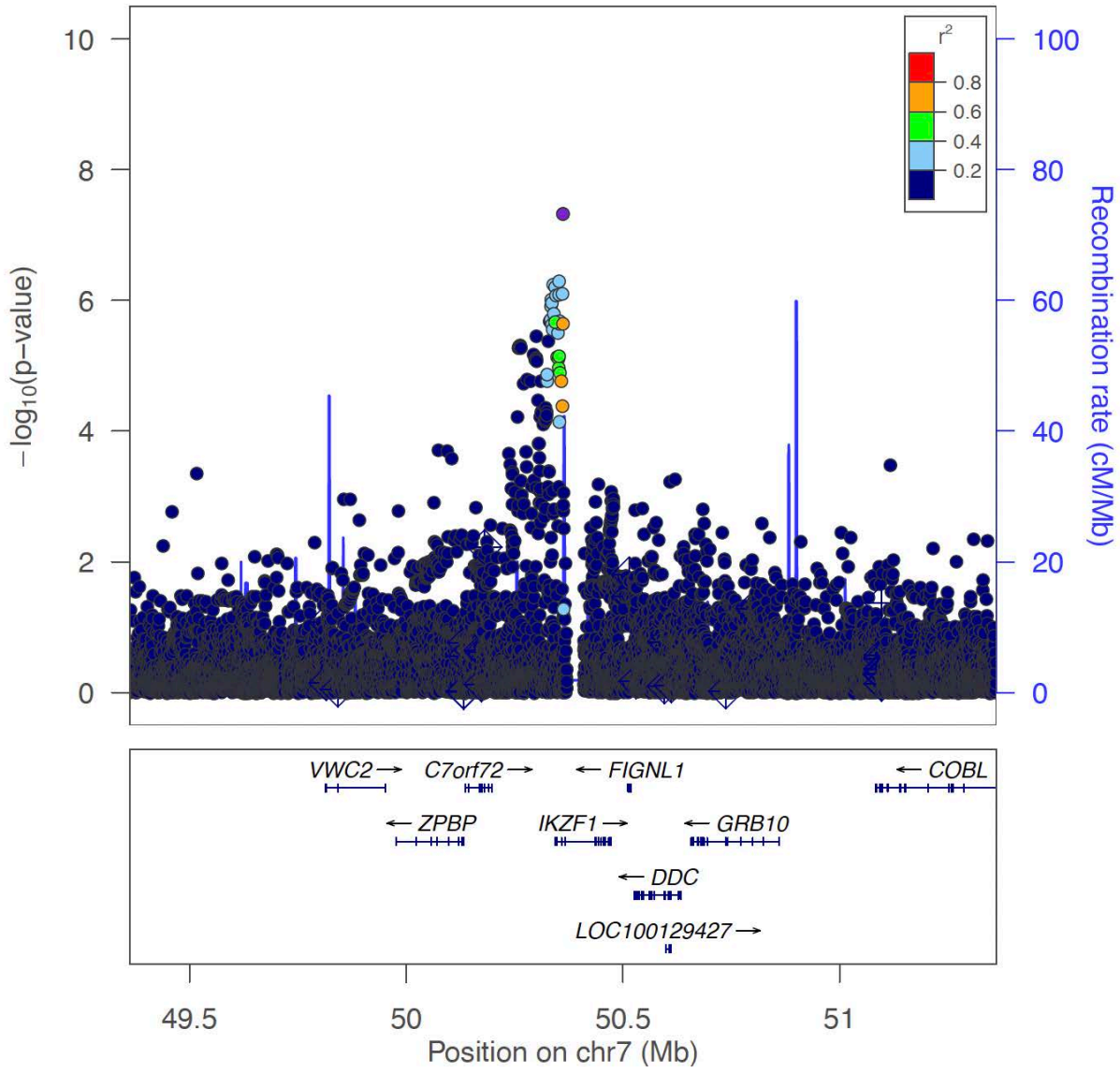

<Locus 61>
7:92250140:T:G (rs42044)
Multi-GWAS (combined)
Known locus

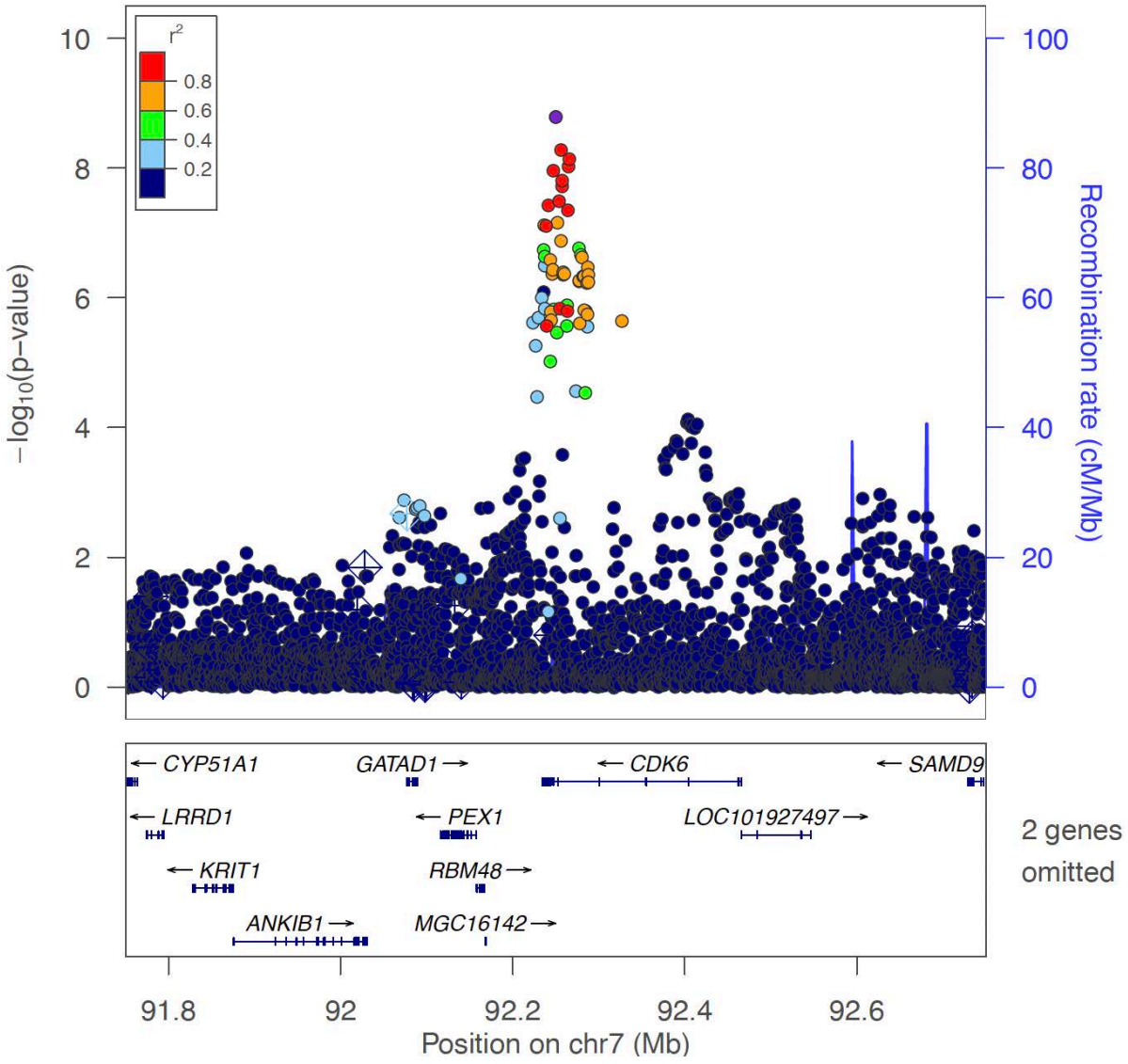

<Locus 62>
7:99893148:C:G (rs6979218)
Multi-GWAS (combined)
Novel locus

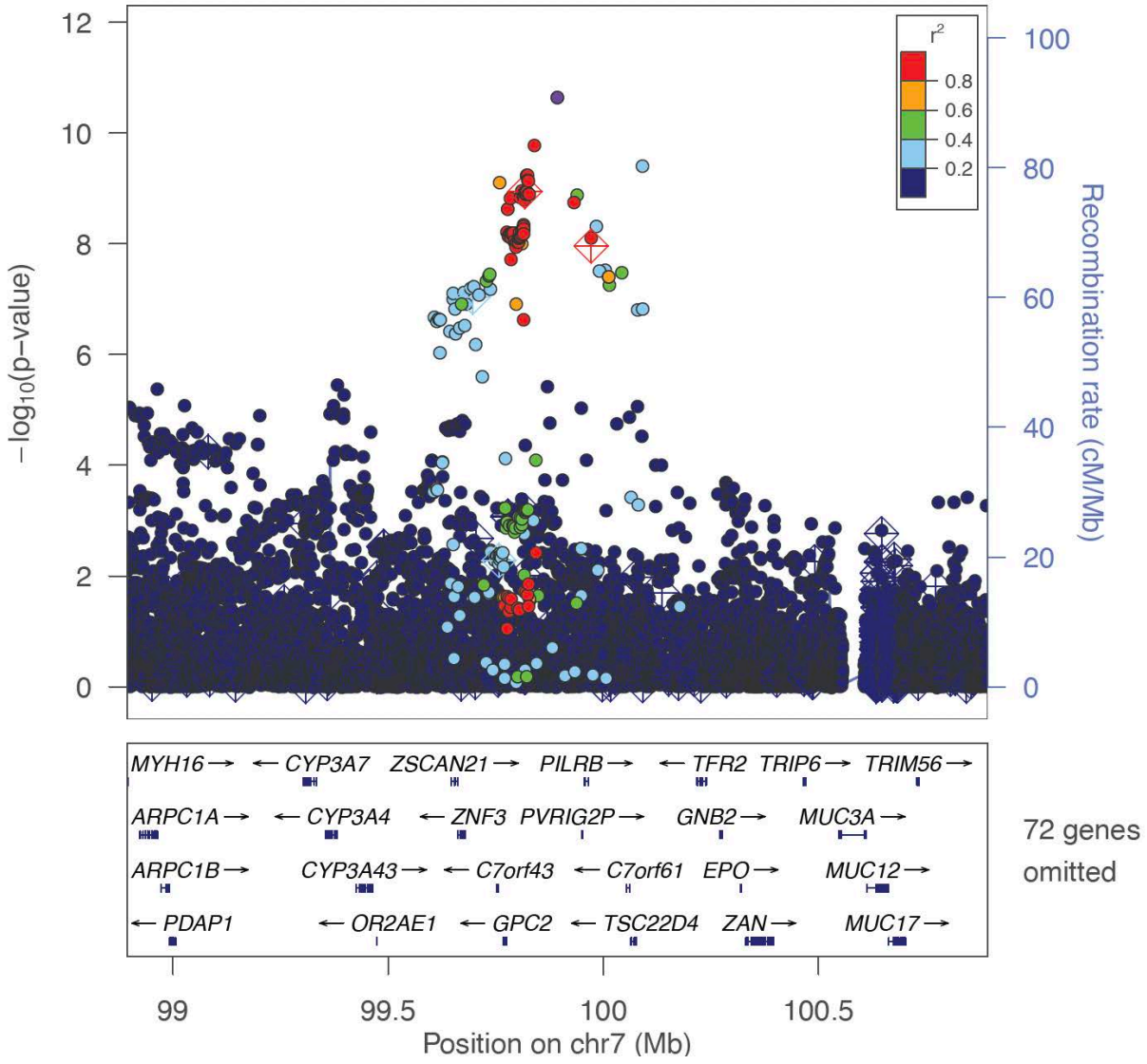

<Locus 63>
7:128576086:T:C (rs3757387)
Multi-GWAS (combined)
Known locus

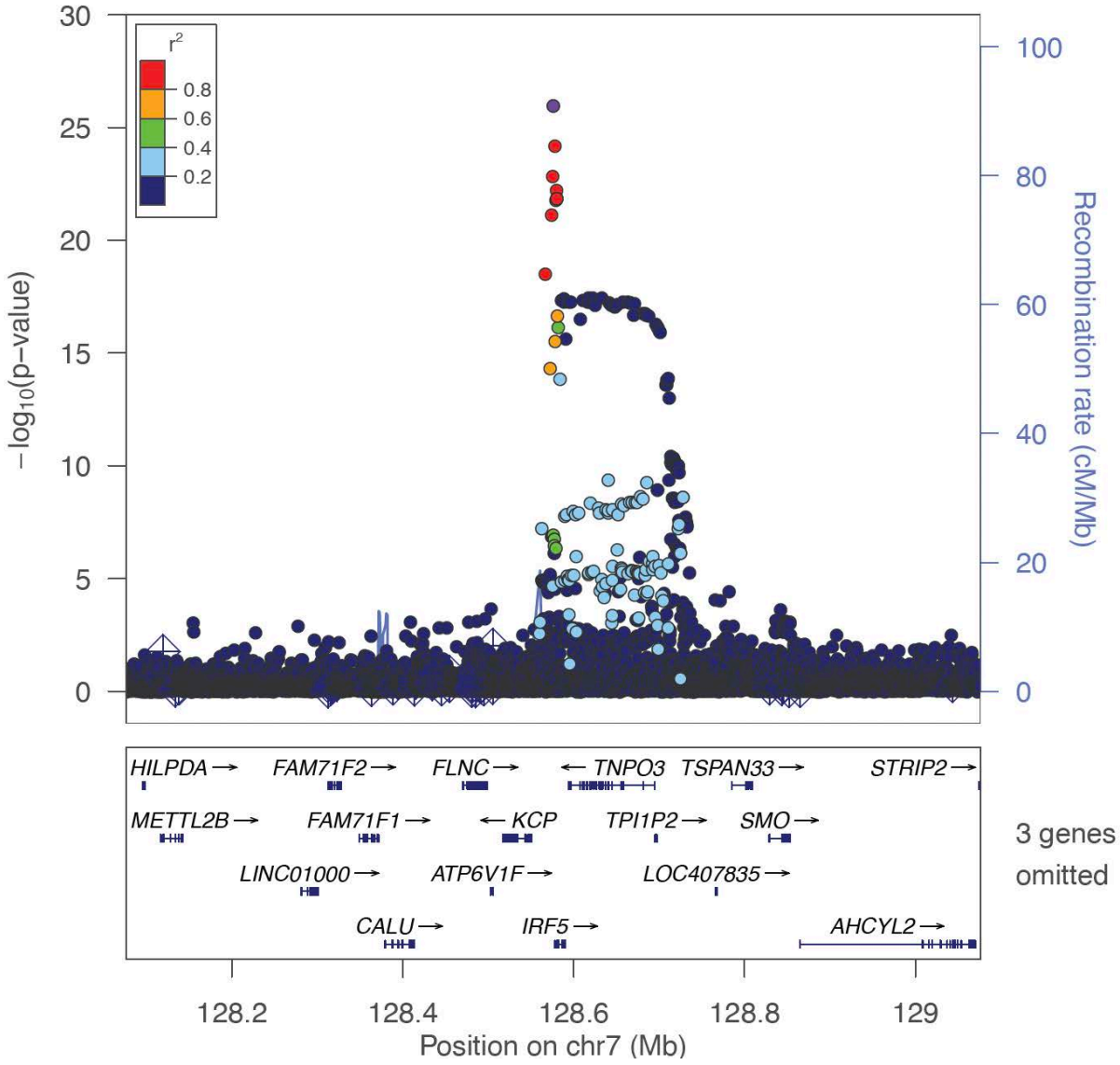

<Locus 64>
8:11343973:C:T (rs2736340)
Multi-GWAS (combined)
Known locus

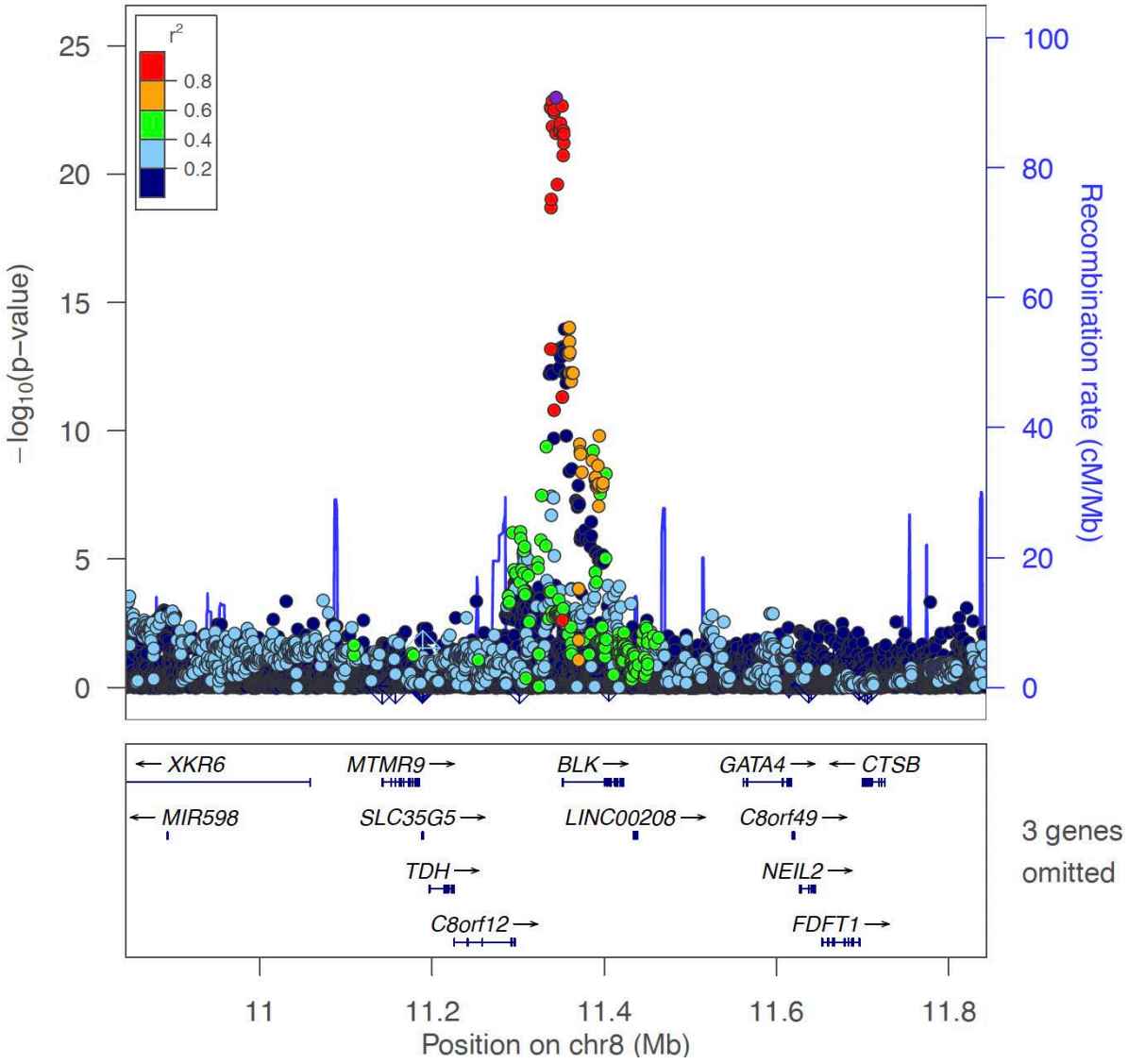

<Locus 65>
8:81135682:T:C (rs10453119)
Multi-GWAS (combined)
Known locus

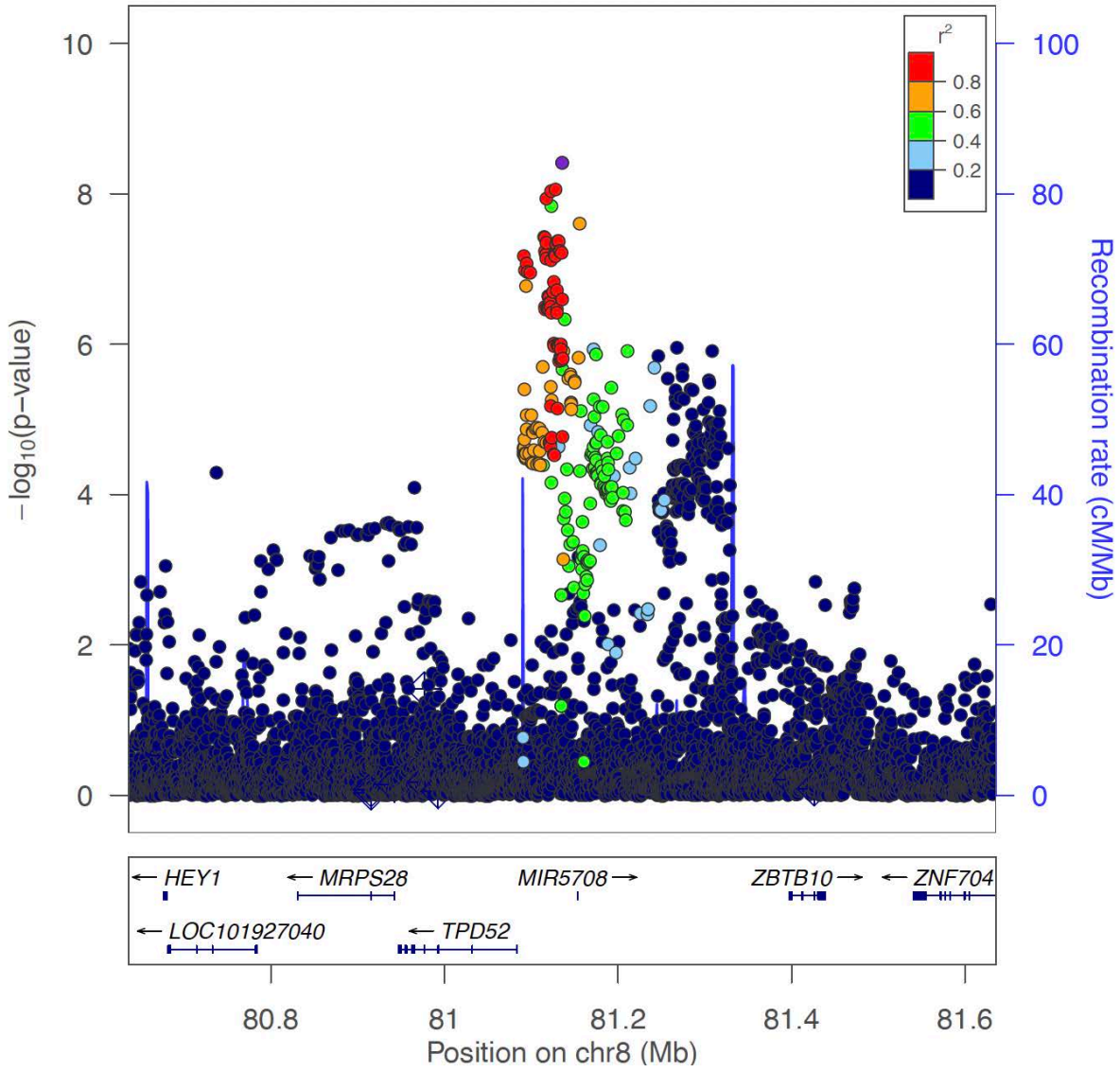

<Locus 66>
8:102453350:T:C (rs1264600)
Multi-GWAS (combined)
Known locus

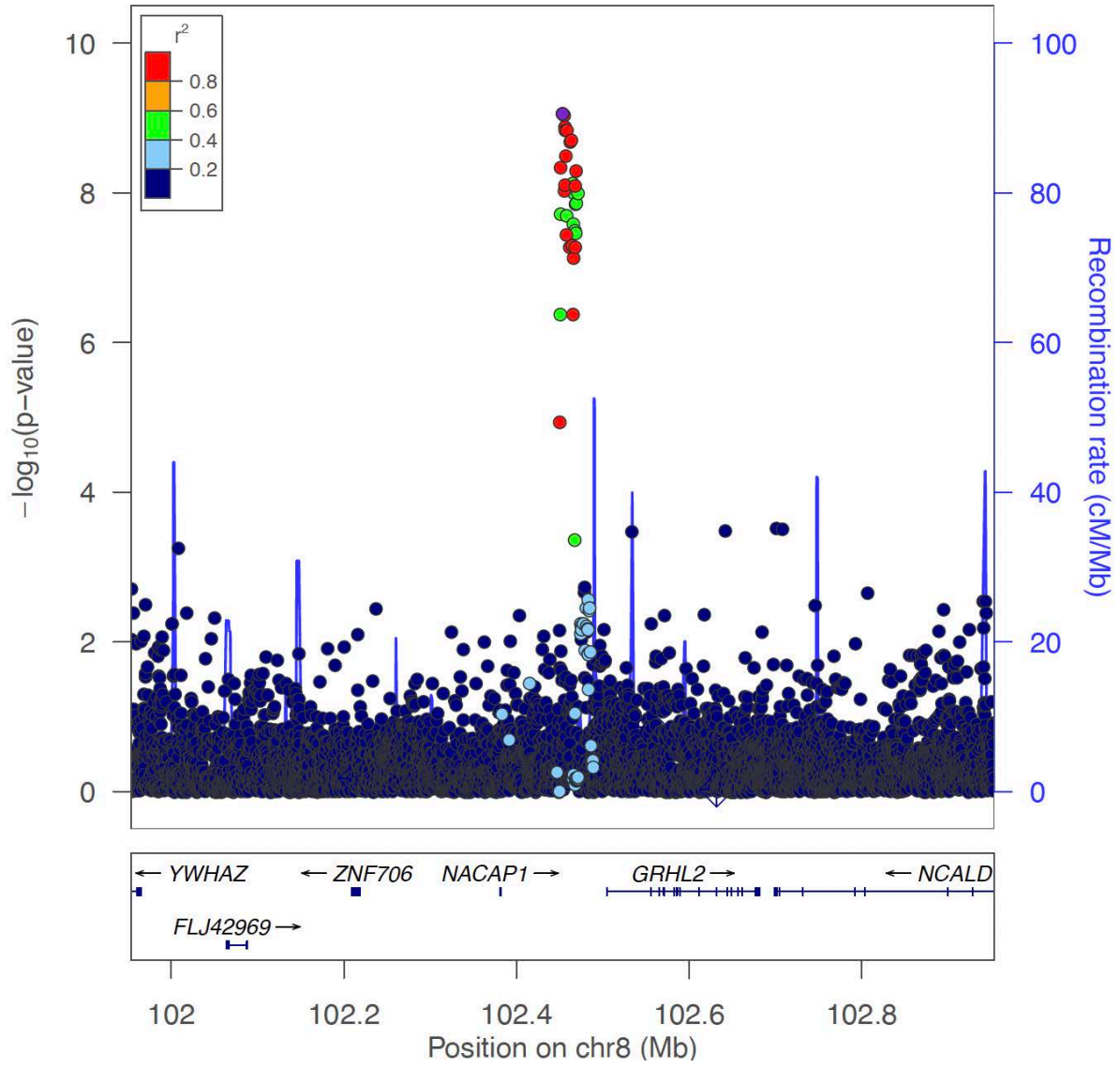

<Locus 67>
8:129576477:T:C (rs16903108)
Multi-GWAS (combined)
Known locus

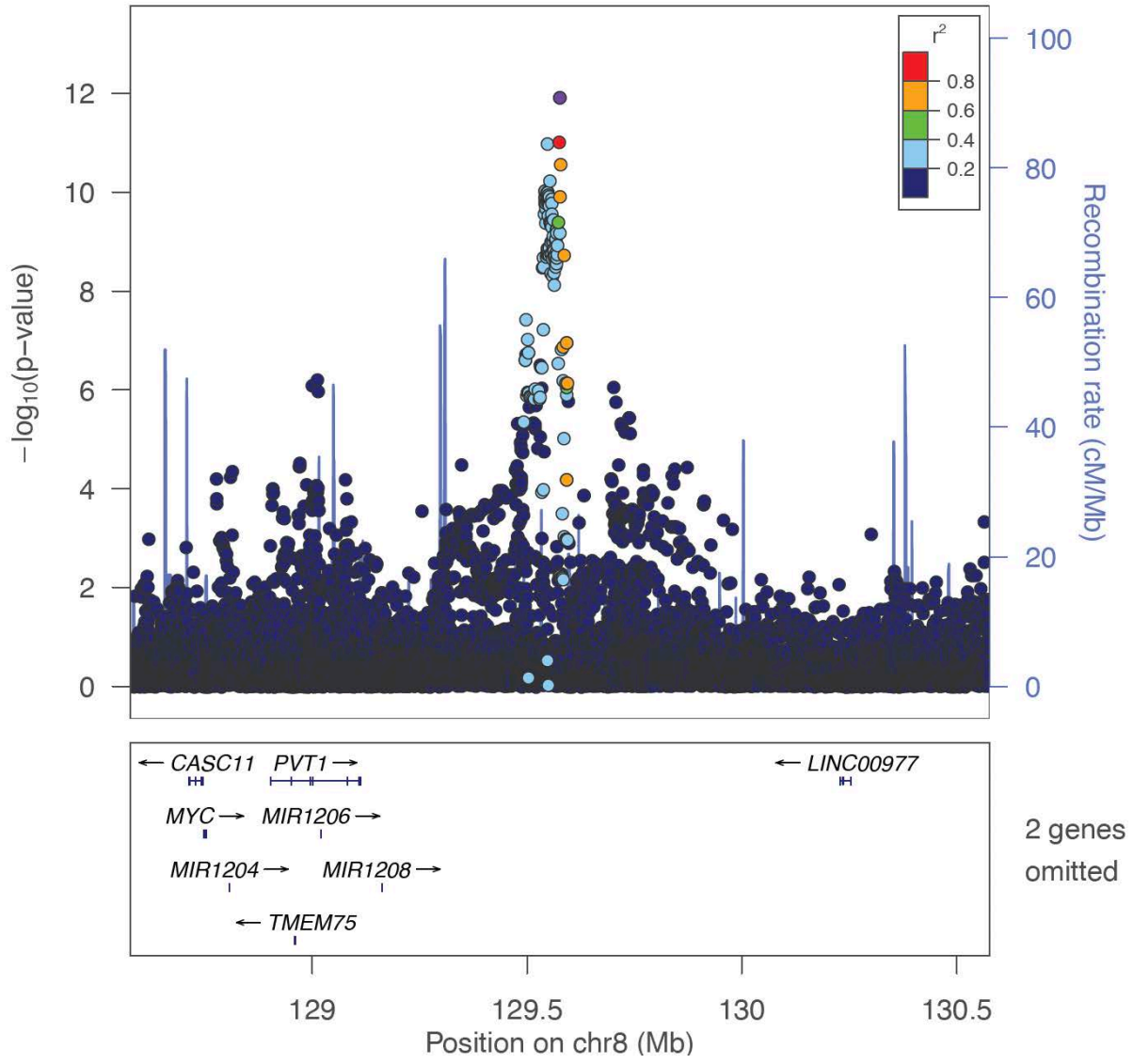

<Locus 68>
8:134211965:G:A (rs11777380)
Multi-GWAS (combined)
Novel locus

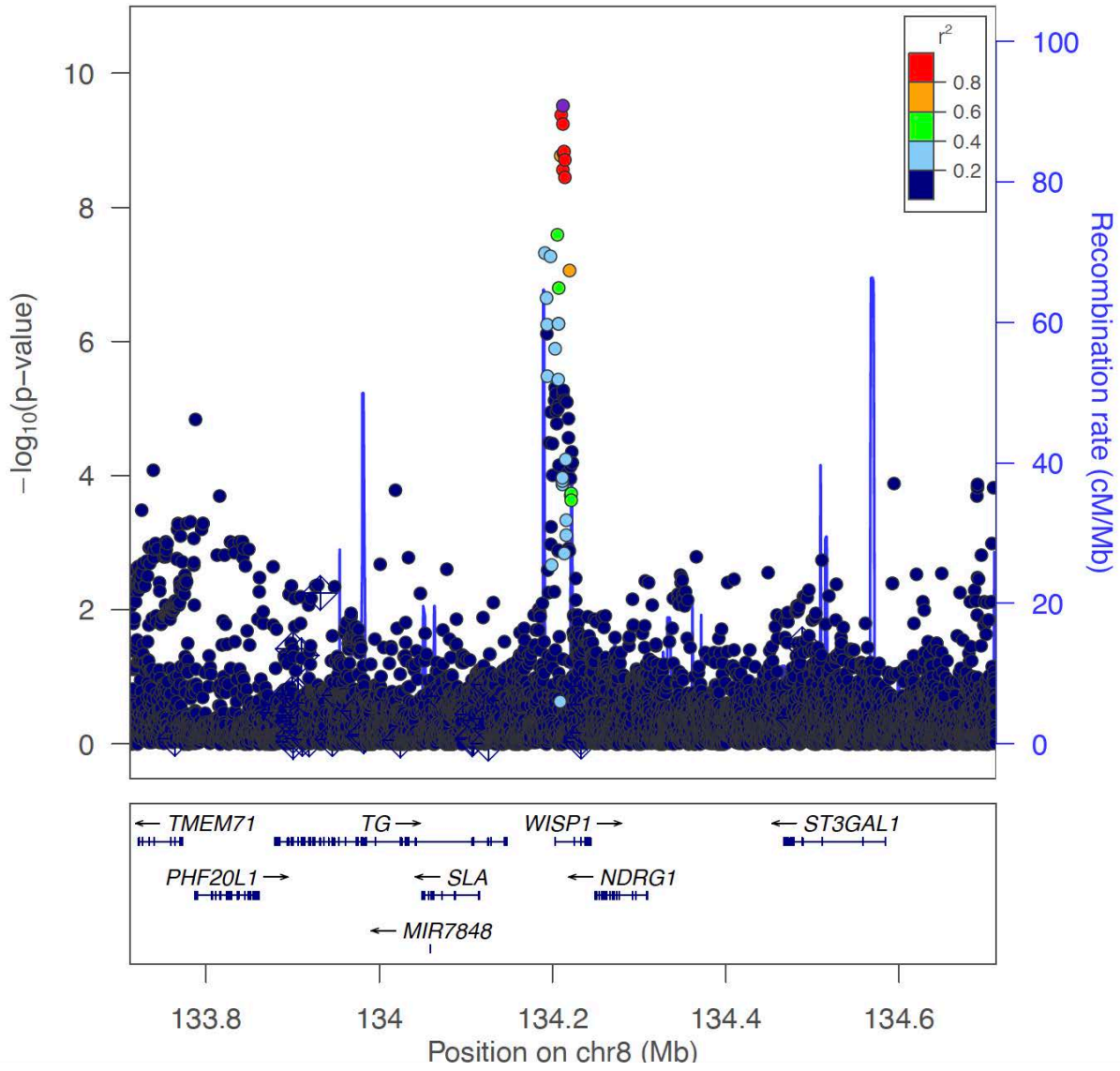

<Locus 69>
9:5438435:C:A (rs911760)
EUR-GWAS (seroposi)
Novel locus

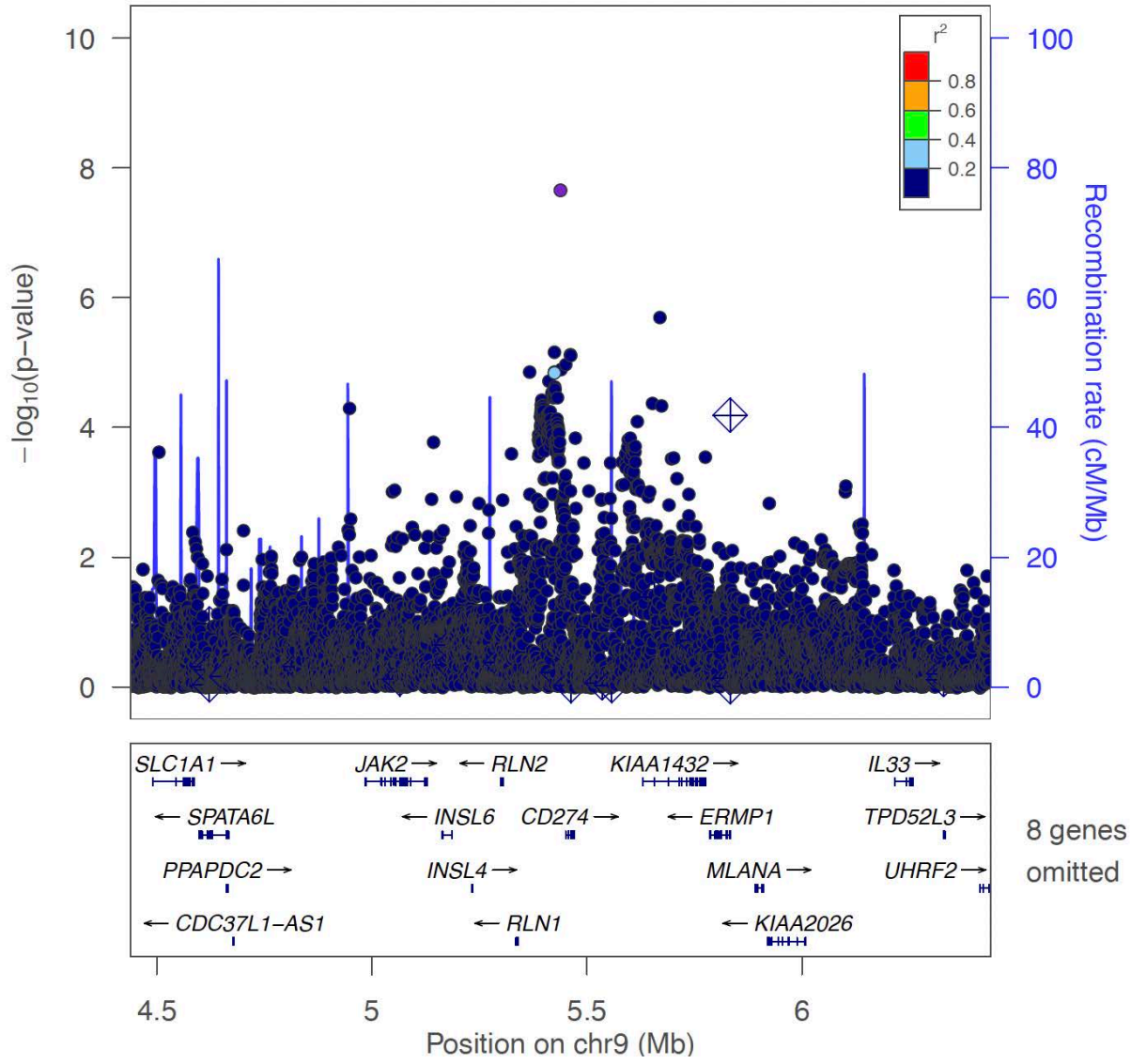

<Locus 70>
9:34710260:G:A (rs2812378)
Multi-GWAS (combined)
Known locus

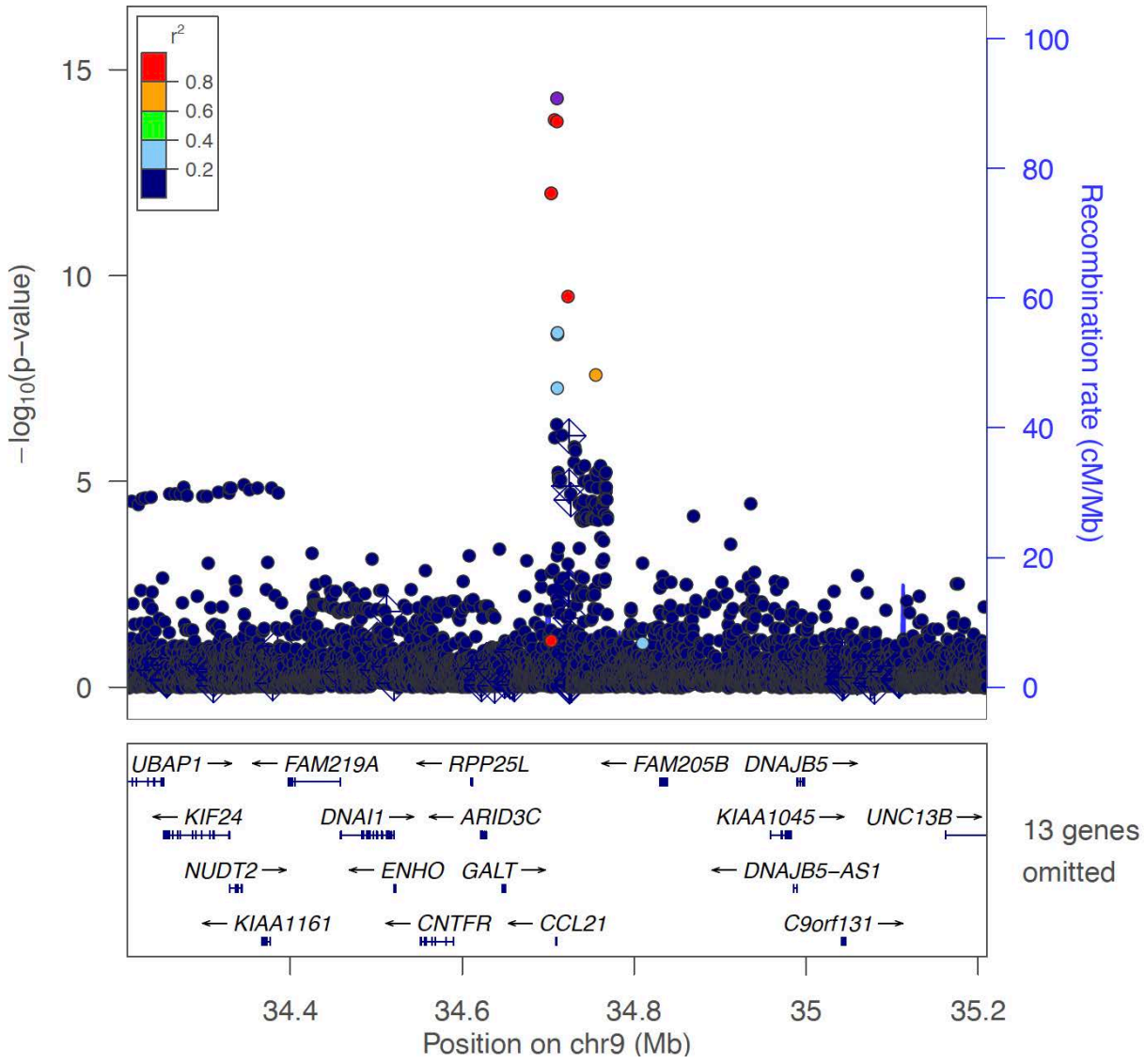

<Locus 71>
9:123640500:T:C (rs1953126)
Multi-GWAS (combined)
Known locus

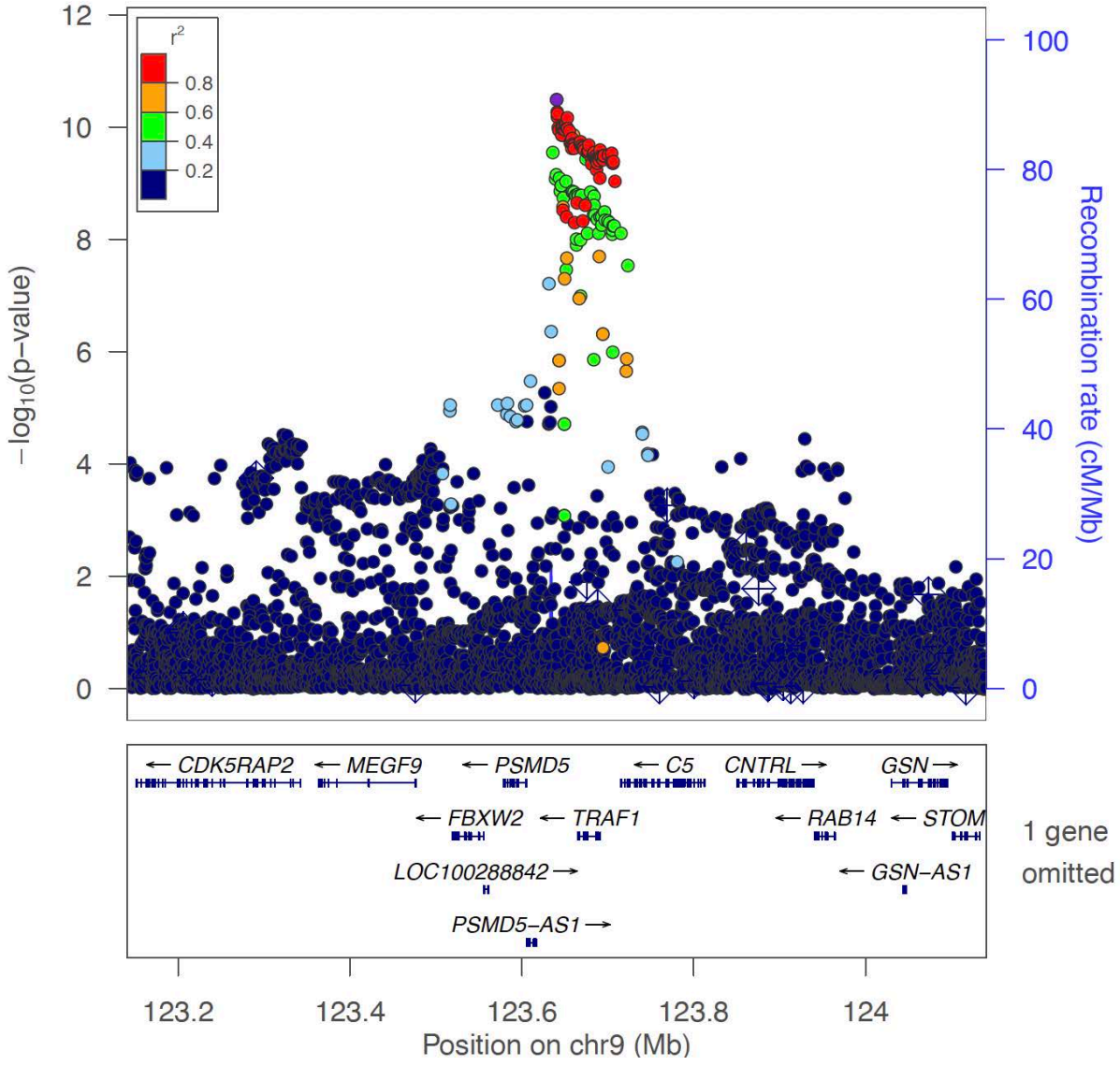

<Locus 72>
10:6100725:G:A (rs3134883)
Multi-GWAS (combined)
Known locus

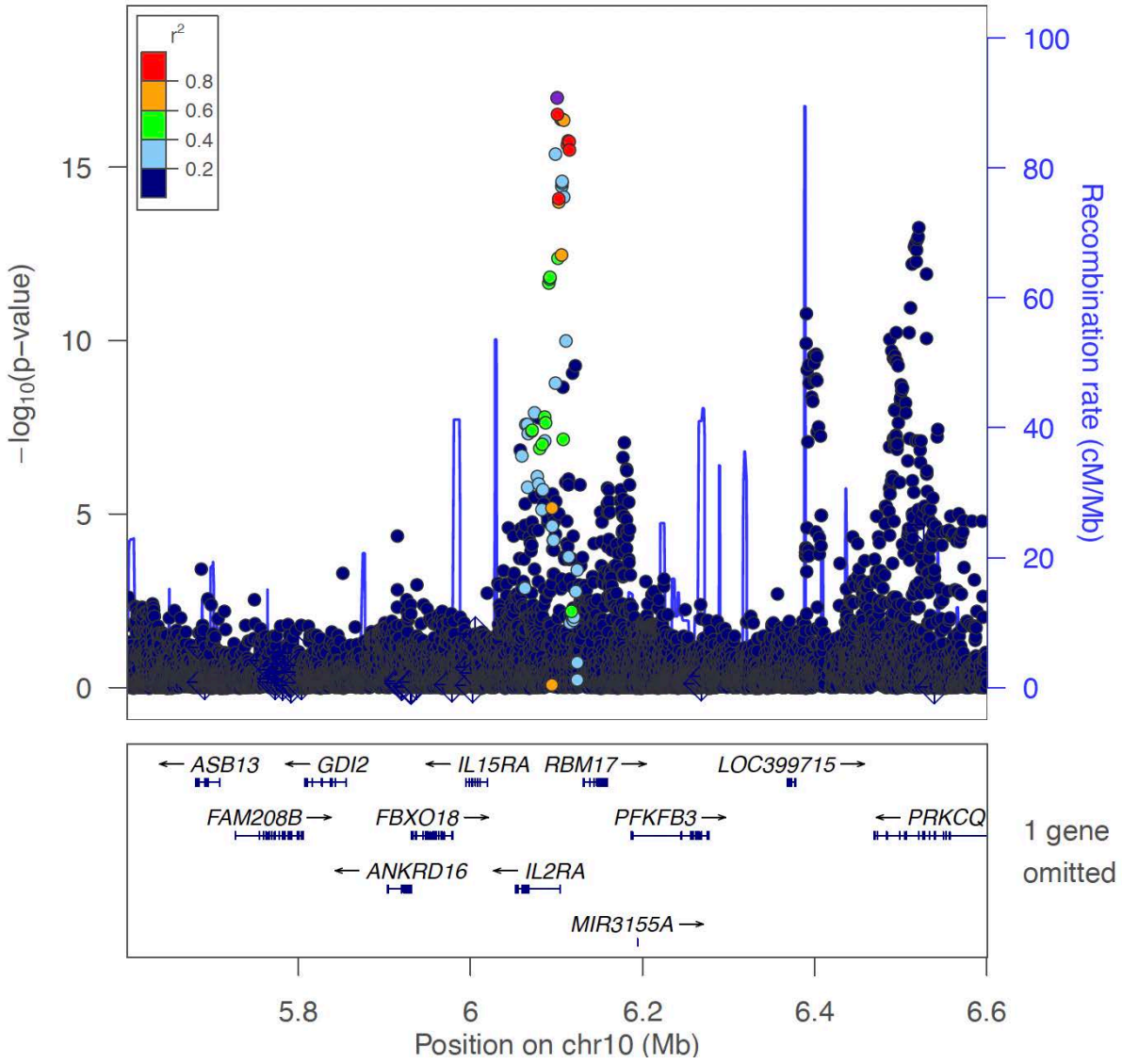

<Locus 73>
10:8115362:C:A (rs10905284)
Multi-GWAS (combined)
Known locus

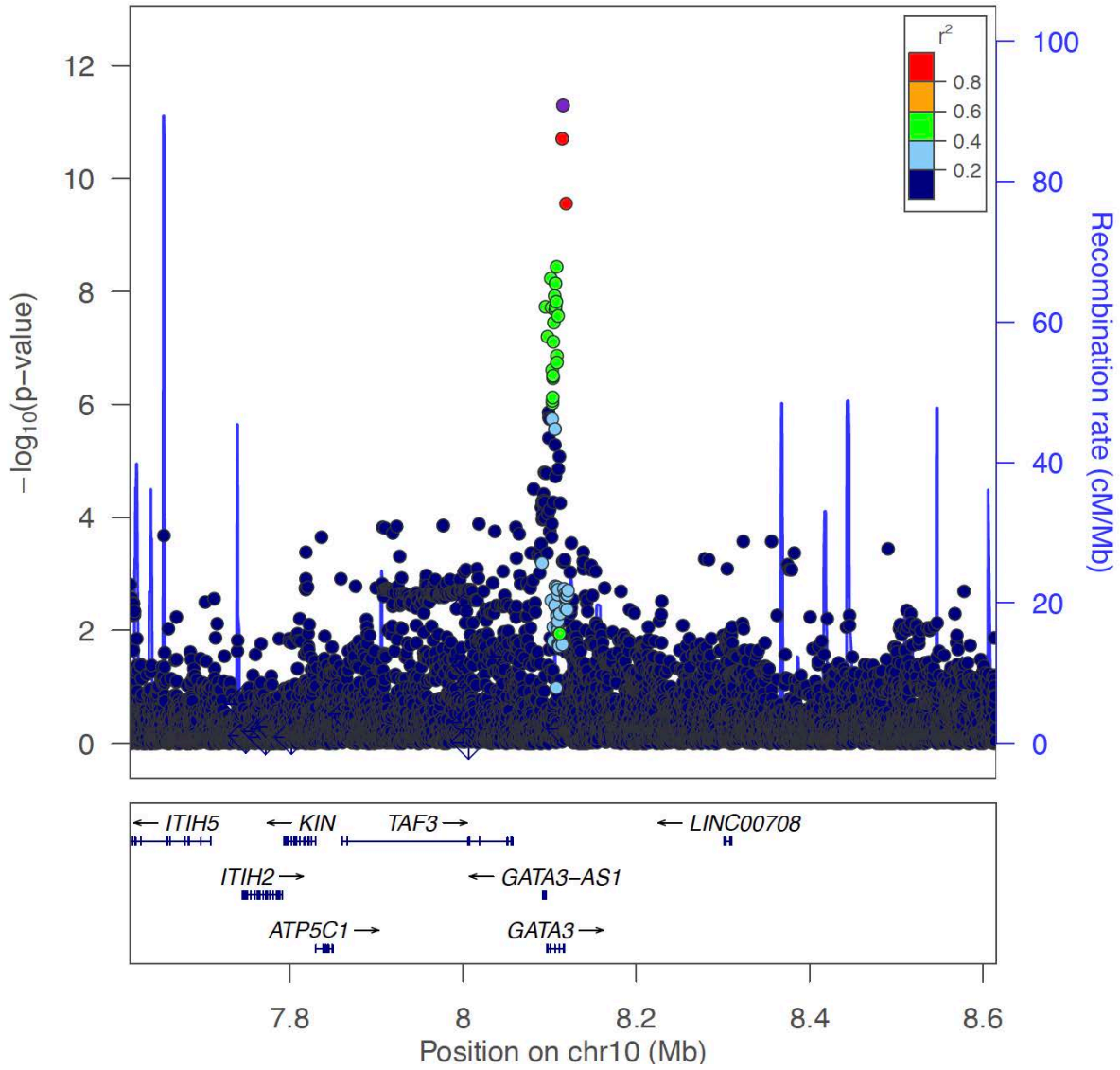

<Locus 74>
10:31385974:C:T (rs793095)
Multi-GWAS (combined)
Known locus

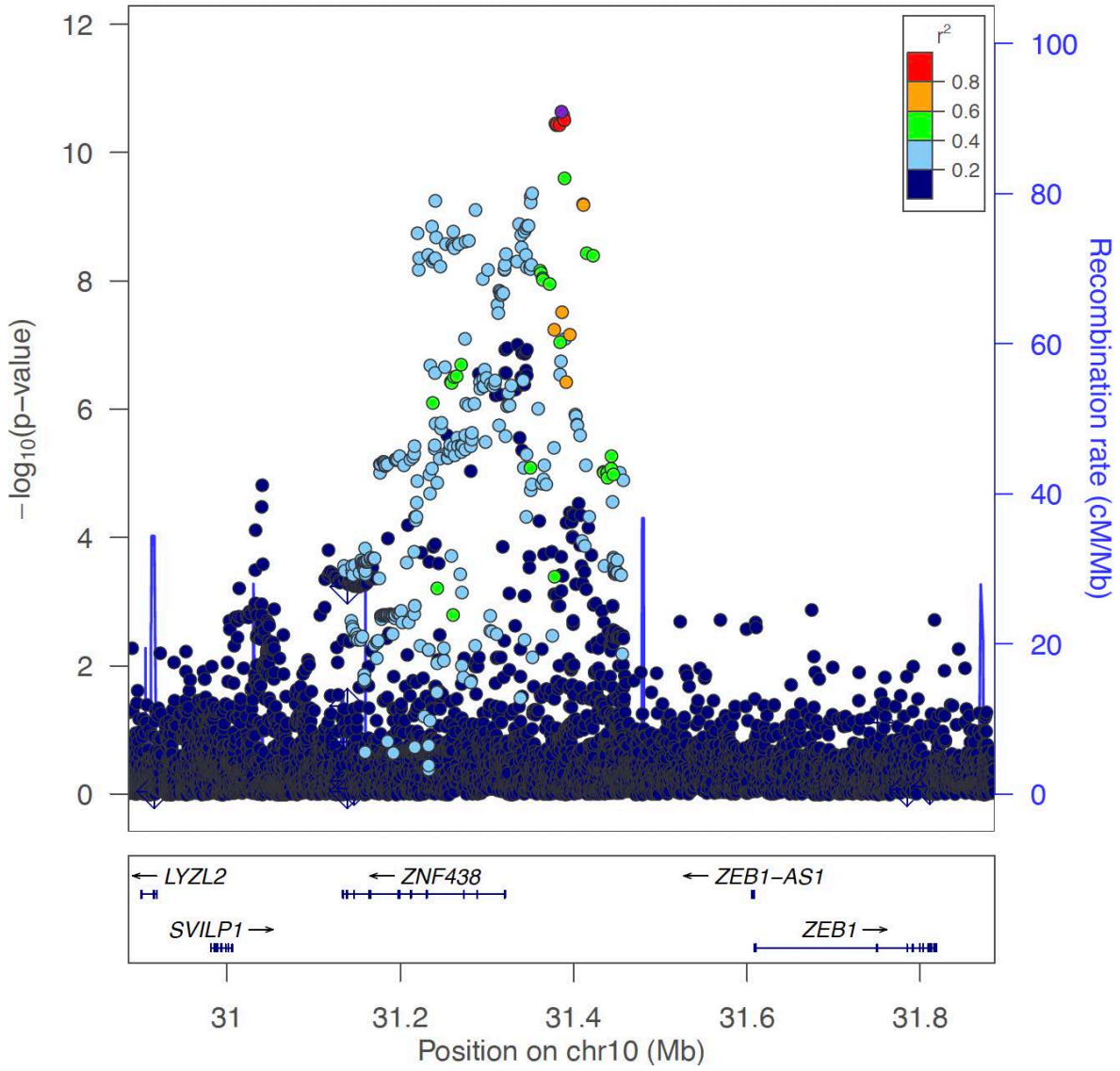

<Locus 75>
10:50025396:G:A (rs7097397)
Multi-GWAS (combined)
Known locus

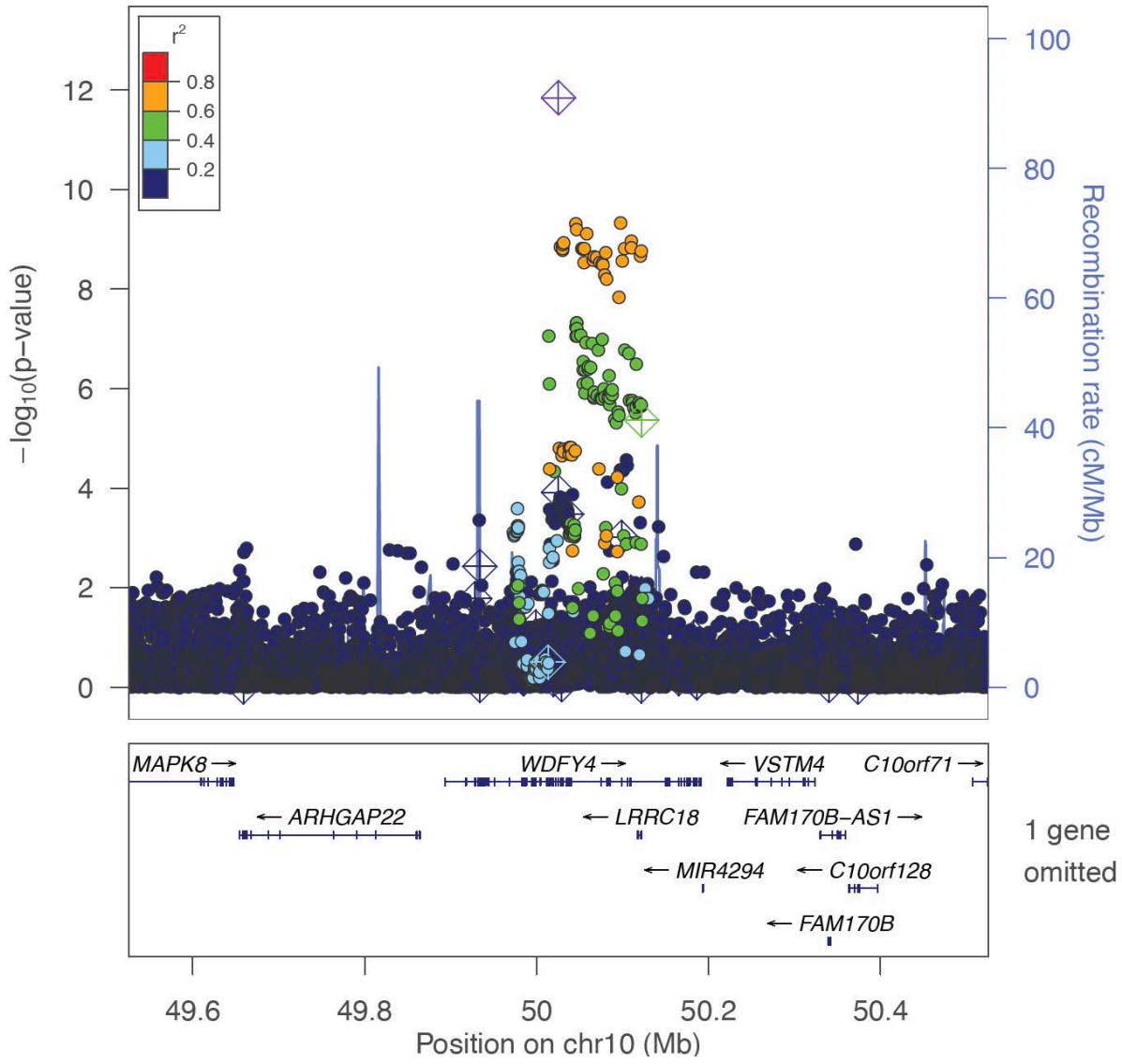

<Locus 76>
10:63801030:C:T (rs7902146)
Multi-GWAS (combined)
Known locus

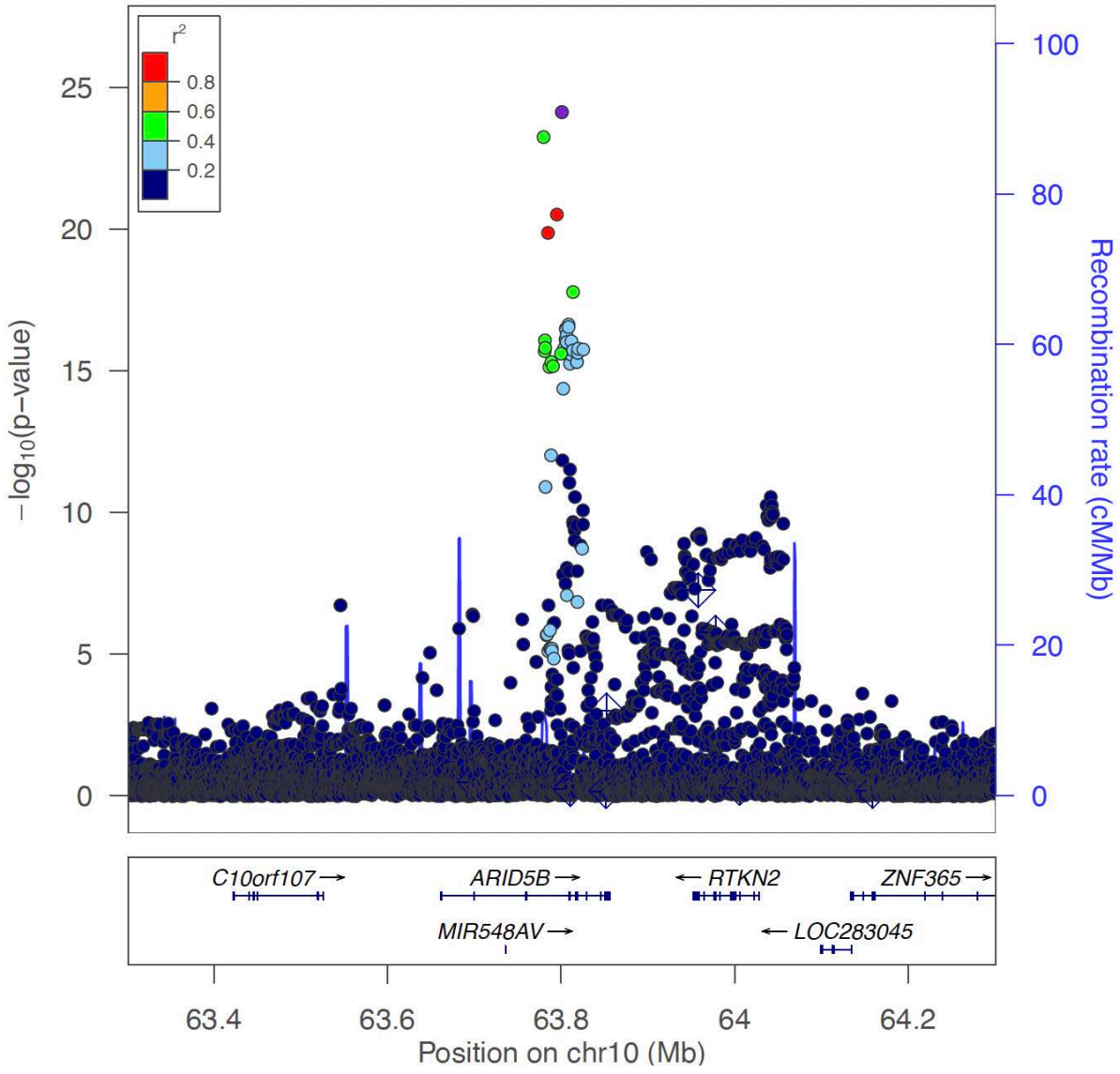

<Locus 77>
11:2323220:G:A (rs734094)
Multi-GWAS (seroposi)
Novel locus

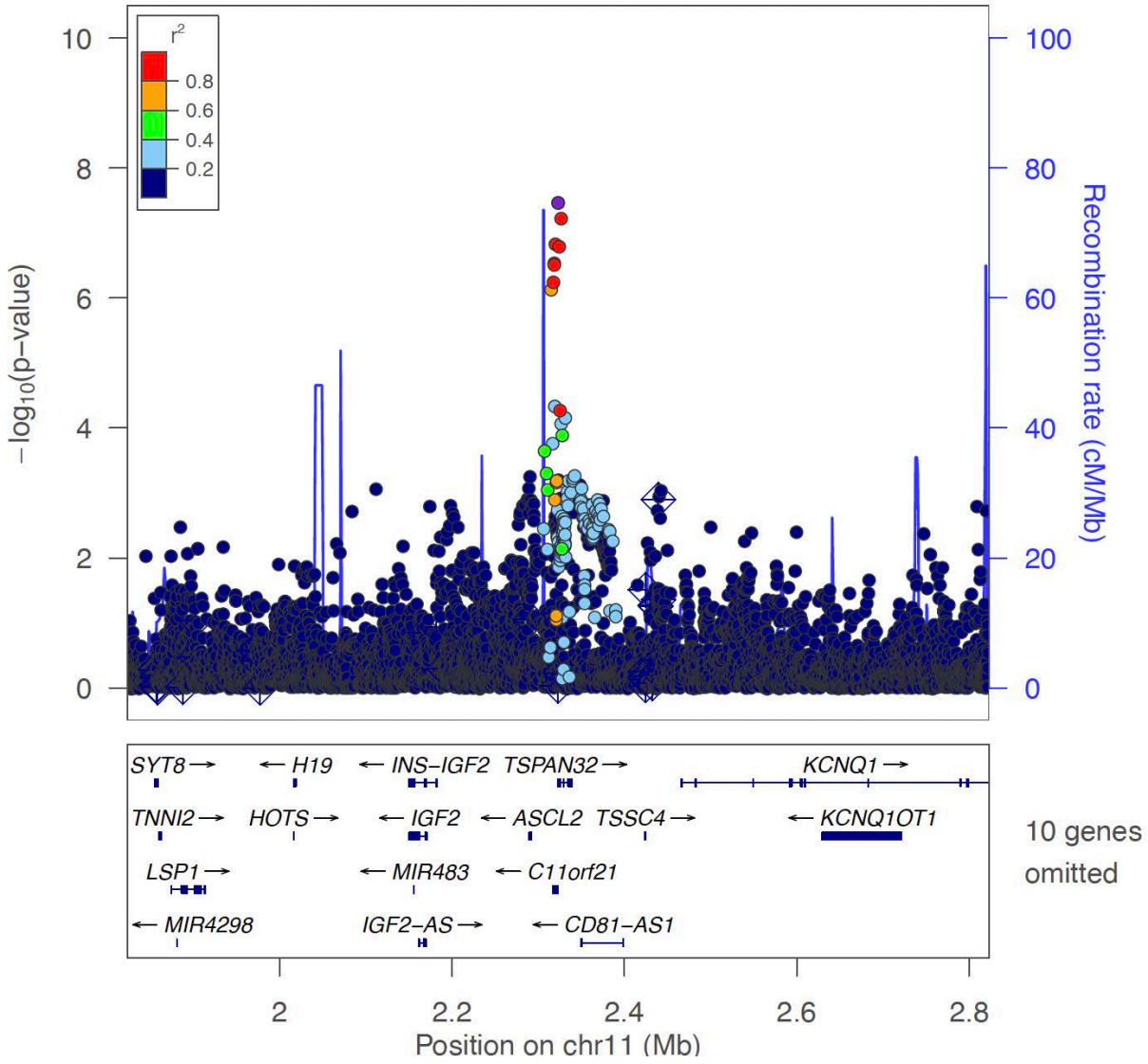

<Locus 78>
11:61547068:G:A (rs7943728)
Multi-GWAS (combined)
Known locus

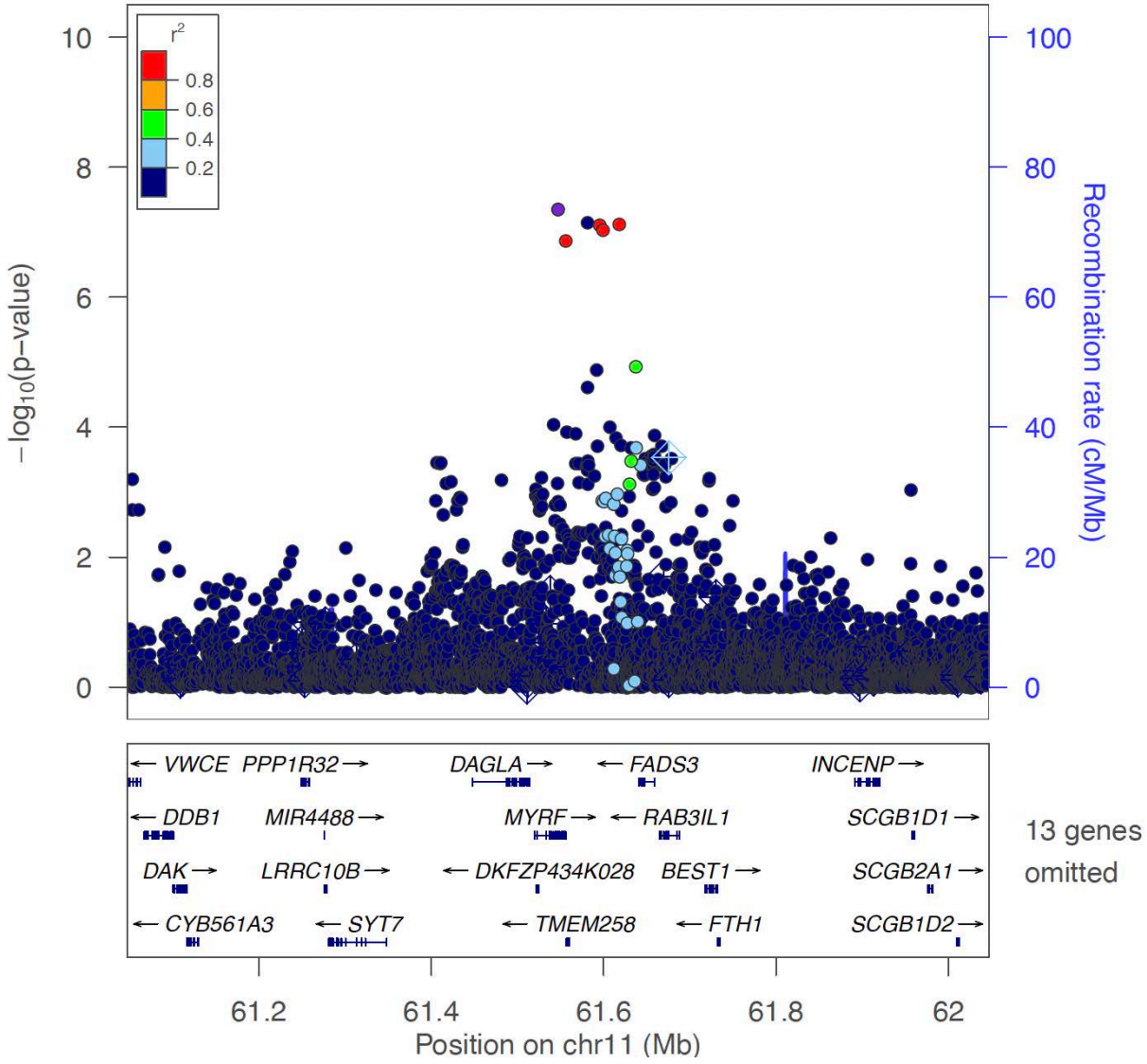

<Locus 79>
11:64107477:T:C (rs479777)
Multi-GWAS (combined)
Known locus

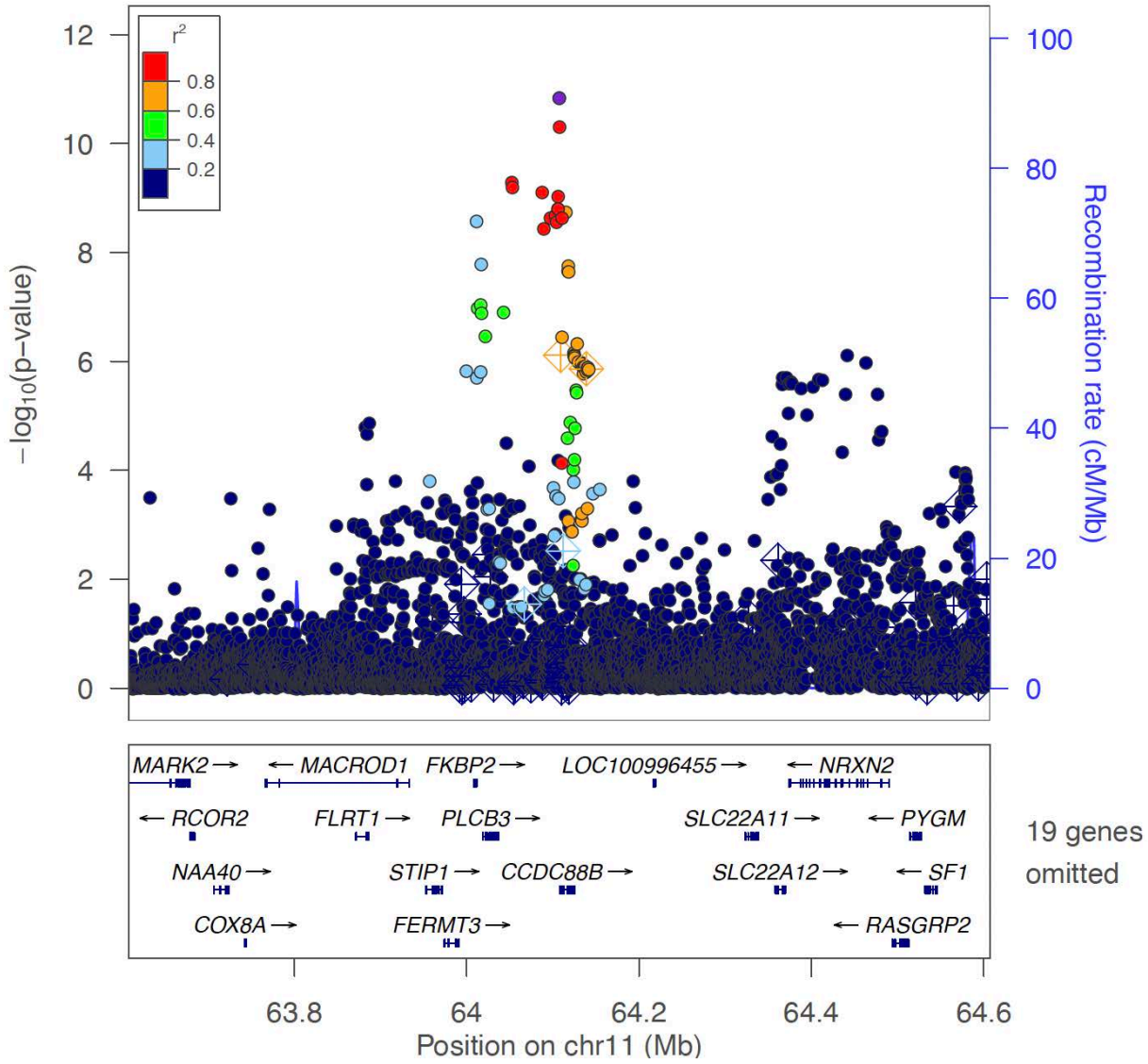

<Locus 80>
11:72404893:C:T (rs79145843)
Multi-GWAS (combined)
Known locus

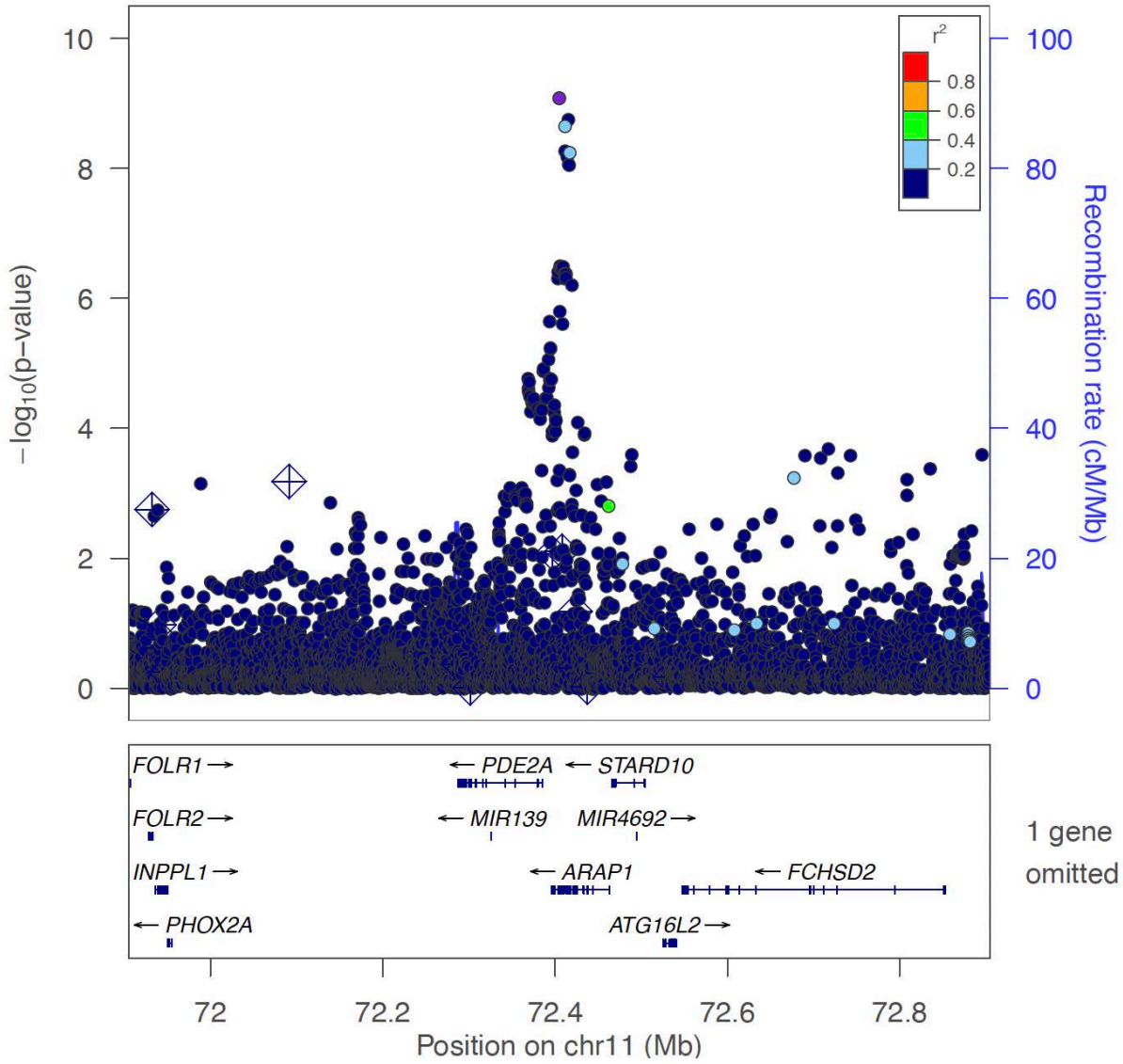

<Locus 81>
11:95311422:T:C (rs4409785)
Multi-GWAS (combined)
Known locus

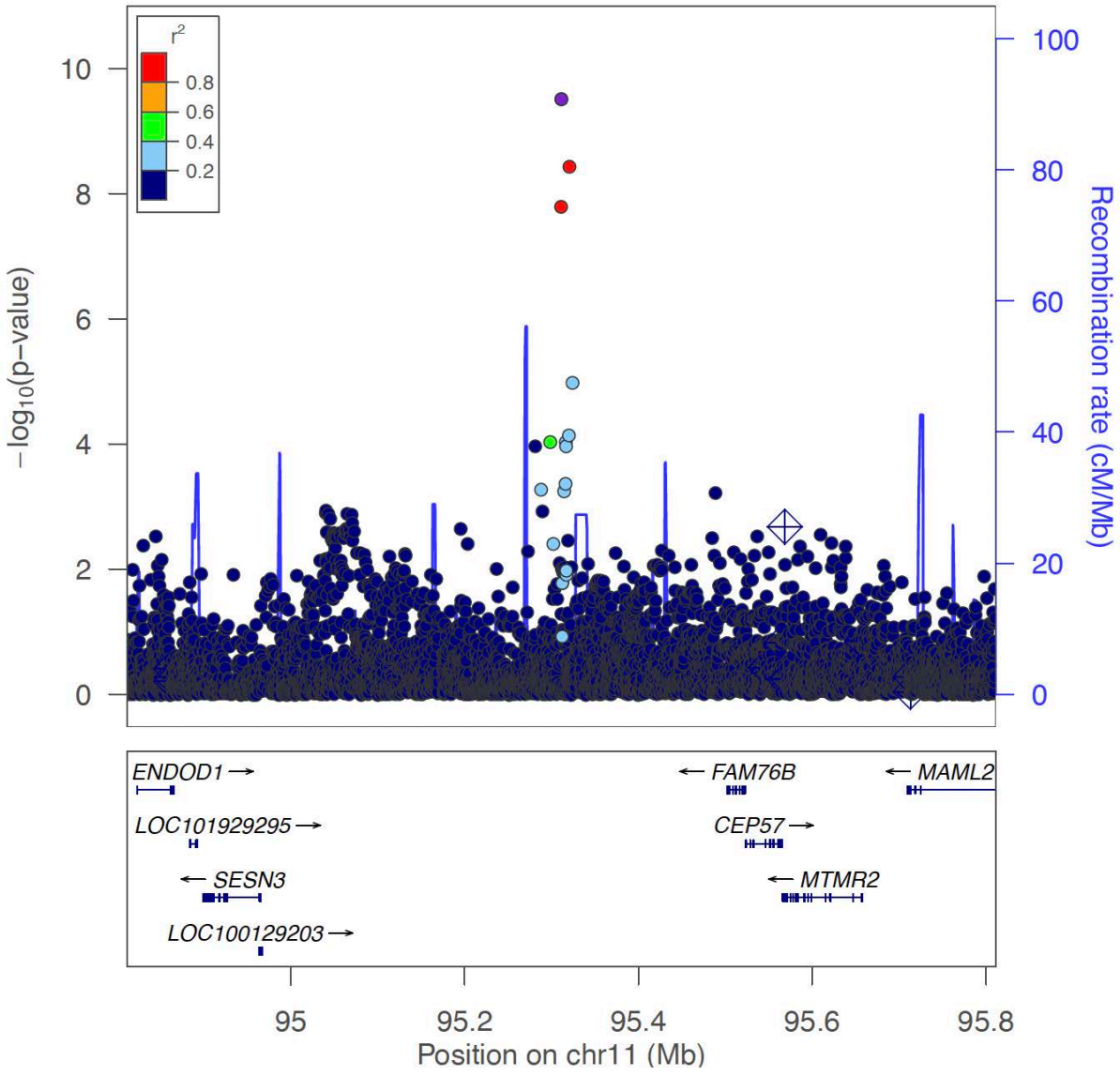

<Locus 82>
11:118681079:A:G (rs73005423)
Multi-GWAS (combined)
Known locus

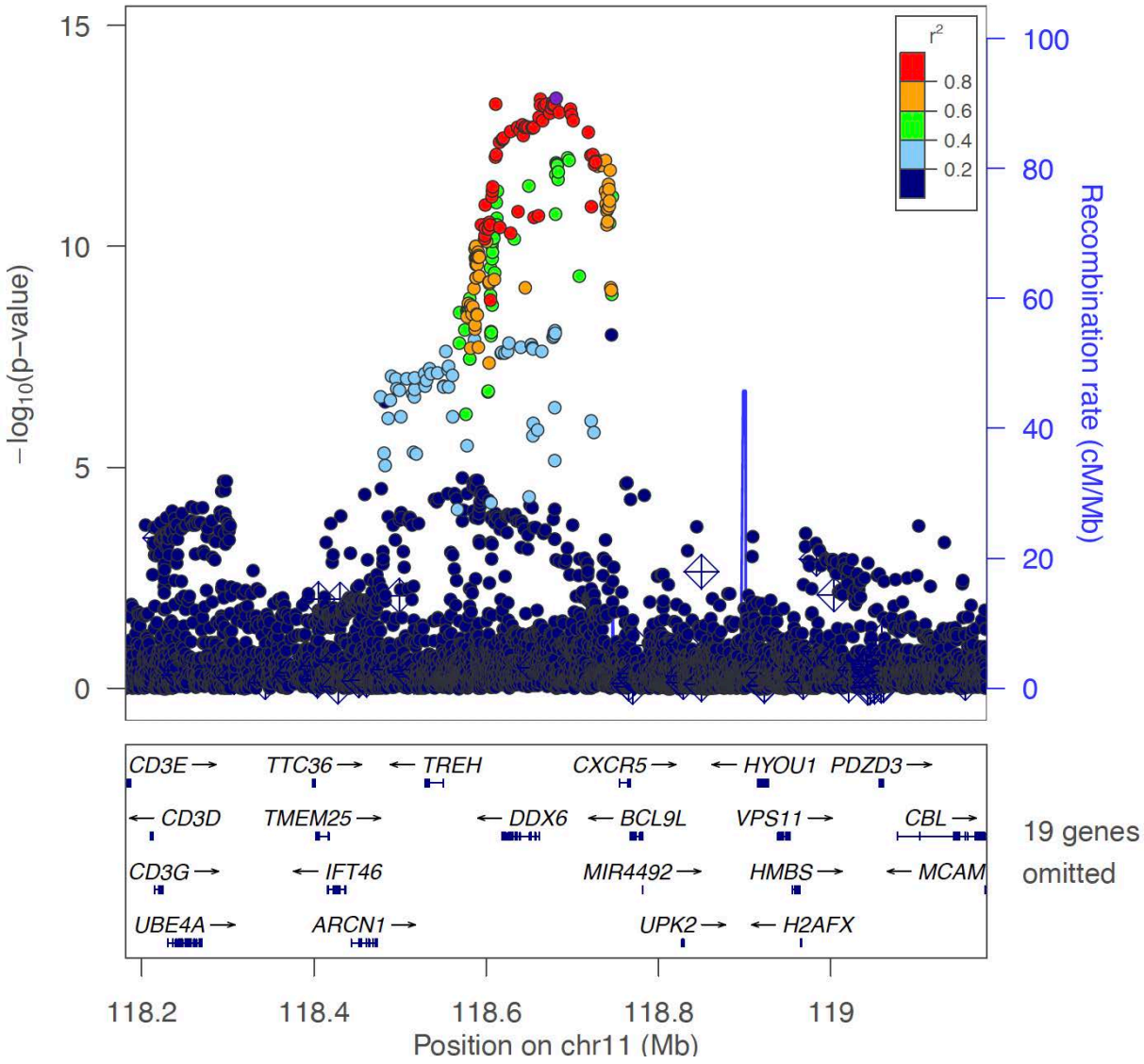

<Locus 83>
11:128486141:ATG:A (rs10556591)
Multi-GWAS (combined)
Known locus

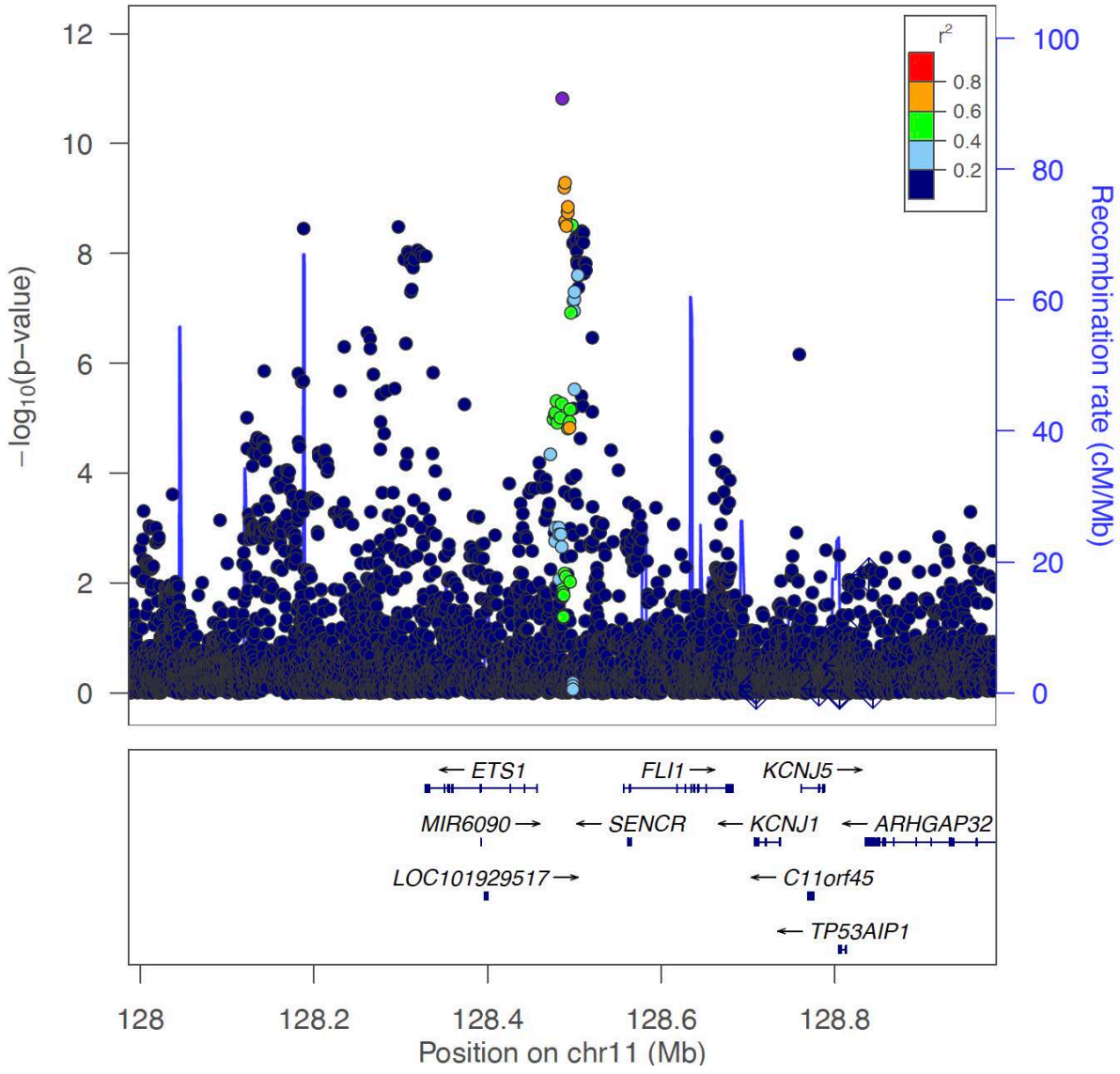

<Locus 84>
12:46370116:C:G (rs1427749)
Multi-GWAS (combined)
Novel locus

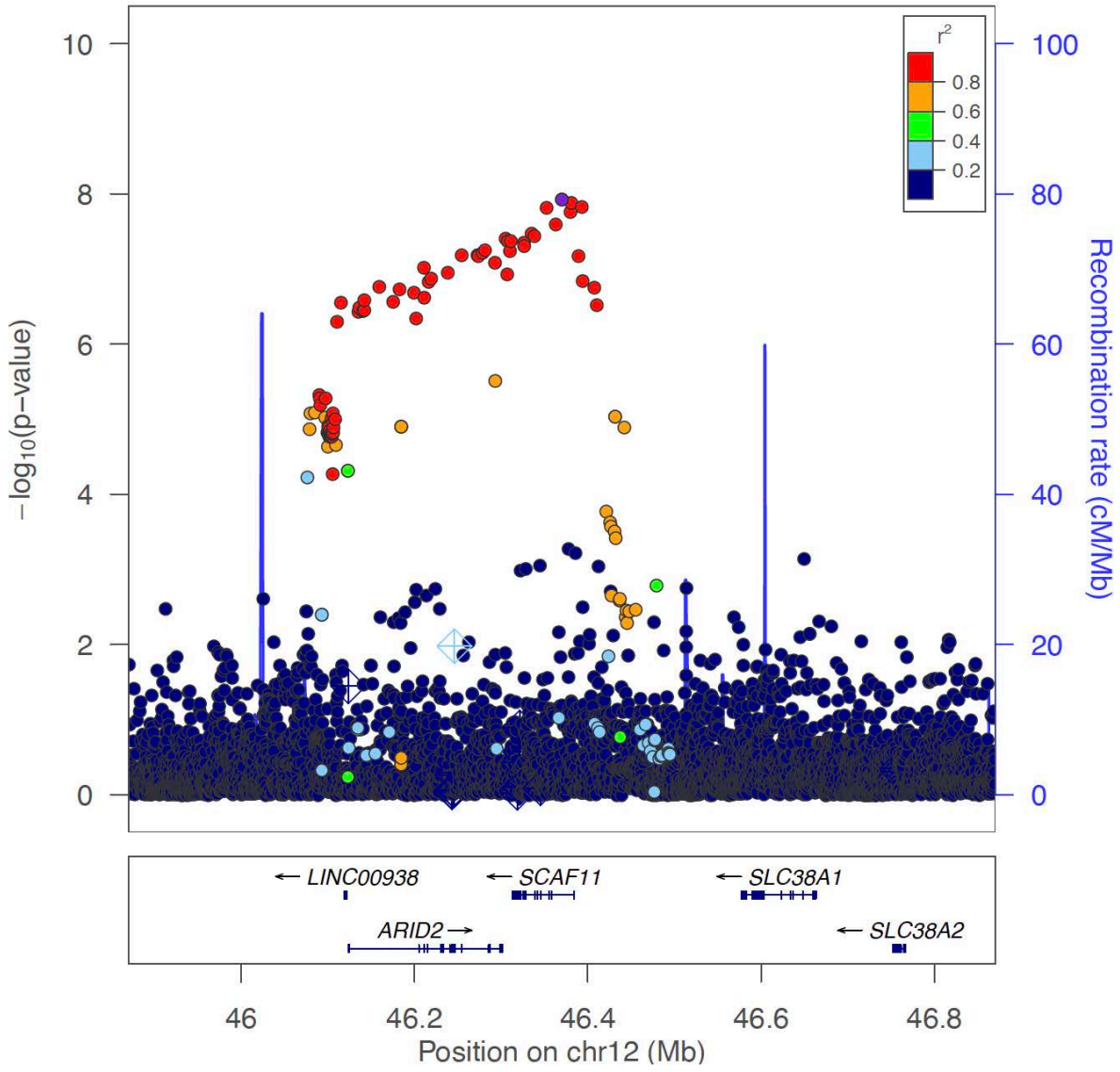

<Locus 85>
12:56389293:T:C (rs705700)
Multi-GWAS (combined)
Known locus

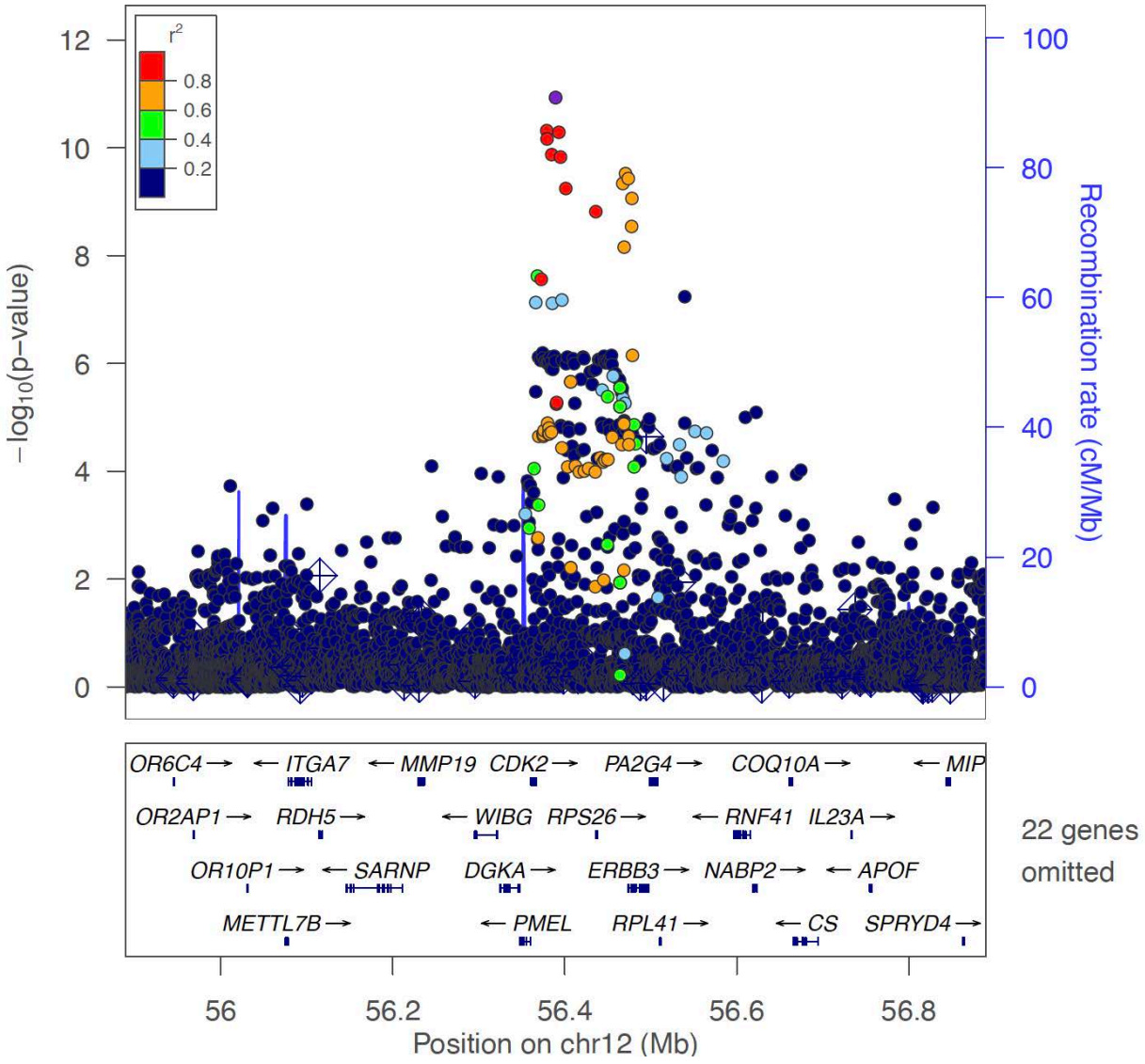

<Locus 86>
12:58116397:T:C (rs1696466)
EUR-GWAS (combined)
Known locus

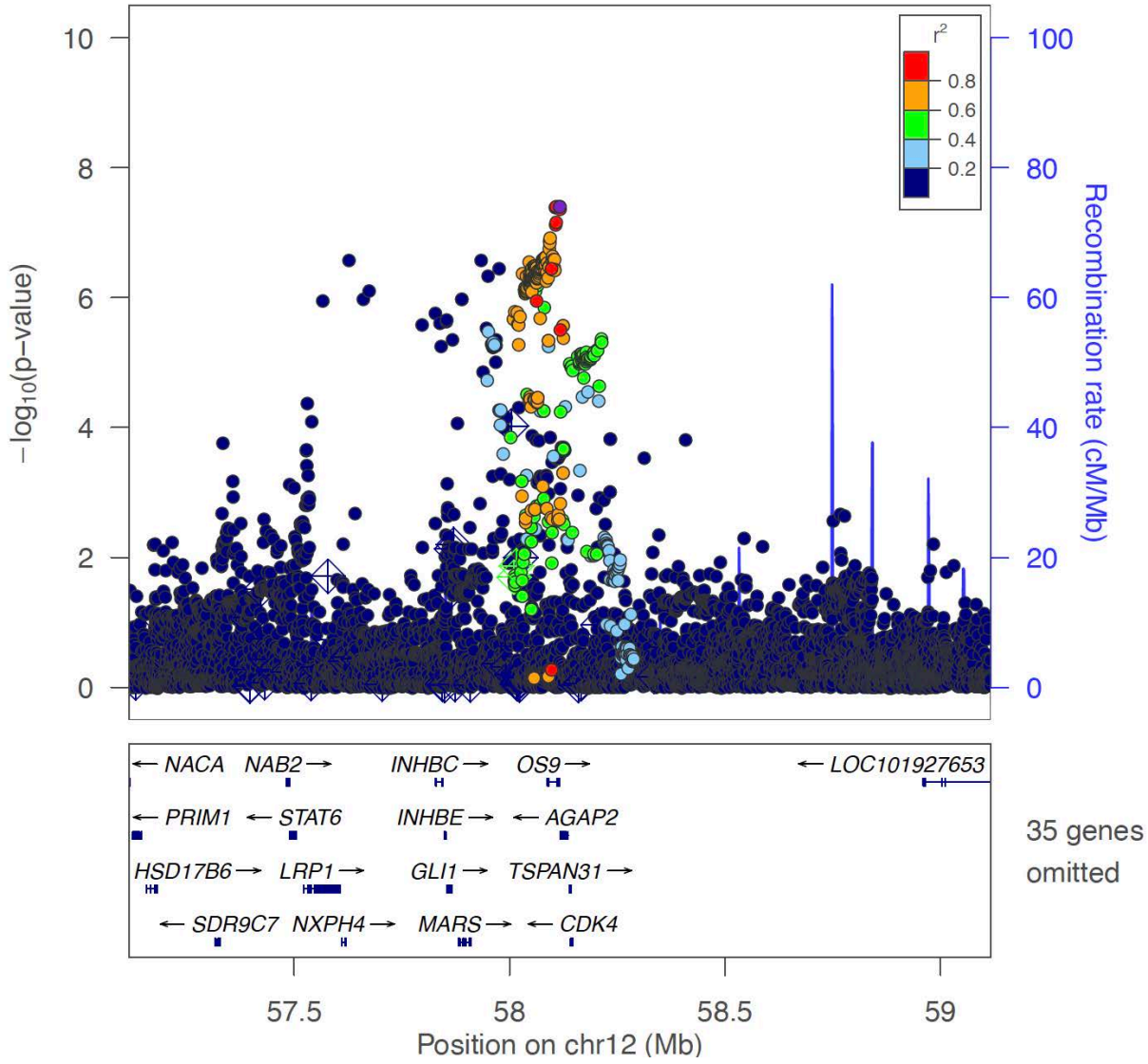

<Locus 87>
12:111884608:T:C (rs3184504)
Multi-GWAS (combined)
Known locus

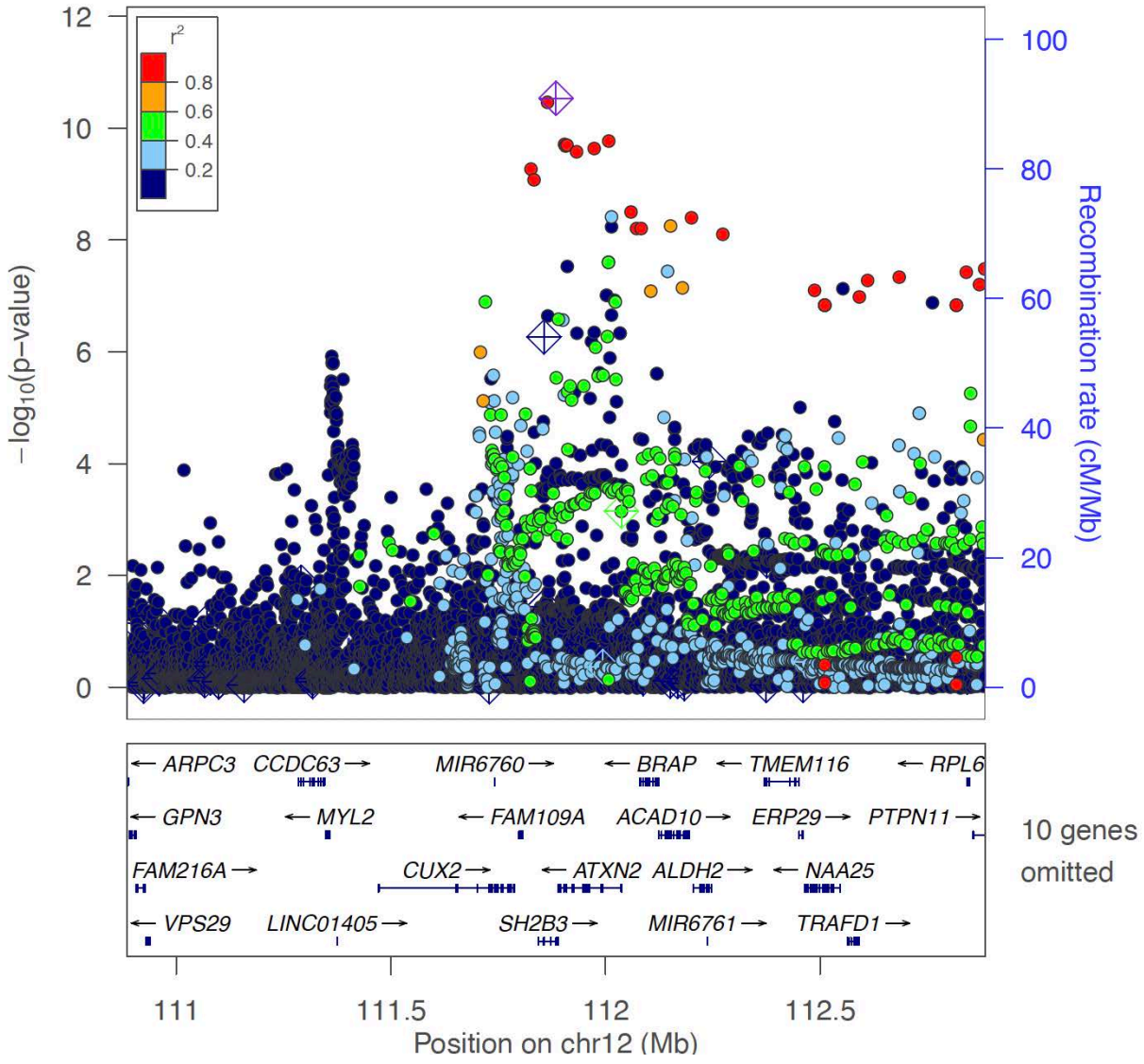

<Locus 88>
13:28634933:G:A (rs61944750)
Multi-GWAS (combined)
Novel locus

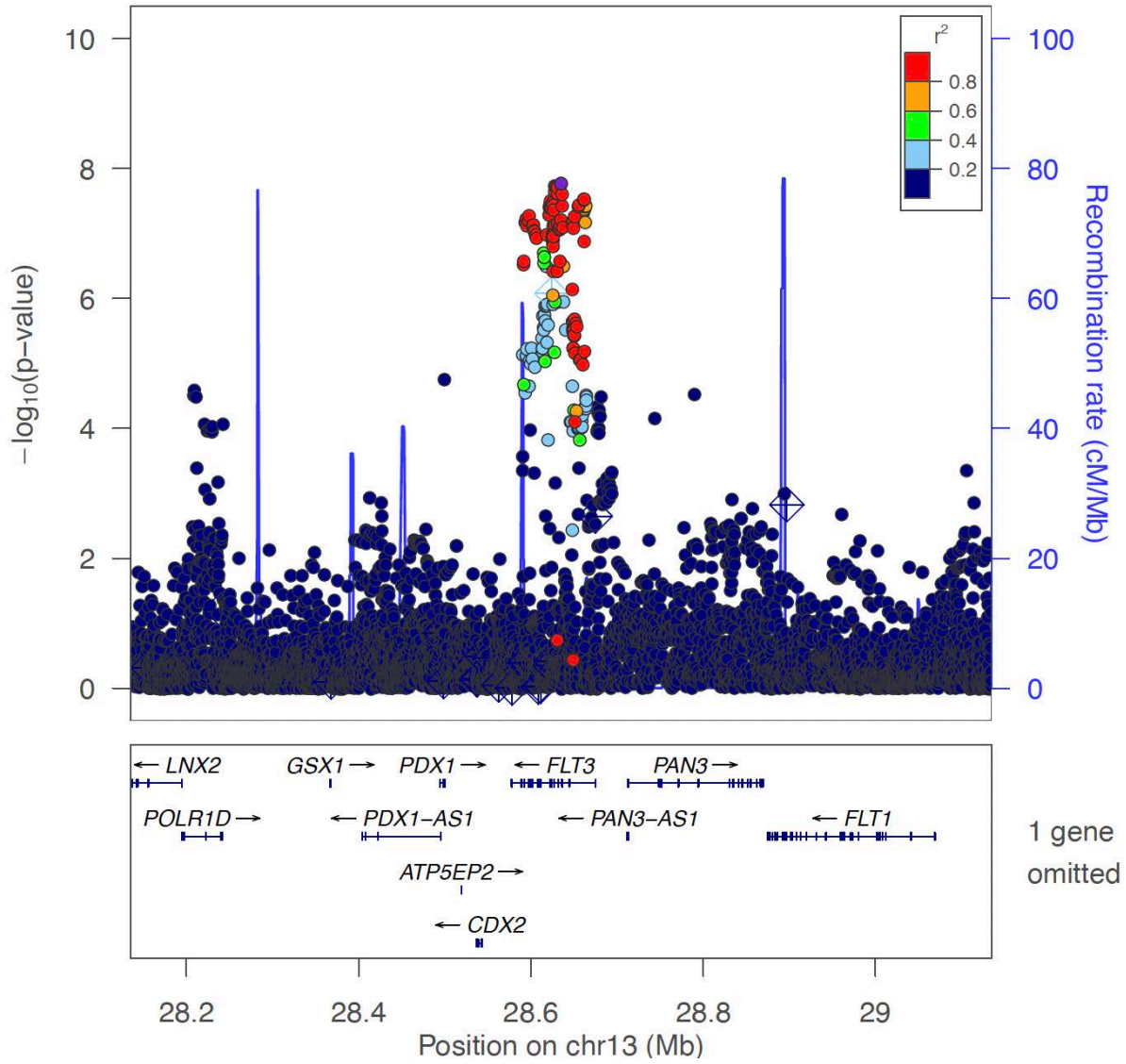

<Locus 89>
13:40355913:T:C (rs9532434)
Multi-GWAS (combined)
Known locus

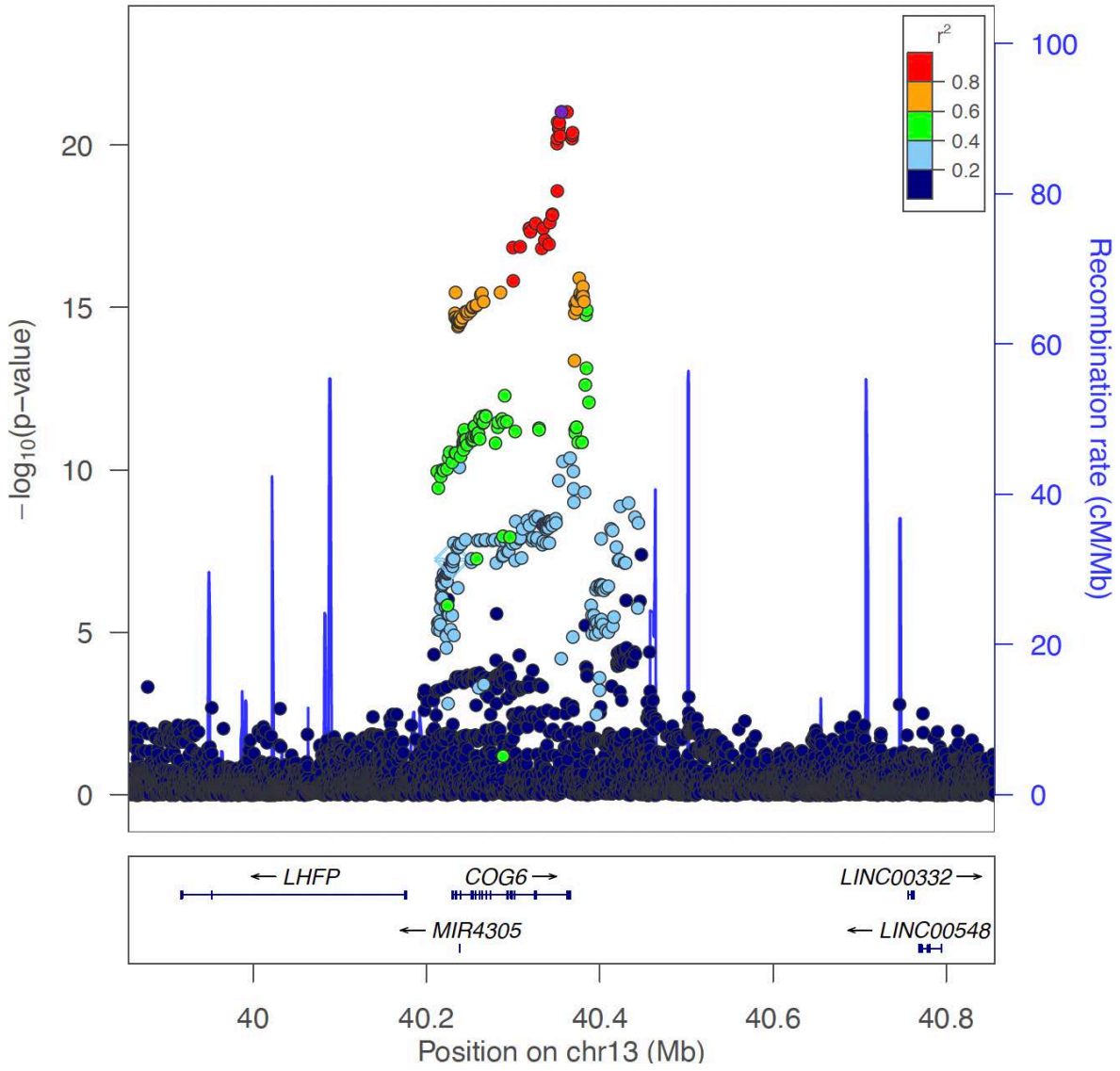

<Locus 90>
13:42982302:A:T (rs2147161)
Multi-GWAS (seroposi)
Novel locus

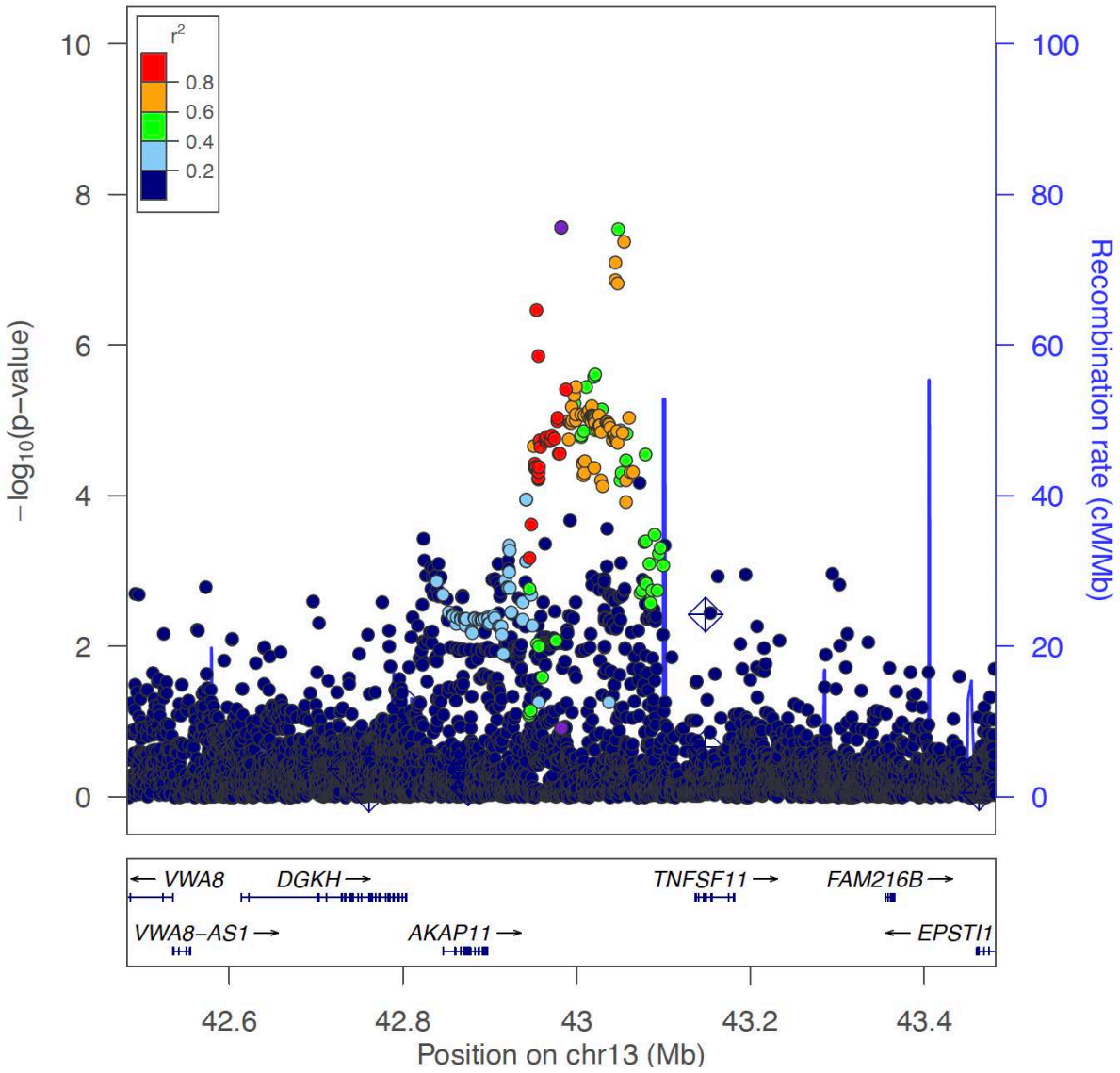

<Locus 91>
14:61926738:A:AT (rs146492555)
Multi-GWAS (combined)
Known locus

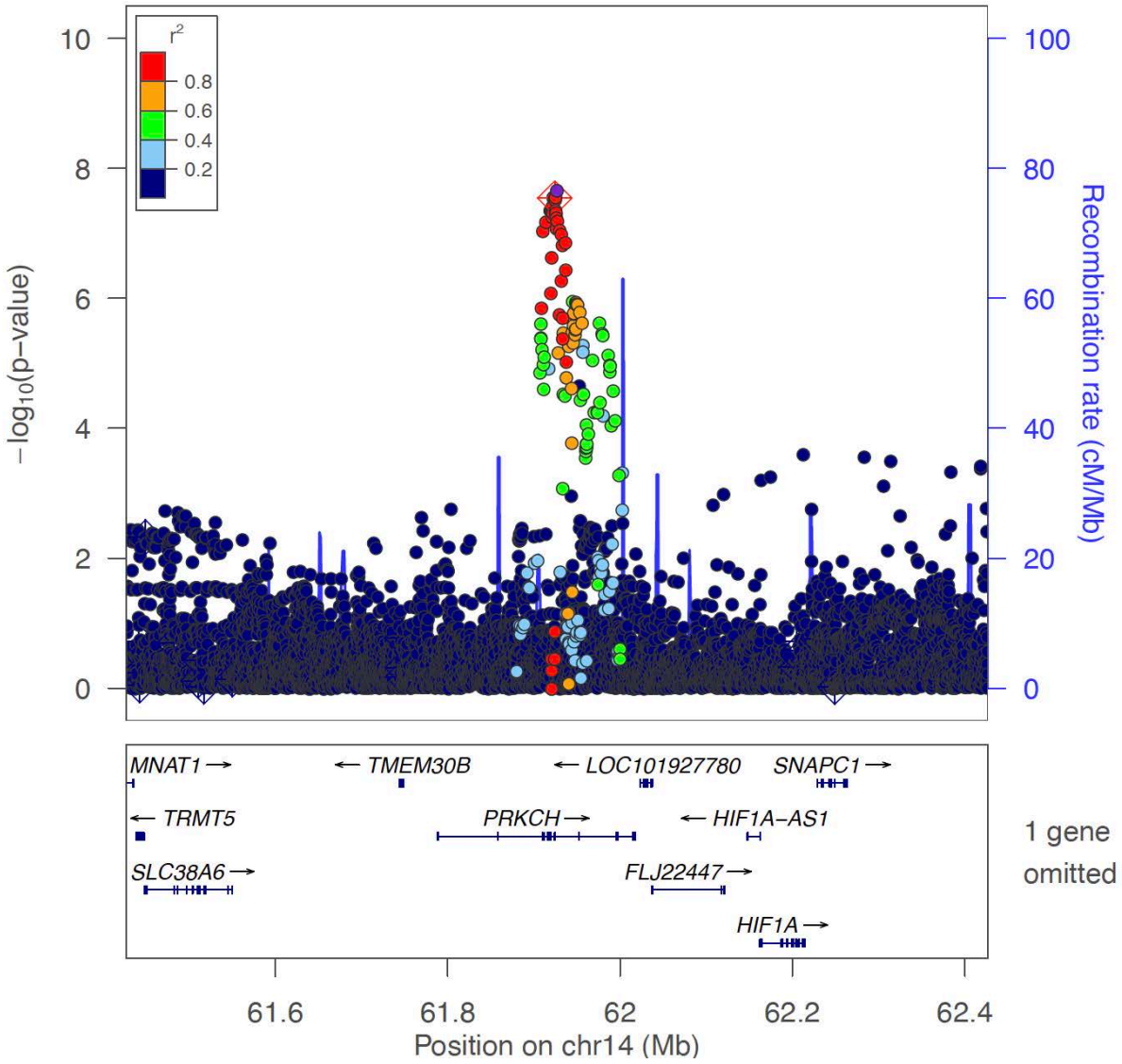

<Locus 92>
14:68754695:G:A (rs1885013)
Multi-GWAS (combined)
Known locus

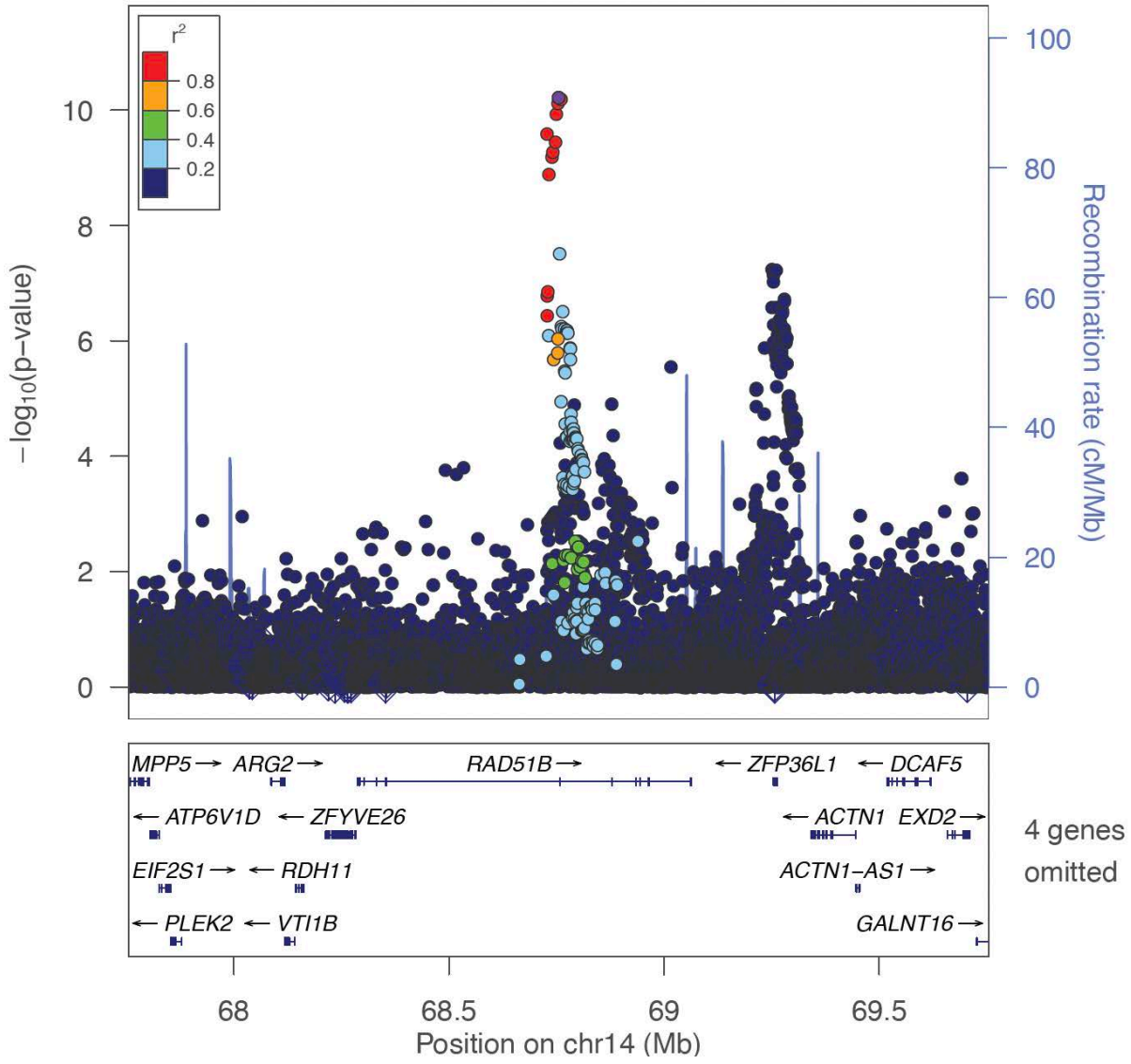

<Locus 93>
14:75981856:T:C (rs175714)
Multi-GWAS (combined)
Novel locus

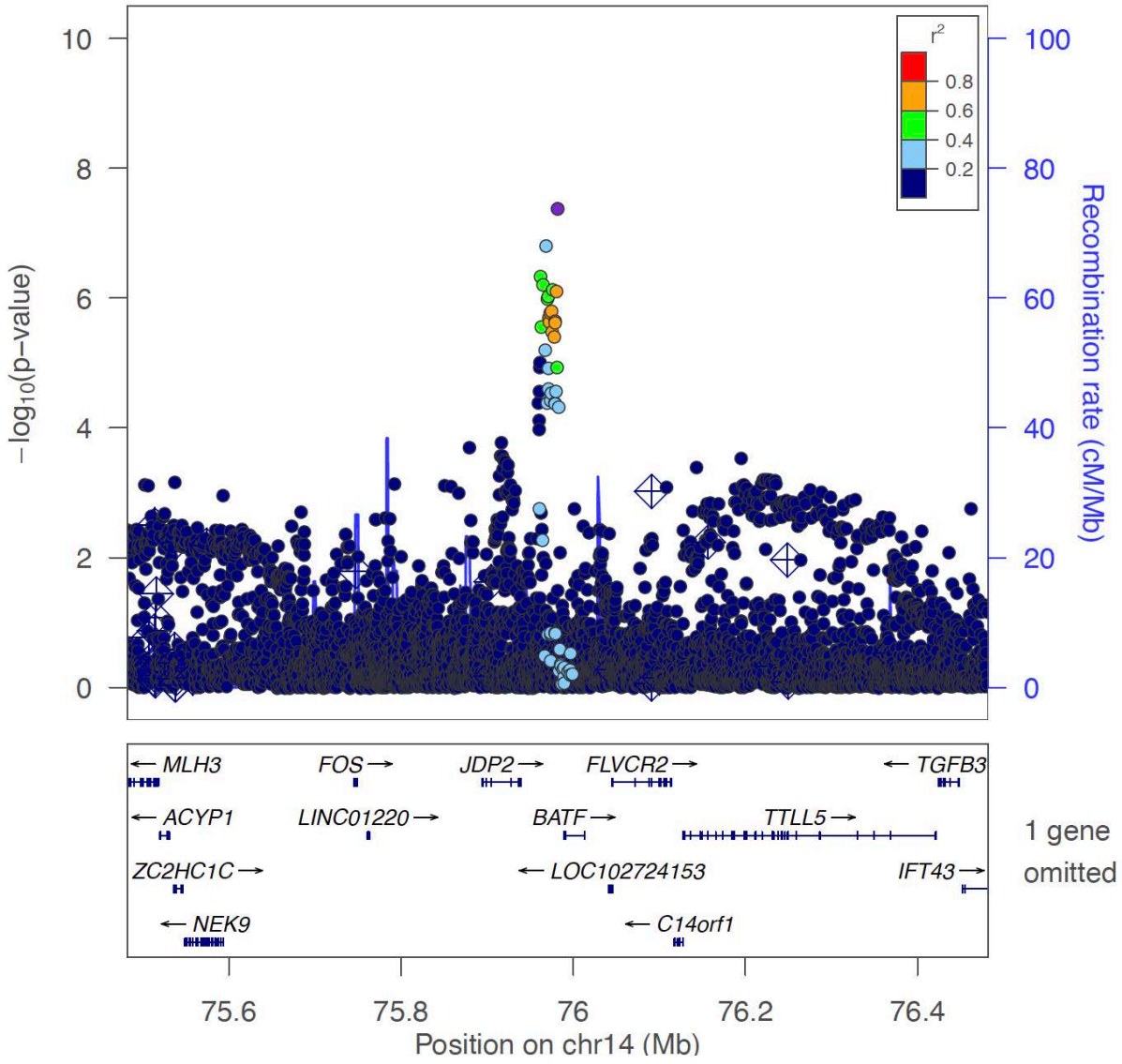

<Locus 94>
14:105386511:G:A (rs3001423)
Multi-GWAS (combined)
Known locus

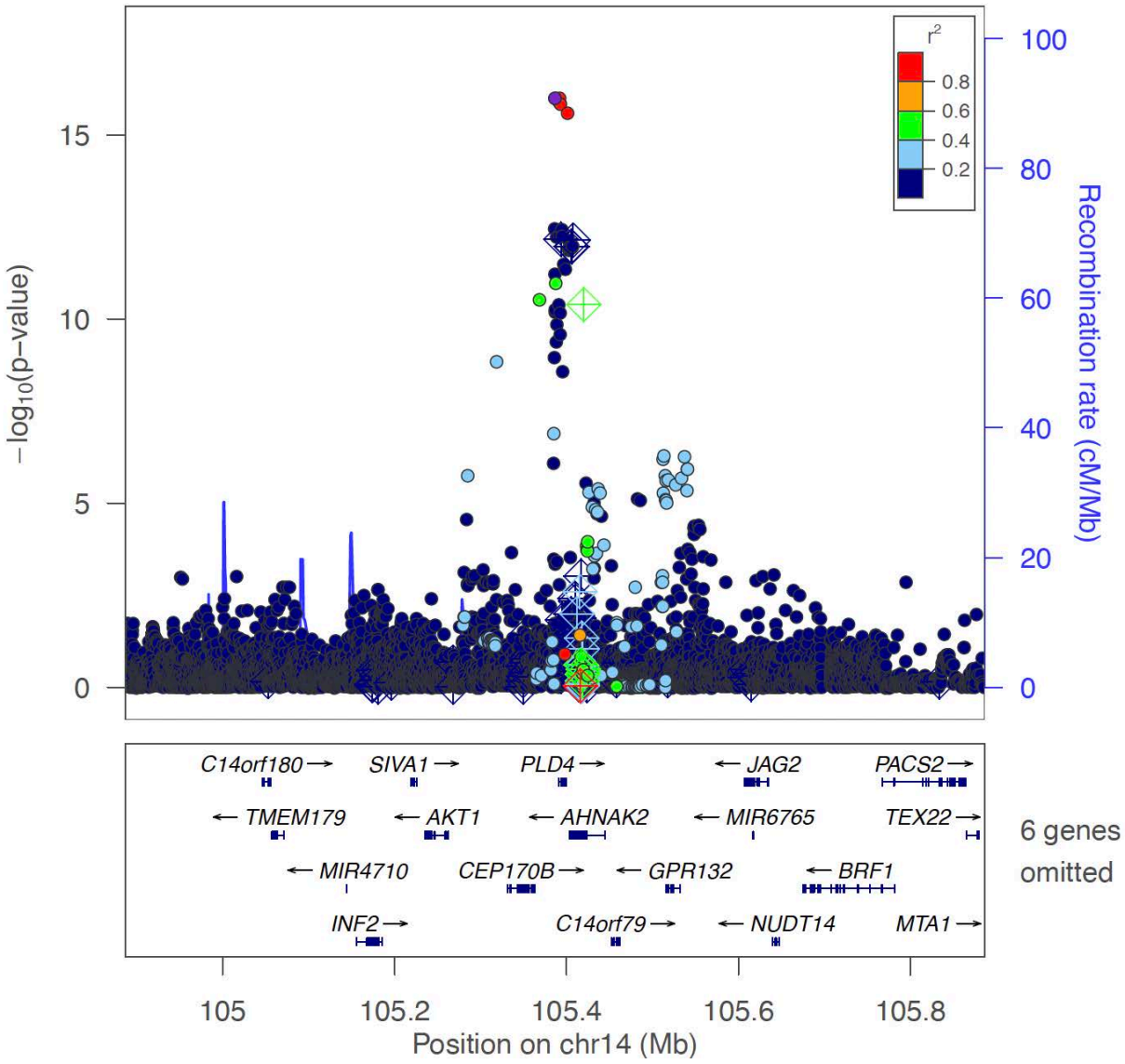

<Locus 95>
15:38847359:C:T (rs6495979)
Multi-GWAS (combined)
Known locus

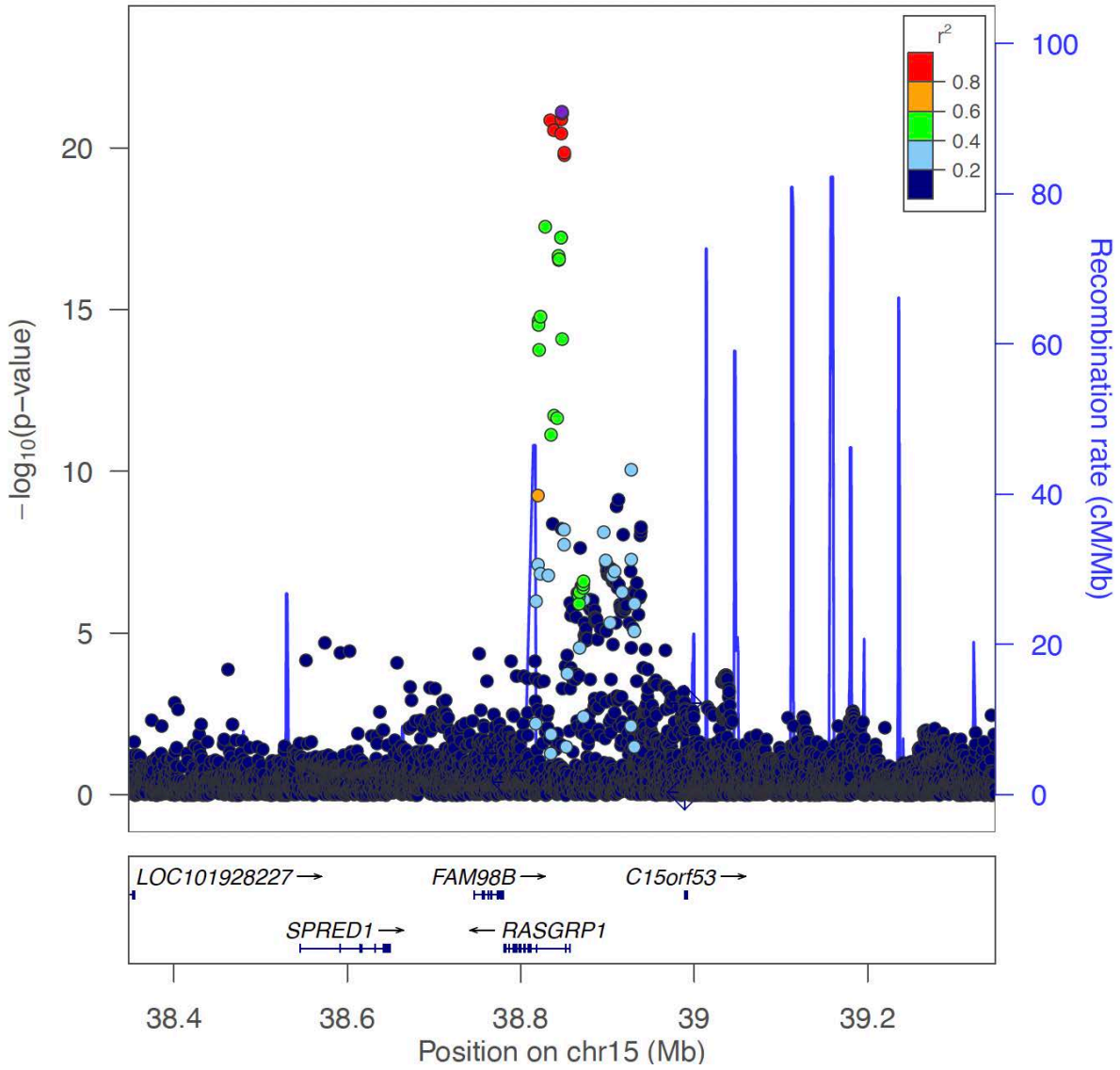

<Locus 96>
15:69991417:G:A (rs8026898)
Multi-GWAS (combined)
Known locus

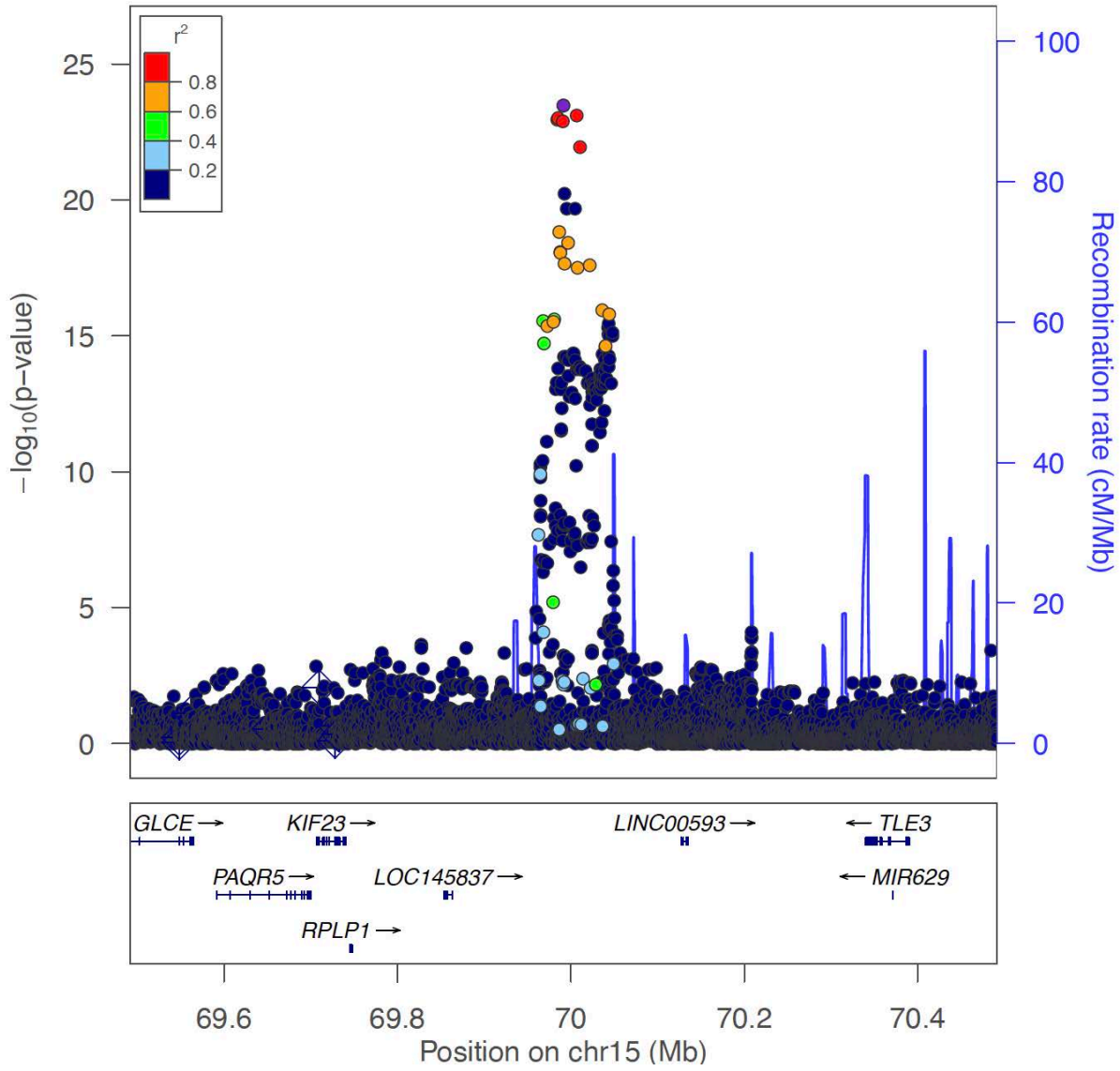

<Locus 97>
15:77326836:T:C (rs115284761)
Multi-GWAS (combined)
Novel locus

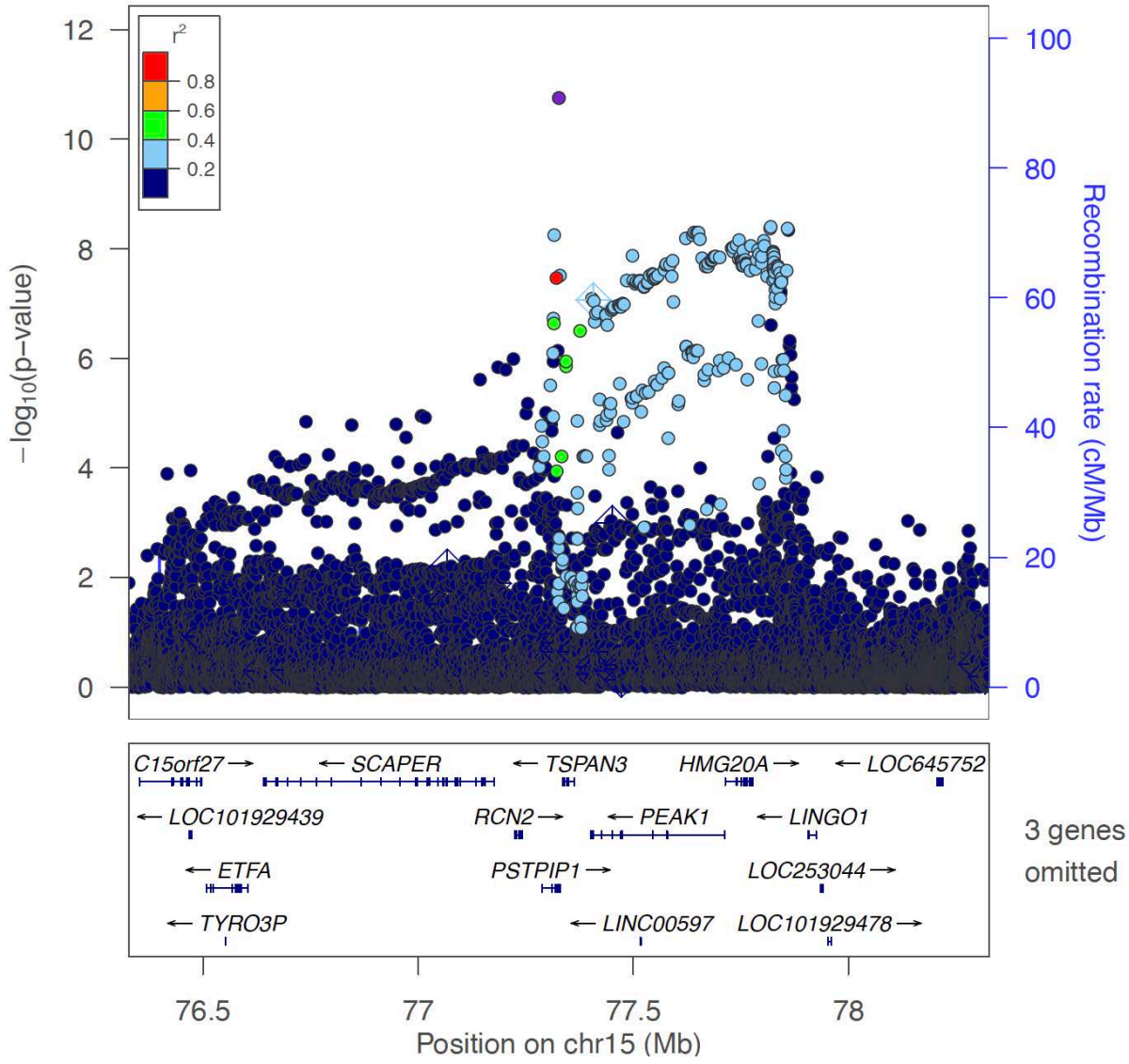

<Locus 98>
15:90904858:G:A (rs7171617)
Multi-GWAS (combined)
Known locus

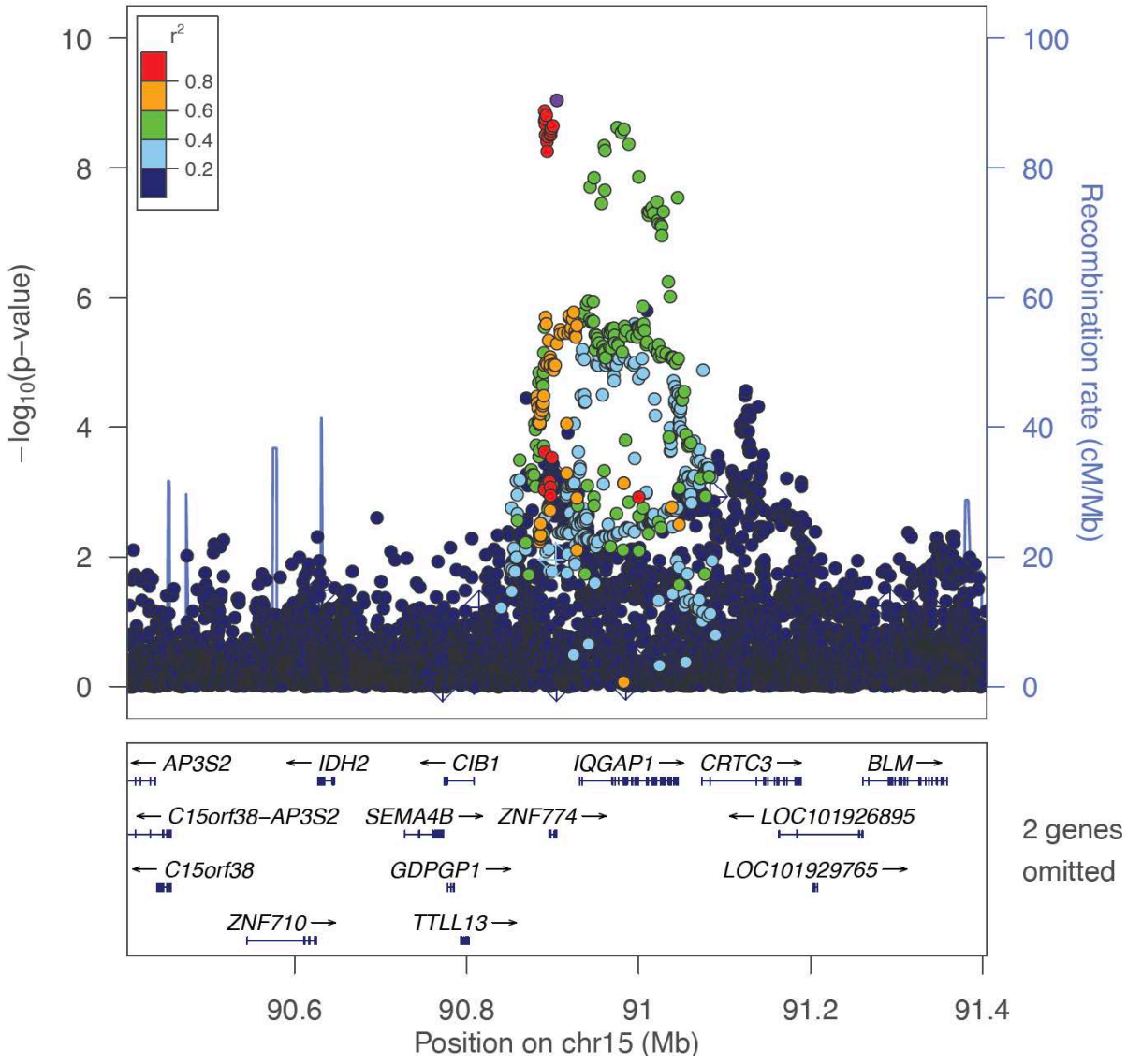

<Locus 99>
16:11798758:C:T (rs4584833)
Multi-GWAS (combined)
Known locus

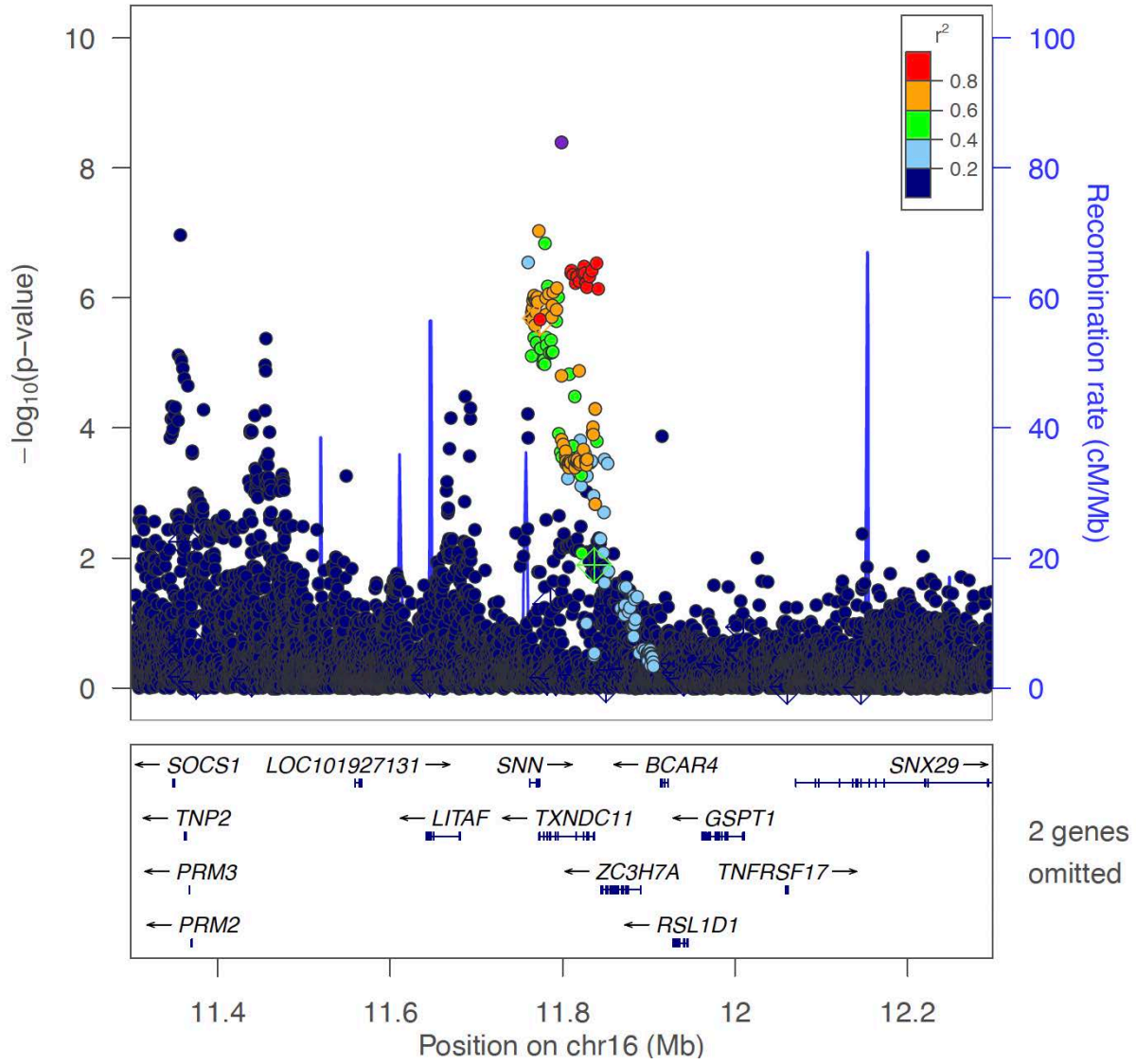

<Locus 100>
16:30798689:G:A (rs34480360)
Multi-GWAS (combined)
Known locus

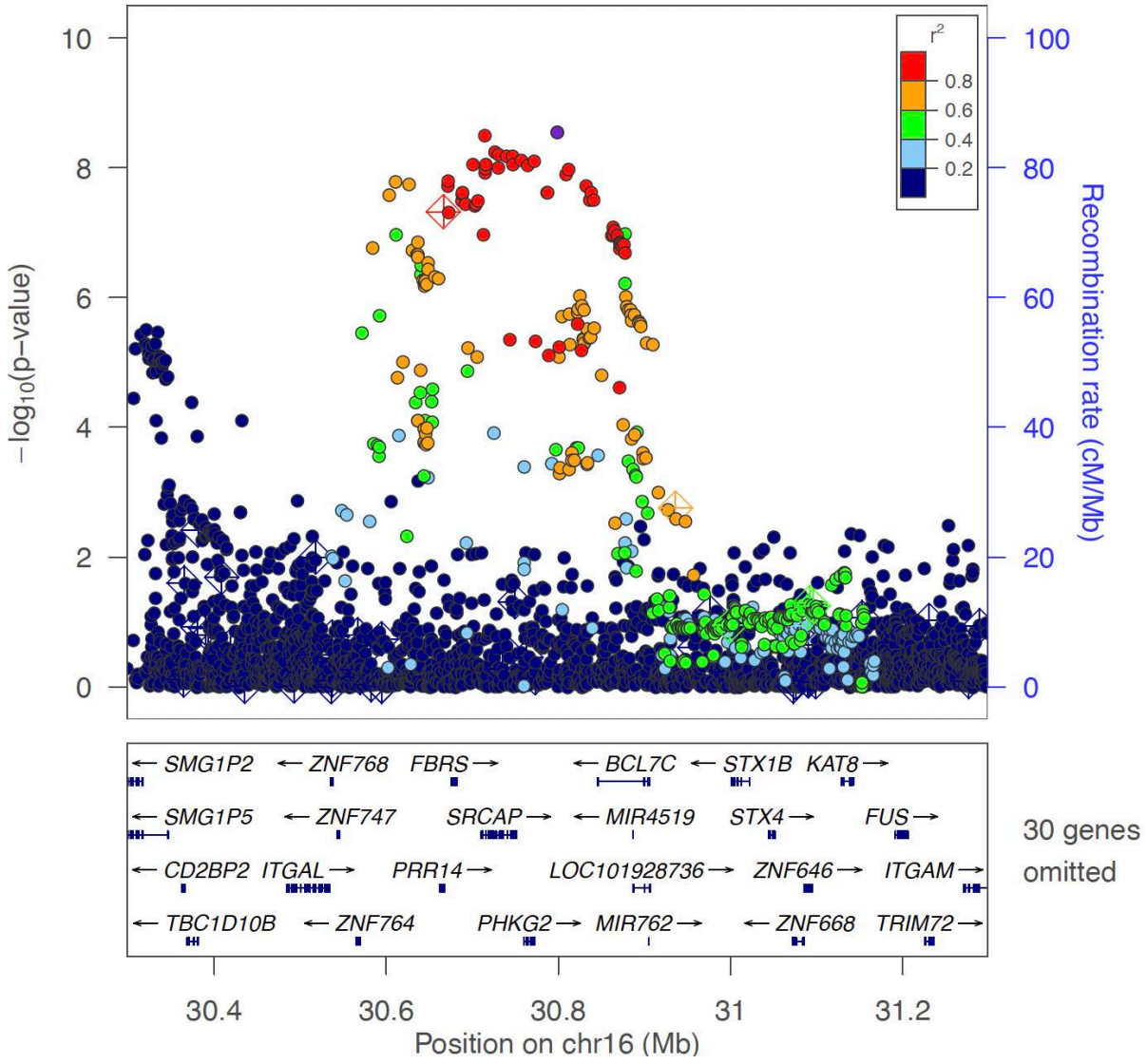

<Locus 101>
16:86016401:C:G (rs9927316)
Multi-GWAS (combined)
Known locus

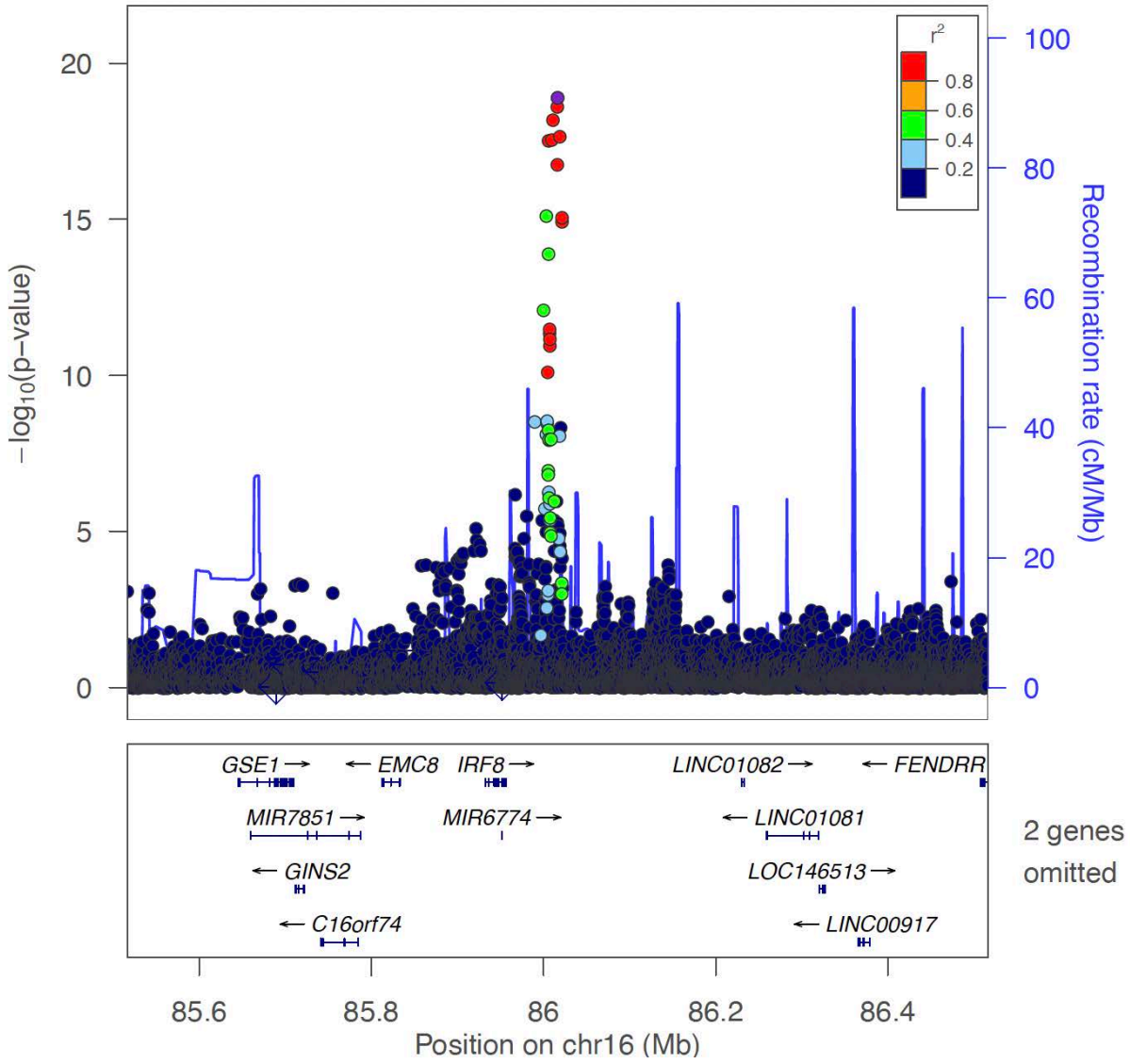

<Locus 102>
17:5147239:G:A (rs8073171)
Multi-GWAS (combined)
Known locus

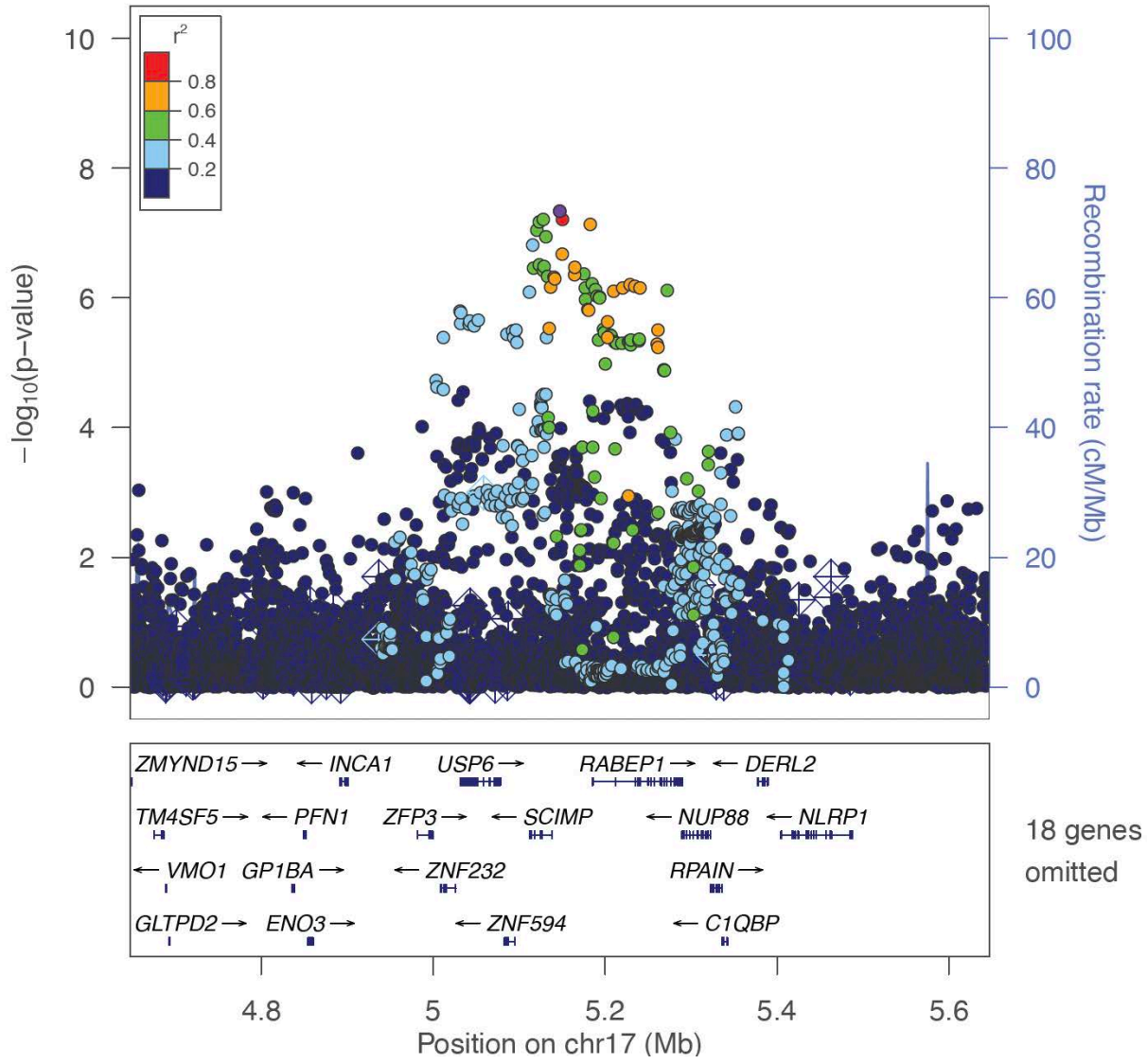

<Locus 103>
17:25904074:G:GT (rs11375064)
Multi-GWAS (seroposi)
Novel locus

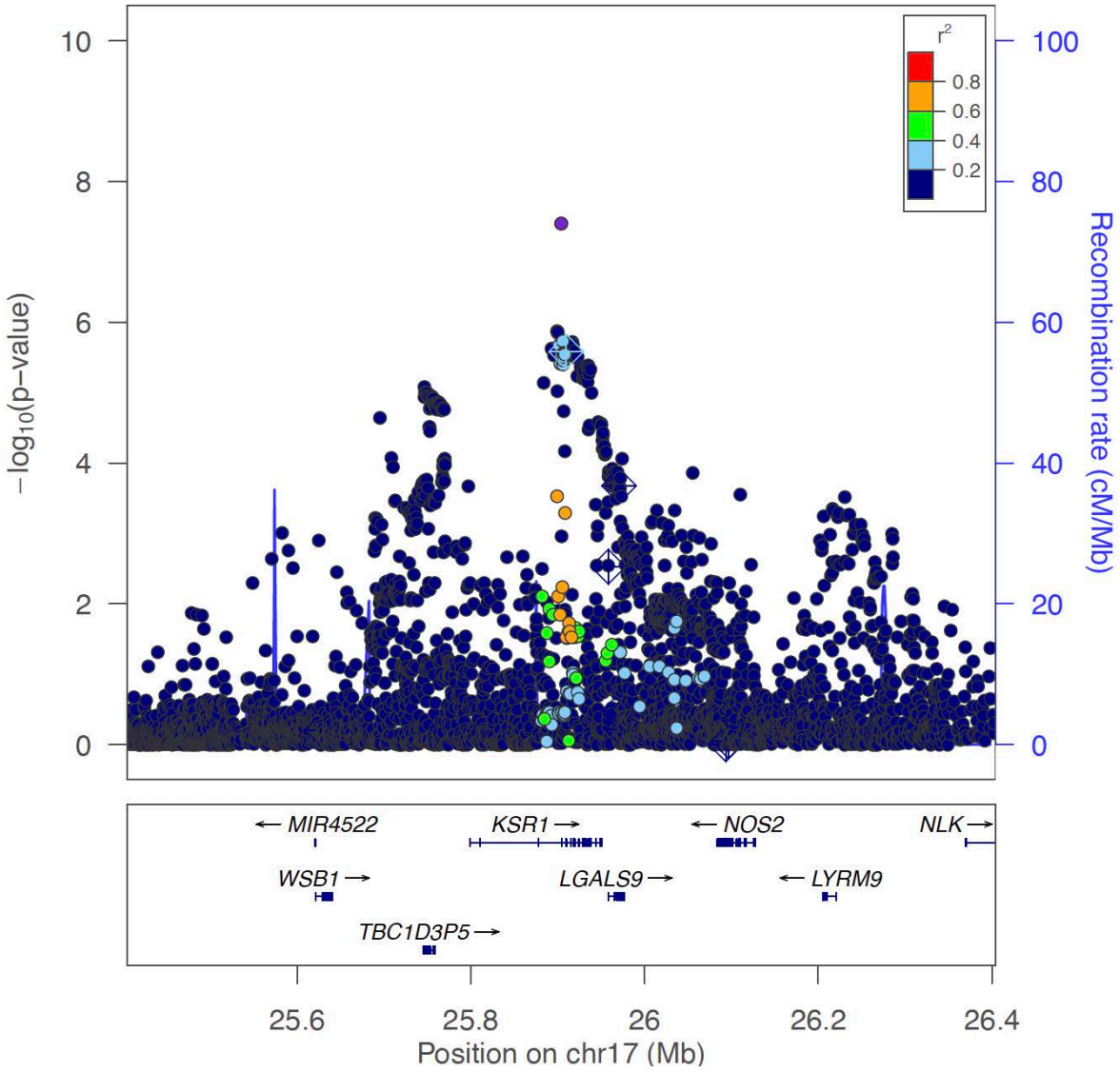

<Locus 104>
17:38062944:A:C (rs56750287)
Multi-GWAS (combined)
Known locus

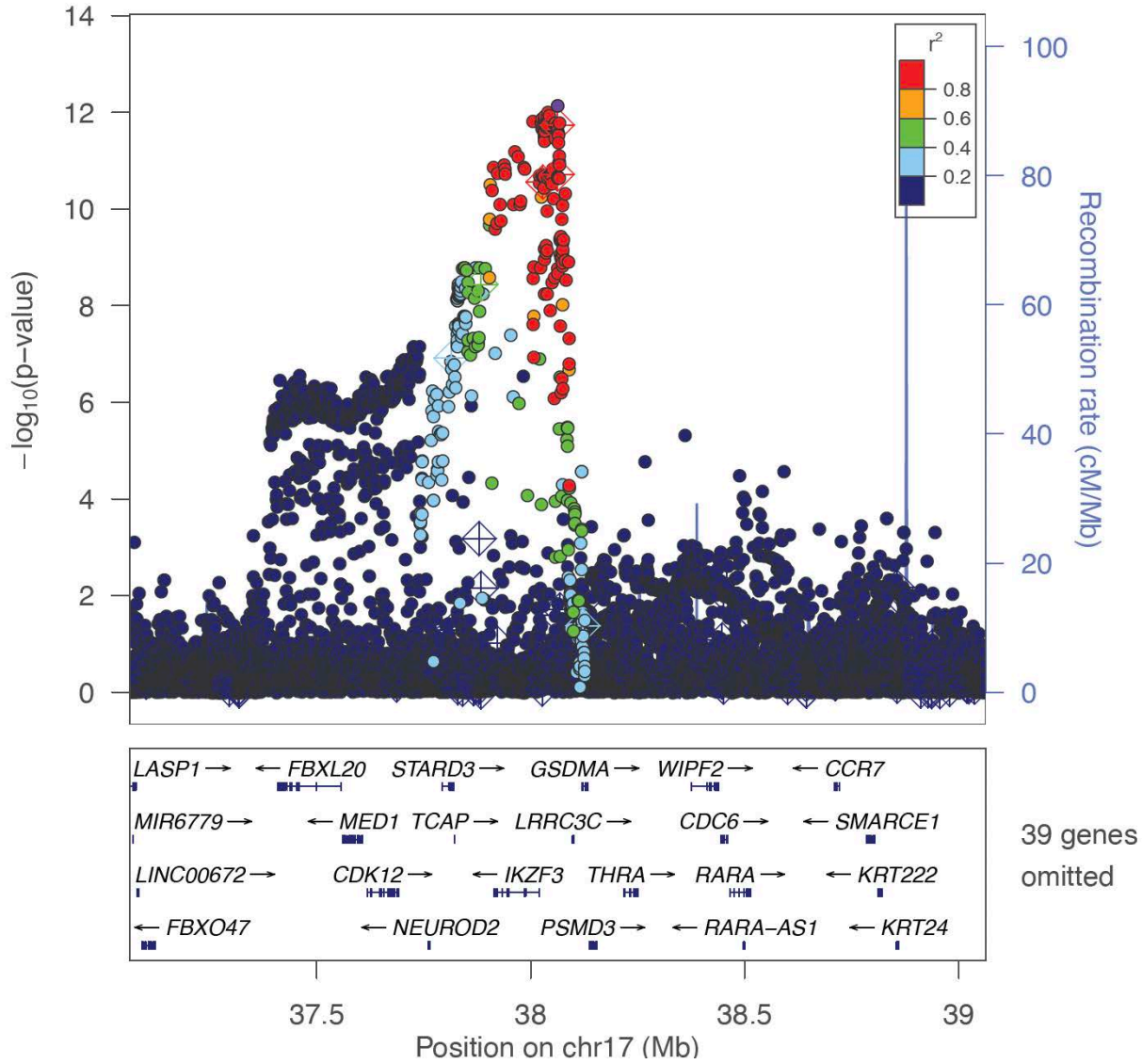

<Locus 105>
18:3542247:T:C (rs591549)
Multi-GWAS (combined)
Novel locus

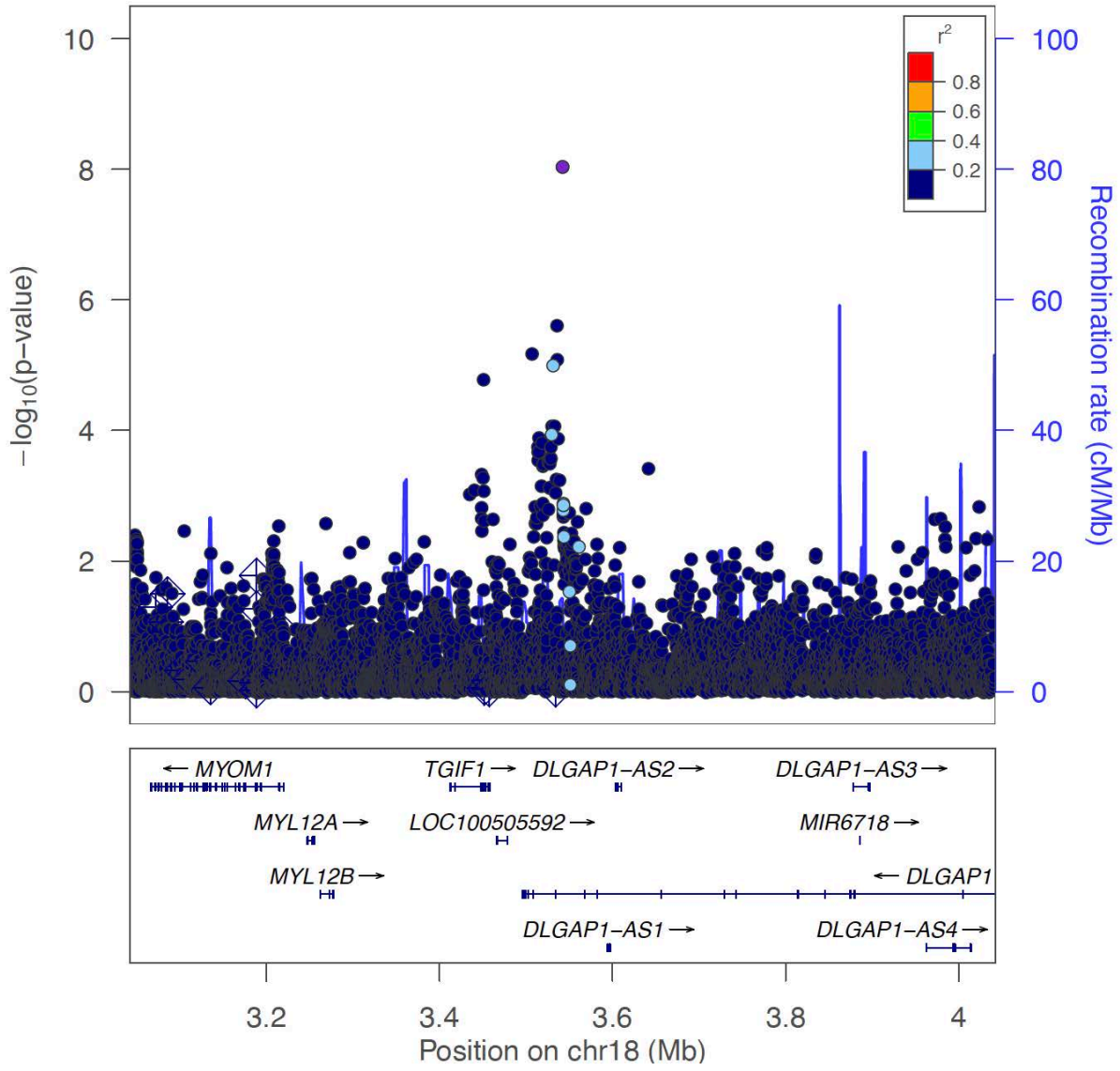

<Locus 106>
18:12880206:A:G (rs7241016)
Multi-GWAS (combined)
Known locus

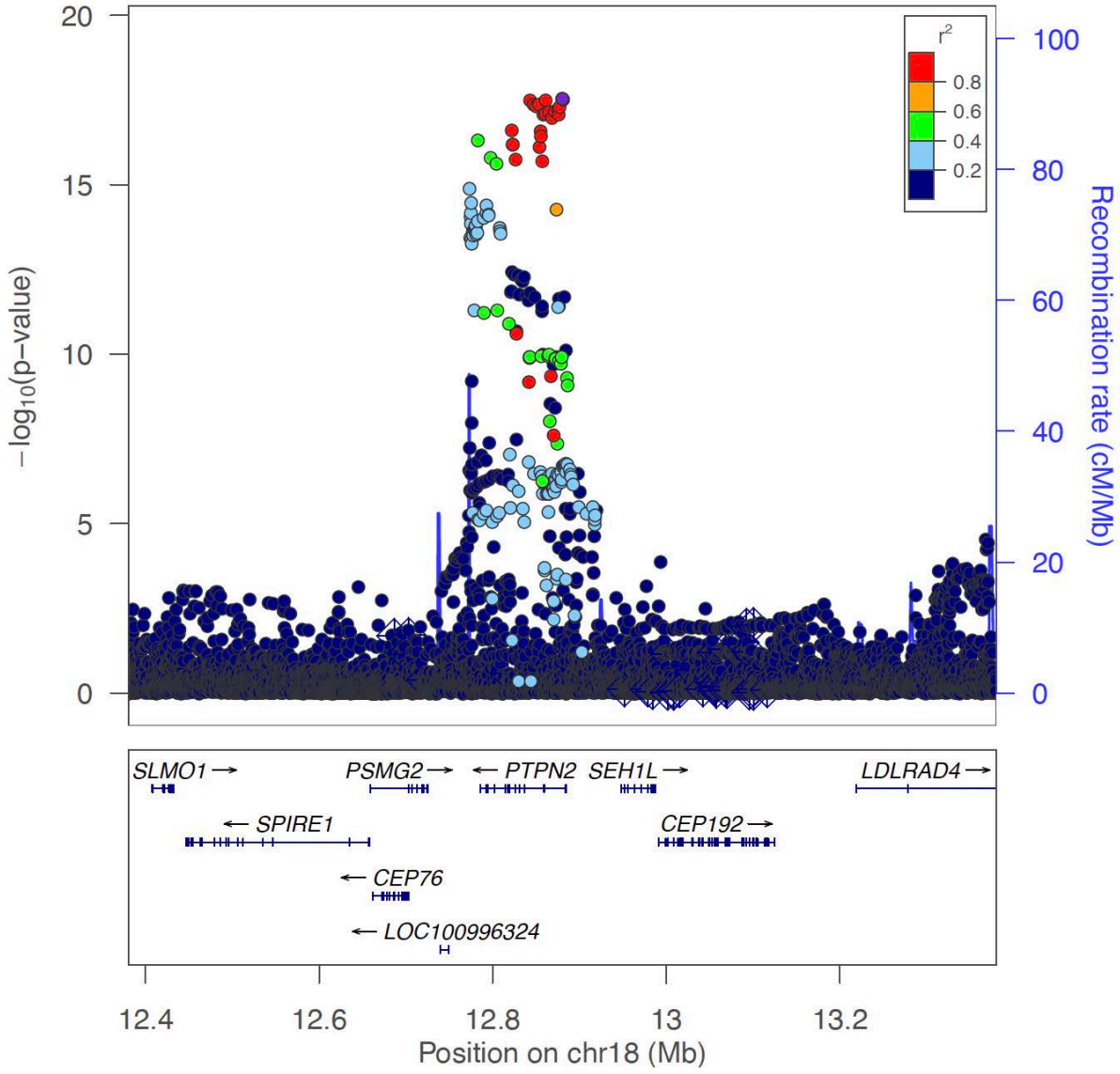

<Locus 107>
18:60009634:C:CAAAAAAAAAA (rs371734407)
Multi-GWAS (seroposi)
Novel locus

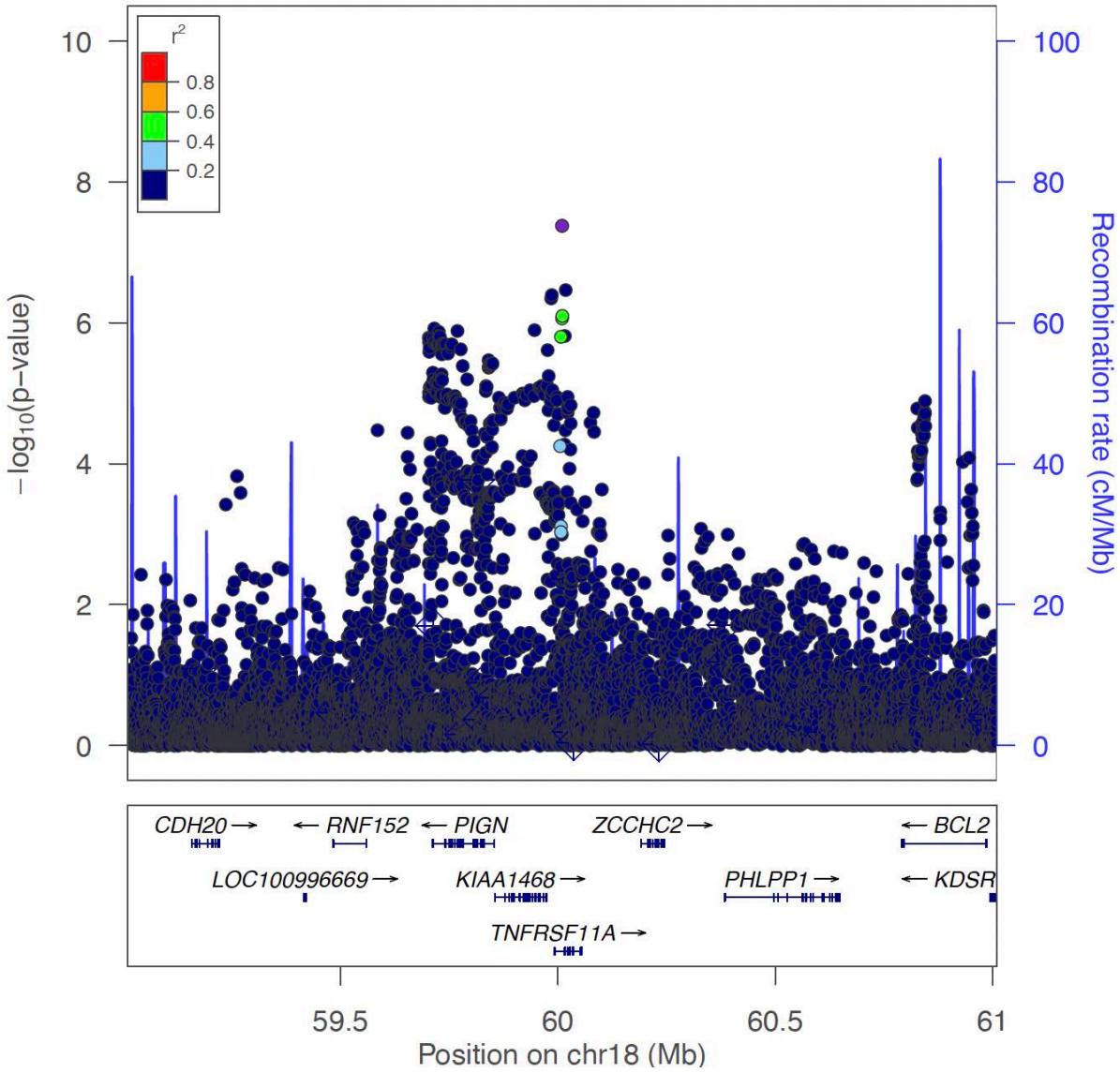

<Locus 108>
18:67547439:AAGGC:A (rs143107126)
Multi-GWAS (combined)
Known locus

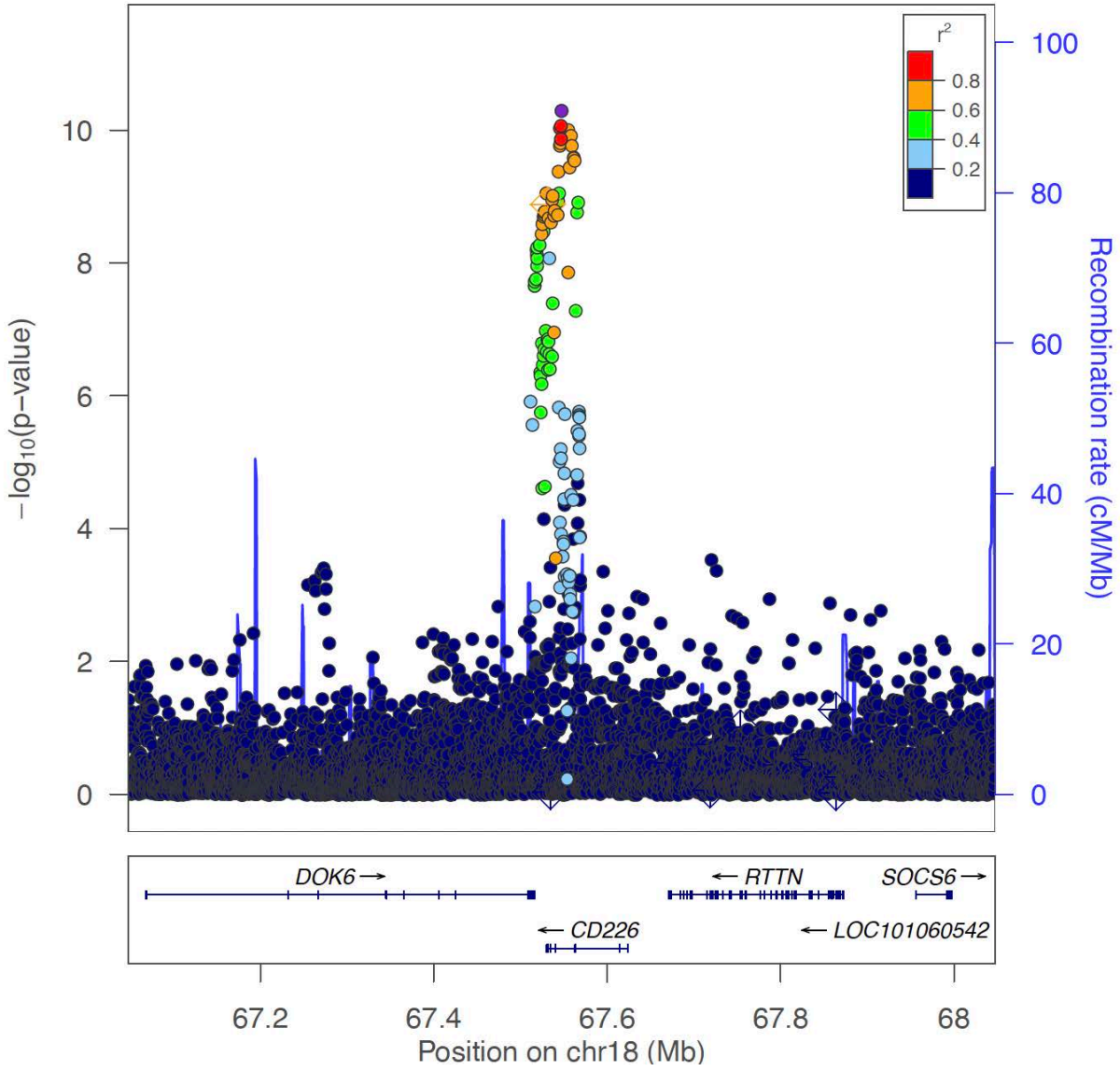

<Locus 109>
19:941603:A:G (rs10415976)
Multi-GWAS (combined)
Novel locus

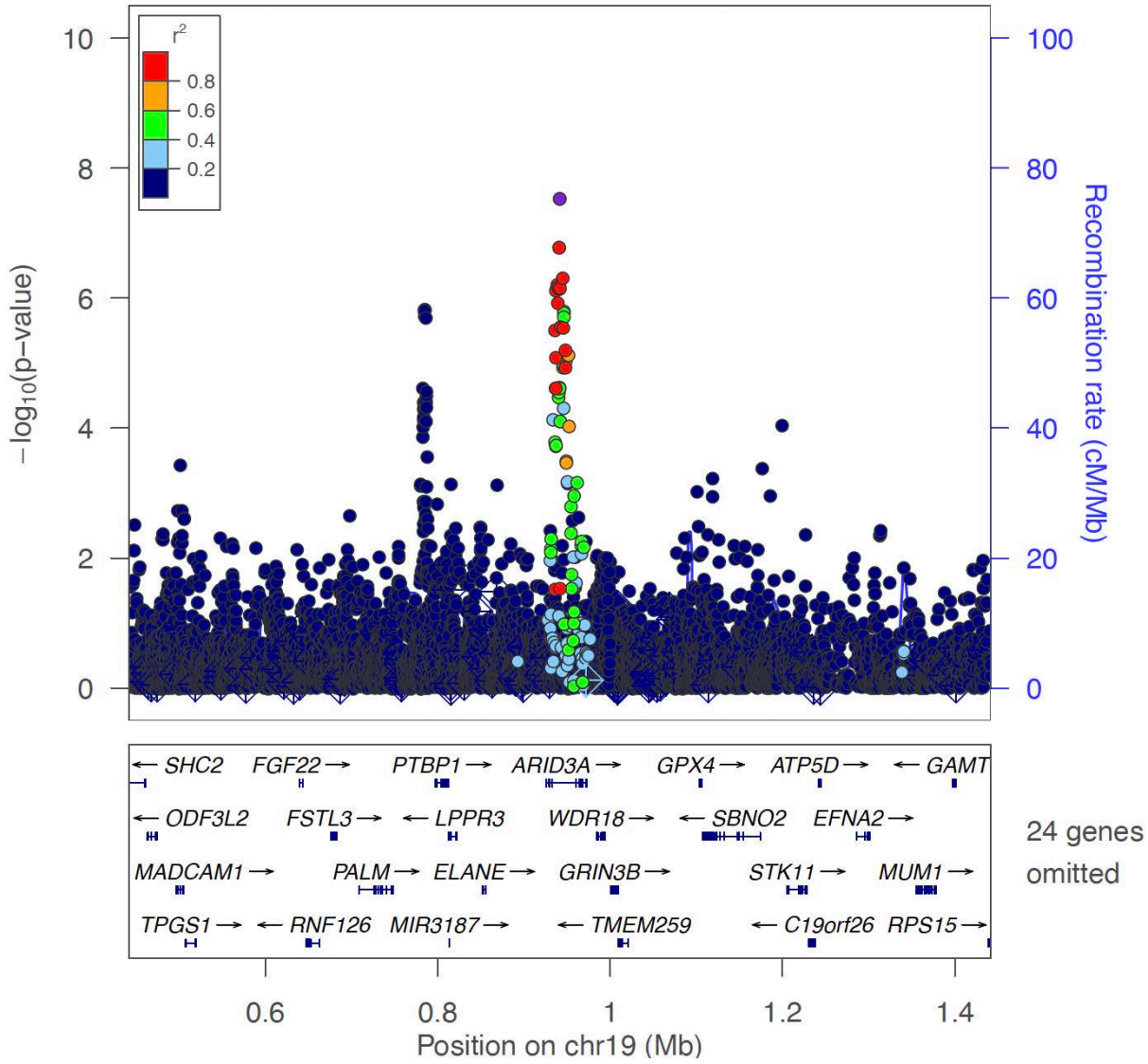

<Locus 110>
19:10463118:G:C (rs34536443)
Multi-GWAS (combined)
Known locus

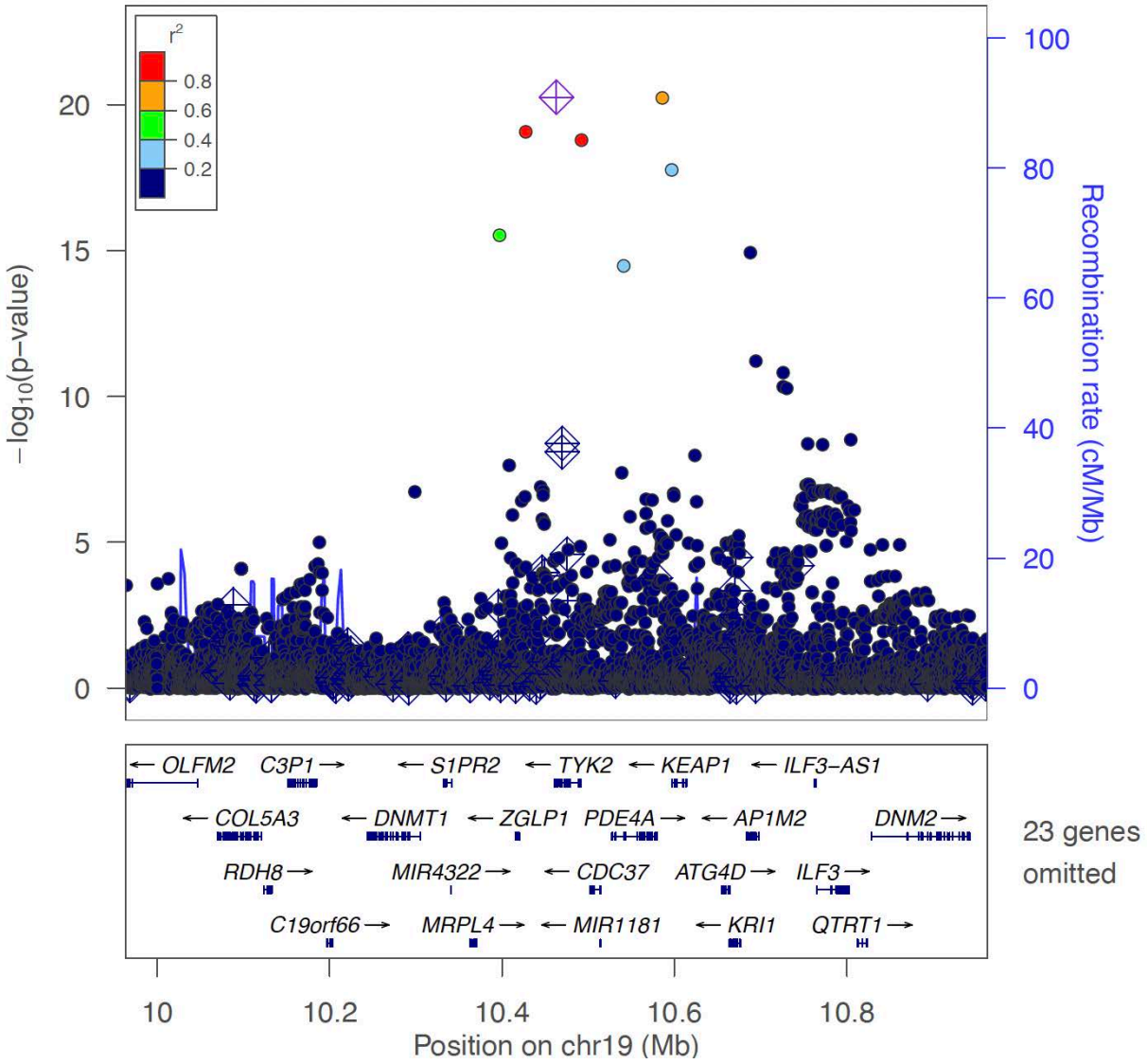

<Locus 111>
19:19367319:C:G (rs55762233)
Multi-GWAS (combined)
Novel locus

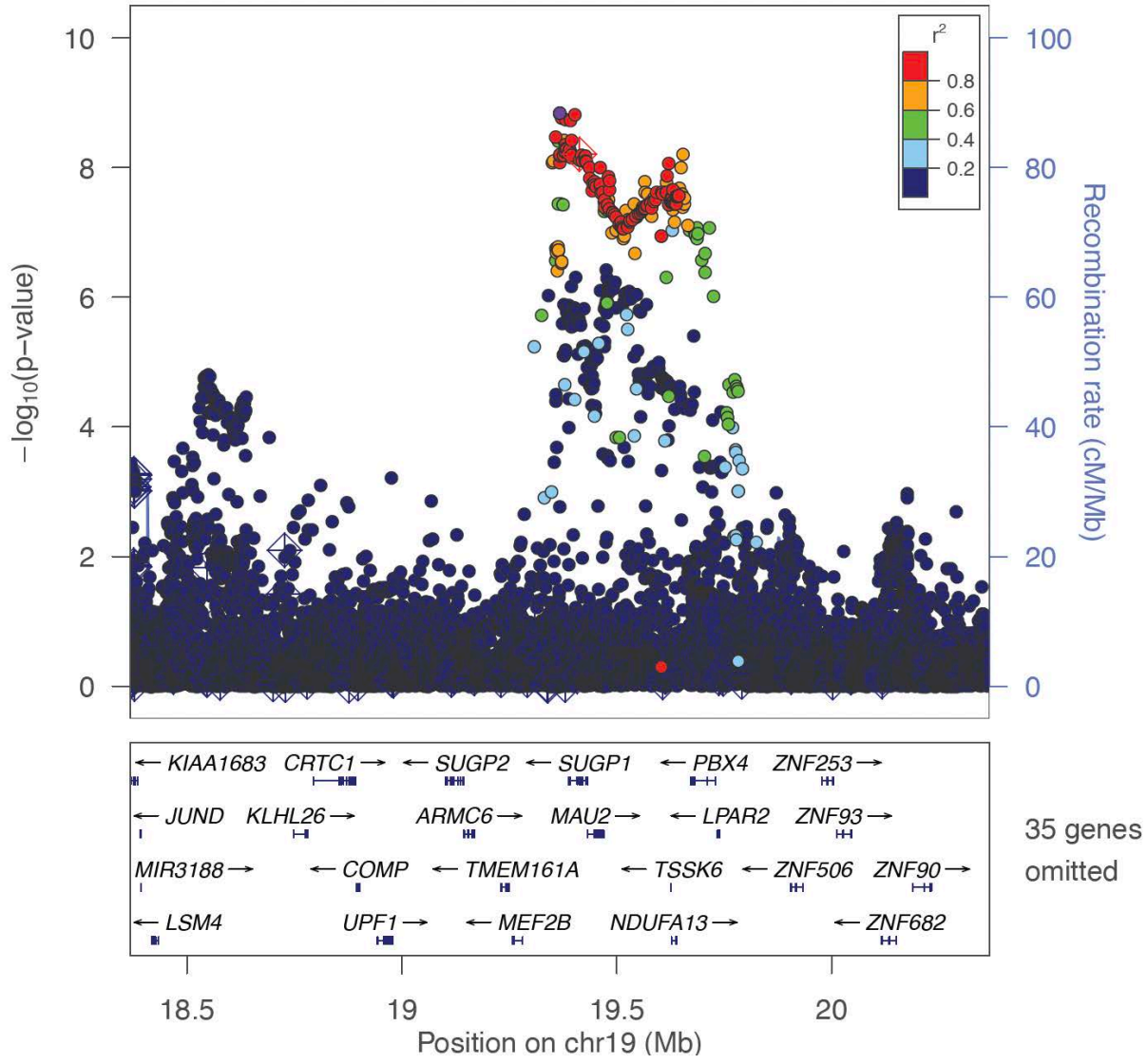

<Locus 112>
19:36213072:A:G (rs28373672)
Multi-GWAS (combined)
Novel locus

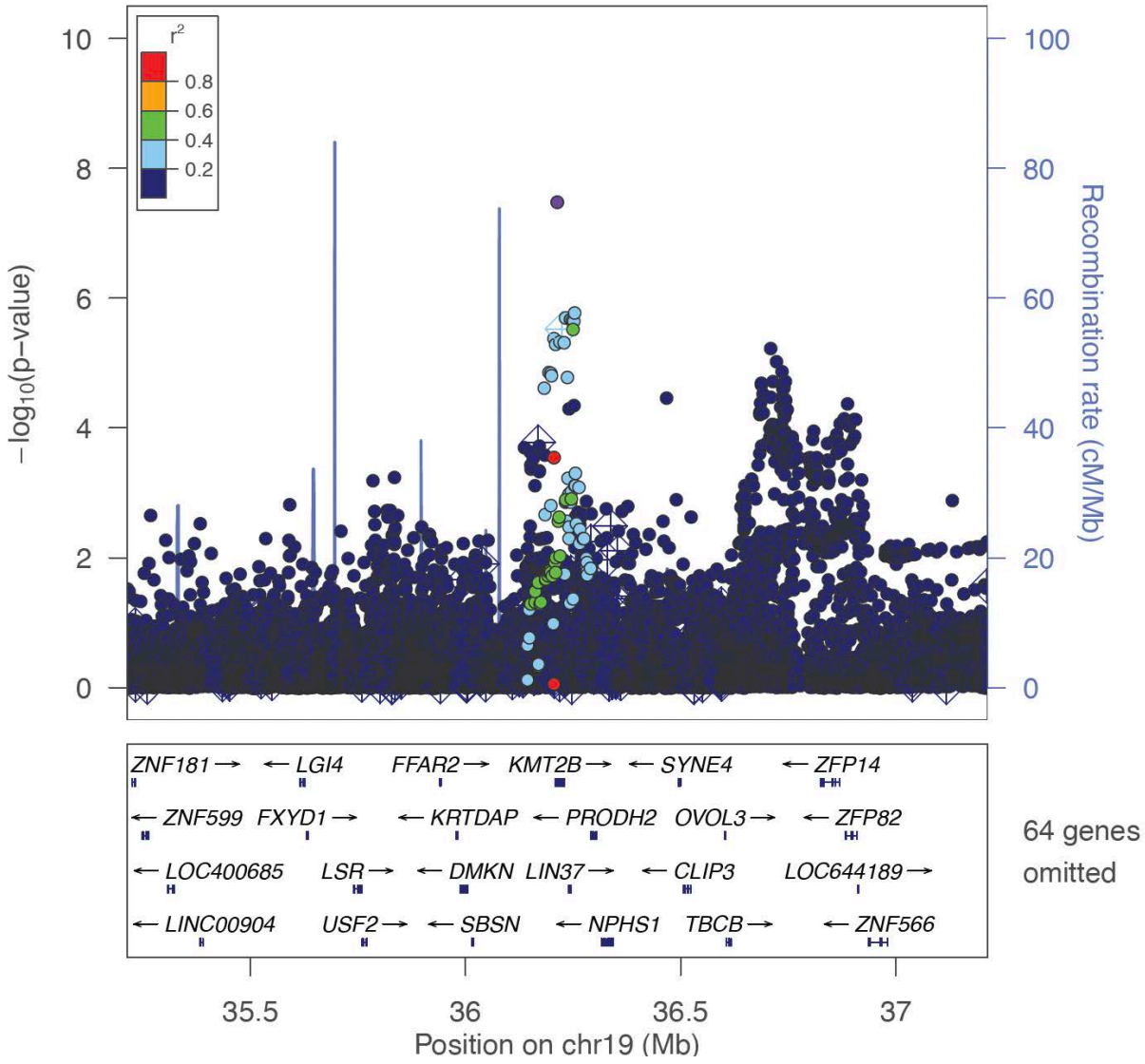

<Locus 113>
19:52017940:C:T (rs8106598)
Multi-GWAS (seroposi)
Novel locus

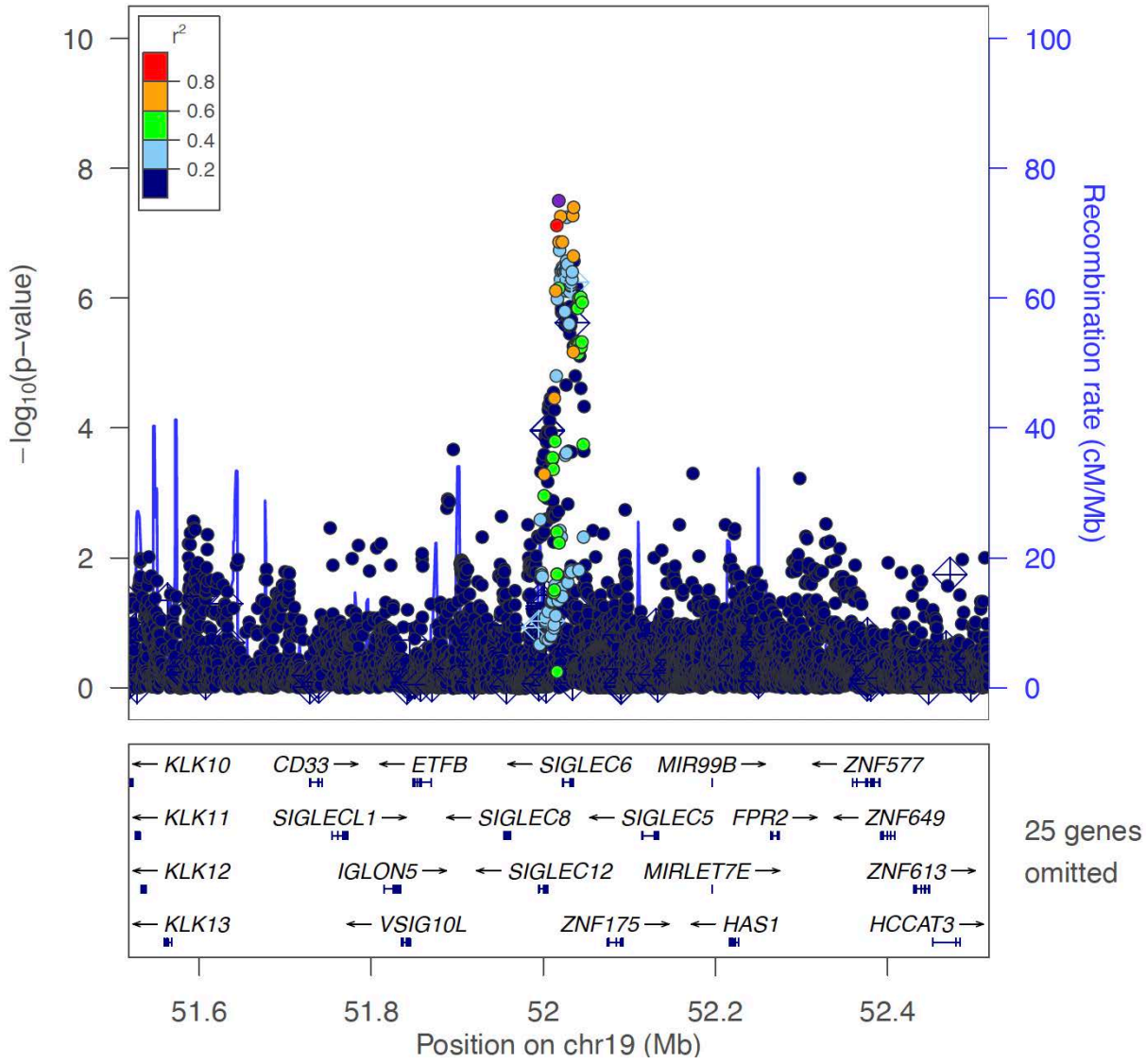

<Locus 114>
20:44746982:T:C (rs1883832)
Multi-GWAS (combined)
Known locus

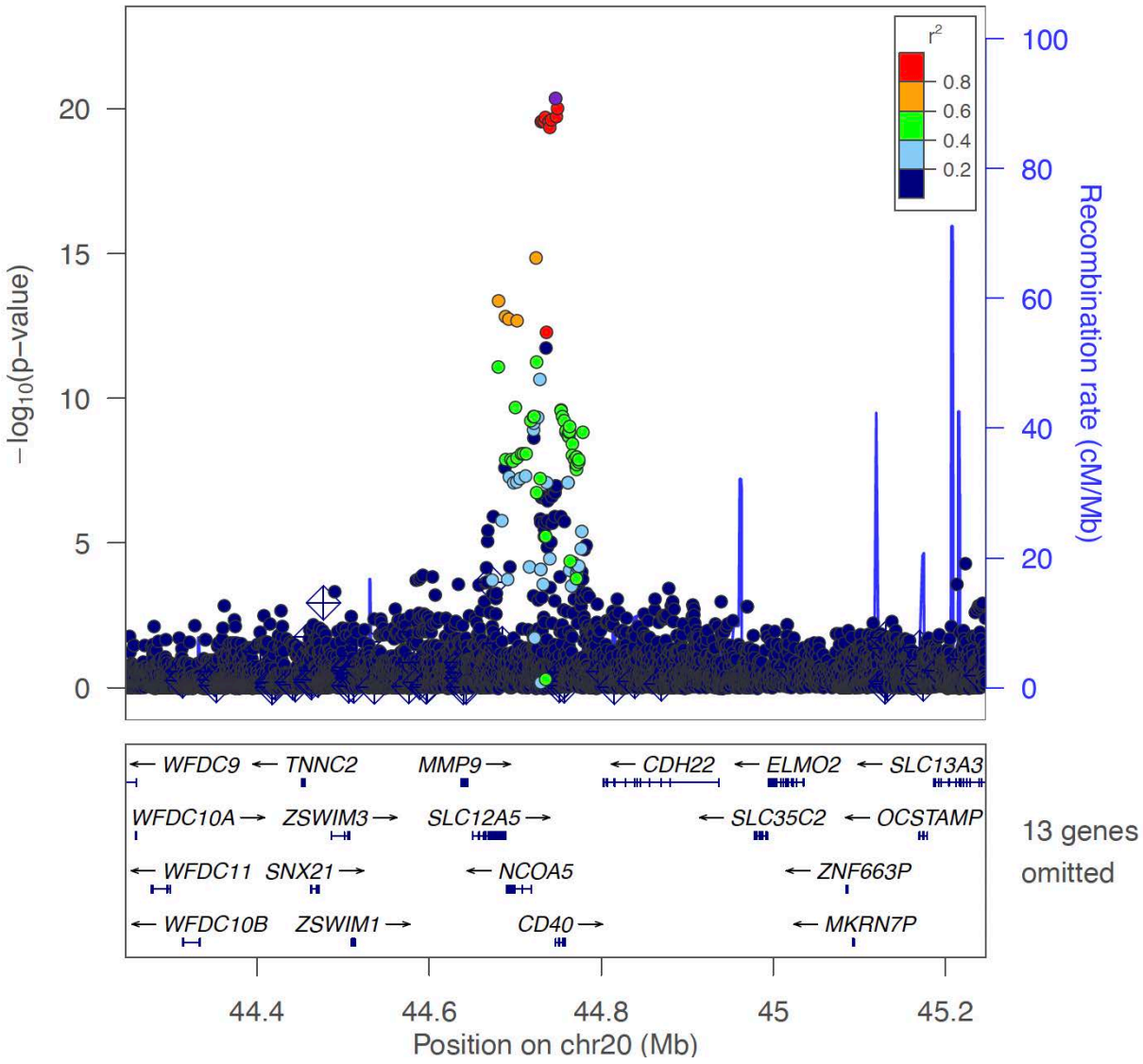

<Locus 115>
20:62480898:C:T (rs4809371)
Multi-GWAS (combined)
Known locus

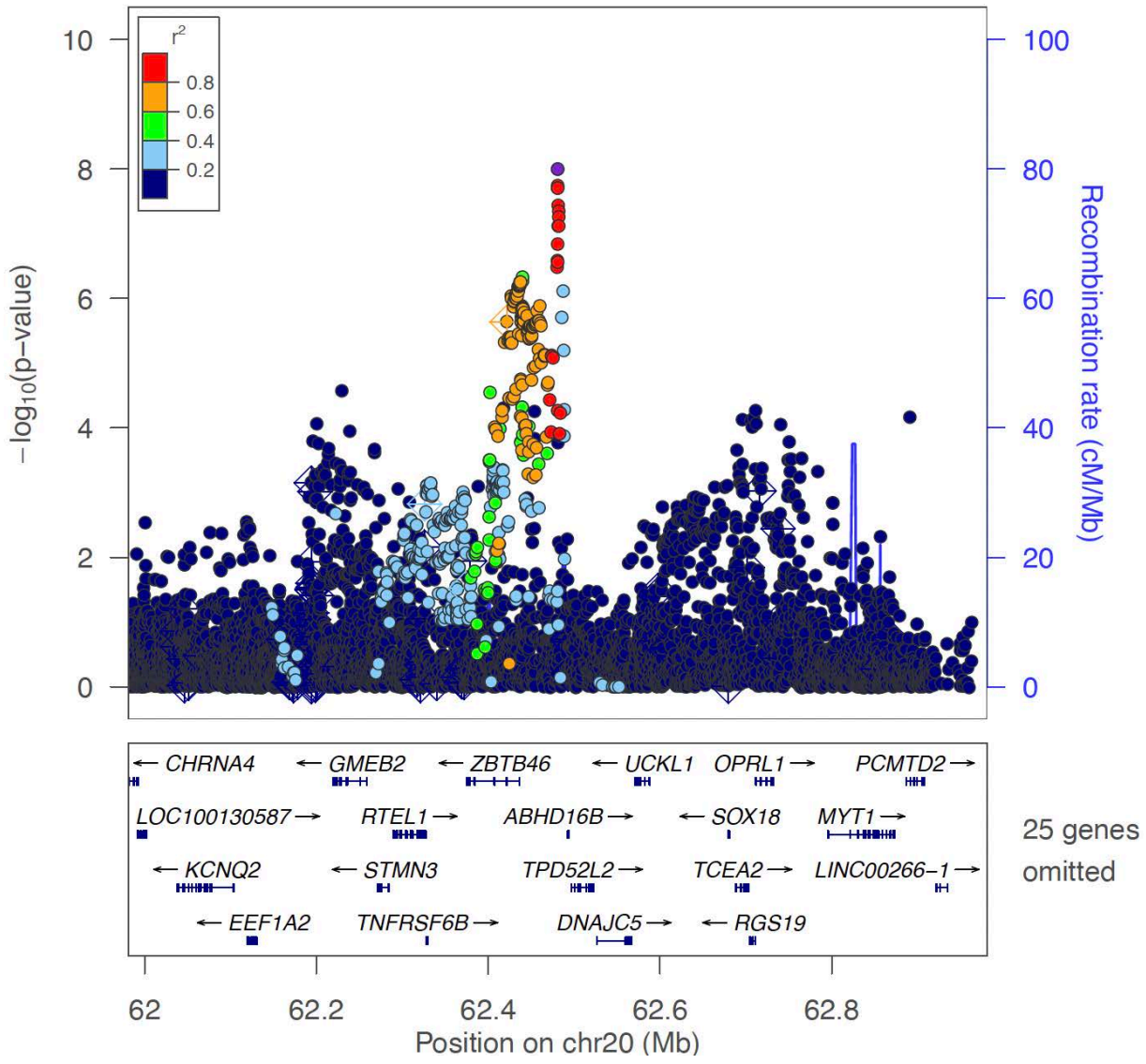

<Locus 116>
21:34788739:A:T (rs2300373)
Multi-GWAS (combined)
Known locus

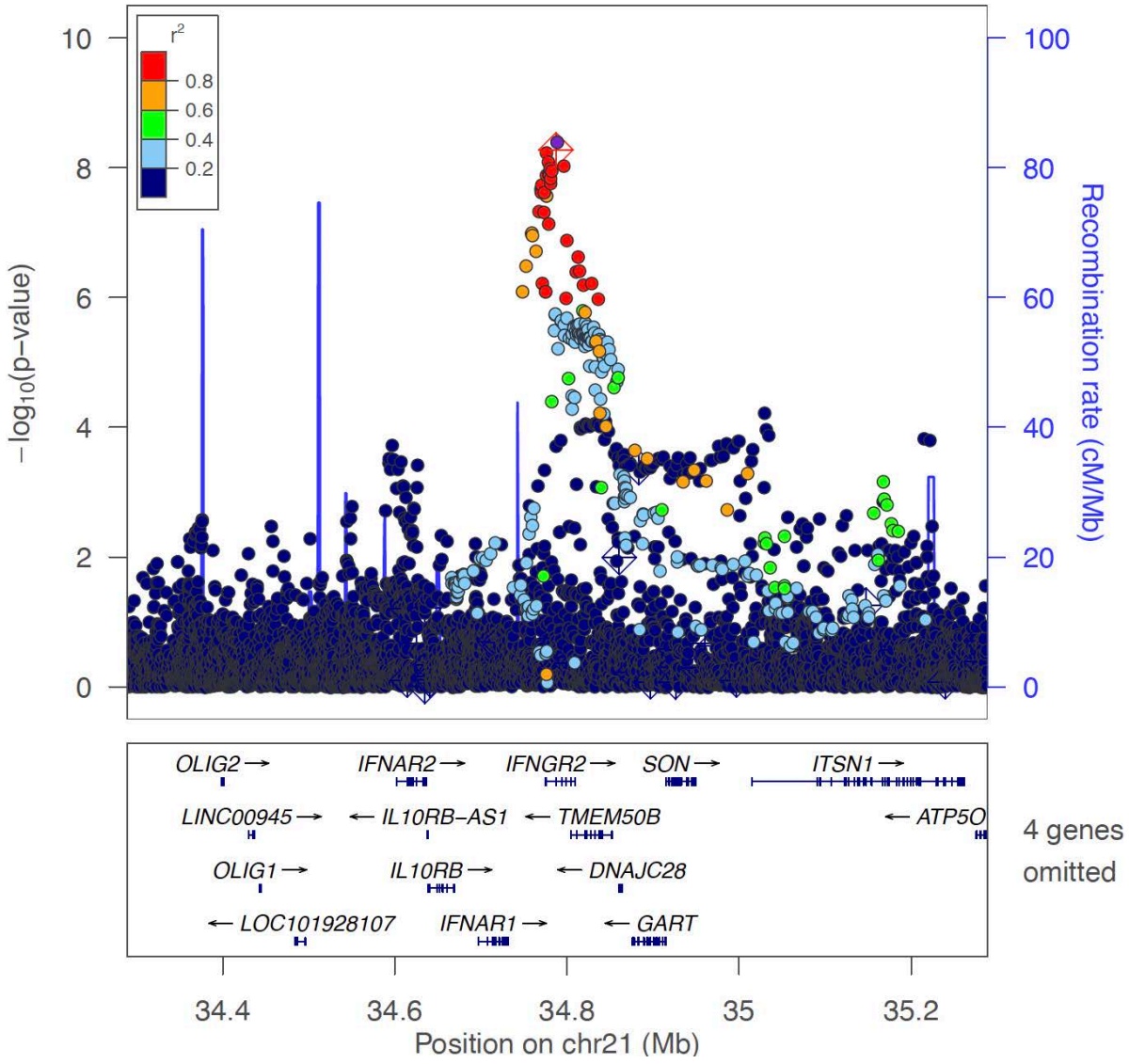

<Locus 117>
21:36714980:TATGCAA:T (rs66922517)
Multi-GWAS (combined)
Known locus

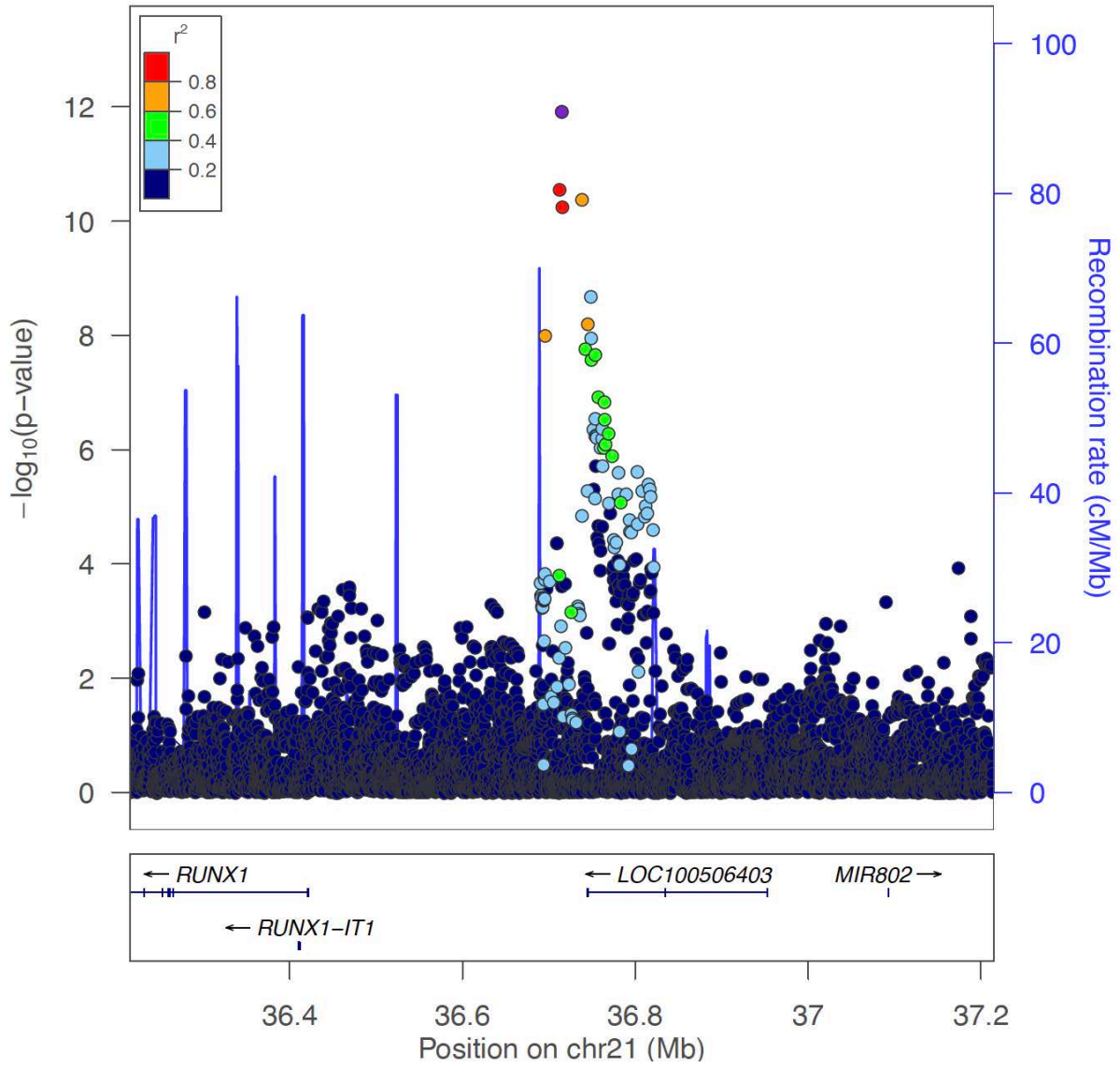

<Locus 118>
21:43855067:A:C (rs1893592)
Multi-GWAS (combined)
Known locus

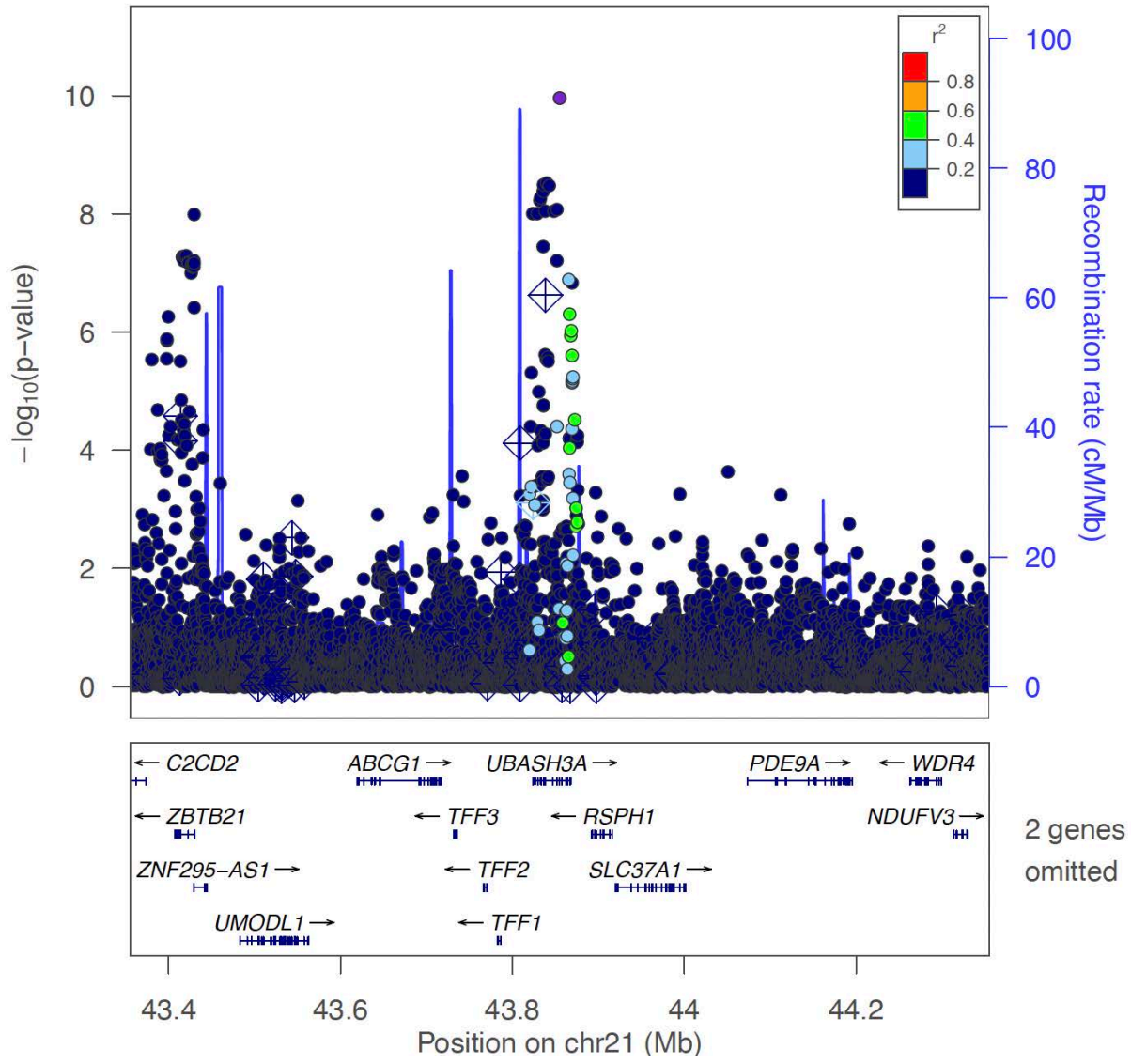

<Locus 119>
21:45709161:A:AC (rs11454989)
Multi-GWAS (combined)
Known locus

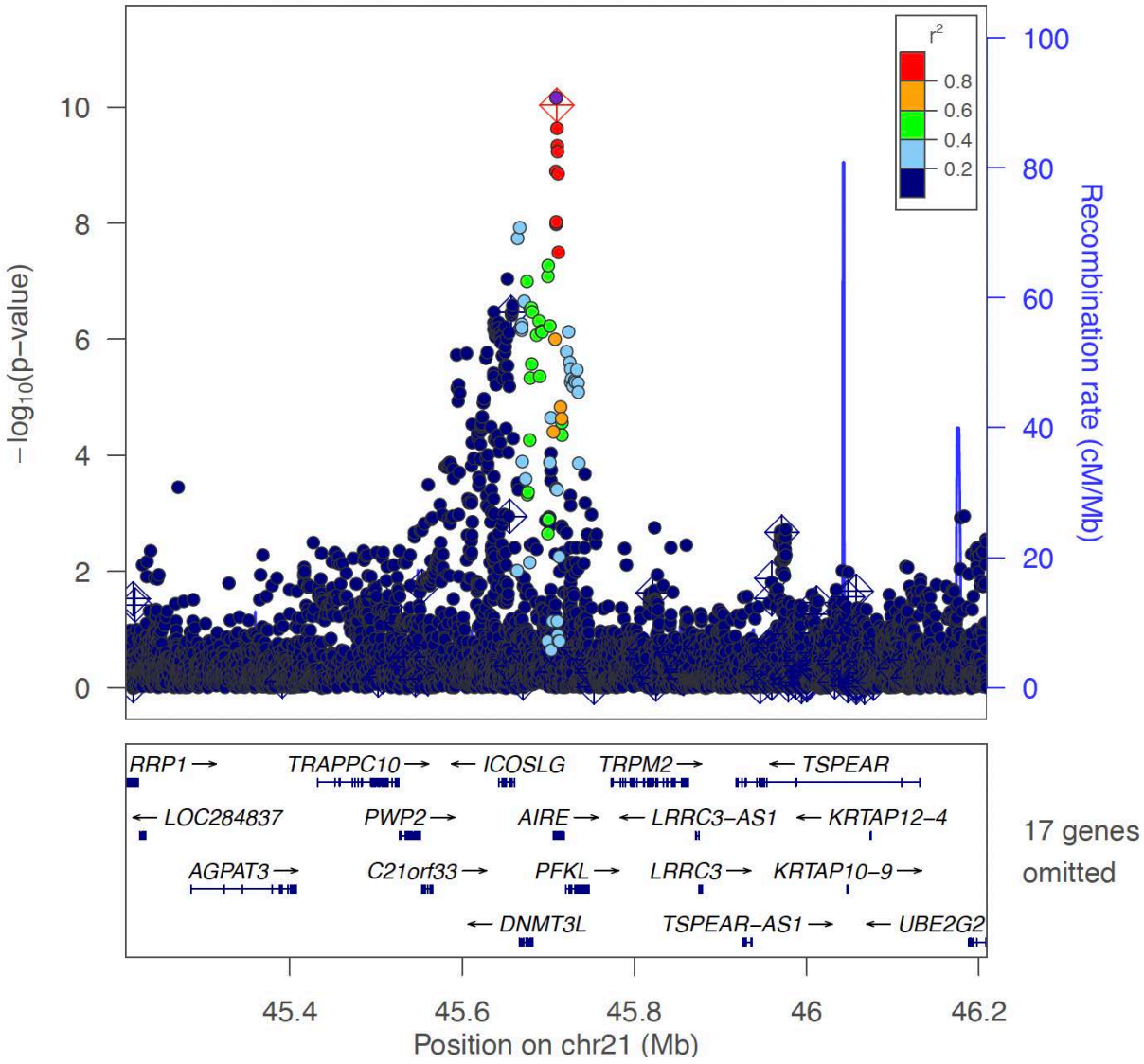

<Locus 120>
22:21916166:T:C (rs5754100)
Multi-GWAS (combined)
Known locus

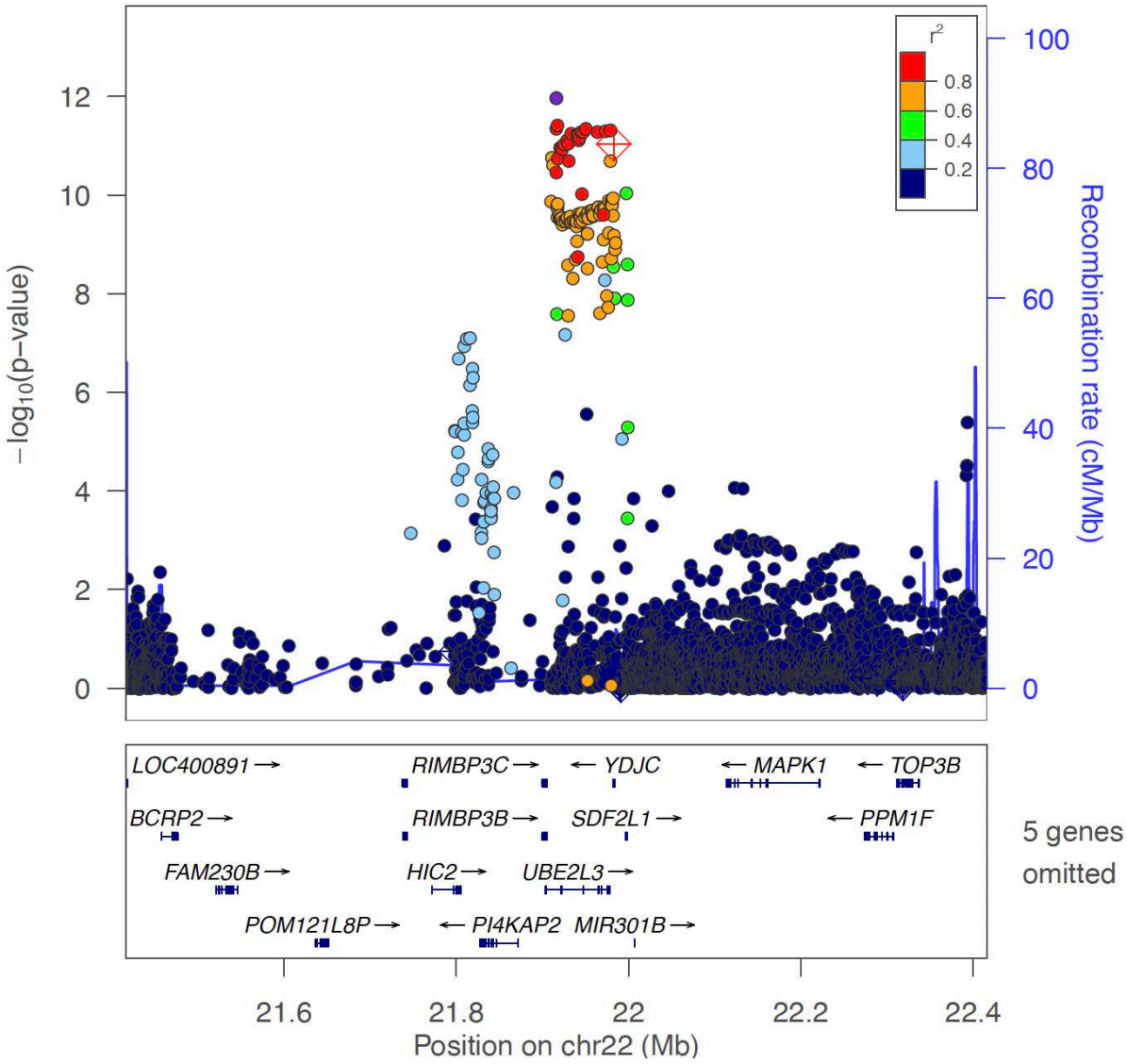

<Locus 121>
22:37316259:T:C (rs5756407)
Multi-GWAS (combined)
Known locus

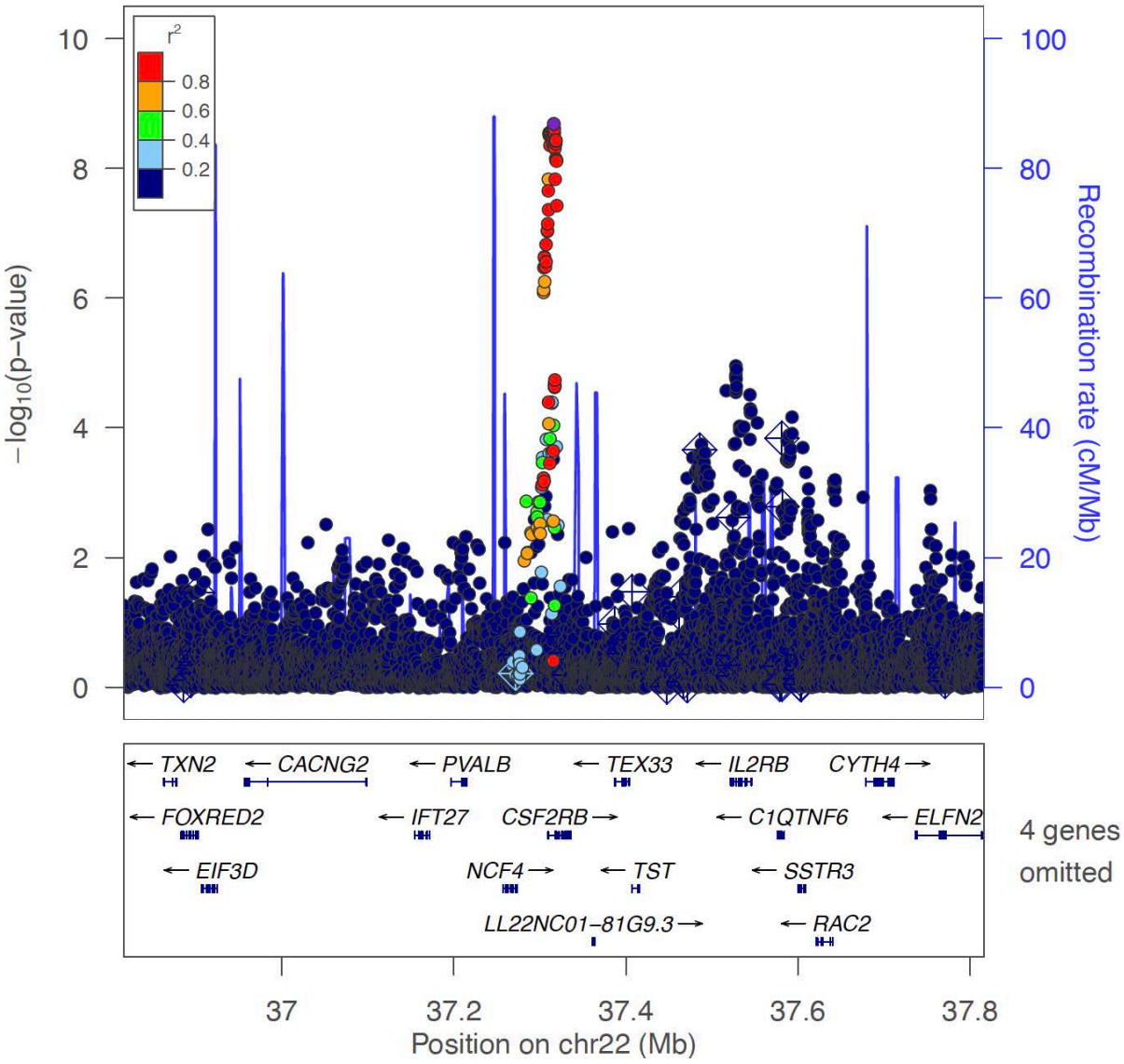

<Locus 122>
22:39747780:G:A (rs2069235)
Multi-GWAS (combined)
Known locus

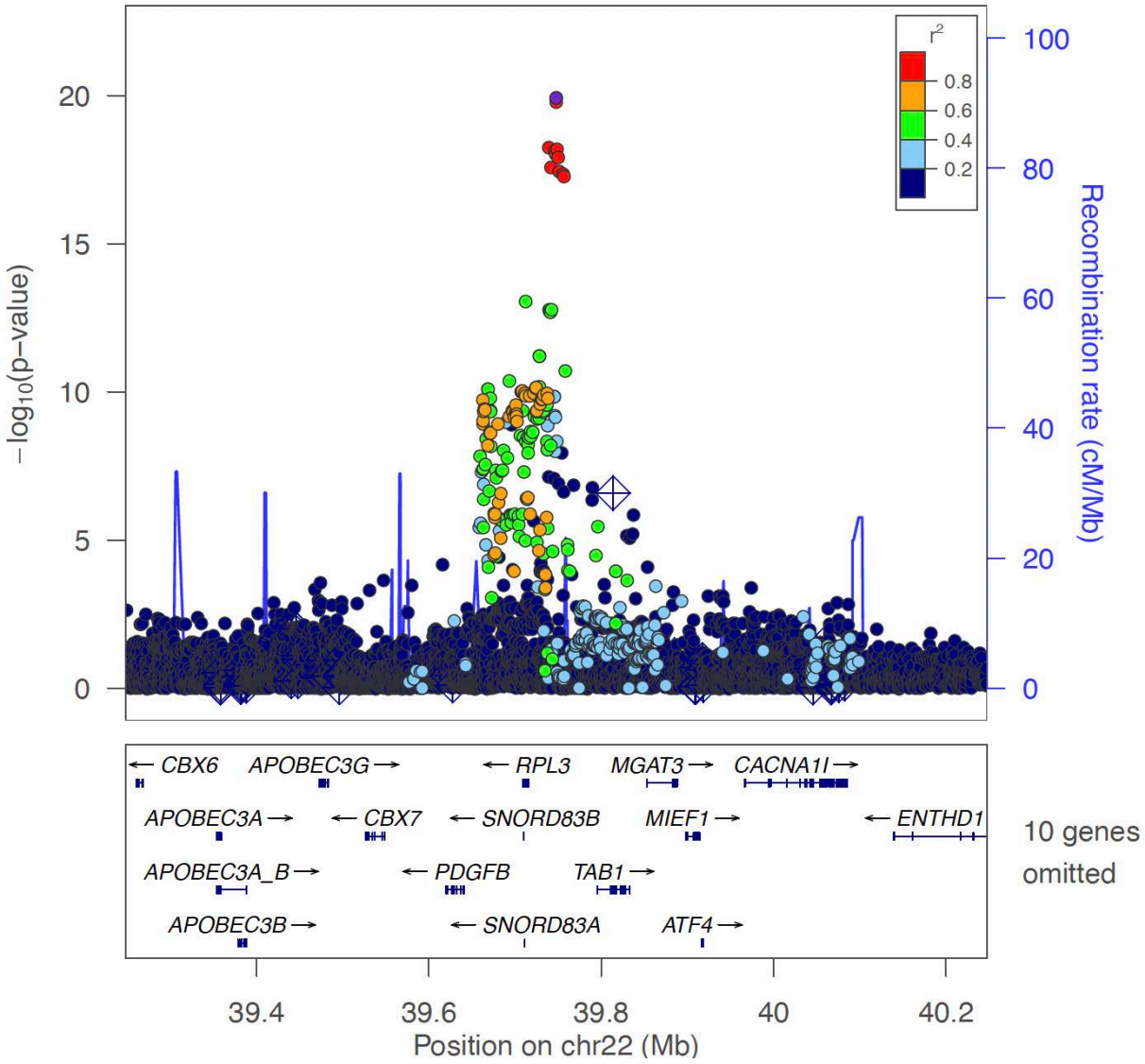

<Locus 123>
X:78332396:G:A (rs74842123)
Multi-GWAS (combined)
Known locus

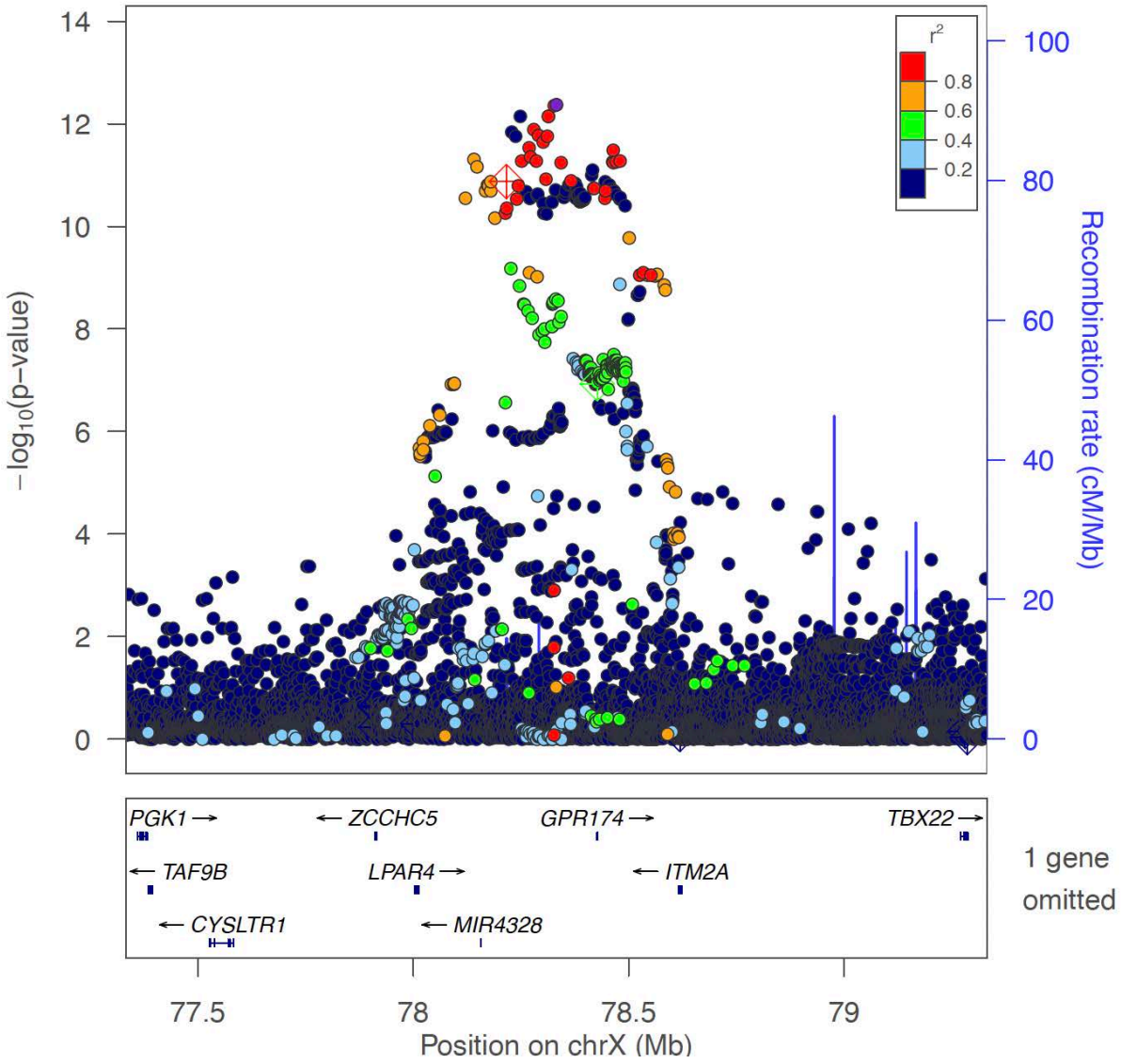

<Locus 124>
X:153298874:G:C (rs3027933)
Multi-GWAS (combined)
Known locus